Dottorato di Ricerca in Ingegneria Civile e Industriale-

Università della Calabria

UNIVERSITÀ DELLA CALABRIA

Dipartimento di Ingegneria Meccanica energetica e Gestionale (DIMEG)

Dottorato di Ricerca in Ingegneria Civile e Industriale

CICLO XXXVI

OPTIMIZATION STRATEGIES FOR AIR CONDITIONING SYSTEMS BASED ON THE INTEGRATION OF HEAT PUMPS AND RENEWABLE SOURCES

Settore Scientifico Disciplinare ING-IND/11

Coordinatore: **Ch.mo Prof. Domenico Mundo**

Firma _____ Domenico Mundo 23.12.2024 13:29:54 GMT+02:00

Supervisore: **Ch.mo Prof. Natale Arcuri**

Firma_____ Natale Arcuri 18.11.2024 12:10:13 GMT+02:00

Dottoranda: Dott.ssa Stefania Perrella

Stefania Perrella 18.11.2024 11:30:52 GMT+02:00

Firma _____

Anno Accademico 2023/2024

Abstract

The energy transition is a non-negotiable goal for the planet and future generations. The research examines the crucial need to implement advanced energy solutions to combat climate change and promote sustainability in the building sector. The primary focus is on the integration of heat pumps with renewable energy sources, particularly solar energy, and the utilization of thermal and electric storage systems to enhance the energy efficiency of buildings. The study begins by analysing the European and Italian regulatory frameworks, highlighting policies such as the European Green Deal and the "Fit for 55%" package, which aim to significantly reduce greenhouse gas emissions by promoting renewable energy adoption and energy efficiency. The Italian legislative context, including the Legislative Decree No. 199/2021, emphasizes the need for renewable energy integration in new and significantly renovated buildings. The core of the research explores the functionality, components, and classifications of heat pumps, emphasizing their role in reducing dependency on fossil fuels and minimizing environmental impact. Detailed simulations using the TRNSYS software model various scenarios of HVAC system enhancements, including the replacement of existing systems with solar-assisted heat pumps (SAHPs) and centralized systems with thermal storage. Key findings demonstrate that integrating solar thermal collectors, photovoltaic systems, and thermal storage significantly improves the performance of heat pumps, especially in cold climates where traditional systems may falter. The deployment of advanced control strategies further optimizes energy consumption, reduces CO_2 emissions, and enhances energy self-sufficiency. The dissertation also includes comparative analyses of different renewable energy systems, such as PV-assisted heat pumps versus biomass boilers, to determine the most effective configurations for various climatic conditions. The research highlights the critical role of thermal storage in stabilizing energy supply, reducing peak demand, and increasing the resilience of the energy system. Overall, this work provides comprehensive insights into the technological and strategic advancements necessary for the successful integration of heat pumps with renewable energy sources. The findings offer practical recommendations for policymakers, industry stakeholders, and researchers to drive the transition towards a sustainable and resilient built environment.

Index

1 Introduction and motivations

1.1 Background and motivations

Among the foremost challenges of our time is the energy sector, which aims to mitigate dependence on fossil fuels-polluting, obsolete, and exhaustible sources-and the concentration of CO_2. This issue occupies a significant place in the global landscape. Furthermore, the increasing demand for energy necessitates the creation of a feasible scenario capable of steering energy consumption towards a sustainable development model that reduces pollutant emissions by prioritizing renewable energy sources.

In Europe, policies to counter climate change have translated into short and medium-term objectives, such as those established by the Climate Energy Package of 2009, updated in 2014. These policies mandate that Member States achieve three major goals by 2030: a 40% reduction in greenhouse gas emissions, an increase in the share of renewables, and a 27% improvement in energy efficiency [1].

In this context, the construction sector plays a crucial role, as it generates significant environmental impacts (responsible for 39.7% of final energy consumption and 36% of greenhouse gas emissions in the European Community) that must be addressed and mitigated through the development of alternative solutions [2].

In such an energy scenario, heat pumps assume a strategic role. These devices, typically used for the air conditioning of buildings, operate by transferring low-temperature heat from one medium (or environment) to another at a higher temperature, following the thermodynamic regeneration of that heat with a specific energy input. During heating, low-temperature heat is extracted from an external medium to the building (air, surface water, slurry, or ground) and transferred to the building itself. During cooling, heat is captured inside the building and transferred to the outside air, water, or ground.

This versatility, which enables both air conditioning and domestic hot water (DHW) production with a single device, makes heat pumps suitable for the air conditioning of many civil buildings, positioning them as highly sustainable tools. Moreover, when adequately integrated with other renewable technologies, heat pumps become a fundamental strategic basis for constructing "smart" buildings. These buildings can provide increasingly sophisticated air conditioning services and interact with the grid, establishing new assets.

Consequently, this research is situated within a growing focus on the urgent need to develop advanced energy solutions to tackle global challenges related to climate change and environmental sustainability.

Renewable energy adoption forms the strategic foundation for achieving ambitious goals in building energy performance and emissions reduction. Renewable energy sources can fully satisfy both current and future energy demands with minimal environmental impact, especially when compared to traditional energy sources. Among the various renewable sources, solar energy is the most abundant.

To realize a rational use of renewable resources, solar energy can play a key role, providing savings and clean energy for both heating and cooling applications. In such a context, among the available options, the heat pump must be considered not only for the direct use of renewable energy present in the environment (air, water, soil) but also, and above all, for the possibility of combining its use with other renewable sources, such as electricity produced by solar panels or thermal energy produced by solar thermal collectors.

These considerations are closely linked to the obligations imposed by Legislative Decree of 8 November 2021, No. 199 [3], which transposes Directive (EU) 2018/2001 on the promotion of the use of renewable energy. The decree establishes binding objectives for the share of renewable energy to be used in various sectors, including the building sector, with the aim of significantly increasing the use of renewable energy in Italy by 2030.

This obligation makes the integration of heat pumps, thermal solar photovoltaic installations, and energy storage systems even more crucial. In fact, in the search for innovative solutions to improve the energy efficiency of buildings, heat pumps emerge as a central and strategic element. However, in cold climates, their performance can be

compromised. It is here that intelligent integration with other renewable energy sources, such as photovoltaic and solar thermal systems, ensures performance.

Renewable technologies, such as heat pumps and solar systems, have been extensively studied in the literature, but technical and management challenges remain that require more in-depth analysis. Among these challenges, there is a pronounced need to efficiently integrate thermal storage with large-scale distributed systems and to optimize heat pump performance in harsh climate conditions.

The role of thermal storage is critical in the rational management of thermal energy, particularly when applied to distributed climate control systems within energy communities. Most studies in the literature have focused on the efficiency of solar-assisted heat pumps, examining both direct and indirect configurations, yet they often overlook the potential of an integrated approach that utilizes centralized thermal storage to optimize energy efficiency in large-scale residential contexts [4-12]. One of the aims of this thesis is to propose a systemic approach demonstrating how the integration of centralized thermal storage can increase overall system efficiency, while also enabling a more rational and flexible management of renewable energy production, yielding tangible benefits in terms of energy consumption optimization. Moreover, unlike the primary studies reviewed, which are limited to theoretical models and experiments on single residences, the role of thermal storage in centralized systems has been evaluated through detailed dynamic simulations of energy performance across an aggregate of real buildings.

Beyond the importance of thermal storage, a key issue lies in the performance of heat pumps in cold climates. Air-to-water heat pumps, while widely adopted, experience a significant drop in their coefficient of performance (COP) in low external temperatures, making it challenging to synchronize thermal demand with the availability of solar radiation. Most existing studies have focused on air-to-water solutions or on models that manage thermal storage in a limited manner [13-16]. To address these limitations, this thesis proposes the integration of water-to-water heat pumps with solar thermal collectors and storage tanks, demonstrating how this solution can significantly improve efficiency in harsh climates. The proposed approach utilizes solar energy not only for heating but also to raise the temperature of the heat pump's cold source, thereby improving the COP and optimizing renewable resource utilization. This strategy maximizes the contribution

of solar resources even in cold climates, enhancing the overall energy efficiency and sustainability of heating systems.

Additionally, the adoption of advanced control systems and parametric simulations in TRNSYS allows for the identification of optimal configurations that maximize solar energy use and significantly reduce non-renewable primary energy consumption. A crucial aspect, closely tied to heat pump optimization, is the implementation of advanced control strategies for managing photovoltaic surplus. The optimization of control logic that combines electrical and thermal storage remains underexplored in the literature [17-21]. This research proposes a dynamic resource management approach that capitalizes on photovoltaic surplus by enhancing overall system efficiency through advanced control strategies for the simultaneous management of thermal and electrical storage in solar-assisted heat pump systems. Unlike traditional approaches, this research goes beyond passive solar energy management, introducing an innovative mode of utilizing photovoltaic surpluses through dynamic exceeding the thermal storage set-point intentionally. In this way, the thermal storage system transitions from merely serving as a buffer to functioning as an active energy storage device, capable of absorbing excess electricity and converting it into heat to be used during periods of low solar radiation availability. This solution increases the operational flexibility of the system, enabling proactive management of solar energy.

Finally, the comparative assessment of solar-assisted heat pumps and biomass boilers, in terms of primary energy consumption, is an essential step to complete the analysis of the examined technological solutions. This comparison serves as a critical phase in understanding which of these technologies offers greater overall energy efficiency while ensuring optimized management of available renewable resources. Such analysis is fundamental for identifying the most suitable approach to reducing dependence on non-renewable energy sources, highlighting the potential and limitations of alternative thermal solutions concerning their sustainability and adaptability to large-scale residential contexts.

While heat pumps represent a highly efficient solution in moderate climates, they suffer a significant performance drop in low-temperature environments. Conversely, biomass boilers, despite generally having lower efficiency than heat pumps, offer a more stable and effective solution in cold climates where heat pump efficiency is compromised. The literature has generally addressed these technologies separately or focused on

specific aspects, such as environmental benefits or life cycle assessment (LCA), without providing a systematic comparison in terms of non-renewable primary energy [22-26]. The comparative analysis of the two solutions, based on the share of non-renewable primary energy and performance across various climatic conditions, aims to offer a more robust foundation for identifying the optimal system.

This research also aims to provide practical recommendations for key stakeholders in the building and energy policy sectors. It is hoped that the results of this research can inform and guide the adoption of more effective and future-oriented policies, promoting a transition to a more sustainable and resilient energy system.

1.2 Methodology

This section outlines the methodology adopted to analyse and optimize the air conditioning systems based on the integration of heat pumps and renewable energy sources. In the process of developing and analysing the research, it is essential to adopt a rigorous methodological approach that ensures the scientific robustness of the results obtained. Using sophisticated and reliable tools is crucial. In this context, the TRNSYS [27] software emerges as a critical resource, offering a versatile and powerful platform for the dynamic simulation of building energy systems.

TRNSYS, developed by the Solar Energy Laboratory at the University of Wisconsin-Madison, is widely recognized for its ability to simulate complex systems and their thermal and energy dynamics over time. This approach allows for precise evaluation of the impact of various plant configurations on energy and environmental performance. Using TRNSYS enables detailed dynamic simulations that account for temporal variations, climatic conditions, and the complex interactions between building elements and the air conditioning systems [28]. This results in more accurate and realistic outcomes compared to static or simplified simulations. Furthermore, TRNSYS provides the capability to integrate advanced models to realistically represent both building components and energy generation and distribution systems. Among the main advantages of TRNSYS are its flexibility and modularity, allowing users to create detailed and customized models of systems, integrating a wide range of components and subsystems. This allows for realistic representation of various air conditioning systems technologies, including heat pumps, solar thermal panels, energy storage systems, and control strategies. Using TRNSYS, it is possible to simulate various operational scenarios,

considering climatic variables, energy consumption profiles, and the specific characteristics of buildings. In this research, the methodology includes several key phases. Initially, detailed data on energy consumption and building operational conditions will be collected through an in-depth analysis of architectural and HVAC characteristics. Subsequently, detailed models of HVAC systems will be developed, integrating heat pumps with selected renewable energy sources. Dynamic simulations will then be performed to analyse system performance under different operational and climatic conditions. This approach will enable evaluation of energy efficiency, indoor comfort, and environmental impact of the integrated systems, identifying optimal configurations and best practices for implementation. Additionally, sensitivity analyses will be conducted to understand the influence of key variables on the overall system performance. The goal is to identify optimal configurations and formulate practical recommendations to rationalize the adoption of renewable energy sources.

To assess the advantages of the proposed solutions, several evaluation parameters are considered, including the non-renewable primary energy consumed by the systems, the coefficients of performance (COP) of the heat pumps, the seasonal coefficient of performance (SCOP) of the heat pumps, the levels of energy self-sufficiency, and the CO_2 emissions avoided compared to conventional systems. These parameters provide a comprehensive assessment of the energy and environmental performance of the proposed solutions, enabling the comparison and evaluation of different scenarios.

1.3 Thesis outline

This thesis is a compilation of results published in scientific journals and presented at conferences. It provides an overview of the main topics addressed, highlighting the interconnections between the various subjects discussed in the four selected papers. In particular, this introductory chapter aims to offer a comprehensive overview of the current context and the challenges related to energy sustainability in the construction sector. It explores the foundational reasons for the research work. The focus is on the importance of integrating heat pumps with renewable sources to enhance the energy efficiency of buildings and reduce carbon emissions. The methodology employed in the study is described, and the overall structure of the thesis is presented.

The second chapter provides an in-depth analysis of the European and Italian regulatory frameworks on the energy transition. Key initiatives and policies at the

European level, such as the Green Deal and Agenda 2030, are examined and compared to Italian national regulations.

The third chapter, on the other hand, offers a theoretical examination of heat pumps.

Subsequently, the thesis is structured into five papers.

As outlined in the "Background and Motivations" section, each article is closely connected to a specific theme concerning the integration of heat pumps with renewable energy sources. Each study is designed to explore a fundamental aspect of this integration, highlighting the interdependence among the various research areas and providing a coherent and comprehensive overview of innovative solutions aimed at enhancing energy efficiency and reducing emissions in the construction sector. In particular:

1. **The role of thermal accumulation in distributed air conditioning plants: energy and environmental analysis** [29]*:* this article focuses on analysing the effect of thermal storage. Through dynamic simulations conducted in the TRNSYS environment, potential reductions in energy consumption and environmental emissions are assessed for an aggregated building comprising four structures. Specifically, two scenarios for improving the HVAC system are compared: replacing the existing system with air-source heat pumps, supported by photovoltaic installations. The performance achieved with individual heat pumps and a centralized system with thermal storage is evaluated, identifying configurations that maximize energy efficiency.
2. **Energy evaluations of a new plant configuration for solar assisted heat pumps in cold climates** [30]**:** this article investigates an innovative solar-assisted heat pump (SAHP) system specifically designed for cold climates. This system integrates advanced technologies to optimize energy efficiency and reduce CO_2 emissions. The SAHP system comprises four primary components: solar thermal panels, a water-to-water heat pump, two thermal storage tanks, and a photovoltaic system with electrical storage. The solar thermal panels capture solar energy and transfer it to the storage tanks for later use. The water-to-water heat pump utilizes this thermal energy to heat water, enhancing the heating process's efficiency. A distinctive technical feature of the SAHP is its capability to elevate the thermal level of the cold source, thereby improving overall system efficiency and reducing reliance on non-renewable energy sources. This is particularly beneficial in

climates where low external temperatures can hinder the performance of conventional heat pumps. A parametric study was conducted to evaluate the impact of the solar collector size and the thermal storage tank volume on overall system performance. It was found that increasing the solar collector area and thermal storage tank volume not only boosts the amount of thermal energy collected but also the percentage of energy demand met directly by the solar collectors, thereby further enhancing the overall efficiency of the SAHP.

3. **Optimization of a solar assisted heat pump system to increase thermal efficiency working on the cold sink** [31]: Building on the previous study's findings and within the broader context of the "Tech for You" project, the SAHP system was implemented in a demonstration building at the University of Calabria, used as a residence. Preliminary investigations, conducted through dynamic simulations in the TRNSYS environment, allowed for accurate system sizing. The installed SAHP system includes a significant area of solar thermal collectors, a water-to-water heat pump, thermal storage tanks, and a photovoltaic system. This configuration was chosen to optimize energy efficiency and ensure a consistent supply of thermal energy even during periods of low insolation. Specifically, the system is designed to elevate the thermal level of the cold source, enhancing overall efficiency and reducing reliance on non-renewable energy sources. The system implementation at the University of Calabria is scheduled for completion and commissioning by the end of the year. During this phase, detailed operational data will be collected to validate the developed virtual model. The collection of empirical data will extend the model's reliability and applicability, providing a solid foundation for further optimizations and applications in other building contexts.
4. **Solar-assisted heat pump with electric and thermal storage: the role of appropriate control strategies for the exploitation of the solar source** [32]**:** this article aims to analyse the effectiveness of control strategies for optimal solar utilization in heat pumps assisted by electrical and thermal storage. Through dynamic simulations under various climatic conditions, the impact of two different control strategies is evaluated: a conventional strategy and one specifically designed to maximize the use of solar energy. The results are compared in terms of electrical self-consumption, CO_2 emission reduction, and

meeting the demand for domestic hot water, highlighting the effectiveness of the optimized control strategy in reducing dependence on the electrical grid.

5. **The choice of appropriate generator systems to enhance the renewable energy share in buildings. A comparison between PV-assisted heat pumps and biomass boilers** [33]: this article compares two options for generation systems to increase the use of renewable energy in buildings: heat pumps assisted by photovoltaic systems and biomass boilers. Through dynamic simulations, the non-renewable primary energy consumption is determined for two buildings located in different climatic contexts. The conditions under which heat pumps assisted by photovoltaics outperform biomass boilers in terms of energy efficiency and environmental impact are highlighted, considering both seasonal efficiency and the actual contribution of self-produced solar energy.

In the ninth chapter, a comprehensive synoptic analysis of the research findings will be presented, highlighting the logical progression and interconnections between the various studies. This chapter will synthesize the results, providing a cohesive narrative that illustrates the overarching themes and insights derived from the integration of heat pumps with renewable energy sources. The analysis will clarify the effectiveness and efficiency of different configurations and control strategies, offering a detailed understanding of their impact on energy sustainability and building performance.

Finally, the tenth chapter will present the conclusions of the thesis. It will summarize the key findings, critically evaluating the methodologies and results. This chapter will also discuss the broader implications of the research, suggesting avenues for future investigations and practical applications.

1.4 References

[1] «European Consilium,» [Online]. Available: https://www.consilium.europa.eu/it/policies/green-deal/.
[2] «IEA50,» [Online]. Available: https://www.iea.org/.
[3] *Renewables Decree 199/2021,* Official Gazette of the Italian Republic, No. 285, November 30, 2021.
[4] Y. H. Kuang and R. Z. Wang, “Performance of a multi-functional direct-expansion solarassisted heat pump system,” Sol. Energy, 2006. https://doi.org/10.1016/j.solener.2005.06.003
[5] Y. W. Li, R. Z. Wang, J. Y. Wu, and Y. X. Xu, “Experimental performance analysis on a direct-expansion solar-assisted heat pump water heater,” Appl. Therm. Eng., 2007. https://doi.org/10.1016/j.applthermaleng.2006.08.007

[6] A. Moreno-Rodríguez, A. González-Gil, M. Izquierdo, and N. Garcia-Hernando, "Theoretical model and experimental validation of a direct-expansion solar assisted heat pump for domestic hot water applications," Energy, 2012. https://doi.org/10.1016/j.energy.2012.07.021

[7] M. Mohanraj, S. Jayaraj, and C. Muraleedharan, "Performance prediction of a direct expansion solar assisted heat pump using artificial neural networks," Appl. Energy, 2009. https://doi.org/10.1016/j.apenergy.2009.01.001

[8] Q. Wang, Y. Q. Liu, G. F. Liang, J. R. Li, S. F. Sun, and G. M. Chen, "Development and experimental validation of a novel indirect-expansion solar-assisted multifunctional heat pump," Energy Build., 2011. https://doi.org/10.1016/j.enbuild.2010.09.013

[9] S. J. Sterling and M. R. Collins, "Feasibility analysis of an indirect heat pump assisted solar domestic hot water system," Appl. Energy, 2012. https://doi.org/10.1016/j.apenergy.2011.05.050

[10] K. Bakirci and B. Yuksel, "Experimental thermal performance of a solar source heat-pump system for residential heating in cold climate region," Appl. Therm. Eng., 2011. https://doi.org/10.1016/j.applthermaleng.2011.01.039

[11] M. Pinamonti, I. Beausoleil-morrison, A. Prada, and P. Baggio, "Water-to-water heat pump integration in a solar seasonal storage system for space heating and domestic hot water production of a single-family house in a cold climate," Sol. Energy, vol. 213, no. August 2020, pp. 300–311, 2021. https://doi.org/10.1016/j.solener.2020.11.052

[12] C. Liang, X. Zhang, X. Li, e X. Zhu, «Study on the performance of a solar assisted air source heat pump system for building heating», Energy & Buildings, vol. 43, n. 9, pagg. 2188–2196, 2011, doi: 10.1016/j.enbuild.2011.04.028.

[13] L. Xu, Y. Zhang, e X. Luo, «Applicability and comparison of solar-air source heat pump systems between cold and warm regions of plateau by transient simulation and experiment», pagg. 1697–1708, 2021.

[14] M. Bakker, H. A. Zondag, M. J. Elswijk, K. J. Strootman, e M. J. M. Jong, «Performance and costs of a roof-sized PV / thermal array combined with a ground coupled heat pump», vol. 78, pagg. 331–339, 2005, doi: 10.1016/j.solener.2004.09.019.

[15] W. W. S. Charters e C. Chaichana, «Solar heat pump systems for domestic hot water», vol. 73, n. 3, pagg. 169–175, 2002.

[16] C. J. Banister e M. R. Collins, «Development and performance of a dual tank solar-assisted heat pump system», Applied Energy, vol. 149, pagg. 125–132, 2015, doi: 10.1016/j.apenergy.2015.03.130.

[17] Miglioli, A.; Aste, N.; Del Pero, C.; Leonforte, F. Photovoltaic-thermal solar-assisted heat pump systems for building applications: Integration and design methods. Energy Built Environ. 2023, 4, 39–56. https://doi.org/10.1016/j.enbenv.2021.07.002.

[18] Ning, Z.; Zhang, X.; Ji, J.; Shi, Y.; Du, F. Research progress of phase change thermal storage technology in air-source heat pump. J. Energy Storage 2023, 64, 107114, https://doi.org/10.1016/j.est.2023.107114.

[19] Long, J.Y.; Zhu, D.S. Numerical and experimental study on heat pump water heater with PCM for thermal storage. Energy Build. 2008, 40, 666–672. https://doi.org/10.1016/j.enbuild.2007.05.001.

[20] Georges, E.; Cornélusse, B.; Ernst, D.; Lemort, V.; Mathieu, S. Residential heat pump as flexible load for direct control service with parametrized duration and

rebound effect. Appl. Energy 2017, 187, 140–153. https://doi.org/10.1016/j.apenergy.2016.11.012.
[21] Kreuder, L.; Spataru, C. Assessing demand response with heat pumps for efficient grid operation in smart grids. Sustain. Cit-ies Soc. 2015, 19, 136–143. https://doi.org/10.1016/j.scs.2015.07.011.
[22] T. Olkowski, S. Lipiński, and A. Olędzka, E3S Web Conf. 19, (2017)
[23] J. A. Lozano Miralles, R. López García, J. M. Palomar Carnicero, and F. J. R. Martínez, Renew. Energy 152, 1439 (2020)
[24] M. J. Stolarski, M. Krzyzaniak, K. Warmiński, and D. Niksa, Energy Convers. Manag. 121, 71 (2016)
[25] A. Saari, T. Kalamees, J. Jokisalo, R. Michelsson, K. Alanne, and J. Kurnitski, Appl. Energy 92, 76 (2012)
[26] B. Hebenstreit, R. Schnetzinger, R. Ohnmacht, E. Höftberger, J. Lundgren, W. Haslinger, and A. Toffolo, Biomass and Bioenergy 71, 12 (2014)
[27] «TRNSYS 18: A Transient System Simulation Program, Solar Energy Laboratory, (2021),» [Online]. Available: http://sel.me.wisc.edu/trnsys.
[28] M. Mgni, F. Ochs, S. De Vries, A. Maccarini e F. Sigg, «Detailed cross comparison of building energy simulation tools results,» *Energy & Buildings,* 2021.
[29] P. Bevilacqua, S. Perrella, D. Cirone, R. Bruno e N. Arcuri, «The role of thermal accumulation in distributed air conditioning plants: energy and environmental analysis»., *International Journal of Architectural Engineering Technology, 2020. https://doi.org/10.15377/2409-9821.2020.07.7*
[30] S. Perrella, R. Bruno, P. Bevilaqua, D. Cirone e N. Arcuri, «Energy Evaluations of a New Plant Configuration for Solar-Assisted Heat Pump in Cold Climate,» *Sustainability,* 2023. https://doi.org/10.3390/su15021663
[31] P. Bevilacqua, S. Perrella, R. Bruno, D. Cirone e D. Kaliakatos, «Optimization of a solar assisted heat pump system to increase thermal,» in *BSA*, Bolzano, 2024.
[32] S. Perrella, F. Bisegna, P. Bevilacqua, D. Cirone e R. Bruno, «Solar-Assisted Heat Pump with Electric and Thermal Storage: The Role of Appropriate Control Strategies for the Exploitation of the Solar Source,» *Buildings,* 2023. https://doi.org/10.3390/buildings14010296
[33] R. Bruno, P. Bevilacqua, S. Perrella, D. Cirone e N. Arcuri, «The choice of appropriate generator systems to enhance the renewable energy share in buildings. A comparison between PV-assisted heat pumps and biomass boilers,» E3S Web of Conferences 312:02014, DOI: 10.1051/e3sconf/202131202014

2 Energy transition: the European and Italian regulatory framework

2.1 Introduction

The European energy transition is a multifaceted process involving a shift towards renewable energy, electrification of end uses, development of carbon capture technologies, and creation of zero-carbon fuels [1].

Despite these promising developments, the transition also poses significant challenges. These include the need to upgrade infrastructure, manage the phase-out of fossil fuels, ensure a just transition for workers and communities, and address the increase in electricity prices. The EU is addressing these challenges through various measures, including the creation of a new 'Social Climate Fund' to support vulnerable households and small businesses, and the 'Just Transition Mechanism' to aid regions heavily dependent on fossil fuels [2].

This chapter delves into the intricate dynamics of this transition, addressing the associated challenges and the strategies employed by the European Union (EU) to overcome them.

2.2 The 2030 Agenda

The 2030 Agenda for Sustainable Development, adopted by the United Nations and supported by the European Union (EU), is a global action plan aimed at ending poverty, protecting the planet, and ensuring prosperity for all by 2030 [3]. This program is structured around 17 Sustainable Development Goals (SDGs) that address a wide range of global challenges, including climate change, economic and social inequalities, environmental degradation, peace, and justice (Figure 2-1).

Figure 2-1- Sustainable Development Goals of the 2030 Agenda

The EU plays a key role in implementing the 2030 Agenda by integrating the SDGs into its internal and external policies, with a particular emphasis on the European Green Deal. This ambitious plan aims to transform Europe into the first climate-neutral continent by 2050 through a series of initiatives promoting environmental, economic, and social sustainability. A crucial aspect of the European Green Deal is energy efficiency, which is considered fundamental for reducing greenhouse gas emissions and limiting global warming.

The United Nations High-Level Political Forum (HLPF) is the main platform for reviewing and verifying the progress of the SDGs. During these meetings, the EU assesses the advancements made and discusses strategies to accelerate the implementation of the SDGs. The 2021 forum, for example, highlighted the importance of using the SDGs as a guide for post-pandemic recovery, promoting a sustainable growth model that addresses the interconnected challenges of the climate, economic, and social crises.

In the context of the COVID-19 pandemic, the EU recognized the need for a global and integrated approach to recovery. The implementation of the SDGs was seen as a compass to guide recovery policies, aiming to build a more resilient and sustainable society. In this framework, energy efficiency plays a crucial role not only in reducing

emissions but also in creating green jobs, stimulating technological innovation, and improving citizens' quality of life.

In summary, the 2030 Agenda and the SDGs provide a clear and ambitious vision for a sustainable future. The EU, through the European Green Deal, is committed to achieving these goals by promoting energy efficiency, transitioning to renewable energy, and fostering a green and inclusive economy. These efforts are essential for addressing global climate and environmental challenges while ensuring sustainable and resilient development for future generations.

2.3 The European Green Deal

The European Green Deal represents one of the European Union's most ambitious initiatives to address contemporary environmental and climate challenges. Presented by the European Commission in December 2019, the Green Deal aims to transform Europe into the first climate-neutral continent by 2050 [4]. This holistic vision not only addresses climate change mitigation but also encompasses sustainable economic growth, social inclusion, and biodiversity protection (Figure 2-2).

Figure 2-2- Graphical schematisation of the objectives of the European green deal

2.3.1 Main Objectives

Climate Neutrality by 2050

The central objective of the European Green Deal is to achieve climate neutrality by 2050. This means that the EU commits to reducing its net greenhouse gas emissions to zero, balancing any residual emissions with carbon absorption activities such as reforestation or carbon capture and storage (CCS) technologies.

55% Emissions Reduction by 2030

The Green Deal includes the intermediate target of reducing greenhouse gas emissions by 55% by 2030 compared to 1990 levels. This milestone is essential to set the EU on the right path towards climate neutrality and requires an acceleration of decarbonization measures across all economic sectors.

2.3.2 Key Sectors and Strategies

Clean and affordable energy

One of the pillars of the Green Deal is the transition to a clean, sustainable, and secure energy system. The main actions include:

- **Increase in renewable energy**: significant increase in the share of energy from renewable sources such as wind, solar, and hydroelectric in the EU's energy mix.
- **Energy efficiency**: improvement of energy efficiency in all sectors, with particular attention to buildings, which are a major source of energy consumption.
- **Energy interconnections**: strengthening of energy infrastructure and interconnections between Member States to ensure a stable and secure supply of renewable energy.

Circular Economy

The Green Deal promotes a circular economy where products and materials are kept in use for as long as possible. Key initiatives include:

- **Eco-Friendly design**: promotion of products designed to last longer, be repairable, reusable, and recyclable.
- **Waste reduction**: introduction of measures to reduce waste production, improve waste management, and increase recycling rates.
- **Sustainable industry**: incentives for adopting more sustainable production processes and efficient use of natural resources.

Sustainable mobility

The transition to sustainable mobility is another core element of the Green Deal. The main strategies include:

- **Electrification of transport**: Promotion of electric vehicles and the installation of large-scale charging infrastructure.
- **Public transport**: improvement of public transport systems and promotion of intermodal transport solutions to reduce dependence on private vehicles.
- **Emission reduction in aviation and maritime sectors**: Introduction of stricter emission standards for the aviation and maritime sectors, encouraging the use of alternative fuels and clean technologies.

Biodiversity and Sustainable Agriculture

Protecting biodiversity and promoting sustainable agricultural practices are essential for ecosystem resilience and food security. The planned actions include:

- **Biodiversity Strategy**: Restoration of degraded ecosystems, protection of natural habitats, and promotion of agricultural biodiversity.
- **Sustainable Agriculture**: Support for farmers to adopt sustainable agricultural practices, such as organic farming and reducing the use of pesticides and chemical fertilizers.
- **Reforestation and Forest Management**: Plans to increase forest cover and improve the sustainable management of existing forests.

Green Finance and Innovation

The Green Deal requires substantial public and private investments to finance the green transition. The main initiatives include:

- **Green investments**: mobilization of funds through financial instruments such as the InvestEU Fund and the Just Transition Mechanism to support sustainability projects.
- **Research and innovation**: Funding of research and innovation programs to develop new green technologies and promote the EU's competitiveness in sustainable technologies.
- **Financial regulation**: Introduction of standards to encourage sustainable investments and incentivize companies to integrate ESG (environmental, social, and governance) criteria into their operations.

The European Green Deal represents a transformative vision for a sustainable and resilient future. Through integrated policies and concrete actions in key sectors, the EU commits to leading the fight against climate change and promoting sustainable economic and social development. The active participation of all actors, from governments to businesses, citizens to international organizations, will be crucial for the success of this ambitious initiative.

2.4 Fit for 55% Package

The "Fit for 55%" package aims to translate the ambitions of the Green Deal into legislative measures. It comprises a series of proposals to renew climate, energy, and transport legislation, to implement new initiatives aligning EU regulations with its climate goals [5]. The package includes:

- A revision of the EU Emissions Trading System (EU ETS), incorporating maritime transport and revising aviation emission rules, along with the establishment of a separate emission trading system for road transport and buildings.
- A revision of the Effort Sharing Regulation, governing member states' reduction targets in sectors not covered by the EU ETS.
- A revision of the LULUCF Regulation, addressing greenhouse gas emissions and removals resulting from land use, land-use change, and forestry.
- An amendment to the regulation setting CO_2 emission standards for cars and vans.
- A revision of the Renewable Energy Directive.
- A revision of the Energy Taxation Directive.
- A revision of the Alternative Fuels Infrastructure Directive.
- The establishment of a Social Climate Fund.
- A revision of the Energy Performance of Buildings Directive.
- Measures to reduce methane emissions in the energy sector.
- A revision of the "energy" package concerning gas.

In light of the commitment to reduce greenhouse gas emissions by at least 55% by 2030, it is evident that the EU must become significantly more energy-efficient. Energy savings play a crucial role, as using less energy has direct positive impacts on the environment. It is the most cost-effective and climate-friendly solution, as lower energy

consumption results in fewer greenhouse gas emissions and more affordable energy prices for citizens.

The legislation will mandate a reduction in energy consumption across the EU, currently averaging 29%. The current targets aim for a 24% reduction in both primary energy consumption—indicating the total energy demand of a country—and final energy consumption—indicating the amount of energy used by end-users. The new targets aim for a 39% reduction in primary energy consumption and a 36% reduction in final energy consumption. Member states will then set their own targets based on national specifics. Additionally, they will need to reduce their final energy consumption by 1.5% per year, almost double the current mandate of 0.8%.

The public sector will be required to contribute to energy efficiency by:

- Reducing its final energy consumption by 1.7% per year, or alternatively by at least 1.9% per year if public transport and armed forces are excluded.
- Renovating 3% of the floor area of public buildings annually to improve energy performance.
- Reviewing public procurement procedures to better integrate efficiency requirements.

Another key focus of the "Fit for 55%" package is combating energy poverty, providing more assistance to low-income consumers to protect them from energy price increases. Funding will come from the Social Climate Fund and revenues from the emission trading systems.

The main sectors affected by the package include buildings, industry, and transport. Further emission reductions are anticipated through the creation of a new emission trading system (ETS) covering all three sectors.

For the buildings sector, new publicly owned buildings must be nearly zero-emission by 2028, and all other new buildings by 2030. Energy Performance Certificates (EPCs) will be mandatory for all new buildings starting in 2030. From that date onwards, solar installations will be required on all new residential buildings, with an earlier deadline for public buildings.

2.5 Energy Efficiency Directive (2018/2002)

The new Energy Efficiency Directive (2018/2002), which amends Directive 2012/27/EU, is a key component of the European Green Deal. The directive aims to

enhance energy efficiency across the European Union (EU) with the goal of achieving a 32.5% improvement by 2030 [6].

The directive stipulates that by 2030, the EU must reduce primary energy consumption to 1,273 Million Tonnes of Oil Equivalent (Mtoe) and final energy consumption to 956 Mtoe, corresponding to a 32.5% improvement in energy efficiency. Member States are required to achieve annual energy savings of at least 0.8% of final energy consumption during the period 2021-2030. This target can be met through policy measures adopted both during the obligation period and in preceding periods, provided that the resulting individual actions are implemented in the new period.

Member States are encouraged to leverage new business models and technologies to promote and facilitate the adoption of energy efficiency measures, including innovative energy services for both large and small customers. It is crucial to raise awareness among EU citizens about the benefits of energy efficiency and to provide them with accurate information on how to achieve it. This includes strengthening consumers' rights to timely and precise information about their energy consumption.

The directive aims to mobilize private financing for energy efficiency measures and renovations by engaging both public and private financial institutions and improving data on the energy and financial performance of investments.

2.6 Energy Efficiency Directive for buildings (2018/844)

The new Energy Efficiency Directive for buildings, adopted by the European Parliament and the Council, aims to support the renovation of the European Union's building stock with the goal of achieving nearly zero-energy buildings by 2050 [7]. This directive updates and complements previous regulations, including Directive 2010/31/EU on the energy performance of buildings and Directive 2012/27/EU on energy efficiency.

Among its key provisions, the directive mandates the adoption of long-term national renovation strategies by Member States to support the transformation of existing buildings into highly energy-efficient and low-carbon buildings. It promotes smart technologies and interconnected buildings, as well as the development of skills in the energy efficiency sector. The directive calls for the implementation of automation and control systems to optimize energy use in buildings, especially non-residential ones, and requires the installation of charging points for electric vehicles in new non-residential buildings and those undergoing major renovations.

The directive is part of the broader European Green Deal, which aims to make Europe the first climate-neutral continent by 2050, promoting decarbonization and improving energy efficiency in the building sector, which represents a significant portion of overall energy consumption and CO_2 emissions in the EU. These measures are designed to reduce energy consumption in buildings, increase the use of renewable energy, and improve air quality, thereby contributing to the European Union's climate and environmental goals.

2.7 Directive on the Promotion of the Use of Energy from Renewable Sources (2018/2001)

The Directive on the Promotion of the Use of Energy from Renewable Sources (Directive (EU) 2018/2001), commonly known as the Renewable Energy Directive (RED II), establishes a comprehensive framework to facilitate the transition to renewable energy within the European Union (EU). The directive sets ambitious targets to increase the share of energy from renewable sources in the EU's total energy consumption to at least 32% by 2030 [8].

Member States are required to contribute to the collective target by setting their own national renewable energy targets, which are reviewed periodically to ensure alignment with the overall EU objective. The directive promotes the integration of renewable energy across various sectors, including electricity, heating and cooling, and transport, with specific measures designed to support the uptake of renewable energy in these sectors.

To attract investments, Member States are encouraged to implement support schemes for renewable energy projects, ensuring stability and predictability. These schemes can include feed-in tariffs, premiums, and auction systems. Additionally, the directive aims to streamline and simplify administrative procedures for renewable energy installations, reducing barriers to deployment and accelerating project development timelines.

A system for guarantees of origin is established to ensure transparency and traceability of renewable energy sources, allowing consumers to verify the origin of their energy. The directive also includes sustainability criteria for biofuels, bioliquids, and biomass, ensuring that their production and use contribute to greenhouse gas emission reductions and do not cause adverse environmental or social impacts.

2.8 Italian Regulatory Context

Italy has implemented various regulations to meet the objectives of the European Green Deal and the "Fit for 55" package. Here are some of the key Italian regulations), with detailed information for each decree, law, or plan:

Decree Law 34/2020 [9]

This decree includes the "Superbonus 110%," a measure that incentivizes energy efficiency improvements in residential buildings through tax deductions. These deductions cover interventions such as thermal insulation, installation of photovoltaic systems, and replacement of winter heating systems. The Superbonus aims to significantly reduce energy consumption and carbon emissions, promoting sustainable building practices.

Legislative Decree 73/2020 [10]

This decree, effective from June 19, 2020, implements the EU Directive 2018/2002 on energy efficiency, modifying the previous 2012 directive. It introduces energy-saving obligations for public and private buildings and establishes measures to improve energy efficiency in the industrial and transport sectors. The decree emphasizes the need for energy audits, mandatory energy management systems, and incentives for adopting energy-efficient technologies.

Law 120/2020 [11]

Enacted on September 11, 2020, this law converts Decree Law 76/2020 into legislation, introducing amendments to the Public Procurement Code to facilitate the implementation of green projects and renewable energy infrastructure. It simplifies the administrative procedures for obtaining permits and approvals for energy efficiency projects and renewable energy installations, aiming to accelerate the green transition.

Decree Law 77/2021 [12]

This decree, effective from May 31, 2021, introduces procedural simplifications to accelerate the ecological and digital transition, with a particular focus on promoting renewable energy and energy efficiency. It includes measures to streamline the approval process for sustainable mobility infrastructure and encourages the adoption of innovative technologies in the energy sector.

National Recovery and Resilience Plan (PNRR) [13]

Adopted on October 13, 2021, the PNRR allocates significant investments towards the ecological transition, with a particular emphasis on sustainable mobility, building energy efficiency, and industrial decarbonization. It also includes measures to promote the circular economy and reduce CO_2 emissions. The plan aims to stimulate economic growth while addressing environmental challenges.

Renewables Decree 199/2021 [14]

This decree, effective from November 8, 2021, implements Directive (EU) 2018/2001 on the promotion of the use of energy from renewable sources. It sets binding targets for renewable energy adoption by 2030, encouraging the development of renewable energy projects and supporting the integration of renewable energy into the national energy system. The decree also includes provisions for simplifying the authorization process for renewable energy installations and promoting innovative renewable energy technologies.

National Integrated Energy and Climate Plan (PNIEC) [15]

The PNIEC, published on July 30, 2024, outlines Italy's strategy to achieve the targets set by the European Union for 2030. It focuses on increasing the share of renewable energy, improving energy efficiency, and reducing greenhouse gas emissions. The plan includes specific measures for the energy sector, transportation, and buildings, aiming to create a more sustainable and resilient energy system.

Considering that the central theme of this thesis focuses on the integration of renewable energy sources with heat pumps, the following section will provide a detailed examination of the decree related to renewable energy.

2.8.1 Renewables Decree 199/2021

This decree aims to accelerate the country's sustainable growth trajectory by establishing provisions for energy from renewable sources, in line with European decarbonization objectives for 2030 and complete decarbonization by 2050. The utilization of renewable energy sources remains central to achieving the goals of improving building energy performance and reducing harmful atmospheric emissions.

In new buildings and buildings undergoing significant first-level renovations, the designer must certify compliance with the renewable energy integration requirements as specified in Legislative Decree No. 199 of 8/11/2021, Annex III. According to this decree, for new buildings or buildings undergoing substantial renovations—defined as existing

buildings with a useful surface area greater than 1,000 m² and renovations involving the entire building envelope—thermal energy production systems must be designed and implemented to ensure the simultaneous coverage of energy needs through renewable energy sources, as follows:

- 60% of the anticipated consumption for domestic hot water (65% for public buildings);
- 60% of the combined anticipated consumption for domestic hot water, winter heating, and summer cooling (65% for public buildings).

There are no less stringent requirements for historic centres. These obligations cannot be fulfilled using renewable energy systems that exclusively produce electricity (e.g., photovoltaic systems) to power devices or systems for producing domestic hot water, heating, and cooling.

For new buildings or buildings undergoing significant renovations, the electrical power of renewable energy systems, which must be installed on or within the building or its relevant areas, is calculated using the following formula:

$$P_{PV} = S_{gross}\ K\ [kW]$$

where *K* is a multiplication coefficient with the following values:

- K = 0,025 *for existing buildings*
- K = 0,05 f*or new buildings*

For public buildings, the required electrical power of the systems to be installed is increased by 10%. There are no exceptions for historic centres, a provision that differs from the previous regulation.

When using solar thermal or photovoltaic panels installed on building roofs, these components must be adherent to or integrated into the roofs with the same inclination and orientation as the roof slope. Non-compliance with the described obligations regarding the integration of renewable energy sources will result in the denial of the building permit, as stipulated in paragraph 4, article 26 of Legislative Decree 199/2021.

2.9 References

[1] "European Council," Council of the European Union, 05 06 2024. [Online]. Available: https://www.consilium.europa.eu/it/policies/how-the-eu-is-greening-energy/.

[2] "European Commission," [Online]. Available: https://climate.ec.europa.eu/eu-action/eu-emissions-trading-system-eu-ets/social-climate-fund_en.

[3] "Parlamento Italiano-Camera dei deputati," [Online]. Available: https://temi.camera.it/leg19DIL/area/19_1_38/agenda-2030.html.

[4] "European Consilium," [Online]. Available: https://www.consilium.europa.eu/it/policies/green-deal/.

[5] "European Council," [Online]. Available: https://www.consilium.europa.eu/it/policies/green-deal/fit-for-55/.

[6] *Directive (EU) 2018/2002 of the European Parliament and of the council of 11 December 2018,* 2018.

[7] *Directive (EU) 2018/844 of the European Parliament and of the Council of 30 May 2018.*

[8] *Directive (EU) 2018/2001 of the European Parliament and of the Council of 11 December 2018 on the promotion of the use of energy from renewable sources (recast),* 2018.

[9] *Decreto Legge 34/2020,* Official Gazette of the Italian Republic, No. 180, July 18, 2020, 2020.

[10] *Legistlative Decree 73/2020,* Official Gazette of the Italian Republic, No. 175, July 07, 2020.

[11] *Law 120/2020,* Official Gazette of the Italian Republic, No. 228, September 14, 2020, 2020.

[12] *Decree Law 77/2021,* Official Gazette of the Italian Republic, No. 129, May 31, 2021.

[13] "Ministry of economy and finance," [Online]. Available: https://www.mef.gov.it/en/focus/The-National-Recovery-and-Resilience-Plan-NRRP/.

[14] *Renewables Decree 199/2021,* Official Gazette of the Italian Republic, No. 285, November 30, 2021.

[15] *National Integrated Energy and Climate Plan,* Ministry of Environment and Energy Security.

3 Heat pumps

Heat pumps are increasingly recognized as a crucial technology for reducing carbon emissions across various applications, including heating and cooling. Recently, they have gained targeted political support in several countries [1]. In 2022, there was a record increase in heat pump sales in both Europe and the United States, and early signs in 2023 suggest this growth is continuing. For instance, Germany and Sweden have reported growth rates of 100% and 20%, respectively. However, heat pumps currently fulfill only about 10% of the global heating and cooling demand for buildings. To achieve the "Net Zero Emissions by 2050" (NZE) scenario, the global stock of heat pumps must nearly triple by 2030, covering at least 20% of the global heating and cooling demand. Furthermore, additional political support and technological advancements are required, particularly to reduce initial costs, eliminate market barriers to renovations, enhance energy efficiency and durability, leverage flexibility potential, and further develop products and systems using refrigerants with lower climate and environmental impacts [2].

This chapter examines the operating principles of heat pumps, their classification, and their integration into advanced air conditioning systems.

3.1 Principle of operation

Heat pump technology has been known and utilized since the 1970s, during the first oil crises, and today it is available on the market with various system solutions that make it suitable and easy to apply for all needs. The heat pump derives its name from its ability to transfer heat from a low-temperature source to a higher-temperature sink. This process is the reverse of what occurs naturally and is only possible by supplying energy to the machine.

The thermodynamics of the ideal vapor compression cycle are summarized in Figure 3-1 which represents the variation in temperature and entropy that occurs during

the cycle. Observing the bell-shaped graph, the area to the left of the bell identifies the liquid region. Entering the bell, there is a two-phase mixture of liquid and vapor until the right curve of the bell is reached, where complete vaporization of the fluid occurs [3].

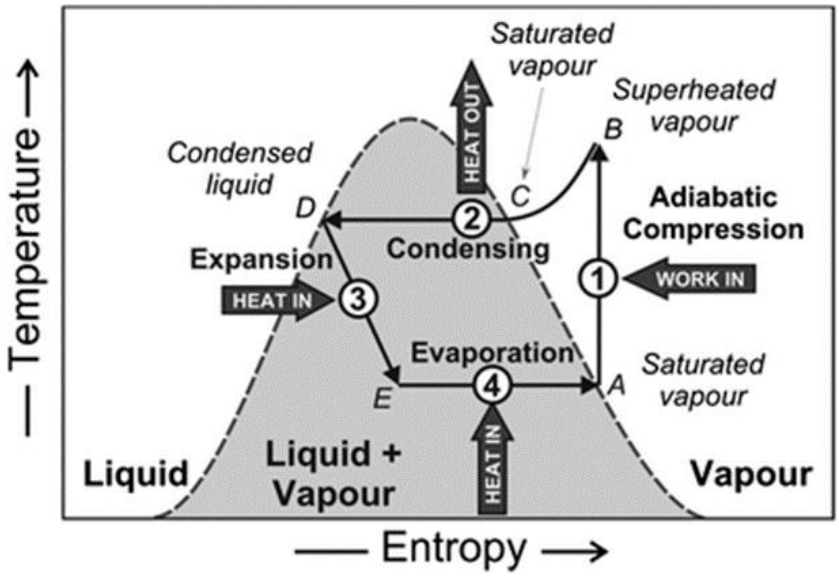

Figure 3-1- Thermodynamic phases of the ideal cycle

The transformations that the cycle undergoes are:

1) **Compression:** The working fluid in the dry vapor phase (A) undergoes an isentropic compression, heating the gas to a superheated state (B). This is due to the introduction of work into the system in the form of electrical energy via the compressor.
2) **Condensation**: The second process involves first removing the superheat (B–C) and then the heat of condensation (C–D). This occurs at constant pressure, and it is here that heat is absorbed and transferred to the hotter location.
3) **Expansion:** The now-liquid working fluid then passes through an expansion valve (3), where its pressure drops sharply, causing evaporation and the corresponding absorption of heat from the low-temperature reservoir.
4) **Evaporation**: The liquid-vapor mixture is then fully vaporized by absorbing heat from the cooler environment (4), returning the working fluid to a dry vapor state.

The set of these transformations constitutes the ideal cycle; in reality, pressure drops due to friction, thermodynamic irreversibility during compression, non-ideal gas behaviour, and the finite temperature difference between heat exchangers cause the cycle to deviate from this ideal and reduce the ratio of output heat to input heat and work.

The main advantage of the heat pump lies in its ability to deliver more energy than it requires for its operation. The efficiency of a heat pump in heating mode is measured by the Coefficient of Performance (COP), which is the ratio of the energy delivered (i.e., heat transferred to the medium to be heated) to the energy consumed. In cooling mode, the efficiency is measured by the Energy Efficiency Ratio (EER). The COP of a heat pump depends on the model, climatic conditions, and is higher when the temperature difference between the cold and hot sources is smaller.

With reference to the winter scenario, the COP decreases as the temperature to which the hot fluid must be heated increases, which in turn must supply the delivery terminals. Excellent performance is achieved when using radiant systems that require moderate temperatures (30-35°C), but they also pair well with fan convectors (T=45-50°C). Performance decreases when the fluid must be heated to high temperatures (65-70°C) to supply radiators.

The cold source also significantly influences the COP. An air-to-water heat pump, generally used for heating buildings, performs well in moderate climates but is less efficient in cold climates. In such cases, external air is often not used as a thermal source; instead, groundwater (typically at around 12°C) or the ground itself (geothermal heat pumps) is used, where heat is extracted from the soil and transferred to the thermal fluid [4] .

3.2 Heat Pump Components

The heat pump itself consists of a compressor, which moves a refrigerant through a refrigeration cycle, and a heat exchanger, which extracts heat from the source. The heat is then passed on to a heat sink through another heat exchanger.

The compressor serves as the central component of a heat pump. Its function involves drawing in low-pressure refrigerant vapor and compressing it to a higher pressure necessary for condensation at elevated temperatures. There are two main types of compressors:

- Volumetric compressors
- Centrifugal compressors

In volumetric compressors, which are the most commonly used, compression is achieved by trapping a volume of gas at suction pressure, progressively reducing the available space and thereby increasing the pressure. In centrifugal compressors, on the

other hand, compression is obtained through the centrifugal force exerted on the gas by a high-speed rotating element. These are primarily employed in high-capacity machinery.

The compressor also plays a crucial role in power modulation. The simplest method to adapt the machine's power to the required load is the on-off control. In this mode, the compressor operates at nominal power until a signal, such as a thermostat detecting a certain ambient temperature, stops it for a predetermined time interval, then restarts it when the temperature falls below another set point value. However, this technology has several drawbacks: on-off operation reduces the coefficient of performance (COP) due to losses during transient start-stop phases. Additionally, the two temperature set points must be sufficiently spaced to avoid excessive start-stop cycles, especially under low-load conditions. The greater the distance between the start and stop set points, the greater the temperature oscillation in the environment, potentially causing discomfort for the occupants. To address these issues and ensure proper modulation, inverter motors are utilized. These electronic devices can vary the frequency of the alternating electric current, allowing for variable compressor speed. This technology offers several advantages: increased occupant comfort, as the system precisely provides the required load at any given moment, and higher system efficiency with COP values at partial loads often surpassing those at nominal load. At partial load, the refrigerant flow rates necessary to transfer heat from the evaporator to the compressor are lower, reducing temperature differences and making the thermodynamic cycle more efficient. Furthermore, the machine startup is smoother, with no voltage surges, as it begins at the minimum rotational speed, and the compressor is then accelerated by the inverter to the required operating speed [4].

Condensers and evaporators are components responsible for facilitating heat exchange with the internal environment or with the heat source or sink. In reversible cycle machines, their roles are exchanged between summer and winter operation. The refrigerant fluid changes state within the two exchangers: it transitions from liquid to gaseous in the evaporator, and from gaseous to liquid in the condenser.

The expansion valve connects the condenser (at higher pressure) to the evaporator (at lower pressure). It acts as a "throttling" point, allowing the passage of the amount of refrigerant that the compressor processes, accommodating the pressure drop between the high and low sides of the cycle.

The cycle of a heat pump is schematically illustrated in the Figure 3-2.

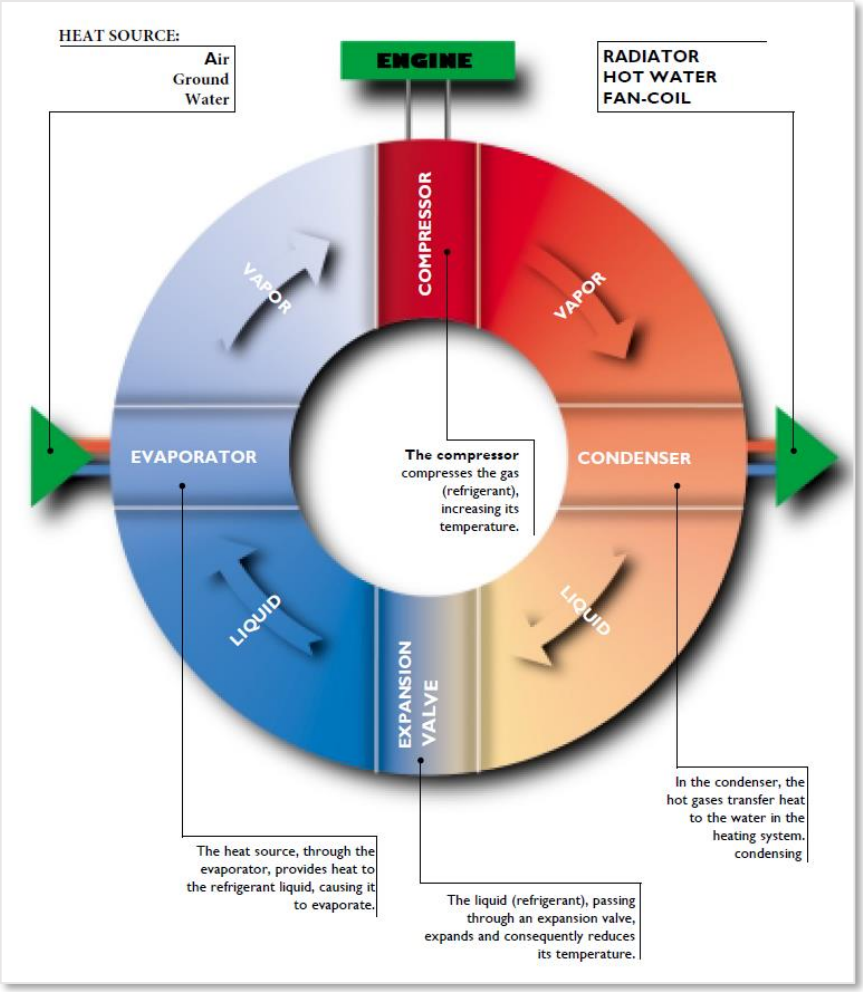

Figure 3-2 Schematic representation of a heat pump cycle [5]

3.3 Refrigerant Fluids

Refrigerants are substances used in air conditioning cycles and in water heating and refrigeration systems for environmental climate control. Additionally, they are applied in refrigeration machines due to their unique physical properties. Any substance that can transition from liquid to vapor and vice versa can be used as a refrigerant; however, the application scope of a substance varies depending on the pressure and temperature range within which the transformation occurs. Over time, it has been discovered that these synthetic fluids have a negative impact on the environment: chlorine-containing compounds damage the ozone layer, while fluorine-containing ones contribute to global warming [6].

In the early years of this century, the environmental emergency due to global warming necessitated legislative measures at the global (Kigali Amendment), European

(EU Regulation 517/2014), and national levels to reduce the use of products that cause the greenhouse effect when released into the atmosphere. Both mentioned regulations aim to progressively reduce the amount of F-gas available on the market, expressed in terms of CO_2 equivalent: the EU F-gas Regulation does not ban the use of HFC compounds but progressively limits their availability.

The most commonly used parameter to assess the climate impact of each compound is the GWP (Global Warming Potential). This parameter measures how much a molecule of a given greenhouse gas contributes to the greenhouse effect. The index is based on a relative scale that compares each gas with carbon dioxide, which has a GWP of 1 by definition. The GWP value is valid within a certain time interval and can thus vary in the medium term; indeed, the GWP of a molecule depends on the time interval over which it was calculated. For example, methane has a GWP of 25 over a hundred-year period but 72 over a twenty-year period.

Next-generation refrigerants, HFOs, have a low GWP due to their short atmospheric lifecycle and low radiative efficiency.

HFCs are typically used in heat pumps and include: R-410A, R-407C, and R-134A. The market penetration percentages of these refrigerants are illustrated in Figure 3-3 [7].

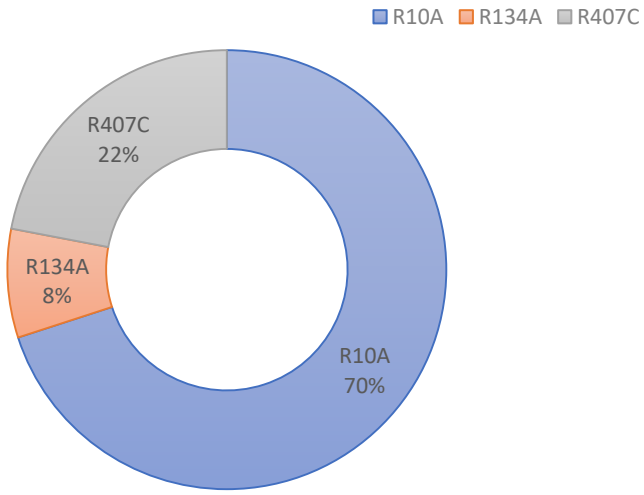

Figure 3-3-Market penetration percentages of refrigerant fluids

New generation refrigerants have been proposed as replacements for the fluids currently used in heat pumps, considering the possibility of a drop-in replacement for machines currently on the market. It would also be possible to use natural refrigerants

such as ammonia and CO_2, but these would require significant redesigns of the machines. The selected fluids that allow for a drop-in replacement without excessive costs and substantial modifications to the heat pump are: R-32, R-1234yf, R-1234ze, R-454B, and R-452B. Below is a brief description of these fluids, with reference to the most widely used refrigerant for heat pump applications, R-410A (Figure 3-3.):

R-32: This is a pure refrigerant suitable for heat pump applications. It has no impact on the ozone layer and has a significantly lower GWP compared to R-410A. It is classified as slightly flammable. R-32 has a high volumetric capacity compared to R-410A, allowing for a reduction in refrigerant charge while maintaining very similar system performance.

R-1234yf: This refrigerant has no impact on the ozone layer and a very low GWP. However, it is highly flammable, posing high risks and significant limitations in applicability. Despite this, it has been frequently used as a replacement for R-134A.

R-1234ze: Due to its low vapor pressure and low latent heat, it requires a larger unit to achieve performance similar to R-410A. R-1234ze has a GWP of 1 and an atmospheric lifetime of about 18 days. It requires some modifications, though not significant, to the machine for use. In the safety data sheet, it is classified as non-flammable, although this classification is valid only for transport and storage.

R-454B: This moderately flammable fluid has a low GWP (78% lower than R-410A) and ensures better performance. It has properties similar to R-410A, making replacement easy and convenient without requiring significant modifications.

R-452B: This is a non-azeotropic mixture, composed of the same substances as R-410A, with a higher percentage of R-1234yf at 26%, while the percentages of R-32 and R-125 are 67% and 7%, respectively. Its GWP is 67% lower than that of R-410A.

Among the selected fluids, the most energy-efficient refrigerant is R-1234ze [6].

3.4 Classification of Heat Pumps

Heat pumps can be classified based on various criteria. The primary classifications include:

Based on the energy used [8]

- *Electric-powered heat pumps*, currently the most widely used type.

- *Gas-powered heat pumps*, these systems use mechanical energy produced by an internal combustion engine to power the compressor.

- *Absorption heat pumps*, these heat pumps utilize a heat source (such as natural gas, solar-heated water, or geothermal-heated water) to drive the refrigeration cycle. They are less common but are used in specific applications where waste heat is available or where electric power is expensive or scarce. These heat pumps utilize a heat source (such as natural gas, solar-heated water, or geothermal-heated water) to drive the refrigeration cycle. They are less common but are used in specific applications where waste heat is available or where electric power is expensive or scarce.

Based on the source used [8]

- Aerothermal Heat Pumps: These utilize external air. This source is always available, but the output power decreases as the temperature drops, and a defrosting system is necessary.
- Hydrothermal Heat Pumps: These utilize water as a source. This type has better performance and is independent of the climate, but it is costlier.
- Geothermal Heat Pumps: These utilize the ground as a source.

The performance of a heat pump is highly influenced by the type of heat source it uses. During the winter season, the ground and water sources outside typically retain more warmth compared to the surrounding air. As a result, heat pumps that draw from the ground or water generally use less electricity than those that draw from the air, resulting in a higher efficiency (COP). This is particularly true in colder regions, where air-source heat pumps need additional energy for defrosting their external components. However, setting up ground-source heat pumps is more expensive because they require an underground heat exchanger, which involves either deep vertical boreholes or an extensive network of pipes buried at least a meter underground. Likewise, connecting a water-source heat pump to nearby rivers, groundwater, or wastewater systems can also be costly. For these reasons, heat pumps using ground or water sources are generally less widespread than those using air. Globally, nearly 85% of all heat pumps sold for building applications are air-source because they are easier to install. Many of these are air-to-air units, but in regions with higher heating demands, air-to-water (hydronic) systems are becoming more common. In Europe, hydronic air-source systems are more prevalent than

in other areas, accounting for almost half of all units sold. Ground-source heat pumps and hybrid systems, which combine a heat pump with another heating source like a gas boiler, currently make up a small portion of global sales but represent a significant market share in some countries. In Sweden, which leads the market for ground-source heat pumps, one in four homes is equipped with such a system. The market for these pumps is also steadily growing in China, where they often replace coal-based heating systems, thereby reducing CO_2 emissions and improving air quality [9].

Single-family homes and apartments can utilize one or multiple small units, or in multifamily and commercial buildings, a centralized unit can provide heating and cooling to several units. In Asia, individual air-to-air units are common in multifamily housing, but in Europe, regulatory restrictions in multifamily housing make heat pumps less common outside single-family homes. Centralized heat pumps can heat entire multifamily and commercial buildings but currently constitute a small fraction of the total installed heat pump capacity. For instance, in Europe, only 10% of units sold in 2021 were large, centralized systems for multifamily housing [10]. Commercial buildings are particularly suitable for centralized heat pumps due to their substantial year-round cooling needs, such as for hospitals, supermarkets, or large server rooms in offices, in addition to space heating requirements. Commercial systems can achieve high efficiency and reduce electricity consumption by using waste heat from cooling to meet heating needs.

Heat pump technology is advanced, and their production and installation can theoretically be scaled up rapidly. Nonetheless, there are significant barriers to increasing their deployment, including the high initial installation costs and various supply chain issues, such as a shortage of skilled workers. Comprehensive efforts are needed to reduce market and regulatory obstacles and to strengthen supply chains, as seen in the recent wave of new government policies and roadmaps encouraging the adoption of heat pumps, such as the European Union's Repower EU Plan and the United States' Inflation Reduction Act, both introduced in 2022.

3.4.1 Aerothermal Heat Pumps

3.4.1.1 Air-to-Air Heat Pumps

The operational mechanism of Air Source Heat Pumps (ASHPs) is depicted in Figure 3-4. A fan draws in ambient outside air, directing it over a series of pipes. Inside the evaporator, a refrigerant with a very low boiling point absorbs heat from the air and vaporizes. This vaporized refrigerant is then compressed, which increases its pressure and temperature. The heated refrigerant then flows through the condenser, transferring its heat to the building's heating system. Finally, the refrigerant returns to the evaporator via the expansion valve. This cycle of evaporation and condensation continuously transfers heat from the outside air to the heating system [11].

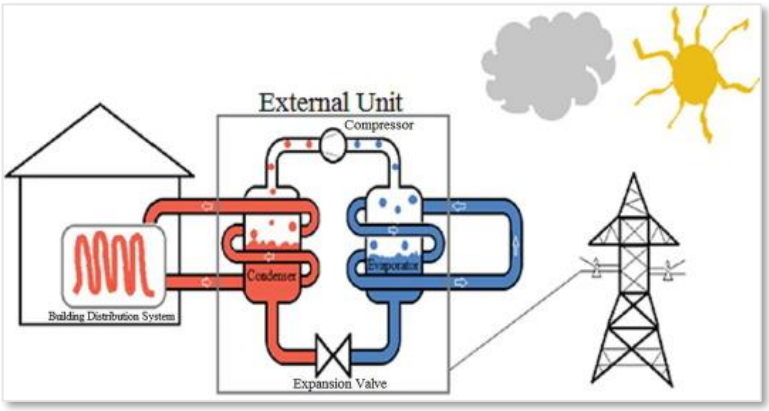

Figure 3-4- Heat pump system schematic diagram

An Air Source Heat Pump (ASHP) transfers heat between the external air and the interior of a building, functioning in both directions depending on the season. ASHPs can be either monobloc units, which house both components in a single box, or split systems. Monobloc ASHPs are typically installed on rooftops with ductwork extending through a wall, primarily used in large-scale applications for commercial buildings.

On the other hand, split systems comprise two separate units: an outdoor unit and an indoor unit (Figure 3-5). These systems are often smaller and are referred to as mini-split heat pumps (MSHPs). MSHPs are widely used in various regions of Europe and Asia due to their cost-effective cooling and heating capabilities. The ductless design of MSHPs simplifies installation for both residential and commercial purposes and eliminates energy losses associated with ductwork, which can account for up to 30% of energy consumption in space heating, especially when ducts are located in unconditioned spaces.

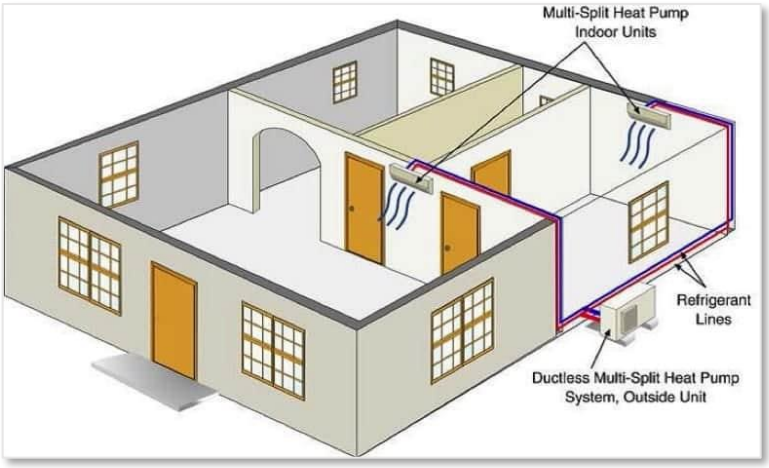

Figure 3-5-Multi-split system

MSHPs also offer flexible design options: the compact outdoor unit and indoor air handling unit can be positioned in multiple ways to optimize performance. The indoor unit can be wall-mounted, ceiling-hung, or floor-mounted, with some models providing floor-standing options. Furthermore, multiple indoor units can be connected to a single outdoor unit, known as a multi-split heat pump, enabling multi-zone conditioning within a building. Typically, the only connections between the outdoor and indoor units are refrigerant lines, requiring a small wall opening of approximately 5-6 centimetres for insulated conduits to pass through, preventing heat loss.

Among residential heat pumps, air-source systems are the most commonly used. Their advantages include rapid temperature regulation within a room, unlimited availability of air, and low installation costs. However, they also have several drawbacks: air-source heat pumps are often noisy, particularly those installed externally, and can be less effective in extremely cold winter conditions. When temperatures drop significantly below freezing, they may not provide sufficient space heating as standalone devices [12].

3.4.1.2 Air-to-Water Heat Pumps

The operation of an air-to-water heat pump system involves drawing in outside air with an electrically powered fan. This air heats a coil containing liquid refrigerant, converting it into a gas. The gas is then pressurized by a compressor, which is the primary electricity consumer of the heat pump, to increase its temperature. This high-temperature refrigerant gas travels to a second heat exchanger, the condenser, where the heat is transferred from the refrigerant to a separate closed water circuit. This heated water is

then used for space heating and/or domestic hot water production. The now-cooled refrigerant passes through an expansion valve and returns to the evaporator [13]. This cycle repeats continuously, as illustrated in Figure 3-6.

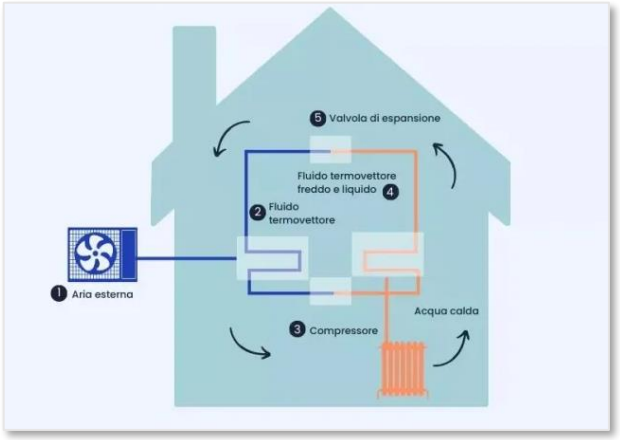

Figure 3-6- Operation of the air-to-water heat pump

Air-to-water heat pumps operate similarly to earlier technologies, but the heat extracted from the outside air is used to warm water, which then circulates through the internal distribution system. Currently, in European countries such as Spain, France, and Italy, air-to-water heat pumps (AWHPs) are widely adopted as the primary solution for domestic hot water (DHW), heating, and cooling needs, replacing traditional direct expansion HVAC systems. The primary reasons for this shift are the high thermal performance of AWHPs and their ability to meet the minimum renewable energy contribution mandated by Directive 2009/28/EC of the European Parliament and Council.

AWHPs can be paired with various terminal units, including fan coils, radiant floor heating, or radiators. In fact, the traditional trend of using a ducted direct expansion inverter system with on/off control for a single zone in residential sectors has been replaced by air-to-water heat pumps, which can support multiple terminal units like fan coils [14]. While pairing AWHPs with traditional radiators is possible, it is not the most efficient choice, as it requires heating water to high temperatures, often above 70°C. Conversely, pairing a heat pump with a radiant system, where water circulates at 25-30°C, significantly increases system efficiency. This solution is perhaps the most prevalent in the construction of new buildings.

3.4.2 Hydrothermal Heat Pumps

Water source heat pumps (WSHPs) extract heat from water sources such as groundwater or underground wells. Compared to air-source heat pumps, WSHPs take advantage of water's more stable temperatures, leading to superior performance. The heat can be transferred inside the building through either air or water, depending on the distribution system installed. Water sources offer more favourable temperature conditions than air, resulting in higher energy efficiency and reduced particulate emissions due to the system's high efficiency. Interest in water-based heating and cooling systems has significantly increased due to these benefits. Various water sources such as rivers, raw water, seawater, lakes, and groundwater are used. WSHP systems are designed to utilize these resources in different configurations, including closed-loop and open-loop systems. Closed-loop systems, which do not exchange directly with the external environment, prevent contamination issues and exhibit less variation with external conditions [8].

3.4.3 Geothermal heat pumps [8]

The term "geothermal heat pump" refers to all types of systems that use groundwater, soil, and surface water as heat sources. The American Society of Heating, Refrigerating and Air-Conditioning Engineers (ASHRAE) has classified geothermal heat pump systems into:

- Groundwater Heat Pumps (GWHP)that use groundwater as a heat source.
- Surface Water Heat Pumps (SWHP) that use surface water as a heat source.
- Ground-Coupled Heat Pumps (GCHP) that systems use the ground as a heat source.

In the Figure 3-7 the diagrams for the various systems are illustrated.

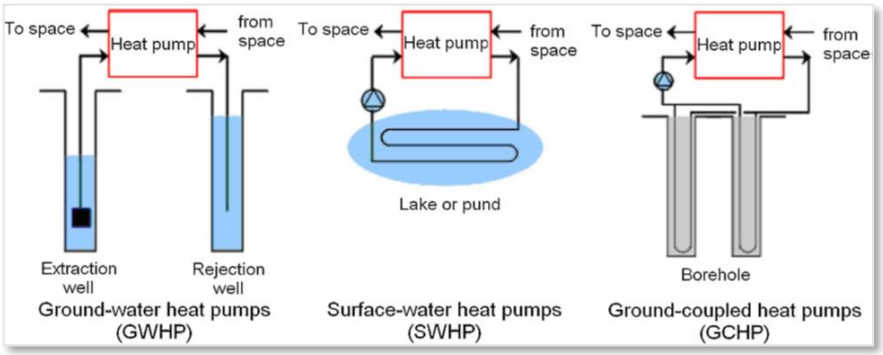

Figure 3-7- Generic Diagram of GSHP Systems

3.4.3.1 Ground Water Heat Pumps (GWHP)

The GWHP system is an open-loop heating/cooling system that uses groundwater as a heat source and/or sink. The advantage of this system lies in the fact that the temperature of groundwater remains almost constant throughout the year, provided the groundwater is deep enough. Therefore, a sufficiently deep well must be drilled to extract this water. This results in a higher initial investment cost compared to using surface water. However, this can be partially offset by the simplicity of construction, the reduced land area required compared to other types of systems, and especially the improvement in operational performance due to the fact that the extracted water does not experience thermal exchange, a factor that affects surface waters.

There are two different types of systems:

- Direct use system.
- Indirect use system.

In direct use systems, the groundwater is pumped directly into the heat pump's exchanger, while in indirect use systems, there is an intermediate exchanger that allows the groundwater to pass to the heat pump. In any case, great care must be taken with potential corrosion problems, since groundwater quality is poor; it may be contaminated or full of impurities. Therefore, filtration processes and water treatments are necessary to eliminate any contaminants. These impurities impact direct use systems more, so these systems are only used for smaller installations and moderate depths because otherwise, energy consumption increases and overall efficiency decreases. For these reasons, indirect use systems are used in most installations.

There is a further classification of GWHP systems based on the type and number of wells constructed. It is possible to have separate wells for extraction and reinjection, as shown in Figure 3-8 (a). Having only two wells is certainly economical; however, this configuration can lead to regulatory issues related to the reinjection of water into the subsoil at a higher temperature or the significant extraction of groundwater, which can alter the equilibrium of the aquifer. There are also systems that feature a single well, known as a standing column well, which serves both the extraction and injection of groundwater. As shown in Figure 3-8 (c), it consists of a submersible pump located at least 100 meters deep, to take advantage of water stratification. The well extracts

groundwater at a certain depth and partially or entirely returns it at a different depth after the thermal exchange.

Finally, there is a third configuration, less commonly used than the others, which involves extracting groundwater through a well and then discharging it into a surface water body, as shown in Figure 3-8(b). However, this changes the surrounding environmental conditions and severely affects the ecosystem, as the decrease in groundwater can cause the death of downstream life forms.

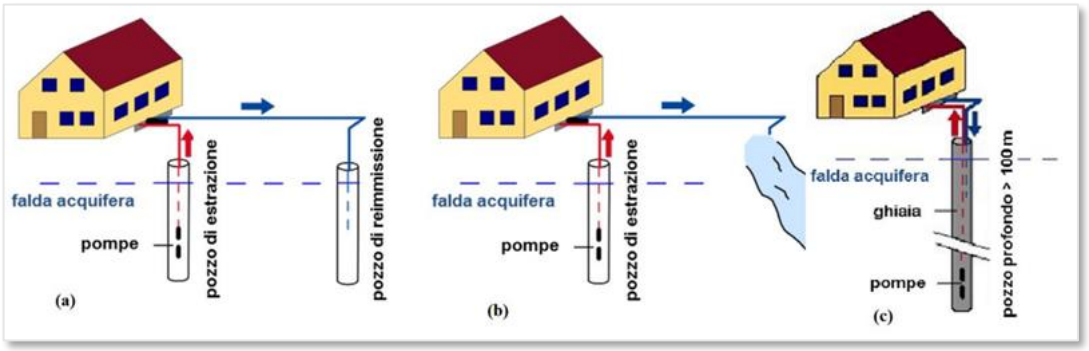

Figure 3-8 Open loop system configurations

3.4.3.2 Surface Water Heat Pumps (SWHP)

These systems use surface water from a lake, pond, or stream as a heat source or sink. The temperature of surface waters is influenced by climatic conditions, especially in winter; this can degrade the system's performance and therefore the COP value.

There are several configurations of surface water heat pumps (SWHP), with the main types being:

- Closed-loop system.
- Open loop system.

Closed-loop systems feature a water-to-air or water-to-water heat pump, which acts as a heat exchanger, connected to a coil placed at an adequate depth within the lake, pond, or water reservoir. Heat exchange occurs through the working fluid circulating within the coil. The operation of closed-loop SWHP systems is well represented in the diagram in Figure 3-9. The heat exchange surfaces consist of a series of pipes laid out or coiled. This construction presents challenges, both in terms of damage—requiring more robust solutions—and particularly in terms of corrosion. Since these pipes are submerged

in water, they are prone, especially the coiled ones, to accumulate underwater debris and sediments, causing wear.

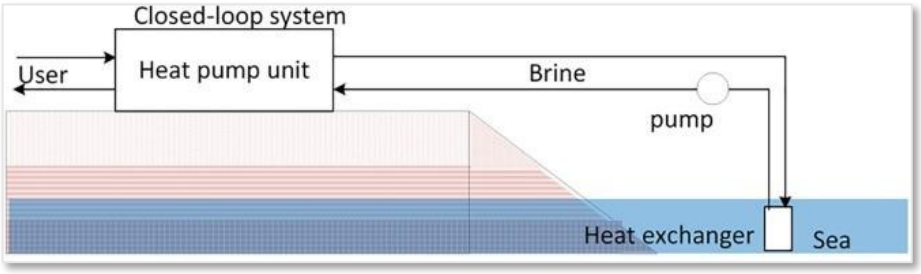

Figure 3-9 Closed-loop system

Regarding open-loop systems, as depicted in Figure 3-10, these systems draw water from the source (lake, reservoir, pond) through a heat exchanger located outside the water and return it at a certain distance from the point of extraction. This heat exchanger is not the same as the evaporator but serves as an intermediate exchanger, which is beneficial because the directly extracted water from the source would otherwise contaminate the circuit. Additionally, the presence of this exchanger allows for the variation of fluid flow rates, thereby improving thermal exchange.

However, before the water is sent to the heat exchanger, it passes through a filtration section, which has the disadvantage of causing pressure losses, thus increasing the energy consumption of the pumps and sometimes leading to cavitation as it lowers the pressure in the pumps.

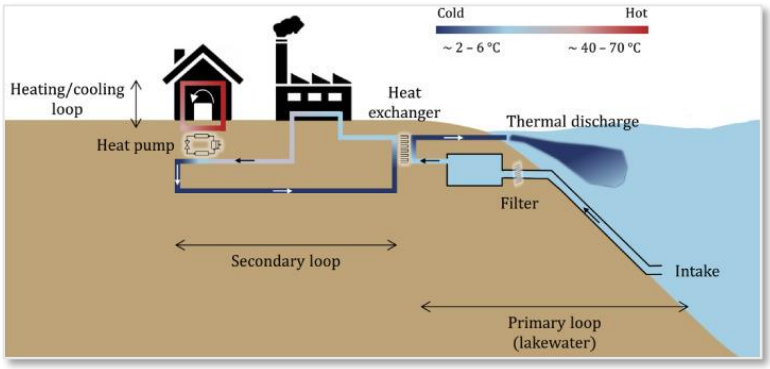

Figure 3-10 Open loop system

3.4.3.3 Ground Coupled Heat Pumps (GCHP)

Ground-Coupled Heat Pumps (GCHP) refer to closed-loop heat pumps where heat is extracted from the ground via a Ground Heat Exchanger (GHE) almost entirely buried

underground. Within the exchanger, a refrigerant, which can be either pure water or an antifreeze solution, circulates through typically high-density polyethylene (HDPE) pipes, facilitating thermal exchange between the fluid and the ground. Depending on the pipe layout, ground-coupled heat pumps can be categorized into two types:

- vertical loop system
- horizontal loop system

Additionally, there is another configuration known as direct expansion, which consists of copper pipes buried in the ground through which the refrigerant of the heat pump circulates directly. These pipes effectively replace the evaporation circuit.

Vertical heat exchangers: In this arrangement, the GHE typically consists of one, dozens, or hundreds of wells with depths ranging from 20 to 200 meters and diameters between 100 and 200 mm. Each of these wells contains single or double U-pipes or coaxial pipes through which the thermal exchange fluid circulates.

Given the significant depths, it is crucial to select durable piping materials to ensure longevity. These materials must be corrosion-resistant to prevent groundwater contamination, possess good mechanical properties, and have good thermal conductivity. Typically, special mixtures containing bentonite are used; alone, this mineral has a low thermal conductivity value but, when mixed with other elements such as sand or cement, achieves higher values.

Among the two pipe types, U-pipes are most commonly used because they statistically experience fewer failures. This design allows the fluid to descend into the deep well and subsequently rise after thermal exchange with the ground. When multiple pipes are present, they are positioned in parallel to each other to limit pressure losses.

The installation of vertical exchangers incurs higher costs compared to other configurations due to the equipment needed to drill to great depths. If multiple pipes are present, it is important to maintain a distance of at least 5-6 meters between them to avoid thermal interference between adjacent wells. Despite this, the described configuration yields the most efficient performance among GCHP systems.

Horizontal heat exchangers: this configuration features pipes laid horizontally relative to the ground, utilizing very shallow depths, not exceeding 2-3 meters. This makes such exchangers less efficient than other ground-source heat pumps, as the ground temperature at shallow depths varies throughout the year. However, installation costs are significantly lower due to the shallow depth required. Compared to vertical exchangers,

they have lower installation costs and less environmental impact but require large land areas. This requirement makes such exchangers suitable only for small to medium-sized installations. A typical representation of this configuration is shown in Figure 3-11, with distinctions between winter (heating) and summer (cooling) operations.

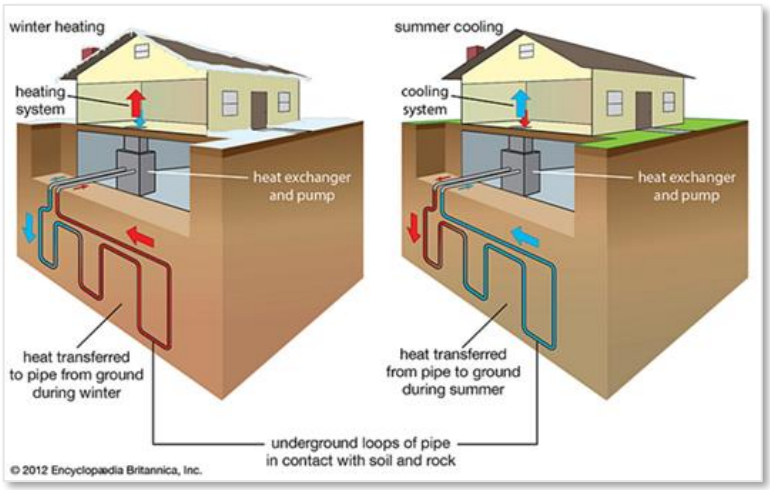

Figure 3-11- Horizontal GCHP System

The pipes can be arranged in different ways:

- single pipe;
- multiple pipes;
- spiral pipes.

The choice depends on the available space, the nature of the ground with its shading areas, and the type of vegetation to be preserved. The ground above the exchangers must be free of plants or other vegetation to avoid shading areas. Single pipe exchangers involve laying a single pipe arranged in a loop, as shown in Figure 3-12, in a trench no deeper than 1.5-2 meters; such excavations are preferable to those made by clearing due to their simplicity and lower cost. The trench is then backfilled with the previously removed soil.

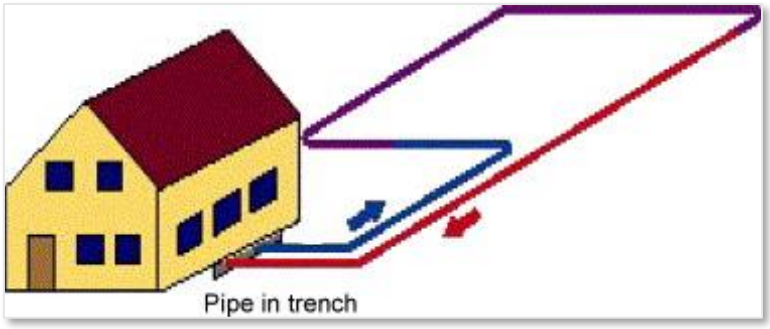

Figure 3-12- Single Pipe Horizontal Exchangers

The second layout uses pairs of pipes, supply and return, placed in the same trench at the same or different depths. Normally, a minimum distance of 7 meters should be maintained between the various trenches where the pipes are located. Special attention should be paid to this distance; if the pipes are positioned farther apart than recommended, the exchangeable power between the various pipes decreases, and if the pipes are too close, the removable thermal flux decreases. This configuration saves ground area and excavation quantity compared to the first but may cause mutual thermal interference due to possible overlaps of the pipe pairs, resulting in lower linear yields. An alternative to trenches is excavation when more ground area is available. This involves removing shallow soil but extending in width, allowing the pipes to be arranged in parallel or serpentine, as indicated in Figure 3-13.

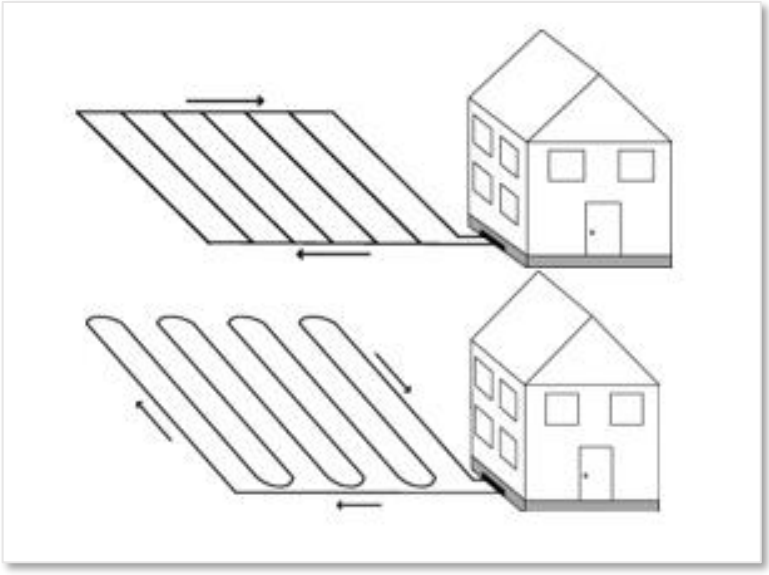

Figure 3-13 Multiple pipe horizontal exchangers, in parallel and serpentine configurations

The spiral configuration, also known as "Slinky," was proposed by the International Ground Source Heat Pump Association to address the problem of excessive surface area usage for such installations. It involves placing pipes at the bottom of vertical trenches similar to those of single and multiple pipe exchangers. The configuration, shown in Figure 3-14, allows more pipes per square meter of ground. This also reduces installation costs, not just the occupied space. However, it reduces thermal efficiency as the pipes can overlap.

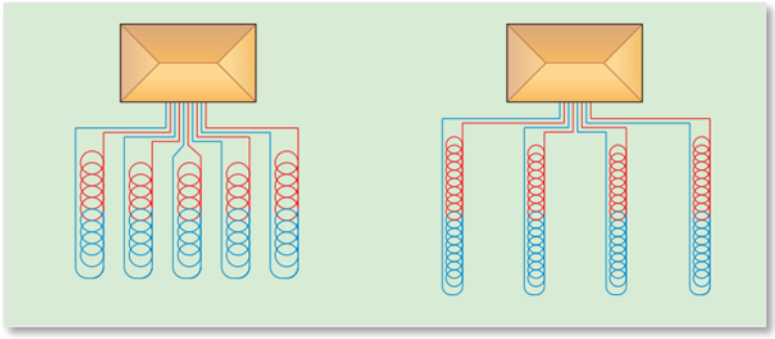

Figure 3-14 "Slinky" method for spiral pipe placement in trenches

An alternative to this method is to position the pipes vertically relative to the ground rather than horizontally. This arrangement is called "Svec" and was proposed by the National Research Council of Canada. It is shown in Figure 3-15.

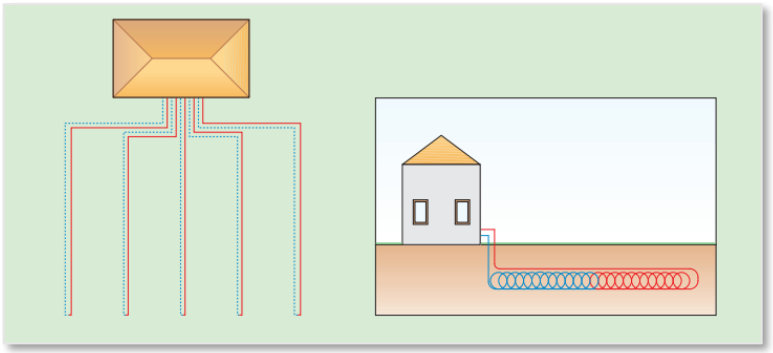

Figure 3-15 "Svec" Method for Spiral Pipe Placement in Trenches

3.5 Solar-assisted heat pump (SAHP)

The solar-assisted heat pump (SAHP) is a system that integrates a traditional heat pump with solar thermal panels into a single unit. Compared to conventional heat pumps, the SAHP system is more efficient and sustainable; it achieves a higher Coefficient of Performance (COP), thus enhancing the operational performance of both the heat pump

and the entire system. Additionally, it contributes to energy savings and CO_2 reduction. The low-temperature thermal requirement of the heat pump combined with the utilization of low-temperature solar energy is what makes this combination mutually advantageous.

SAHP systems can be classified into two categories:

- Direct Expansion Solar-Assisted Heat Pumps (DX-SAHP)
- Indirect Expansion Solar-Assisted Heat Pumps (IDX-SAHP)

In the former, the solar collector and the heat pump are combined into a single unit, whereas in the latter, the thermal fluid cycle and the refrigerant cycle of the heat pump are separated. Both configurations are widely used for heat supply, including space heating, domestic hot water, and cooling [15].

3.5.1 Direct Expansion Solar-Assisted Heat Pumps (DX-SAHP).

A Direct Expansion Solar-Assisted Heat Pump (DX-SAHP), as shown in Figure 3-16, comprises a collector-evaporator, a compressor, a condenser, and an expansion valve, all interconnected to form a closed circuit with pipes filled with refrigerant [16]. The refrigerant, initially at a low temperature and low pressure, is introduced into the collector-evaporator where it absorbs heat from incident solar radiation or ambient air, causing it to vaporize. The compressor then provides mechanical work to the superheated refrigerant vapor from the collector, increasing its temperature and pressure. Subsequently, the refrigerant vapor reaches a condenser where, by releasing heat, it becomes saturated liquid refrigerant. The expansion valve reduces the pressure of the liquid refrigerant exiting the condenser. The low-pressure liquid refrigerant re-enters the collector-evaporator, and the cycle repeats.

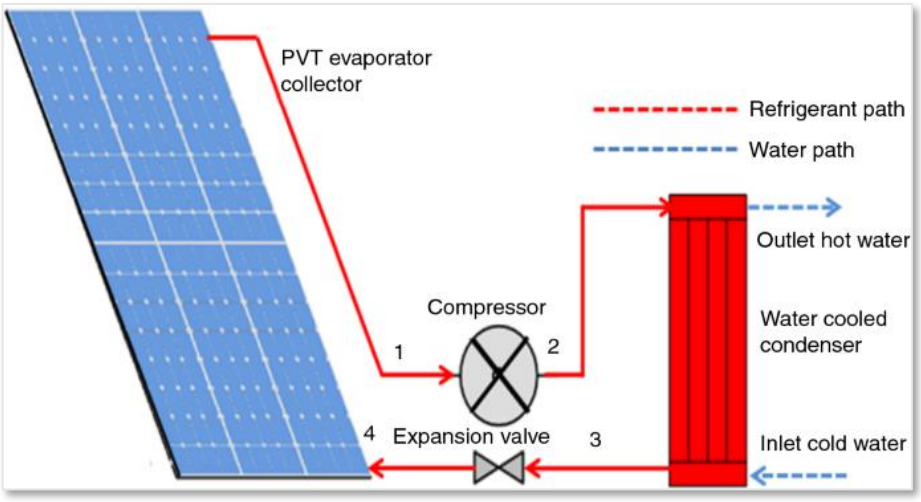

Figure 3-16- Diagram of a DX-SAHP system [16]

The unification of the two cycles, characteristic of this system, allows for a very simple structure but, most importantly, achieves a high evaporation temperature, low heat loss, and thus better thermal performance. Additionally, the presence of refrigerant in the collector-evaporator solves freezing and corrosion issues that often occur in traditional solar collectors using water as the working fluid, and efficiently utilizes both low and high radiation intensities for cooling and heating.

To evaluate the performance of a DX-SAHP system, it is necessary to know the Coefficient of Performance (COP), defined as the ratio of the thermal energy released by the condenser over a certain period to the electrical energy input to the compressor during the same period. Considering negligible heat losses from the condenser, the COP can be expressed by the following equation [17]:

$$COP = \frac{F_R A_{CE}[I_S(\tau\alpha) - U_L(T_{CE} - T_A)] + W_{Comp}}{W_{C_{omp}}} \quad (3.1)$$

where F_R is the collector efficiency factor, A_{CE} is the area of the collector-evaporator, I_S is the solar radiation intensity on the collector surface, τα is the effective absorptance, U_L is the heat loss coefficient of the collector,, T_{CE} is the evaporation temperature, T_A is the ambient temperature, and $W_{C_{omp}}$ is the electrical work absorbed by the compressor. If the solar radiation is zero, the DX-SAHP operates as an air-source heat pump with the evaporation temperature lower than the ambient temperature. The performance indicator for the solar collector alone is efficiency, defined as the ratio of

the useful power provided by the collector over a certain period to the incident solar irradiance on the collector plane during the same period. It is expressed by the following equation:

$$\eta = \frac{F_R A_{CE}[I_S(\tau\alpha) - U_L(T_{CE} - T_A)]}{I_S A_{CE}} \quad (3.2)$$

If the difference between the evaporation temperature of the refrigerant and the ambient air temperature becomes negative, the DX-SAHP system will achieve better performance for a given solar radiation intensity.

3.5.2 Indirect Expansion Solar-Assisted Heat Pumps (IDX-SAHP) [16]

A typical IDX-SAHP system is outlined in Figure 3-17 It consists of a solar collector, a heat pump, and a storage tank. The solar thermal collector (STC) receives solar radiation, converts it into thermal energy, and transfers it to the heat transfer fluid, which is generally an antifreeze solution mixed with water or air. This fluid transports the energy to the evaporator, where the energy is absorbed by the refrigerant in the heat pump. The STC can also be used as a heat source for the heat pump.

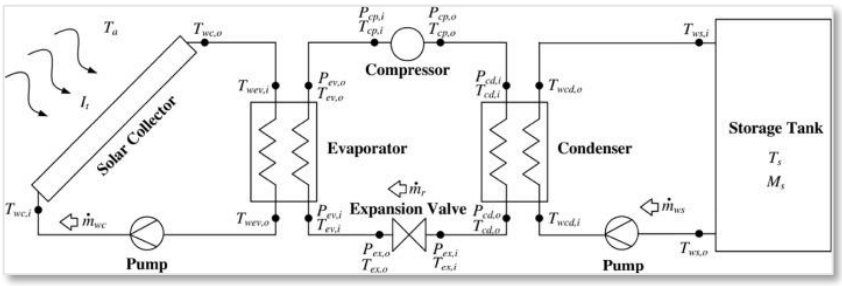

Figure 3-17 Schematic of an IDX-SAHP system

The separation between the heat transfer fluid cycle and the refrigerant cycle of the heat pump allows for different modes of operation with the common goal of heating and cooling spaces, as well as producing domestic hot water.

IDX-SAHP systems can be classified into three types: series, parallel, and dual-source. The common objective is to increase the temperature of the heat transfer fluid by absorbing solar energy.

Series IDX-SAHP systems, schematically represented in Figure 3-18, use solar energy as a heat source and are characterized by the presence of a heat exchanger that facilitates the interaction between the heat pump refrigerant and the heat transfer fluid. In practice, the heat exchanger functions as the evaporator for the heat pump; it has a higher evaporation temperature compared to air, resulting in a higher Coefficient of Performance (COP). Additionally, in these systems, it is possible to bypass the heat pump if the solar energy alone is sufficient to meet the required heating demand.

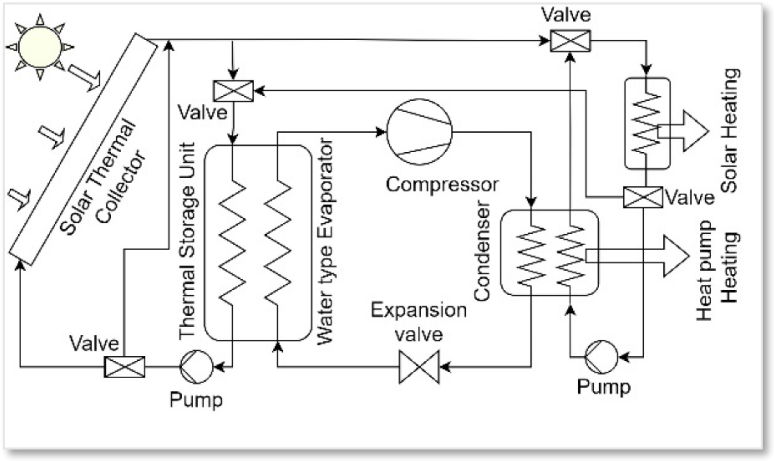

Figure 3-18- Series IDX-SAHP systems

Parallel IDX-SAHP systems also possess this property. They use air as a heat source and, unlike series systems, do not allow interaction between the heat transfer fluid and the refrigerant of the heat pump. The heat transfer fluid passes through a ventilated heat exchanger to reach the heating environment. Figure 3-19 shows a generic system of this configuration.

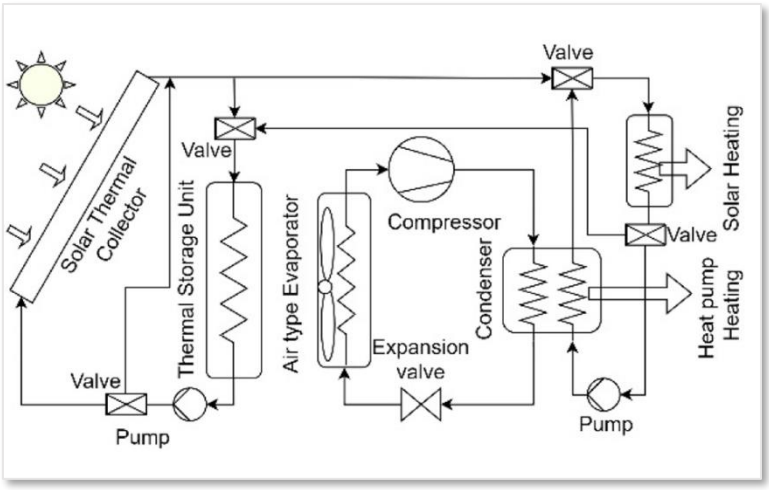

Figure 3-19- Parallel IDX-SAHP systems

Dual-source IDX-SAHP systems, as shown in Figure 3-20 are characterized by two evaporators, each utilizing a different heat source: the first (solar-side evaporator) uses solar energy as a heat source and is integrated with the heat transfer fluid cycle, while the other evaporator (air-side evaporator) uses air as a heat source. The use of a dual-source system allows for better performance compared to the traditional air-source heat pump system, as it increases the evaporation temperature and, consequently, the COP by supplying heat to the heat pump evaporator. Dual-source IDX-SAHP systems are preferred when the ambient temperature is moderate and solar irradiation is insufficient.

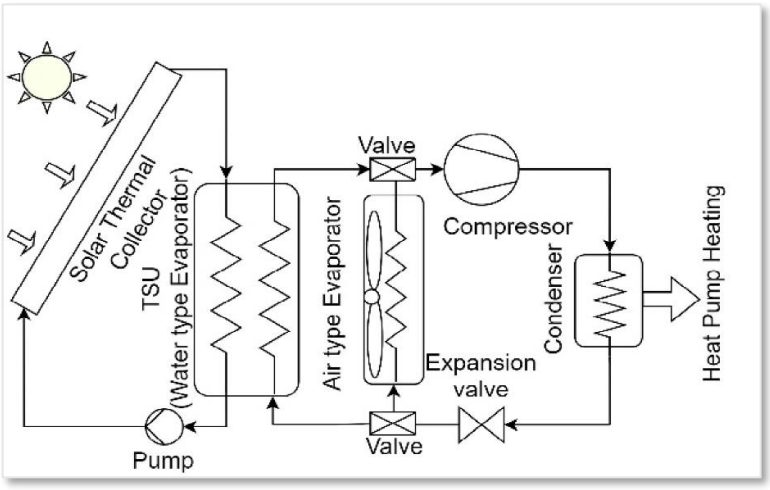

Figure 3-20 Dual-source IDX-SAHP systems

3.6 State of the art on helium-assisted air conditioning systems using heat pumps

The investigation into the state of the art regarding the potential applications of solar-assisted heat pumps for building heating has highlighted the interest of numerous researchers in this methodology. The most noteworthy contributions are listed below.

3.6.1 Study on energy-saving operation of a combined heating system of solar hot water and air source heat pump [18]

The authors J. Long et al. have proposed a hybrid solar hot water and air-source heat pump heating system (HSAHP), the schematic of which is shown in Figure 3-21. Various connection modes can be realized within this system. The evaporator can exchange heat with both the external air and the hot fluid from the solar thermal collector. Additionally, the hot water storage tank can receive heat directly from the solar collector or the heat pump.

The analyses were conducted using the TRNSYS software.

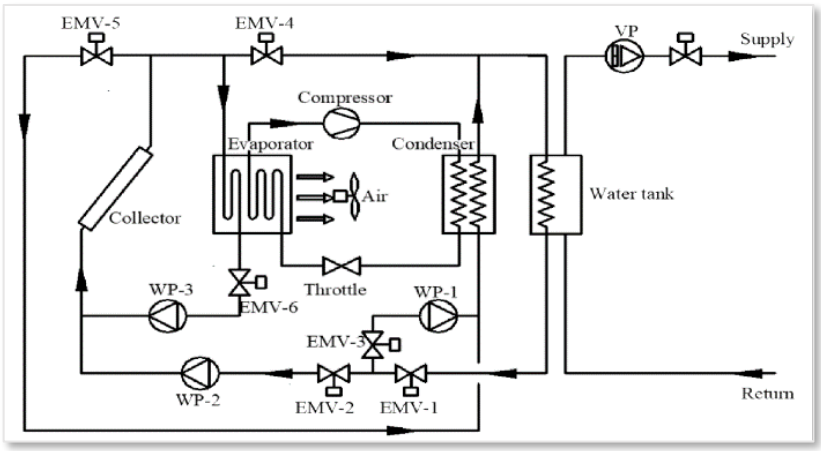

Figure 3-21-System schematic

During the cold season, the energy efficiency of the combined heating system was simulated and analyzed. The results showed that the intensity of solar radiation and ambient temperature are crucial factors influencing the energy efficiency of each connection method of the proposed combined heating system, as illustrated in the graphs in Figure 3-22.

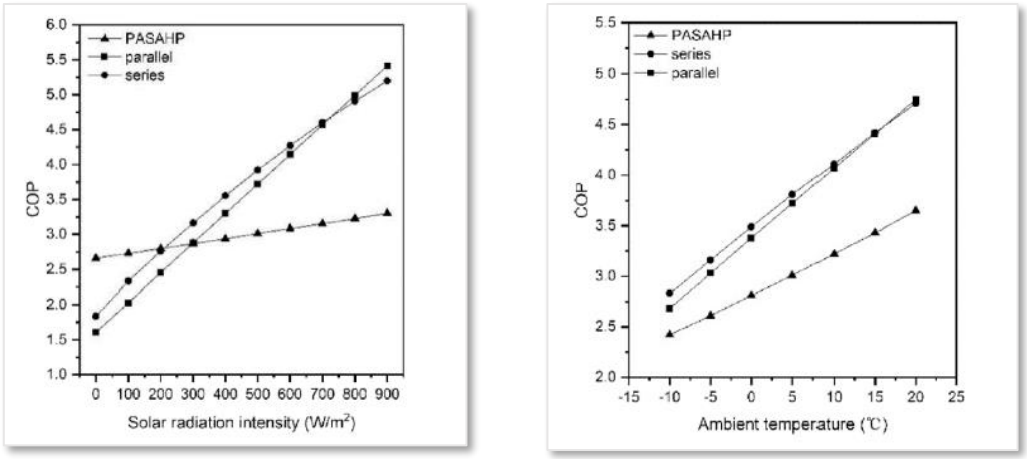

Figure 3-22-Variation of COP as a function of solar radiation and external temperature

The influence of ambient temperature on the COP of the three analyzed systems under two different solar radiation levels was also examined, as shown in Figure 3-23

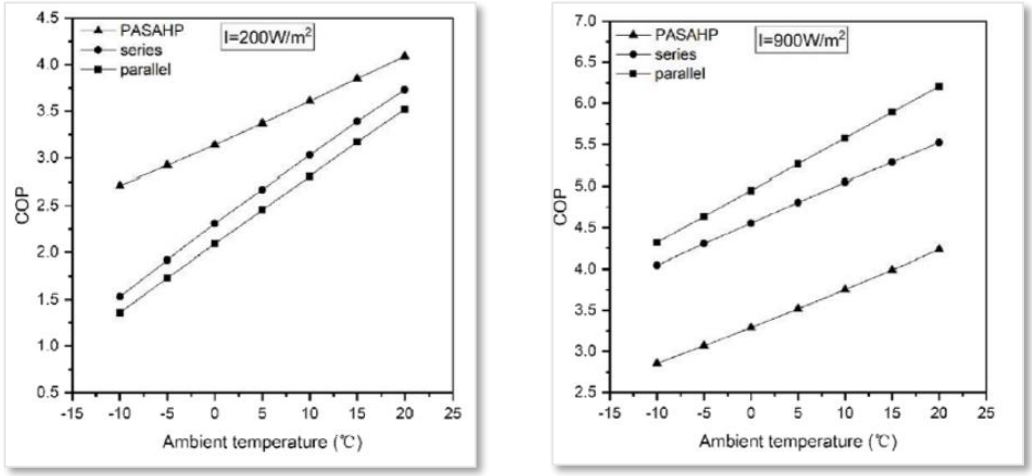

Figure 3-23-Variation of COP as a function of external temperature with two fixed values of solar radiation

Critical issues: The real-world operation of this proposed system faces challenges due to the variability and unpredictability of solar radiation and the consequent heat input, making the system difficult to control.

3.6.2 Applicability and comparison of solar-air source heat pump systems between cold and warm regions of plateau by transient simulation and experiment [19]

L. Xu et al. propose an interesting application for heating domestic hot water and residential spaces using a heat pump system that uses external air as the cold source (solar-ASHP) and feeds a storage tank, which is also heated by the fluid from evacuated tube solar collectors. The schematic proposed by the study is shown in Figure 3-24.

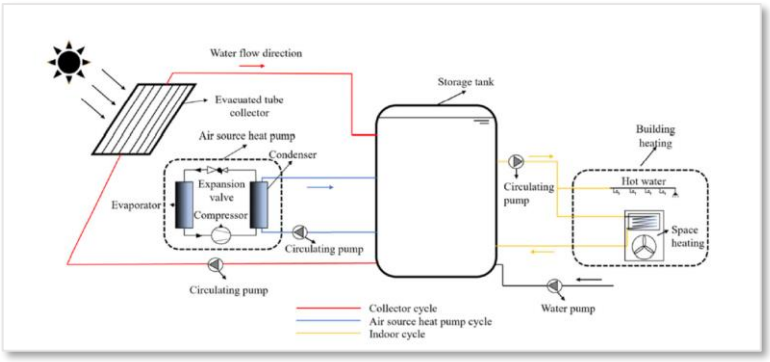

Figure 3-24-Schematic of the proposed system

This system has the advantage of resolving the intermittent operation of the standalone solar system (due to the presence of the heat pump) and the freezing issue of the standalone ASHP system (due to the storage tank).

The proposed system was installed in a building in Kunming and Shangri-La, two Chinese locations with the following climatic characteristics (Table 3-1)

Table 3-1-Climatic characteristics of the locations

Location	Solar radiation [MJ·m^{-2}·day^{-1}]	Altitudes [m]	Ambient temperature in winter [°C]	Coldest month average temperature [°C]	≤8 °C days of year	≤5 °C days of year
Shangri-La	24.7	3459	-10–12	January/-2.3	189	167
Kunming	20.6	1819	3–15	January/10.7	39	15

The field of evacuated tube collectors has an inclination angle of 35°, the hot water storage tank is made of stainless steel and is insulated with a 5 cm thick rigid polyurethane foam. The heated space has an area of 50 m².

The thermal load of the room in different months is calculated based on the heating requirement for the room to be heated, considering cold air infiltration.

The system is divided into three cycles:

The water in the collector is circulated by the pump when there is solar radiation capable of heating it to at least 45°C; when this is not possible, the ASHP is turned on to help feed the tank, which provides the necessary fluid flow for heating the building.

Considering a typical winter day in January, the variations of solar radiation, external air temperature, solar irradiance, and collector outlet temperature are shown below (Figure 3-25 and Figure 3-26).

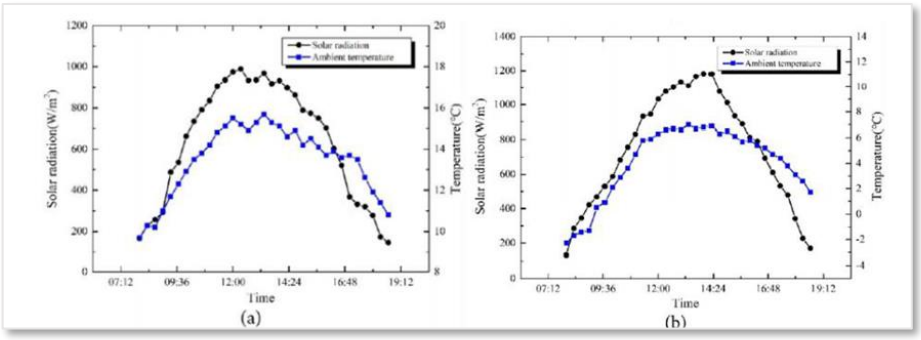

Figure 3-25- Variation of solar radiation and external temperature for Kunming (a) and Shangri-La (b)

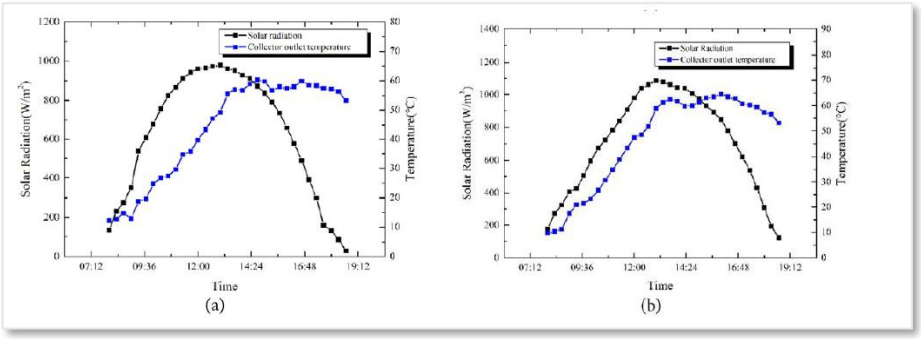

Figure 3-26- Variation of solar radiation and collector outlet temperature for Kunming (a) and Shangri-La (b)

Critical issues: It can be observed that at the end of the day, in the absence of solar radiation, there is a decrease in the collector outlet temperature, which essentially matches the storage tank temperature that stands at about 52°C at 19:12. This indicates that in the absence of solar radiation, due to poor weather conditions and at night, it is necessary to rely solely on the heat pump, which remains significantly disadvantaged in areas with low external air temperatures.

3.6.3 Experimental thermal performance of a solar source heat-pump system for residential heating in cold climate region [20]

K. Bakirci et al. studied the performance of a solar source heat pump system with energy storage in the province of Erzurum (Turkey). For this purpose, an experimental setup was constructed, consisting of twelve flat-plate solar collectors covering an area of 20 m², a thermal energy storage tank, a water plate heat exchanger, a liquid-liquid vapor compression heat pump, circulation pumps, and other measuring equipment. The layout of the experimental setup is illustrated in the Figure 3-27:

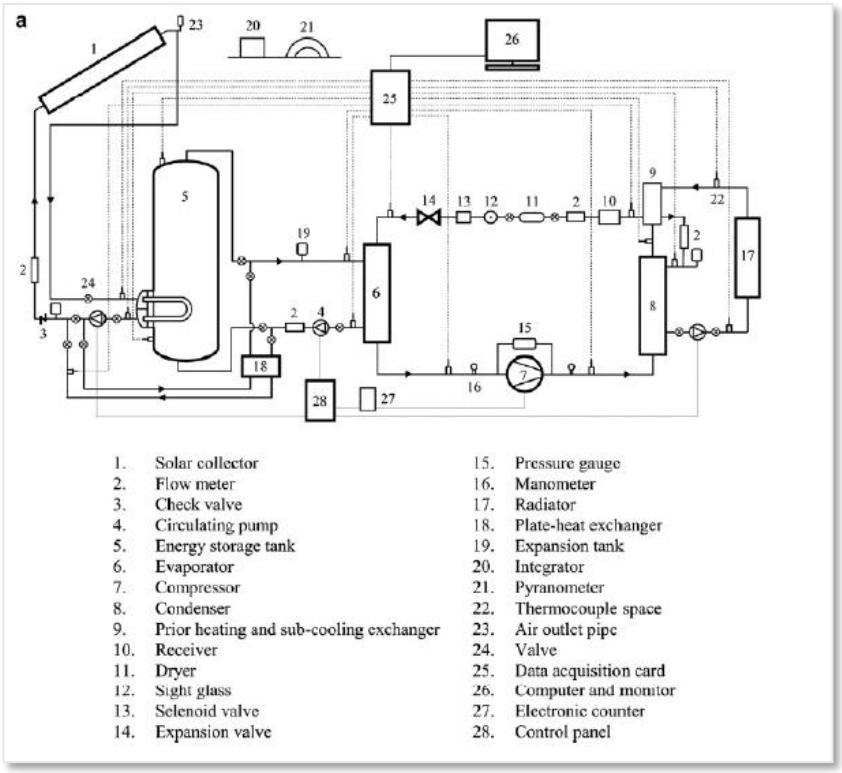

Figure 3-27- Layout of the system and component legend

The experiments were conducted (not continuously) from January to June 2004. The efficiency of the collector, the coefficient of performance (COP) of the heat pump, and the overall performance of the system (COPS) were calculated. During the actual operation months, the outside air temperature ranged from 10.8°C to 14.6°C.

The experiments were performed under clear sky conditions to achieve a quasi-steady state. For most runs, the system was started well before solar noon, and the quasi-steady state of operation was generally reached around noon. Data were obtained for global solar radiation on the collector plane ranging from 300 to 1050 W/m². The condenser outlet temperature varied between 32°C and 58°C. In this context, underfloor heating is preferred over radiators as it is more suitable for supply temperatures of 40-45°C.

In the experimental study conducted from January to June 2004, the outlet water temperature from the condenser, the average COP of the heat pump, the COPS of the entire system, and the average efficiencies of the collector were deduced from the experimental data. The variation of total solar radiation on the inclined surface fluctuated with the time of day, reaching its peak around solar noon at approximately 1050 W/m², as measured by a pyranometer. A typical day's analysis showed that the collector

efficiency varied from 33% to 47% throughout the day (Figure 3-28). Figure 3-29 illustrates the variation in the energy storage tank temperature with respect to the time of day:

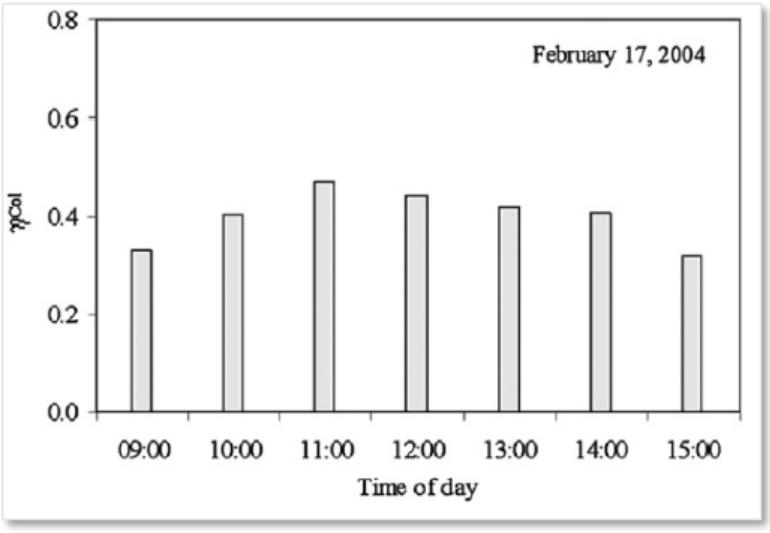

Figure 3-28 Collector efficiency throughout the day

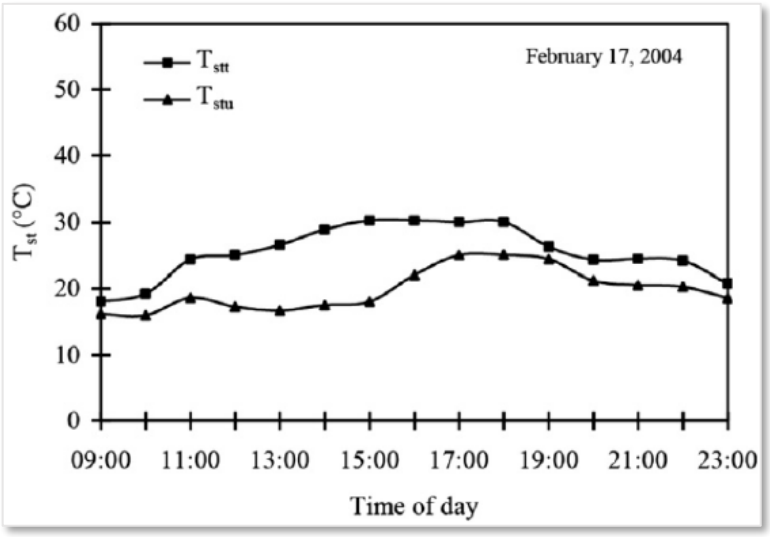

Figure 3-29 Variation in storage tank temperature throughout the day

Figure 3-30 also shows the maximum temperature of the energy storage tank over the months studied. As indicated, the maximum storage temperature steadily increased from January to June due to the rise in solar radiation.

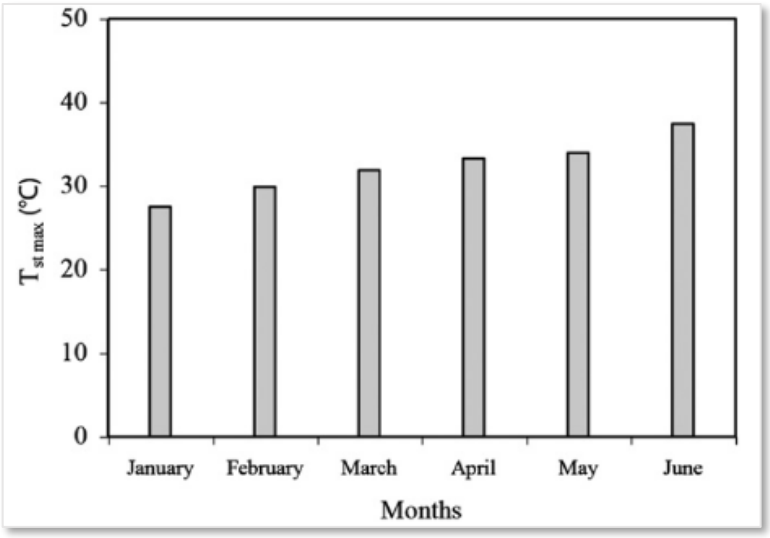

Figure 3-30- Maximum storage tank temperature

Figure 3-31 shows the inlet temperature of the collector (T1), the outlet temperature of the collector (T2), and the inlet temperature of the heat exchanger (T3) for the heat transfer fluid (water and ethylene glycol) with respect to the time of day. All temperatures (T1, T2, and T3) peaked around solar noon. Additionally, T2 equalled T3 at 16:00 local time when the sun had set and the circulation pump for the collector loop was turned off, indicating a rapid decrease in incident solar energy on the collector surface.

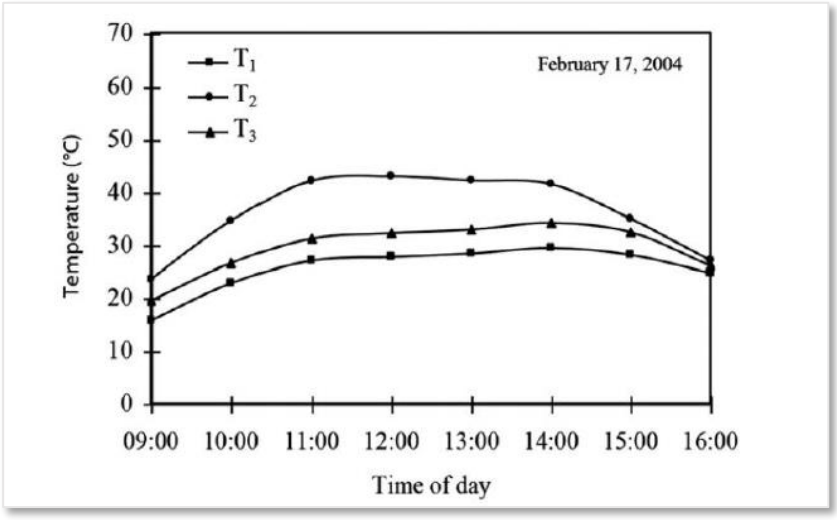

Figure 3-31- Collector inlet/outlet and heat exchanger inlet temperatures throughout the day

Figure 3-32 shows the inlet temperature of the evaporator (T4) and the condenser outlet temperature (T_{cwo}) of the water with respect to the time of day. The condenser outlet temperature (T_{cwo}) consistently varied between 35 and 48°C. However, the evaporator

inlet temperature peaked at 16:00 because the sun had set between 15:00 and 16:00 and the collector loop was closed. After this period, the evaporator received energy from the storage, causing T4 to rise again at 17:00 local time.

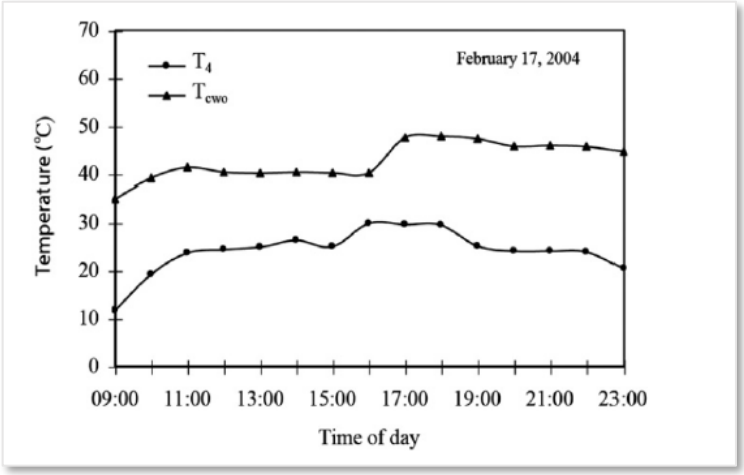

Figure 3-32- Evaporator inlet (T4) and condenser outlet (Tcwo) temperatures throughout the day

In this system, hot water from the collectors first goes to the energy storage tank, where it transfers some energy, then passes through the plate heat exchanger, and is used as a heat source by the water evaporator during the day. Finally, the heat transfer fluid is sent back to the solar collectors by a circulation pump. However, on nights and cloudy days, the lower-temperature water from the heat pump evaporator is sent to the energy storage tank instead of the solar collectors. The cold-water extracts energy from the storage tank before flowing into the evaporator to be used as a heat source.

The inlet water temperature to the evaporator (T_4) and the outlet water temperature from the condenser (T_{cwo}), as well as the COP and COPS values, increase due to the rise in solar irradiance during the day. The energy storage tank is used for night-time operation. However, during the night, the lower-temperature water from the heat pump evaporator is directed to the energy storage tank instead of the solar collectors. The performance is as follows (Figure 3-33):

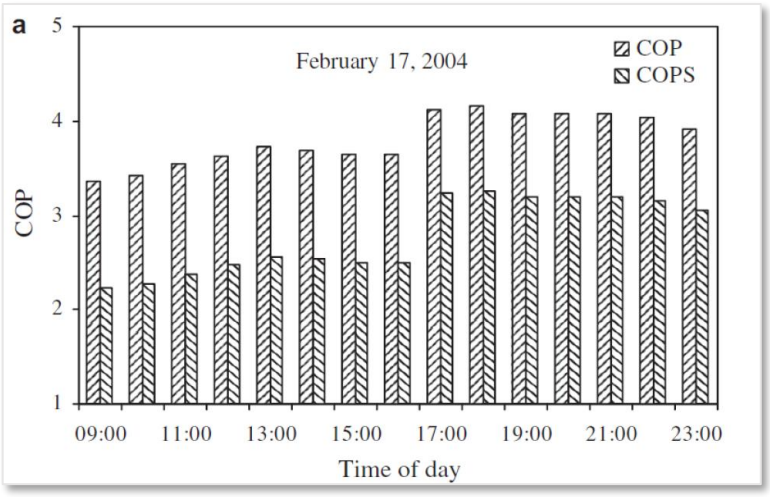

Figure 3-33- COP and COPS performance throughout the day

This study demonstrated that the analysed system could be used for residential heating in the province of Erzurum, which has the coldest climate in Turkey.

Critical issue: analysis of the collector efficiency and the water temperature trends in the storage tank indicates an undersized collector surface and collectors that are not highly efficient. Additionally, there is a lack of direct connection with the building in cases where the tank temperatures are compatible with the delivery terminals.

3.6.4 Energy analysis of a thermal system composed by a heat pump coupled with a PVT solar collector [21]

In this work, the energy analysis of a thermal system comprising a heat pump coupled with a hybrid PVT (Photovoltaic Thermal) collector was conducted. The advantages of these systems include providing energy for space heating in winter and hot water during other seasons, along with the simultaneous generation of electricity.

Specifically, the possibility of using a Water Source Heat Pump (WSHP) in a heating system supported by a PVT system with thermal storage for a building was analysed. The PVT collector is utilized to supply electrical energy for the WSHP and thermal energy for space heating across three different European climates (Rome, Milan, and Krakow). The novelty of this work lies in the particular configuration of the WSHP operating with a thermal storage tank that supports the heat pump in heating the building.

The system (shown in Figure 3-34) comprises a photovoltaic thermal panel, a thermal storage tank, a water-to-water heat pump, and emission terminals (fan coils). The PVT panels have dual production: thermal and electrical. The electrical energy is used to

power the water-to-water heat pump and to meet the building's electrical needs; any surplus electricity can be stored in a storage system or fed into the grid. The thermal output of the PVT is used to heat the water contained in the thermal storage tank. The thermal storage is the critical element of the entire system as it is closely linked to the operation of the heat pump.

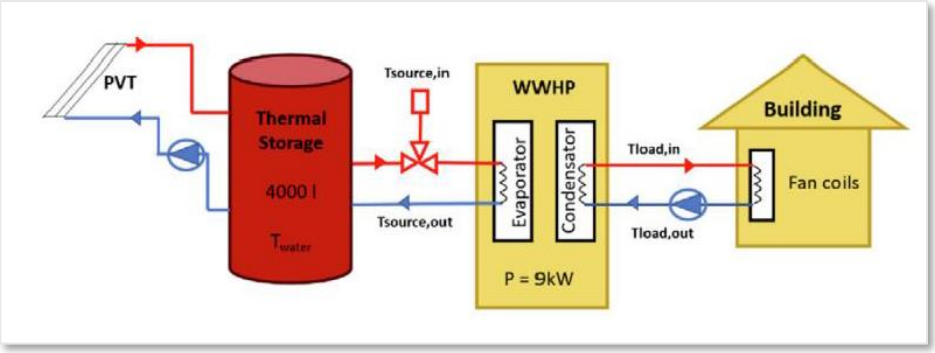

Figure 3-34- System layout [21]

The proposed system performs well for the city of Rome, covering 56% of the total heating demand. For the city of Milan, 52% of the heating demand is covered, while for the city of Krakow, only 37% of the heating demand can be directly met by the heating system. Since the heating demands are not fully covered, auxiliary heating is required: for example, the heat pump can adopt a ground heat exchanger to cover the remaining heating requirements. The analysis conducted allows the conclusion that the proposed system works well for cities with mild climates.

Based on the studies and analyses conducted in this document, it is observed that the prototype system is highly influenced by the climatic conditions in which it operates, as the availability of solar radiation varies with geographical location. It depends on the supply of thermal and electrical energy from the system.

Critical issue Utilizing PVT systems optimizes costs and available surface area but entails the following limitations:

a) For cold climates, this solution prevents the use of evacuated tube collectors, which are more efficient for such climates.
b) The temperature of the water in the storage tank must be limited; otherwise, the efficiency of the PVT photovoltaic panels decreases, resulting in a limitation on the utilization of solar thermal energy for hot water production.

3.6.5 Operating performance of a solar/air-dual source heat pump system under various refrigerant flow rates and distributions [22]

Z. Liu et al. proposed and studied a new dual-source solar/air heat pump system used for space heating, as shown in the following system layout (Figure 3-35):

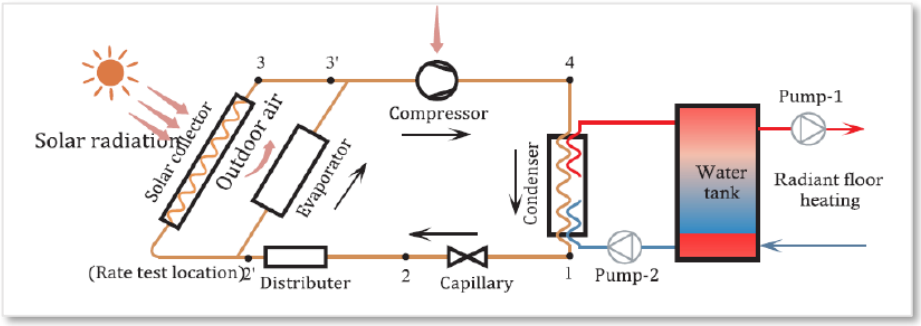

Figure 3-35- System layout

The evaporator exchanges with the source at the higher temperature between the air heated by the solar collectors and the outside air. In this way, when solar radiation is present, the temperatures of the air exchanged by the evaporator are relatively high.

Based on a demonstration building on the Qinghai-Tibetan Plateau in China, a dynamic simulation model was established in TRNSYS and then validated with experimental data.

To leverage the variability of solar radiation, the idea of controlling the refrigerant flow distribution of the heat pump was adopted. The performance of the dual-source heat pump with various refrigerant flow rates and different air flow rates through the solar collector and evaporator was studied and optimized. The results show that the coefficient of performance is maximized when the refrigerant flow rate is 16 g/s. Under this condition, the monthly average coefficient of performance of the dual-source heat pump can generally reach 3.6, and the annual average indoor temperature of the building is generally above 20°C.

Critical issue: The lack of thermal energy storage from the solar air collectors represents a limitation of this configuration, as it cannot always fully utilize solar energy. The surplus energy, beyond what the evaporator can absorb, is lost.

3.7 Potential and challenges of heat pumps in sustainable energy transition

Heat pumps are emerging as one of the most significant technologies for the energy transition, due to their ability to substantially reduce primary energy consumption and greenhouse gas emissions while promoting environmental sustainability. A primary advantage of these systems lies in their high thermodynamic efficiency: rather than generating heat directly, heat pumps transfer thermal energy from a low-temperature source (such as air, water, or ground) to a higher-temperature environment. This process enables them to achieve high coefficients of performance (COP), translating into considerable energy savings, especially when powered by renewable sources like photovoltaics or solar thermal collectors. Integrating these technologies allows for optimized energy flows and minimized use of non-renewable energy, with positive effects on both environmental sustainability and operating cost reduction.

The versatility of heat pumps represents another crucial factor: they can be used for both heating and cooling and can also meet the demand for domestic hot water (DHW). This multifunctionality makes them particularly suitable for high-energy-efficiency buildings, such as nearly zero-energy buildings (nZEB). When combined with appropriate thermal storage systems, heat pumps enable advanced energy management, maximizing the self-consumption of locally produced renewable resources and reducing peak demand on the electricity grid, thereby also benefiting grid stability.

The broad range of available technological configurations provides an additional advantage for this solution. Various types of heat pumps exist, each optimized for specific environmental conditions: aerothermal, which uses ambient air as a heat source; hydrothermal, which leverages surface or groundwater; and geothermal, which extracts heat from the ground. Each of these options offers distinct benefits, making heat pumps adaptable to a variety of climatic contexts. In temperate climates, aerothermal pumps can deliver very high performance, while in colder regions, geothermal pumps—thanks to the stability of ground temperatures—prove to be more efficient.

Despite their many benefits, these technologies present some inherent challenges. For example, in harsh climates, the performance of air-to-water heat pumps can decrease significantly when external temperatures drop very low. Under such conditions, the COP diminishes, leading to increased electricity consumption and reduced overall system efficiency. To maintain functionality in such contexts, it is often necessary to integrate

auxiliary heat sources, such as biomass boilers or electric resistance systems, to offset efficiency losses. Moreover, managing the defrost cycle, essential for air-to-water pumps in cold climates, entails additional energy consumption, further impacting efficiency.

Another challenge relates to the initial investment required for installing these systems, which can be considerably higher than that of traditional heating systems. Adopting a heat pump involves not only the cost of the unit itself but also expenses associated with installation, maintenance, and, in the case of renewable integration, the acquisition of supporting systems (e.g., photovoltaic panels or solar collectors). While long-term energy savings may offset these costs, the payback period can be relatively lengthy, particularly in the absence of adequate financial incentives. This issue has been widely discussed in several studies, which emphasize the need for targeted support policies to encourage the adoption of these sustainable technologies.

An additional critical aspect is the evolution of refrigerants used in heat pumps. Traditional refrigerants, often characterized by a high global warming potential (GWP), are subject to increasingly stringent environmental regulations, driving the shift toward low-impact refrigerants such as carbon dioxide (CO_2) or natural fluids. However, the adoption of these alternatives involves technical and engineering challenges that can increase costs and complicate large-scale implementation, necessitating further advancements in refrigeration technologies.

In conclusion, heat pumps offer a combination of energy efficiency, versatility, and compatibility with renewable sources, positioning them as a favored solution for the energy transition. However, addressing the challenges associated with cold climates, high upfront costs, and the adoption of sustainable refrigerants will be essential for widespread adoption. A successful transition will also depend on the evolution of support policies and the implementation of integrated solutions that make this technology increasingly accessible and efficient.

3.8 References

[1] A. S. Gaur, D. F. Fitiwi e J. Curtis, «Heat pumps and our low-carbon future: A comprehensive review,» *Energy Research & Social Science,* 2020.

[2] «IEA50,» [Online]. Available: https://www.iea.org/.

[3] I. Staffel, D. Brett, N. Brandon e A. Hawkes, «A review of domestic heat pumps,» *Energy & Environmental Science,* 2012.

[4] R. Lazzarin, Pompe di calore, Padova: Servizi Grafici Editoriali, 2011.

[5] ENEA, «La pompa di calore».

[6] C.Menale, A. Mariani, M. Pieve e R. Trinchieri, «Selezione e stima del rischio correlato all'uso di refrigeranti a basso GWP in Pompe di Calore per la climatizzazione residenziale,» ENEA, Report RdS/ptr, 2019.

[7] P. Makhnatch, «Future refrigerant mix estimates as a result of the European Union regulation on fluorinated gases,» *Conference Paper,* 2019.

[8] R. Lazzarin, F. Busato, F. Minchio e M. Noro, Sorgenti termiche delle pompe di calore, Milano: Editoriale Delfino, 2012.

[9] I. E. A. (IEA), «The Future of Heat Pumps,» *World Energy Outlook Special Report,* December 2022.

[10] «EHPA (European Heat Pump Association),» 2021. [Online]. Available: https://www.ehpa.org/market-data.

[11] M. Chesser, P. Lyons, P. O'Reilly e P. Carroll, «Air source heat pump in-situ performance,» *Energy and Buildings,* 2021.

[12] G. Hailu, «Energy systems in buildings,» in *Energy Services Fundamentals and Financing*, Academic Press, 2021, pp. 181-209.

[13] R. O'Hegarty, O. Kinnane, D. Lennon e S. Colclough, «Air-to-water heat pumps: Review and analysis of the performance gap between in-use and product rated performance,» *Renewable and Sustainable Energy Reviews,* 2022.

[14] F. F. Hernández, A. A. Márquez, J. M. Peña Suárez e J. A. Bandera Cantalejo, «Analysis of a HVAC zoning control system with an air-to-water heat pump and a ducted fan coil unit in residential buildings,» *Applied Thermal Engineering,* 2022.

[15] Raghad S. Kamel, A. S. Fung e P. Dash, «Solar systems and their integration with heat pumps: A review,» *Energy and Buildings,* 2014.

[16] A. A., K. Sopian, M. Alghoul e A. Elbreki, «Performance study on photovoltaic/thermal solar-assisted heat pump,» *Journal of Thermal Analysis and Calorimetry,* 2018.

[17] S. K. Chaturvedi e J. Y. Shen, «Thermal performance of a direct expansion solar-assisted heat pump,» *Solar Energy,* 1984.

[18] J. Long, K. Xia, H. Zhong e H. Lu, «Study on energy-saving operation of a combined heating system of solar hot water and air source heat pump,» *Energy Conversion and Management,* 2021.

[19] L. Xu, M. Li, Y. Zhang e X. Luo, «3.6.2 Applicability and comparison of solar-air source heat pump systems between cold and warm regions of plateau by transient simulation and experiment,» *Building Simulation,* 2021.

[20] K. Bakirci e B. Yuksel, «Experimental thermal performance of a solar source heat-pump system for residential heating in cold climate region,» *Applied Thermal Engineering,* 2011.

[21] A. Vallati, P. Oclon, C. Colucci, L. Mauri, R. De lieto Vollaro e J. Taler, «Energy analysis of a thermal system composed by a heat pump coupled with a PVT solar collector,» *Energy,* 2019.

[22] Z. Liu, Q. Wang, D. Wu, Y. Zhang, H. Yin, H. Yu, G. Jin e X. Zhao, «Operating performance of a solar/air-dual source heat pump system under various refrigerant flow rates and distributions,» *Applied Thermal Engineering,* 2020.

4 The Role of thermal storage in distributed air-conditioning plants: energy and environmental analysis

Abstract

Energy efficiency is becoming a crucial target in the construction of a decarbonized society to guarantee sustainable development and tackle climate change issues. The building sector is one of the major players being responsible for a huge amount of primary energy, mostly related to heating and cooling services. Aside from intervening on the building envelope, intending to reduce energy demand, it is of fundamental importance to consider appropriate air-conditioning systems that can easily integrate renewable sources and rationalize energy use. Heat pumps are an appealing solution because of the renewable energy available in the external sources and because of the possibility to drive them with PV systems. Solar assisted heat pumps have therefore become a promising solution for energy efficiency in buildings, allowing lower primary energy demands and generating lower CO_2 emissions. The ulterior integration of thermal storage in the systems allows for a further improvement of energy efficiency. This paper investigates the achievable energy savings after interventions of energy efficiency on a building aggregate composed of four buildings. In particular, two different scenarios of improvement of the HVAC system substituting the existing plant with PV-assisted heat pumps are considered. The performances obtained with the use of single-heat pumps and a centralized one with thermal storage are investigated employing dynamic simulations conducted in the TRNSYS environment.

4.1 Introduction

The need to decarbonize the building sector, which is believed to account for about 40% of primary energy needs in Europe, is pushing toward ambitious targets of energy efficiency in buildings constructions and operation [1], [2]. On one hand, the developed awareness of the importance of the building envelope in providing repair from the outdoor severe climatic conditions has propelled the research and implementation of innovative active [3]–[10] and passive solutions [11]–[13]. Aside from the conspicuous use of thermal insulation, interesting solutions can be represented by the use of green roofs [14]–[26], solar walls [27]–[33], PCM incorporated in building elements [34]–[38]. Nevertheless, the HVAC plant plays an equally important role in determining energy

performances. Recent advancements both in research and field applications are nowadays almost compelling the use of heat pumps as efficient, reliable, and clean generators for the annual air-conditioning of buildings [39]. Furthermore, combining solar source with heat pumps allows a double benefit: on the one hand, the use of solar energy is maximized, and on the other, the efficiency of the heat pump is increased, simultaneously optimizing and rationalizing the use of renewable sources [40]–[47]. Several authors have studied and analysed both experimentally and analytically, the performance of helium-assisted heat pumps configured in direct series operation in relation to the type and characteristics of the components of the two subsets, cataloguing their performance according to the offered service (domestic hot water, heating) and to the reference climate [48]– [51]. Similarly, other authors have investigated the performance of indirect systems [52]– [54], focusing on the effects and role of thermal storage on the performance of subsets [55]– [57]. Raghad S. Kamel et al. have provided a systematic review in which they first analyse and catalogue the solar systems of the literature and then carry out a detailed bibliographic analysis of all the systems that integrate the use of the heat pump with solar collectors. The systems taken into consideration have been analysed according to the type of heat pump used, the type of solar panel used, and the configuration adopted (in parallel, direct, and indirect series) [58]. Pinamonti et al. studied the integration of a water-water heat pump with a solar system equipped with a short-term and long-term storage tank through a dynamic simulation performed using TRNSYS. Long-term storage allowed to store the excess of solar energy collected by solar collectors in summer, and then use it to provide space heating during winter. This system allowed the solar fraction to increase by five percentage points [59]. Cagri Kutlu et al. analysed the integration of an helio-assisted heat pump for the production of DHW with a thermal storage tank made with phase change material. The configuration has been studied by a transient model. The results showed that it is possible to obtain energy savings of about 12% [60]. The energy performances of a smart air-conditioning plant installed at the University of Calabria, made of a heat pump and a storage tank were investigated as an alternative electric storage system because the plant was assisted by a 4kWp PV generator [61]. In such a more complex HVAC plant design, the use of thermal storage is becoming an interesting technical solution as it is capable of providing several benefits [62]–[66]. The heat pump used with thermal energy storage is believed to shift their energy consumption, providing the opportunity to align to price signals to reduce consumer costs, especially in single-

family houses belonging to an energy community. Power-to-heat technology such as heat pumps and thermal energy storage has been shown to both decarbonize heat and enable the cost-effective integration of more renewable electricity into the grid. The impact of different heat storage sizes and heat pump powers on cost savings and shifting potential, when variable electricity prices based on the electricity market are applied, was analyzed in the Luxembourgish context [67]. The author aimed to demonstrate and emphasize the importance of the use of thermal storage, especially combined with renewable sources, to rationalize the use of energy for air-conditioning services of buildings. Recently, researchers are also focusing on developing accurate and reliable optimization algorithms to derive optimal operation schedules for heat pump-based grid-edge technology [68]. The impact of user demand patterns and load shifting scenarios on the volume of energy storage required for a heat-pump installation was analysed in [69]. The authors used monitored data from several family homes to conduct simulations and found that the level of service for the householder is sensitive to the patterns of consumption, the thermal energy storage volume, and the electricity tariff. A residential building in Stuttgart, equipped with a hybrid heat pump, a thermal energy storage unit, and a gas boiler as an integration system was investigated to determine the influence of electricity tariffs on the energy flexibility of the building and associated energy costs. The demand response programs led to higher utilization of thermal energy storage along with increased boiler consumption, by up to 17.1% and 12.1%, respectively, in case of maximum demand response intensity [70]. The capability of a cost-optimal control strategy to activate demand response actions in a building equipped with an air-source heat pump coupled with a water thermal storage system was assessed by comparing the results of a reference scenario with no demand response actions and several demand response scenarios [71]. The results illustrated the effectiveness of thermal energy storage for reducing the total system operational cost and its seasonal primary energy consumption, both with and without demand response actions.

This study presents the result of energy simulation performed on a real building aggregate made of four terraced houses in order to highlight the importance of the HCAV system in reaching goals of energy-saving and carbon emission reductions. The building aggregate is supposed to go through energy renovation actions, implemented only on the air-conditioning plant demonstrating the undoubted advantages of the use of heat pump

and thermal storage and the importance of integration with renewable energy sources such as photovoltaic systems.

4.2 Methodology

4.2.1 Case study building

The chosen case study is an existing building aggregate made of four terraced houses, being part of a bigger complex made of four rows of such constructions. It was chosen for the simulation since it represents a typical example of popular construction built between 1976 and 1980, that shows very poor energy performances, and very prone to be subject to energy renovation interventions. The two-story buildings have a gross surface of about 60 m^2 per floor and a floor height of 3 m (Figure 4-1).

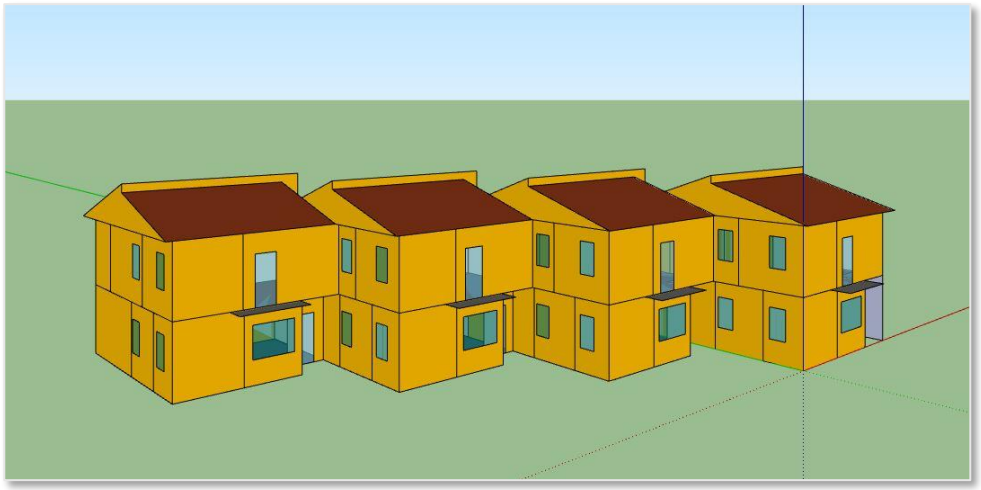

Figure 4-1-Case study

Since the paper aims to investigate the interventions regarding the air-conditioning plant and the effect on the energy efficiency of the building, the envelope was modelled properly considering a thermal insulation layer, to reach the minimum standard imposed by current Italian legislation. The main thermal properties of the layers composing the different building components are reported in Table 4-1to Table 4-3.

Table 4-1- Thermal properties of the external wall layers

External wall				
Material	**Thickness [cm]**	**Density [kg/m³]**	**Specific heat [J/kg K]**	**Thermal conductivity [W/mK]**
Plasterboard	2	1800	1000	0.9
Hollow bricks	8	1800	1000	0.4
Air gap	10	-	-	-
Hollow bricks	12	1800	1000	0.386
Plasterboard	2	1800	1000	0.9
Structural bonding	0.5	1400	1000	0.538
EPS Insulation	6	15	1260	0.031
Skim coat skim coat with reinforcement	2	1400	1000	0.538

Table 4-2- Thermal properties of the ground floor layers

External roof				
Material	Thickness [cm]	Density [kg/m³]	Specific heat [J/kg K]	Thermal conductivity [W/mK]
Plasterboard	2	1800	1000	0.9
Hollow bricks and concrete slab	24	1800	1860	0.858
Waterproofing	0.5	1200	920	0.169
EPS Insulation	8	15	1260	0.031
Air gap	3	-	-	-
Roofing tile	1.2	1800	840	0.825

Table 4-3- Thermal properties of the ground floor layers

Ground floor				
Material	Thickness [cm]	Density [kg/m³]	Specific heat [J/kg K]	Thermal conductivity [W/mK]
Tiles	1.2	400	1000	0.064
Lightened concrete slab	5	1400	1000	0.583
Waterproofing	0.5	1200	920	0.169
EPS Insulation	5	15	1260	0.03
Vapor barrier	0.3	500	1800	0.4
Reinforced concrete slab	10	1200	1000	0.333
Ground floor loose stone foundation	9.5	-	1000	-

The building is located in Crotone (Italy) characterized by hot and dry summers, classified as subtype "Csa" (Mediterranean Climate) in the Köppen Climate Classification. Simulation was performed in TRNSYS 18 environment. For the aim of the study, each building was considered as a single thermal zone. DHW needs were not considered to focus only on the energy requirements for heating and cooling. Internal

gains were defined according to the Italian national standard UNI 11300:1 [39] differentiating them according to a schedule. Natural ventilation was assumed with a rate of 0.3 1/h as suggested by the same national standard. Electrical load requirements for the building equipment' are set according to a weekly schedule (Figure 4-2) defined on the basis of a statistical analysis of data from Italian national consumptions [40]. For two years for a sample of Italian families, the load curves were continuously acquired. In the same period, a set of information on the main electrical uses of the family was acquired every four months. In particular, the presence and type of the main household appliances, the energy class, the frequency, and the day/time of use. The results of the analysis are the four curves displayed in Figure 4-2 each defined for a single season. These loads were properly set in TRNSYS environment.

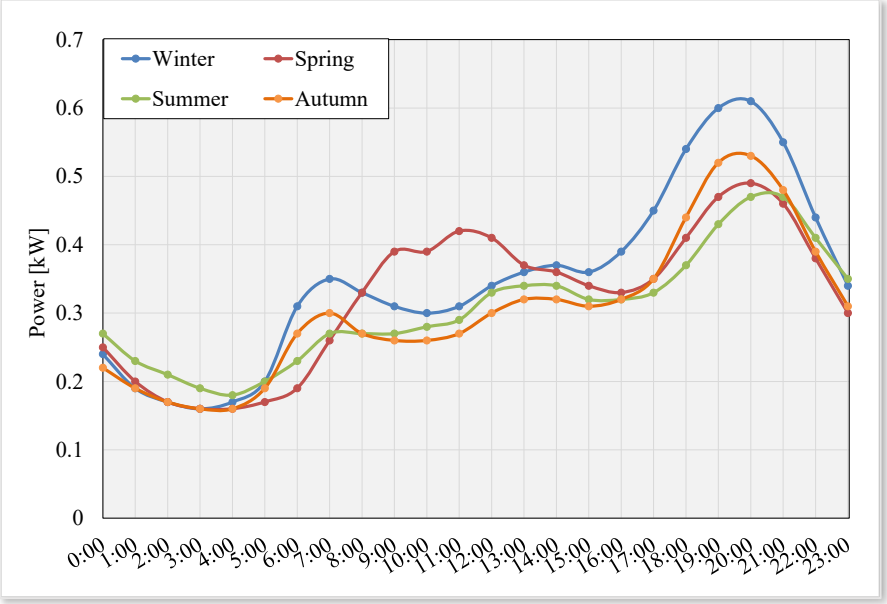

Figure 4-2- Electric load daily profiles of the building, differentiated for season.

4.2.2 Air Conditioning plant

4.2.2.1 Base case plant

The case base building, representing the most likely actual situation, is equipped with a traditional gas boiler supplied by natural gas with traditional radiators as emitters. The main parameters of the multi-stage boiler are reported in Table 4-4. The heating setpoint temperature was assumed equal to 20 °C.

Table 4-4- Main properties of the gas boiler

Boiler	
Fuel	Natural gas
Combustion efficiency	0.92
Boiler efficiency	0.89
Minimum Turn-Down Ratio	0.2
Rated power (kW)	4

Summer air-conditioning is assumed provided by single air-to-air heat pumps, as it is likely in the real case, with the following characteristics.

Table 4-5- Main properties of the heat pump for cooling application

Heat pump	
Type	Air-to-Air
Nominal Cooling Capacity	3.88 kW
Nominal EER	2.55

4.2.2.2 Yearly conditioning with solar heat pumps

A first possible intervention for energy efficiency investigates the substitution of the gas boiler for heating and the air-to-air heat pump for cooling with a single air-to-water heat pump for each building for the yearly air-conditioning, replacing radiators with fan-coils as emission system.

Table 4-6- Main properties of the heat pump for yearly air-conditioning

Heat pump	
Type	Air-to-Water
Nominal Cooling Capacity	3.88 kW
COP	2.55
EER	
Airflow rate	185 l/s

As to improve the overall efficiency and the share from renewable sources another intervention considers the installation of a 3 kW PV plant for each building. The photovoltaic poly-crystalline modules have a nominal power of 280 W with electric characteristics reported in Table 4-7.

Table 4-7- Electrical characteristics of PV panels

Photovoltaic panels	
Panel type	Poly-crystalline silicon
Area	1.627 m^2
Nominal Power	280 W
Voltage at max power	31 V
Current at max power	9.07 A
Short-circuit current	9.76 A
Open circuit voltage	38 V
Temperature coefficient of Isc	-0.31 %/°C
Temperature coefficient of Voc	0.05 %/°C
NOCT	45 °C

4.2.2.3 PV assisted heat pump with thermal storage

In order to achieve a high level of efficiency, and to highlight the importance of thermal storage, the air-conditioning plant of each building was replaced with a centralized air-to-water heat pump assisted by a photovoltaic plant supplying energy to inertial thermal storage. All the buildings are conditioned by fan-coils to be supplied by the centralized thermal storage volume. The main characteristics of the heat pump are reported in Table 4-8

Table 4-8- Main characteristics of the centralized air-to-water heat pump

Heat Pump		
Heat transfer fluid	Water	
Max supply temperature	60 °C	
Airflow rate	1500 l/s	
Heating	Nominal power	15.21 kW
	Power modulation range	7.1-15.9 kW
	Nominal COP	4.1
Cooling	Nominal power	15.69 kW
	Power modulation range	8.7-16.3 kW
	Nominal EER	4.9

This configuration still considers the presence of a PV plant, that instead of being dedicated to every single building, are supposed to form a unique electric generator at the service of the entire building aggregate in an optic of the energy community. The PV modules characteristics are the same as those reported in Table 4-7. Properties of the thermal storage are reported in Table 4-9. The saturation temperatures set for the boiler are respectively 45°C and 7°C for winter and summer, beyond which the eventual surplus is equally transferred to the grid.

Table 4-9- Characteristics of heat cylindrical storage tank

Storage tank	
Heat transfer fluid	Water
Specific heat capacity	4.182 kJ/kg K
Fluid density	992 Kg/m^3
Thermal conductivity of the fluid	0.62 W/m K
Max storage temperature	99 °C
Tank volume	3 m^3
Tank height	1 m
Number of tank nodes	5
Top loss coefficient	0.923 W/m^2 K
Bottom loss coefficient	0.923 W/m^2 K
Edge loss coefficient	0.923 W/m^2 K

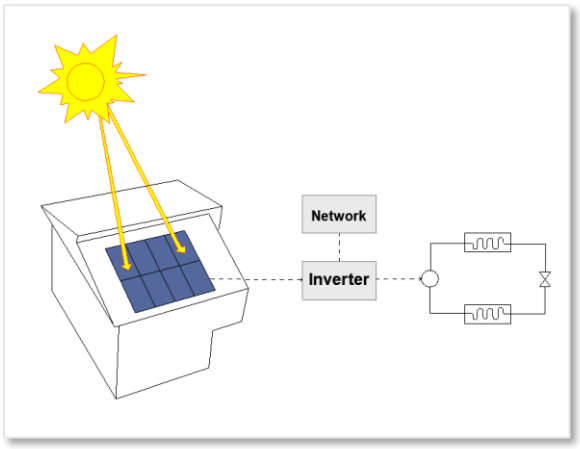

Figure 4-3- Schematization of the solar assisted heat-pump configuration

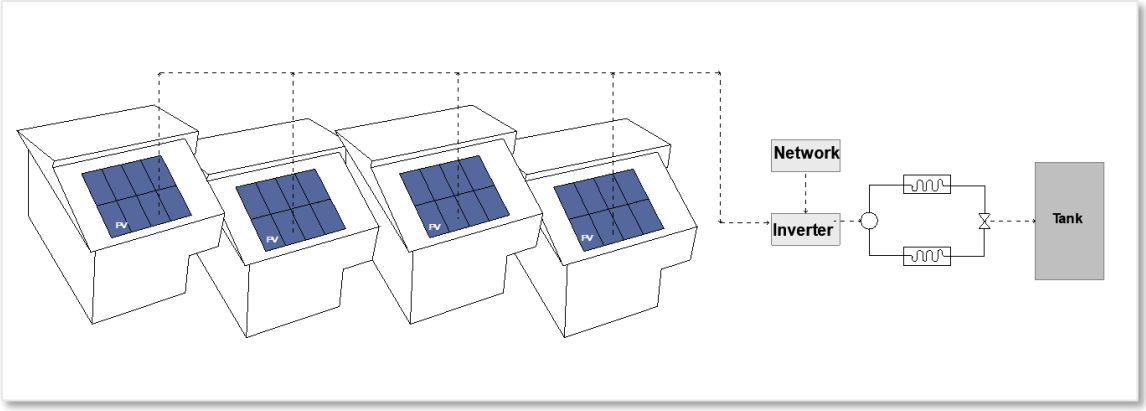

Figure 4-4- Schematization of a centralized solar assisted heat pump with thermal storage

In order to maximize and rationalize the use of the solar source, considering that in the optic of energy community the space available for the installation of a PV plant is not solely confined to the buildings roof area, in the case of centralized system two sizes of PV peak power were considered (12 kW and 16 kW) at a parity of storage tank volume, supposed to be available for the whole aggregate without defining separate plants for each building.

For all the considered plant solutions, the CO_2 emission to the atmosphere has been evaluated considering an emission factor of 0.427 kg CO_2 per kWh of energy produced considering the average thermoelectric production on the Italian territory [41]. The emission factor of natural gas was set as 2,75 kg of CO_2 per kg of burnt natural gas [42].

A final economic analysis is conducted to assess the monetary advantage of the use of the proposed interventions. For such evaluation the following parameters are supposed:

- Cost of electricity from the grid: 0.3 €/kWh.
- Revenue from electricity supplied to the grid: 0.09 €/kWh.
- Cost of natural gas: 1 €/Stm^3.

4.3 Results and discussion

4.3.1 Base case scenario

Figure 4-5 displays the monthly heating and cooling energy needs of the base case scenario for the four buildings belonging to the aggregate. As it can be appreciated, due to the similar geometric configuration, both heating and cooling need are quite similar for

the four buildings, with the two external (B1 and B4) and the two internal (B2 and B3) buildings showing in pair almost equal consumptions.

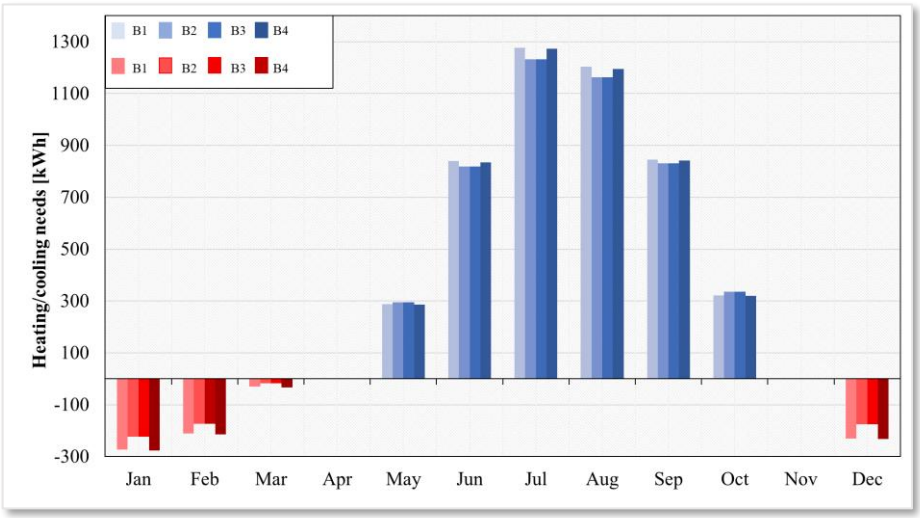

Figure 4-5- Monthly heating and cooling needs of the four buildings for the base case scenario

It is also possible to appreciate how for the considered Mediterranean climate, and for building with an adequate level of thermal insulation of the envelope, the cooling requirements are conspicuously superior than the heating ones. The maximum energy required for the heating season is 756.9 kWh (B4) whereas for the summer season is 4776.8 kWh (B1).

Considering the presence of the traditional boiler and the air-to-air heat pump, Figure 4-6 (left) shows the natural gas consumption to satisfy the winter energy demand and the associated CO_2 emissions into the atmosphere, and Figure 4-6 (right) shows the electric energy for the heat pump summer operations, alongside the associated kilograms of CO_2 emissions. Naturally, these results reflect the trend already observed in Figure 4-6 (left), where the natural gas consumption is almost equal, in pairs, for the four building, with a maximum of 48.63 kg (B1) found in January with a correspondent mass of 133.74 kg of emitted carbon dioxide. As regards the electricity absorption from the electrical grid for the heat pump operation, from Figure 4-6 (right) we can see how in July and August the request is high and similar, with a maximum of 952.2 kWh and a correspondent CO_2 emission of 406.4 kg.

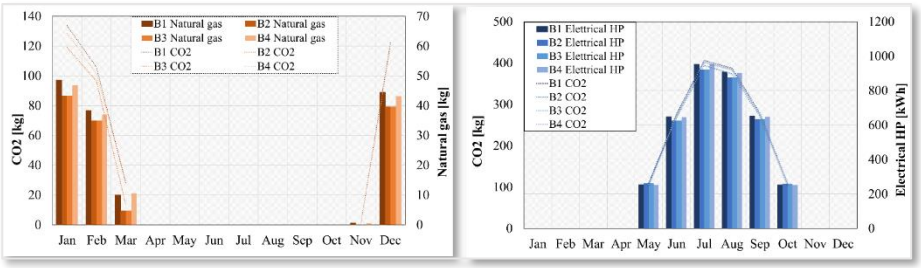

Figure 4-6- Natural gas consumption and CO_2 emissions for the heating service (left) and electrical energy consumption and CO_2 emissions for the cooling service (right) of the base case scenario.

Finally, the monthly total electrical consumption is shown in Figure 4-7, which is the sum of the electric load for house equipment and the request of electricity for the operation of the heat pump. Clearly, in winter months the values reported referring exclusively to the households since the heating service is provided by a boiler

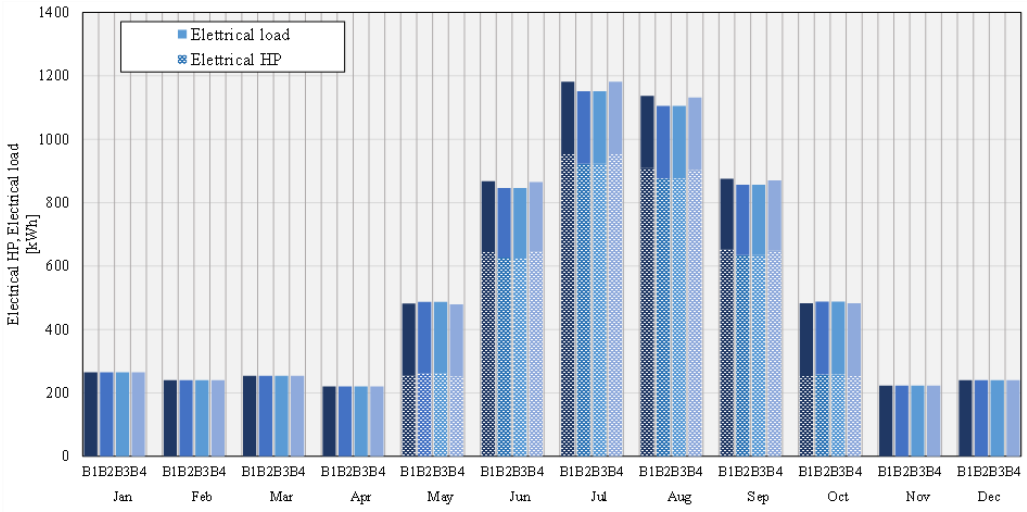

Figure 4-7 Total electric energy consumption for the four analysed buildings in the base case scenario.

Finally, Table 4-10 summarizes the main results obtained for the entire building aggregate.

Table 4-10- Summary of the energy and CO_2 results for the base case

	B1-B4
Heating [kWh]	2683.3
Cooling [kWh]	18878.4
CO_2 [kg]	12 400
Electrical HP [kWh]	14479.3
Electrical tot [kWh]	25666.5

4.3.2 Use of single solar assisted heat pumps

The first intervention supposes the replacement of the natural gas boiler and of the air-to-air HP in each building with an air-to-water HP that supplies the necessary thermal energy for both heating and cooling. Furthermore, for each house, a 3 kW peak PV plant was considered. Such a solution represents a conspicuous step toward a high-efficient and eco-friendly solution for the air-conditioning of dwellings, since the heat pump can provide heating and cooling load through the use of clean energy, and the use of electricity produced by the PV allows to increase the share of self-consumed renewable energy. The PV plant is of the grid-connected type and therefore exchanges energy with the national electric grid.

Table 4-8 shows for each building the electrical consumptions of the heat pump to satisfy the heating and cooling services. The greatest heating demand of 289 kWh is found for B1 house in January, where also the greatest cooling demand of 871 kWh in July is found due to the major exposed surface to solar radiation. Globally, the whole aggregate building requires a demand of 2573.8 kWh for heating and of 13017.4 kWh for cooling.

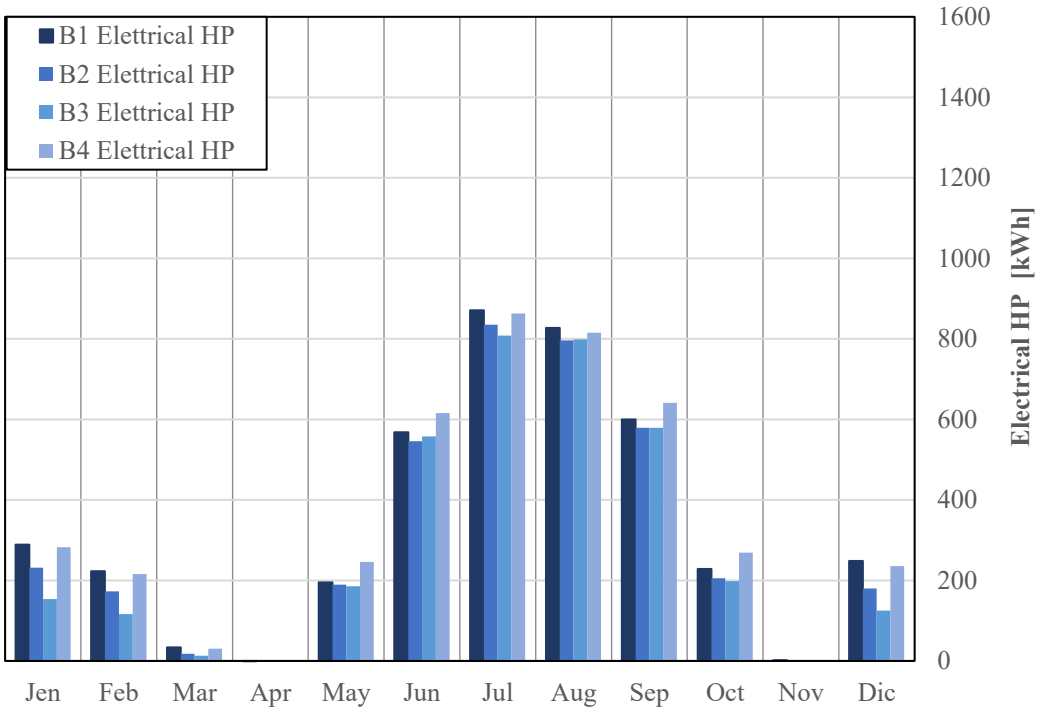

Figure 4-8- Electrical consumption for the heating service and cooling service for the single solar assisted heat pumps

Table 4-11- Electrical consumption for the heating service and cooling service single solar assisted heat pumps

Electrical Hp [kWh]												
	Jen	**Feb**	**Mar**	**Apr**	**May**	**Jun**	**Jul**	**Aug**	**Sep**	**Oct**	**Nov**	**Dec**
B1	289	223	34	0	195	568	871	827	600	228	2	248
B2	232	173	18	0	189	546	835	796	579	205	0	180
B3	154	116	13	0	185	558	808	799	579	198	0	125
B4	283	216	31	0	246	616	863	815	641	269	2	235
B1÷B4	**958**	**728**	**95**	**0**	**816**	**2287**	**3377**	**3237**	**2399**	**901**	**2**	**790**

When domestic users' electric loads are added to the heat pump electric requirements the total electric energy is reported in Figure 4-9. It can be seen how in intermediate seasons, such as April and November, the required electric energy is solely attribute to the domestic loads. The annual sum for the whole aggregate gives 7454 kWh for heating and 18444 kWh for cooling.

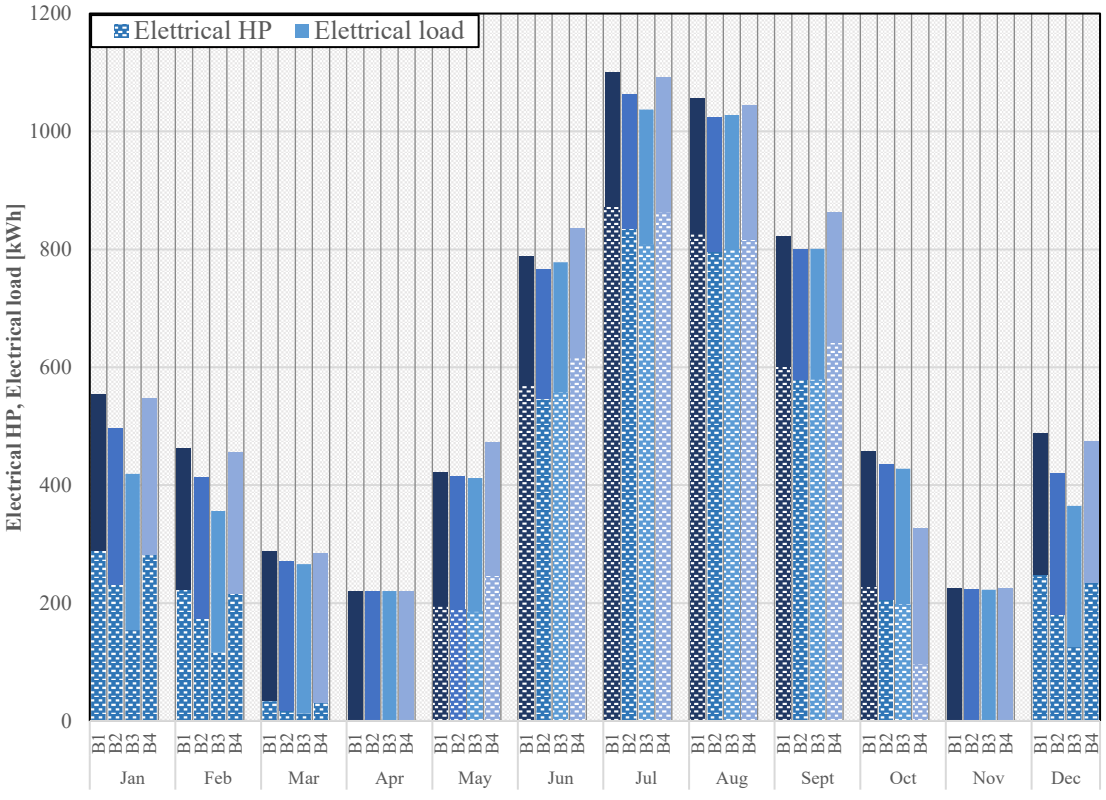

Figure 4-9- Total electric energy consumption for the four analysed buildings for the single solar assisted heat pumps

Considering the presence of the PV plant, thanks to the hourly simulation results, it is possible to account in detail for the electric energy produced by the plant and directly self-consumed by the users. Results of such computations are reported, in monthly summary, in Figure 4-10 along with the CO_2 emissions. The CO_2 emissions are computed considering only the share of electric energy requested from the heat pump and for the domestic loads withdrawn by the electric grid. The total amount of carbon dioxide produced for the four buildings accounts for 11434.2 kg.

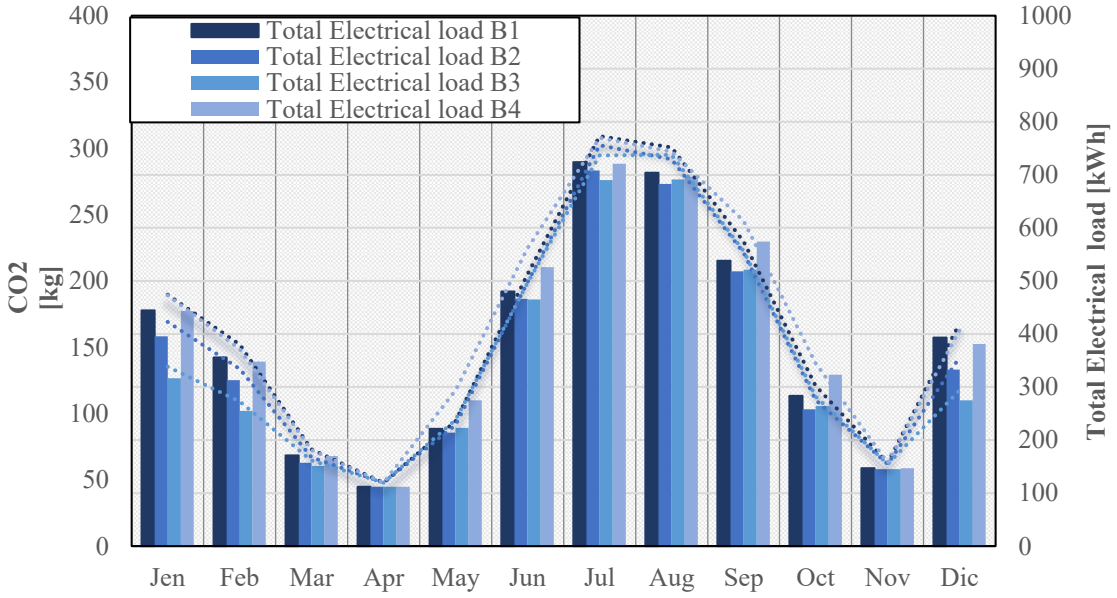

Figure 4-10- Net monthly total electric consumption, considering the PV self-consumed energy

Figure 4-11 shows, for each house, the amount of electricity produced and directly consumed, the amount produced but not consumed instantly and therefore supplied to the national grid, and finally the amount withdrawn from the grid. This last case occurs when the total electric load is greater than the photovoltaic production and/or when a lack of synchronism between demand and production occurs at certain times of the day. For B1 building we can see how the amount of 356 kWh of energy is produced and directly consumed in July against production of 583 kWh. In winter months, on the other hand, proportionally to the production, the self-consumed quota also decreases being of the order of about 100 kWh for all the houses, with a maximum value of 110 kWh self-consumed energy in March against the 155kWh fed into the grid.

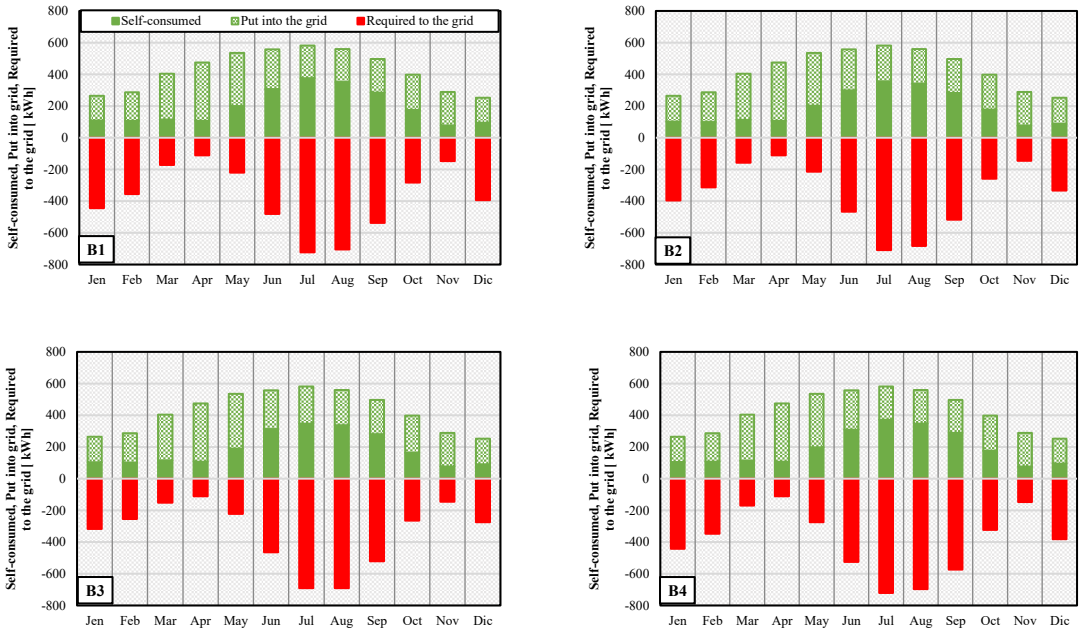

Figure 4-11-Monthly electric energy self-consumed, supplied and withdrawn from the national grid for the four different houses.

Finally, the monthly percentage of self-consumed energy, compared to the total PV production of all houses, is reported in Figure 4-12. The highest percentages of self-consumption are achieved in July and August (62 and 61% respectively) while the lower is found in April and November (23% and 27% respectively) because of the absence of air-conditioning demand. In the coldest winter months of December and January, however, the total self-consumed energy reached an appreciable threshold of 36% and 39% respectively.

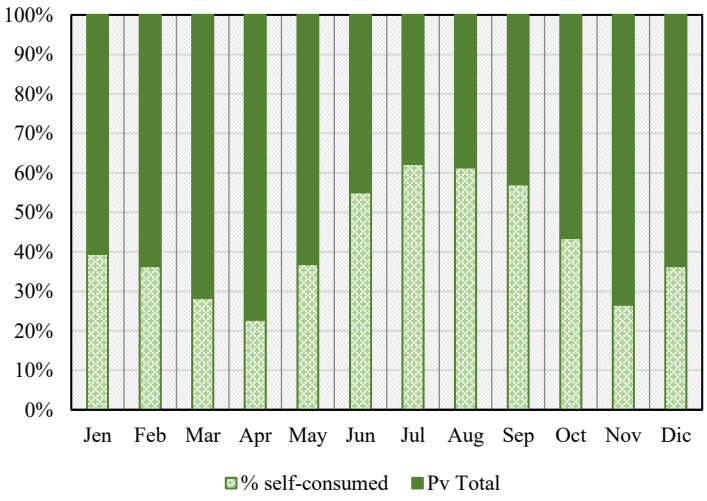

Figure 4-12- Monthly percentages of total self-consumed and produced electric energy for the whole building aggregate

The summary of the findings for the single PV assisted heat pumps scenario is reported in Table 4-12.

Table 4-12- Summary of the results for the single solar assisted heat pumps scenario

	B1-B4
Electrical tot [kWh]	17 700
CO_2 [kg]	7559
PV production [kWh]	20 404
PV consumption [kWh]	9079

4.3.3 Use of a centralized solar assisted heat pump with thermal storage

The second intervention supposes the replacement of the single heat pumps for each building, with a centralized heat pump combined with a thermal storage tank to supply the whole aggregate system. This solution allows to convert electricity into thermal energy using the heat pump, and to use it in deferred mode.

Figure 4-13 shows the total electric consumptions for the building aggregate heating and cooling, including the users' load and without considering the PV production. Again, for the heating period, the consumption is maximum in January where it assumes the value of 1960.7 kWh, while, in the cooling period, the highest consumption occurs in July where it assumes the value of 4073.6 kWh.

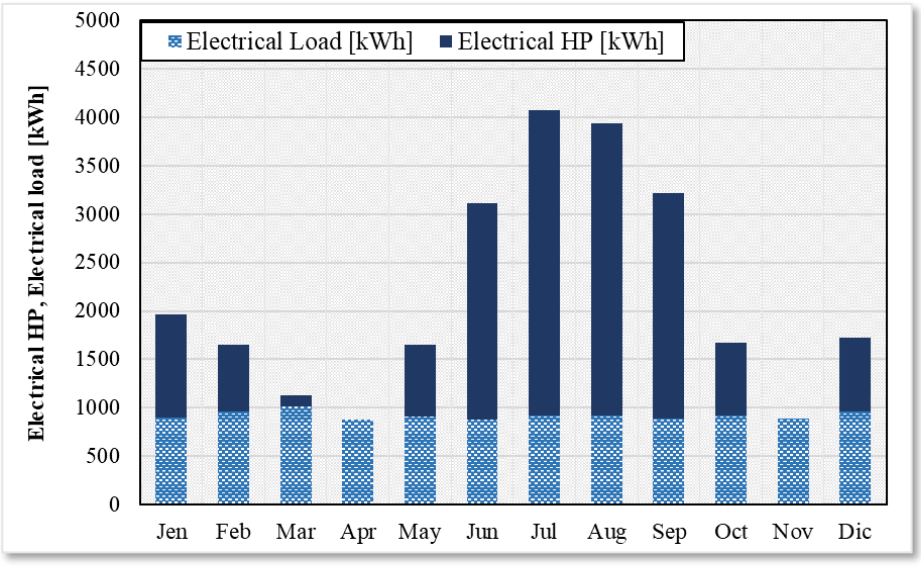

Figure 4-13-Total electric energy consumption for centralized solar assisted heat pump

The consumption related to the sole operation of the heat pump was compared with the case of single heat pumps for each building in Table 4-13, to highlight the

advantage of using a centralized heat pump that supplies a thermal storage. In almost the totality of the months (except for March) a reduction can be appreciated, being the highest, in absolute value, in July where the use of such system allowed to save 215 kWh.

Table 4-13- Comparison of the electric consumption of the heat pump

	Electrical Hp [kWh]											
	Jan	**Feb**	**Mar**	**Apr**	**May**	**Jun**	**Jul**	**Aug**	**Sep**	**Oct**	**Nov**	**Dec**
B1-B4 (Single)	958	728	95	0	816	2287	3377	3237	2399	901	2	790
B1-B4 (Centralized)	900	688	118	0	743	2236	3158	3022	2325	750	0	761
Reduction (kWh)	-58	-40	+23	0	-73	-51	-219	-215	-74	-151	-2	-29
Percentage reduction	-6%	-5%	+24%	0%	-9%	-2%	-6%	-7%	-3%	-15%	-100%	-3%

The monthly net total electric energy consumption for the two cases is reported in Figure 4-14, along with the associated CO_2 emissions. In both cases, the monthly trend is fairly similar, but greater reductions are naturally appreciated when a 16 kW PV plant is installed. Globally for the latter, the annual energy consumption amounted to 15 489 kWh against the 16 023.5 kWh for the 12 kW case. In terms of CO_2, the adoption of a greater PV size led to emissions of 6613.8 kg, 305 kg less than the smaller PV case.

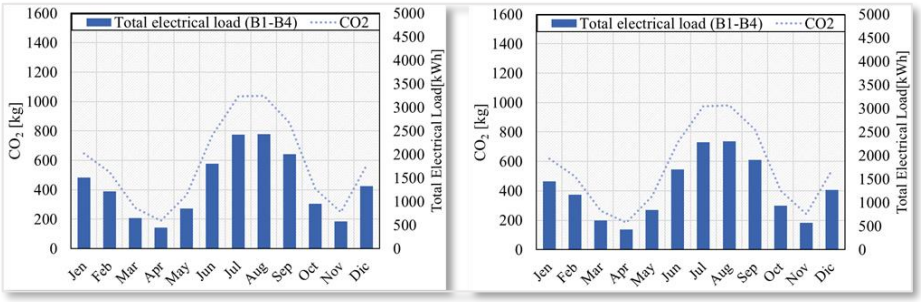

Figure 4-14- Net monthly total electric consumption and CO_2 emissions, considering the PV self-consumed energy with a 12-kW plant (left) and 16 kW plant (right).

Figure 4-15 reports the share of monthly PV electric energy self-consumed, supplied to the national grid and withdrawn from it to satisfy the total electric requirements.

For the 12-kW case, the self-consumed energy ranged from the minimum of 307 kW in November, to the maximum of 1648 kWh in July. The share withdrawn from the grid reached the highest value in August (2432 kWh) whereas the lowest value was found in April (447 kWh). Annually the PV plant produced 20416 kWh. If a PV plant of 16 kW is considered, the yearly production rises to 28568 kWh and the share of self-consumed

energy reaches a maximum of 1788 kWh again in July. The share withdrawn from the grid was reduced to 2299 kWh for the most requiring month of August and to 431 kWh in April. Figure 4-15 reports the share of monthly PV electric energy self-consumed, supplied to the national grid and withdrawn from it to satisfy the total electric requirements.

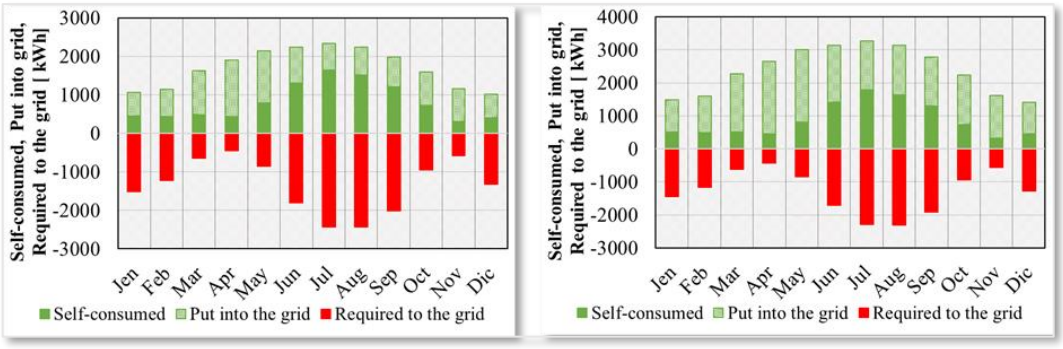

Figure 4-15- Monthly electric energy self-consumed, supplied and withdrawn from the national grid for the whole aggregate with a 12-kW plant (left) and 16 kW plant (right).

For the 12-kW case, the self-consumed energy ranged from the minimum of 307 kW in November, to the maximum of 1648 kWh in July. The share withdrawn from the grid reached the highest value in August (2432 kWh) whereas the lowest value was found in April (447 kWh). Annually the PV plant produced 20416 kWh. If a PV plant of 16 kW is considered, the yearly production rises to 28568 kWh and the share of self-consumed energy reaches a maximum of 1788 kWh again in July. The share withdrawn from the grid was reduced to 2299 kWh for the most requiring month of August and to 431 kWh in April.

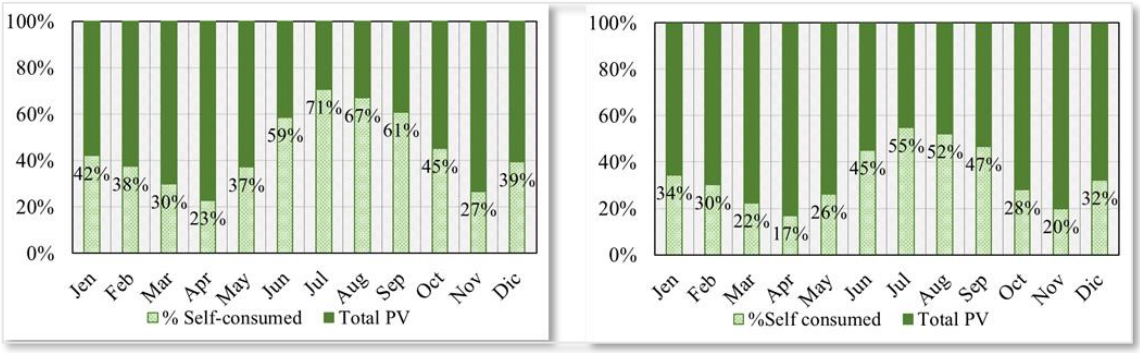

Figure 4-16- Monthly percentages of total self-consumed and produced electric energy for the whole building aggregate with a 12-kW plant (left) and 16 kW plant (right).

In Figure 4-16 the monthly percentages of self-consumed and produced electric energy are reported. In both cases, the lowest self-consumption is found in April and November where there is a very low demand for air-conditioning and the PV plant supplies exclusively the users' electric loads. When the PV plant is increased from 12 kW to 16 kW the self-consumption raises to 71% in July, falling to 59 % in June, while in the coldest winter months the percentage is about 40%.

Data in Table 4-14 shows the percentage increase of electric energy self-consumption compared to the previous case of single heat pumps without thermal storage. Even at a parity of PV peak power (12 kW) the centralized system with thermal storage can rationalize the energy use, providing a percentage increase of up to 14%. If the PV peak power is augmented to 16 kW the self-consumption share increases by 22% and 24% in January and December respectively, and by 23% in July.

Table 4-14- Percentage increase of electric self-consumption compared to the single heat pump use

Percentage increase of single HP	**Jan**	**Feb**	**Mar**	**Apr**	**May**	**Jun**	**Jul**	**Aug**	**Sep**	**Oct**	**Nov**	**Dec**
12 kW	7%	3%	5%	0%	1%	7%	14%	9%	6%	4%	0%	8%
16 kW	22%	16%	11%	4%	2%	15%	23%	19%	15%	5%	4%	24%

The summary of the findings for the centralized solar assisted heat pumps scenario is reported in Table 4-15.

Table 4-15 Summary of the Results for the Centralized Solar Assisted Heat Pumps Scenario

	PV 12 kW	**PV 16kW**
Electrical tot [kWh]	16203.5	15489
CO_2 [kg]	6918.9	6613.8
PV production [kWh]	20416.0	28568.4
PV consumption [kWh]	9686.9	10401.4

4.4 Economic evaluations

Finally, to evaluate the economic advantages of the proposed centralized system, a revenue estimation is carried out considering the operational cost associated with the natural gas for the base case scenario, the cost of electricity withdrawn from the grid, as

well as the economic revenue from selling the surplus PV energy to the grid. Figure 4-17shows the monthly total cost for the heating and cooling services and users' electric loads. The base case scenario offers the highest cost in each month since it relies on a traditional boiler for heating and there is not any renewable source. Moving to the case of the use of single heat pumps for air-conditioning with separate PV plants, a decrement of monthly cost can be observed, which becomes drastic in summer months. In the coldest month of January, the total expense dropped from 563.35 € of the base case to 422.26 € for single heat pumps, to 347.71 € for the centralized plant with 16 kW of PV power. In the hottest month of July, the expenses were for the same cases: 2014.36 €, 773.50 €, and 552.95 € respectively.

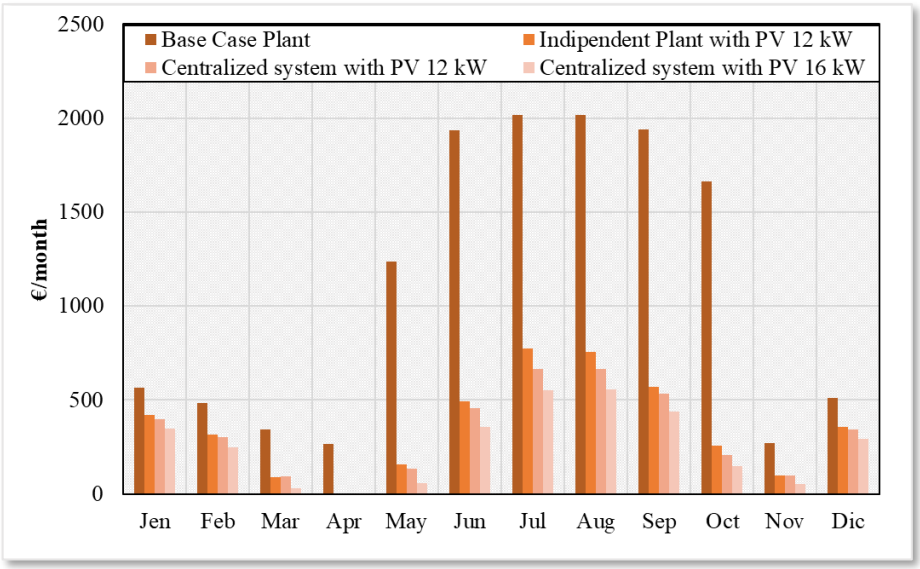

Figure 4-17- Monthly total cost for the heating and cooling services and electric loads demand.

The economic advantage was found to be more evident for the centralized heat pump with the highest PV peak power, where the economic savings were higher than 38% in winter months, and higher than 73% in summer months. On an annual level, the heating, cooling and electric loads energy consumptions reduced from 13 246.70 € of the base case scenario to 3 081.15 € for the centralized HP with 16 kW PV plant. Results confirmed the indisputable supremacy of heat pumps as generators, especially when coupled with a renewable energy source.

4.5 Conclusions

Solar assisted heat pumps have become a promising technology to improve energy efficiency in buildings, allowing lower primary energy demands and CO_2 emissions. This paper investigated the energy, economic and environmental advantages of the use of PV assisted heat pumps for building air-conditioning. With reference to a building aggregate composed of four houses, an intervention of energy efficiency was supposed, by replacing the traditional generators with PV assisted heat pumps. Furthermore, to highlight the benefits of the use of thermal storage, in an optic of energy community, the single heat pumps were supposed to be replaced by a centralized one that works on a thermal storage, which, in turn, supplies the whole building aggregate. The same storage was further considered as a sui-generis system where electricity surplus is transformed into thermal energy, more easily to employ in differed manner.

Hourly dynamic simulations in TRNSYS environment, showed that when the traditional generators are replaced with single heat pumps thanks to the share of renewable energy provided by the aerothermal source combined with the electricity production from the PV plant, a high level of energy efficiency can be achieved with a percentage of self-consumed energy from PV, on an annual level, of 44% and with a conspicuous reduction of CO_2 emissions that dropped to 7 559 kg compared to the 12 400 kg of the case base scenario.

More appealing appeared the use of a centralized heat pump combined with thermal storage to supply the four buildings, which further allowed to reduce the net total electric consumption from 17 700 kWh of the previous case to 16 203.5 kWh with the same PV plant size (12 kW) and to 15 489.1 kWh when a PV plant of 16 kW is used. A higher level of energy efficiency was also detected with a monthly self-consumption percentage that reached 71% in July for the 16 kW PV. From an economic point of view, the total expenses for heating, cooling and electric loads amounted to 13 246.70 € for the base case scenario and fell to 3 081.15 for the centralized HP with a yearly economic reduction of 76.7%.

Conclusions are obtained for a Mediterranean climate, that is characterized by a conspicuous amount of solar radiation. If the same procedure is applied to colder and more continental climates results may be different and, in particular, a reduction of the economic and environmental advantage produced by the PV plant is to be expected.

The study allowed to conclude that the use of a centralized heat pump with a thermal storage system, in an optic of energy community, can be advantageous for different reasons, providing relevant energy and economic savings and allowing to design of a generator with a lower power when compared to the use of single heat pumps for each building.

4.6 References

[1] V. Telichenko, A. Benuzh, G. Eames, E. Orenburova, and N. Shushunova, "Development of Green Standards for Construction in Russia," in Procedia Engineering, 2016. https://doi.org/10.1016/j.proeng.2016.08.233

[2] S. Korol, N. Shushunova, and T. Shushunova, "Indicators of the resource efficiency development in Russia," in MATEC Web of Conferences, 2018. https://doi.org/10.1051/matecconf/201819305075

[3] M. I. Al-Amayreh, A. Alahmer, and A. Manasrah, "A novel parabolic solar dish design for a hybrid solar lighting-thermal application," Energy Reports, 2020. https://doi.org/10.1016/j.egyr.2020.11.063

[4] A. A. Manasrah, S. Alkhalil, and M.Masoud, "Investigation of multi-way forced convective cooling on the backside of solar panels," Int. J. Energy Convers., 2020. https://doi.org/10.15866/irecon.v8i5.19516

[5] A. Manasrah, A. Al Zyoud, and E. Abdelhafez, "Effect of color and nano film filters on the performance of solar photovoltaic module," Energy Sources, Part A Recover. Util. Environ. Eff., 2021.https://doi.org/10.1080/15567036.2019.1631907

[6] M. Nemś and J. Kasperski, "Experimental investigation of concentrated solar air-heater with internal multiple-fin array," Renew. Energy, 2016. https://doi.org/10.1016/j.renene.2016.06.038

[7] M. Nemś, J. Kasperski, A. Nemś, and A. Bać, "Validation of a new concept of a solar air heating system with a long-term granite storage bed for a single-family house," Appl. Energy,2018.https://doi.org/10.1016/j.apenergy.2018.02.020

[8] A. Nemś and M. Nemś, "Analysis and selection criteria of photovoltaic panels for DHW," in E3S Web of Conferences, 2017.https://doi.org/10.1051/e3sconf/20171303003

[9] A. Bać, M. Nemś, A. Nemś, and J. Kasperski, "Sustainable integration of a solar heating system into a single-family house in the climate of Central Europe-A case study," Sustain., 2019. https://doi.org/10.3390/su11154167

[10] M. Nemś, A. Manikowska, and A. Nem Ś, "Linear concentrating collector as an air heater in the heating system of building in Polish climatic conditions," in E3S Web of Conferences,2016. https://doi.org/10.1051/e3sconf/20161000064

[11] G. Ulpiani, S. Summa, and C. di Perna, "Sunspace coupling with hyper-insulated buildings: Investigationof the benefits of heat recovery via controlled mechanical ventilation," Sol. Energy, 2019.https://doi.org/10.1016/j.solener.2019.01.084

[12] G. Ulpiani, E. Di Giuseppe, C. Di Perna, M. D'Orazio, and M. Zinzi, "Thermal comfort improvement in urban spaces with water spray systems: Field measurements and survey," Build. Environ., 2019.https://doi.org/10.1016/j.buildenv.2019.04.007

[13] F. Stazi, G. Ulpiani, M. Pergolini, C. Di Perna, and M. D'Orazio, "The role of wall layers properties on the thermal performance of ventilated facades: Experimental investigation on narrow-cavity design," Energy Build., 2020. https://doi.org/10.1016/j.enbuild.2019.109622

[14] S. Cascone, A. Gagliano, T. Poli, and G. Sciuto, "Thermal performance assessment of extensive green roofs investigating realistic vegetation-substrate configurations," Build. Simul., 2019.https://doi.org/10.1007/s12273-018-0488-y

[15] S. Cascone, "Green roof design: State of the art on technology and materials," Sustainability (Switzerland). 2019. https://doi.org/10.3390/su11113020
[16] A. Gagliano, F. Nocera, M. Detommaso, and G. Evola, "Thermal Behavior of an Extensive Green Roof: Numerical Simulations and Experimental Investigations," Int. J. Heat Technol., 2016.https://doi.org/10.18280/ijht.35sp0206
[17] S. Cascone, G. Evola, C. Leone, and G. Sciuto, "Vertical greenery systems for the energy retrofitting of buildings in Mediterranean climate: A case study inCatania, Italy," in IOP Conference Series: Materials Science and Engineering, 2018. https://doi.org/10.1088/1757-899x/415/1/012054
[18] E. Korol, N. Shushunova, O. Feoktistova, T. Shushunova, and O. Rubtsov, "Technical and economical factors in green roof using to reduce the aircraft noise," in MATEC Web of Conferences, 2018. https://doi.org/10.1051/matecconf/201817001081
[19] E. Korol and N. Shushunova, "Benefits of a Modular Green Roof Technology," in Procedia Engineering, 2016. https://doi.org/10.1016/j.proeng.2016.08.673
[20] S. Korol, N. Shushunova, and T. Shushunova, "Innovation technologies in Green Roof systems," in MATEC Web of Conferences, 2018. https://doi.org/10.1051/matecconf/201819304009
[21] P. Bevilacqua, A. Morabito, R. Bruno, V. Ferraro, and N. Arcuri, "Seasonal performances of photovoltaic cooling systems in different weather conditions," J. Clean. Prod., 2020.https://doi.org/10.1016/j.jclepro.2020.122459
[22] T. Blanusa, M. M. Vaz Monteiro, F. Fantozzi, E. Vysini, Y. Li, and R. W. F. Cameron, "Alternatives to Sedum on green roofs: Can broad leaf perennial plants offer better 'cooling service'?," Build. Environ., 2013. https://doi.org/10.1016/j.buildenv.2012.08.011
[23] C. Gargari, C. Bibbiani, F. Fantozzi, and C. A. Campiotti, "Environmental Impact of Green Roofing: The Contribute of a Green Roof to the Sustainable use of Natural Resources in a Life Cycle Approach," Agric.Agric. Sci. Procedia, 2016. https://doi.org/10.1016/j.aaspro.2016.02.087
[24] A. Gagliano, M. Detommaso, F. Nocera, and G. Evola, "A multi-criteria methodology for comparing the energy and environmental behavior of cool, green and traditional roofs," Build. Environ., 2015. https://doi.org/10.1016/j.buildenv.2015.02.043
[25] V. Costanzo, G. Evola, and L. Marletta, "Energy savings in buildings or UHI mitigation? Comparison between green roofs and cool roofs," Energy Build., 2016. https://doi.org/10.1016/j.enbuild.2015.04.053
[26] G. Evola et al., "UHI effects and strategies toimprove outdoor thermal comfort in dense and old neighbourhoods," in Energy Procedia, 2017.https://doi.org/10.1016/j.egypro.2017.09.589
[27] K. Hami, B. Draoui, and O. Hami, "The thermal performances of a solar wall," Energy, vol. 39, no. 1, pp. 11–16, 2012. https://doi.org/10.1016/j.energy.2011.10.017
[28] F. Stazi, A. Mastrucci, and C. Di Perna, "The behaviour of solar walls in residential buildings with different insulation levels: An experimental and numerical study," Energy Build., vol. 47, pp. 217–229, 2012.https://doi.org/10.1016/j.enbuild.2011.11.039

[29] P. Bevilacqua, F. Benevento, R. Bruno, and N. Arcuri, "Are Trombe walls suitable passive systemsfor the reduction of the yearly building energy requirements?," Energy, 2019. https://doi.org/10.1016/j.energy.2019.07.003
[30] J. Błotny and M. Nemś, "Analysis of the impact of the constructionof a trombe wall on the thermal comfort in a building located in wroclaw, Poland," Atmosphere (Basel)., 2019.https://doi.org/10.3390/atmos10120761
[31] J. Szyszka, "Simulation of modified Trombe wall," in E3S Web of Conferences, 2018. https://doi.org/10.1051/e3sconf/20184900114
[32] J. Szyszka, P. Bevilacqua, and R. Bruno, "An innovative trombe wall for winter use: The thermo-diode trombe wall," Energies, 2020.https://doi.org/10.3390/en13092188
[33] J. Szyszka, "Experimental evaluation of the heat balance of an interactive glass wall in a heating season," Energies, 2020. https://doi.org/10.3390/en13030632
[34] H. Akeiber et al., "A review on phase change material (PCM) for sustainable passive cooling in building envelopes," Renew. Sustain. Energy Rev., vol.60, pp. 1470–1497, 2016. https://doi.org/10.1016/j.rser.2016.03.036
[35] N. Soares, J. J. Costa, A. R. Gaspar, and P. Santos, "Review of passive PCM latent heat thermal energy storage systems towards buildings' energy efficiency," Energy and Buildings. 2013.https://doi.org/10.1016/j.enbuild.2012.12.042
[36] A. De Gracia and L. F. Cabeza, "Phase change materials and thermal energy storage for buildings," Energy and Buildings. 2015.https://doi.org/10.1016/j.enbuild.2015.06.007
[37] E. M. Alawadhi, "Thermal analysis of a building brick containingphase change material," Energy Build., 2008. https://doi.org/10.1016/j.enbuild.2007.03.001
[38] L. F. Cabeza, C. Castellón, M. Nogués, M. Medrano, R. Leppers, and O. Zubillaga, "Use of microencapsulated PCM in concrete walls for energy savings," Energy Build., 2007. https://doi.org/10.1016/j.enbuild.2006.03.030
[39] A. Ramos, M. A. Chatzopoulou, I. Guarracino, J. Freeman, and C. N. Markides, "Hybrid photovoltaic-thermal solar systems for combined heating, cooling and power provision in the urban environment," Energy Convers. Manag., 2017. https://doi.org/10.1016/j.enconman.2017.03.024
[40] M. S. Bukerand S. B. Riffat, "Solar assisted heat pump systems for low temperature water heating applications: A systematic review," Renewable and Sustainable Energy Reviews. 2016.https://doi.org/10.1016/j.rser.2015.10.157
[41] M. Noro, R. Lazzarin, and G. Bagarella, "Advancements in Hybrid Photovoltaic-thermal Systems: Performance Evaluations and Applications," in Energy Procedia, 2016. https://doi.org/10.1016/j.egypro.2016.11.063
[42] A. Chauhan, V. V. Tyagi, and S. Anand, "Futuristic approach for thermal management in solar PV/thermal systems with possible applications," Energy Conversion and Management. 2018.https://doi.org/10.1016/j.enconman.2018.02.008
[43] T. Beck, H. Kondziella, G. Huard, and T. Bruckner, "Optimal operation, configuration and sizing of generation and storage technologies for residential heat pump systems in the spotlight of self-consumption of photovoltaic electricity," Appl. Energy, 2017.https://doi.org/10.1016/j.apenergy.2016.12.041
[44] C. Protopapadaki and D. Saelens, "Heat pump and PV impact on residential low-voltage distribution grids as a function of building and district properties," Appl. Energy, 2017. https://doi.org/10.1016/j.apenergy.2016.11.103

[45] R. Thygesen and B. Karlsson, "An analysis on how proposed requirements for near zero energy buildings manages PV electricity in combination with two different types of heat pumps and its policy implications –A Swedish example," Energy Policy, 2017.https://doi.org/10.1016/j.enpol.2016.11.025
[46] G. B. M. A. Litjens, E. Worrell, and W. G. J. H. M. van Sark, "Lowering greenhouse gas emissions in the built environment by combining ground source heat pumps, photovoltaics and battery storage," Energy Build., 2018. https://doi.org/10.1016/j.enbuild.2018.09.026
[47] J. Ji, K. Liu, T. tai Chow, G. Pei, W. He, and H. He, "Performance analysis of a photovoltaic heat pump," Appl. Energy, 2008. https://doi.org/10.1016/j.apenergy.2008.01.003
[48] Y. H. Kuang and R. Z. Wang, "Performance of a multi-functional direct-expansion solarassisted heat pump system," Sol. Energy, 2006. https://doi.org/10.1016/j.solener.2005.06.003
[49] Y. W. Li, R. Z. Wang, J. Y. Wu, and Y. X. Xu, "Experimental performance analysis on a direct-expansion solar-assisted heat pump water heater," Appl. Therm. Eng., 2007. https://doi.org/10.1016/j.applthermaleng.2006.08.007
[50] A. Moreno-Rodríguez, A. González-Gil, M. Izquierdo, and N. Garcia-Hernando, "Theoretical model and experimental validation of a direct-expansion solar assisted heat pump for domestic hot water applications," Energy, 2012. https://doi.org/10.1016/j.energy.2012.07.021
[51] M. Mohanraj, S. Jayaraj, and C. Muraleedharan, "Performance prediction of a direct expansion solar assisted heat pump using artificial neural networks," Appl. Energy, 2009. https://doi.org/10.1016/j.apenergy.2009.01.001
[52] Q. Wang, Y. Q. Liu, G. F. Liang, J. R. Li, S. F. Sun, and G. M. Chen, "Development and experimental validation of a novel indirect-expansion solar-assisted multifunctional heat pump," Energy Build., 2011. https://doi.org/10.1016/j.enbuild.2010.09.013
[53] S. J. Sterling and M. R. Collins, "Feasibility analysis of an indirect heat pump assisted solar domestic hot water system," Appl. Energy, 2012. https://doi.org/10.1016/j.apenergy.2011.05.050
[54] K. Bakirci and B. Yuksel, "Experimental thermal performance of a solar source heat-pump system for residential heating in cold climate region," Appl. Therm. Eng., 2011. https://doi.org/10.1016/j.applthermaleng.2011.01.039
[55] R. Yumrutaş and M. Ünsal, "Energy analysis and modeling of a solar assisted house heating system with a heat pump and an underground energy storage tank," Sol. Energy, 2012. https://doi.org/10.1016/j.solener.2012.01.008
[56] S. P. Aly, N. Barth, B. W. Figgis, and S. Ahzi, "A fully transient novel thermal model for in-field photovoltaic modules using developed explicit and implicit finite difference schemes," J. Comput. Sci., 2018.https://doi.org/10.1016/j.jocs.2017.12.013
[57] V. Badescu, "Model of a thermal energy storage device integrated into a solar assisted heat pump system for space heating," Energy Convers. Manag., 2003. https://doi.org/10.1016/s0196-8904(02)00184-x
[58] R. S. Kamel, A. S. Fung, and P. R. H. Dash, "Solar systems and their integration with heat pumps: A review," Energy and Buildings. 2015.https://doi.org/10.1016/j.enbuild.2014.11.030
[59] M. Pinamonti, I. Beausoleil-morrison, A. Prada, and P. Baggio, "Water-to-water heat pump integration in a solar seasonal storage system for space heating and

domestic hot water production of a single-family house in a cold climate," Sol. Energy, vol. 213, no. August 2020, pp. 300–311, 2021. https://doi.org/10.1016/j.solener.2020.11.052

[60] C. Kutlu, Y. Zhang, T. Elmer, Y. Su, and S. Riffat, "A simulation study on performance improvement of solar assisted heat pump hot water system by novel controllable crystallization of supercooled PCMs," Renew. Energy, 2020. https://doi.org/10.1016/j.renene.2020.01.090

[61] N. Arcuri, R. Bruno, and C. Carpino, "PV Driven Heat Pumps for the Electric Demand-Side Management: Experimental Results of a Demonstrative Plant," in Proceedings -2018 IEEE International Conference on Environment and Electrical Engineering and 2018 IEEE Industrial and Commercial Power Systems Europe, EEEIC/I and CPS Europe 2018, 2018. https://doi.org/10.1109/eeeic.2018.8493492

[62] G. Alva, Y. Lin, and G. Fang, "An overview of thermal energy storage systems," Energy. 2018. https://doi.org/10.1016/j.energy.2017.12.037

[63] S. Pintaldi, C. Perfumo, S. Sethuvenkatraman, S. White, and G. Rosengarten, "A review of thermal energy storage technologies and control approaches for solar cooling," Renewable and Sustainable Energy Reviews. 2015. https://doi.org/10.1016/j.rser.2014.08.062

[64] J. Lizana, R. Chacartegui, A. Barrios-Padura, and J. M. Valverde, "Advances in thermal energy storage materials and their applications towards zero energy buildings: A critical review," Applied Energy. 2017. https://doi.org/10.1016/j.apenergy.2017.06.008

[65] H. Zhang, J. Baeyens, G. Cáceres, J. Degrève, and Y. Lv, "Thermal energy storage: Recent developments and practical aspects," Progress in Energy and Combustion Science. 2016. https://doi.org/10.1016/j.pecs.2015.10.003

[66] R. Parameshwaran, S. Kalaiselvam, S. Harikrishnan, and A. Elayaperumal, "Sustainable thermal energy storage technologies for buildings: A review," Renewable and Sustainable Energy Reviews. 2012. https://doi.org/10.1016/j.rser.2012.01.058

[67] S. Bechtel, S. Rafii-Tabrizi, F. Scholzen, J. R. Hadji-Minaglou, and S. Maas, "Influence of thermal energy storage and heat pump parametrization for demand-side-management in a nearly-zero-energy-building using model predictive control," Energy Build., 2020. https://doi.org/10.1016/j.enbuild.2020.110364

[68] C. Schellenberg, J. Lohan, and L. Dimache, "Comparison of metaheuristic optimisation methods for grid-edge technology that leverages heat pumps and thermal energy storage," Renew. Sustain. Energy Rev., 2020. https://doi.org/10.1016/j.rser.2020.109966

[69] D. Marini, R. A. Buswell, and C. J. Hopfe, "Sizing domestic air-source heat pump systems with thermal storage under varying load shifting strategies," Appl. Energy, 2019. https://doi.org/10.1016/j.apenergy.2019.113811

[70] P. Fitzpatrick, F. D'Ettorre, M. De Rosa, M. Yadack, U. Eicker, and D. P. Finn, "Influence of electricity prices on energy flexibility of integrated hybrid heat pump and thermal storage systems in a residential building," Energy Build., 2020. https://doi.org/10.1016/j.enbuild.2020.110142

[71] F. D'Ettorre, M. De Rosa, P. Conti, D. Testi, and D. Finn, "Mapping the energy flexibility potential of single buildings equipped with optimally-controlled heat pump, gas boilersand thermal storage," Sustain. Cities Soc., 2019. https://doi.org/10.1016/j.scs.2019.101689

[72] Italian Unification Institution, UNI TS 11300-1: Energy performance of buildings -Part 1: Evaluation of energy need far space heating and cooling. 2014. https://doi.org/10.3403/30133624

[73] A. M. Massimo Gallanti, Walter Grattieri, Simone Maggiore, "Analisi ed evoluzione negli anni dellecurve di carico dei clienti domestici," L'Energia Elettr., vol. 89, no. 6, 2012.

[74] N. N. S. for the P. of the E. (SNPA) Institute for Environmental Protection and Research (ISPRA), Fattori di emissione atmosferica di gas a effetto serra nel settore elettrico nazionale e nei principali Paesi Europei. 2020.

[75] A. Fong, Simon James, Dey, Nilanjan, Joshi, ICT Analysis and applications: Proceedings of ICT4SD, SPRINGER, 2019. Springer Singapore, 2020.https://doi.org/10.1007/978-981-15-0630-7Received on 22-10-2020Accepted on 18-12-2020Published on 30-12-2020DOI: https://doi.org/10.15377/2409-9821.2020.07.7

5 Energy evaluations of a new plant configuration for solar assisted heat pumps in cold climates.

Abstract

Heat pumps in buildings allow for limiting CO_2 emissions by exploiting directly the renewable energy available in the external environment (aerothermal, hydrothermal and geothermal sources). Moreover, other renewable technologies such as active solar systems can be integrated easily. This combination not only increases the share of primary energy provided by renewable sources for heating/cooling but also improves the heat pump performance indices. Nevertheless, in cold climates, air-water heat pumps should be equally penalized due to the unfavourable out-door air temperature. Conversely, a water-water heat pump connected with a solar tank and thermal solar collectors overcome this issue. Indeed, the higher temperature attainable in the cold source allows for reaching greater COPs, and when the solar tank temperature level is enough, emitters can be directly supplied avoiding the absorption of electric energy. In this paper, this plant configuration in which a further tank after the heat pump was considered to manage the produced thermal energy, is investigated. Proper control strategies have been developed to increase the renewable share. Regarding a reference residential building located in Milan, for which the water-water heat pump was sized properly, a parametric study carried out in TRNSYS by varying solar tank volume and collecting surface, has allowed for identifying the optimal system configuration. A renewable share ranging between 54% and 61% as a function of the collecting surface and the storage volume, and an average seasonal coefficient of performance (SCOP) over 4, were detected. Regarding two common heating plant configurations using an assisted PV air-to-water heat pump and a gas boiler, the optimal solution allows for limiting CO_2 emissions of 33% and 53% respectively.

5.1 Introduction

The environmental challenge, aimed at combating dependence on fossil fuels, pollution and CO_2 emission, occupies a prominent place in the world panorama [1]. On the other hand, the energy demand growth has to convey energy consumption towards a sustainable development model that promotes renewable energy sources [2]. In this con-

text, the construction sector plays a crucial role because it impacts considerably on the external environment, being responsible in the EU for 39.7% of the energy consumption of final uses and 36% of the greenhouse gas emissions [3]. In this field, a pragmatic solution that limits these percentages, can be given by heat pumps [4]. Indeed, these devices can lead to exploiting renewable energy sources, including aerothermal, hydrothermal, geo-thermal and solar energy [5]. In the latter case, heat pumps are integrated with active solar systems to obtain the so-called "Solar-assisted Heat Pumps" (SAPH). In the literature several studies concerning SAHP used for heating, cooling and domestic hot water production, are available. Yi Fan et al. have carried out a critical overview of research focused on SAHP. They have found that the principal weaknesses are: unsatisfactory energy performance at low temperatures, difficulty to couple solar collectors to reduce the absorption of electric energy and the lack of synchronism between thermal load demand and solar source availability for heating purposes [6]. Liang et al. studied the performance of a new air-source SAHP for building heating by TRNSYS simulations. The coefficient of performance (COP) of the air source heat pump increased with the solar collector area increase and, in the whole heating season, 40 m^2 of solar collector allowed for saving 453.43 kWh [7]. L.Xu et al. have analysed a system that combines an air-source heat pump connected to a storage tank. The water is also heated by a field of solar collector, to use both for DHW and space heating. The model was successively validated by experimental data. The authors found that the system performance is affected respectively by the outdoor air temperature, the tank volume and collector surface area [8]. SAHP system can be integrated with thermal solar collectors, to use as the heat source, but also with photovoltaic (PV) panels to supply electricity, also in hybrid configurations. For instance, Baker et al. have modelled in TRNSYS a system composed of a ground source heat pump (GSHP) coupled with a field of 25 m^2 of Photovoltaic Thermo (PV/T) panels connected to a storage tank to use directly for space heating and DHW production, or send to the evaporator of the GSHP. They found that the system is able to cover the whole demand both for heating and for the DHW [9].

According to the different integration modalities, SAHPs combined with thermal so-lar collectors are classified as direct (DX-SAHP) and indirect expansion solar-assisted heat pumps (IDX-SAHP). In the first case, thermal solar collectors and the heat pump evaporator are integrated into a single unit that uses solar energy to promote refrigerant evaporation. Charters et al. compared three technologies for producing DHW for the main

Australian cities: a single solar thermal system, a single heat pump and a DX-SAHP. The comparison considered the electricity use, the life-cycle costs and the reductions in green-house gas emissions. The authors found that the right choice strongly depends on the climatic conditions and the local price of electricity [10]. Compared to the direct so-lar-assisted configurations, in indirect solar-assisted solutions (IDX-SAHP) thermal solar collectors and heat pumps are considered as two independent systems. Banister et al. have developed an indirect dual tank SAHP system for domestic hot water heating with a dedicated control strategy to minimize electricity consumption by selecting the best mode, experimentally validated, from those proposed. Annual simulations of system performance for a single-family residential home indicate that the dual tank SAHP system provides significant energy savings in comparison to a traditional solar domestic hot water system [11]. Furthermore, IDX-SAHPs can be classified into three different functioning modes: series, parallel and dual source systems. In the series and the dual source modes, solar energy is employed to improve the heat pump performance, whereas in the parallel system the solar device and heat pump work together to increase the renewable share in energy demand. Usually, in a parallel system solar radiation is used to provide directly heating loads, however when solar radiation is not sufficient, the heat pump intervenes. Pinamonti et al. have analysed the integration of a modulating water-water heat pump in a solar system equipped with a seasonal storage. System performance was evaluated through a series of energy simulations using TRNSYS [12].

The dual-source solar-assisted heat pump is designed to use two evaporators operating with different sources, choosing that with the most favourable temperature [13], but also plant systems equipped with heat pumps operating with more than two sources, have been studied. In this regard, Emmi et al. have determined the performance of a multi-source energy system composed of PV/T solar collectors, heat pumps and two storage tanks, one for the heat source at the evaporator side, and the second one for the DHW production and the space heating of a single-family dwelling located in the North East of Italy. In particular, different sources (air, ground and water) were analysed through the modelling of two plant configurations. The first does not contemplate the integration of solar radiation and thermal energy from the ground. In the second one, the system was conceived to use solar radiation to increase the ground thermal level. The simulations were carried out in a TRNSYS environment and showed that the latter solution was not economically profitable [14]. Liu et. al have proposed a heat pump dual-source (solar and

air) used for space heating in which the evaporator exchanges with the higher temperature between the air heated by the solar collectors and the external air. The performance of the dual-source heat pump has been studied and optimized with various refrigerant and air flow rates supplying the solar collectors. The average monthly coefficient of performance of the dual-source heat pump can generally reach 3.6 and the average annual in-door temperature of the building is generally above 20 ° C. One drawback of this installation setup is definitely the absence of a storage system that hinders a rational exploitation of solar surpluses [15]. Taoufik et al. investigated the performance of a double tank indirect parallel solar-assisted heat pump photovoltaic/thermal (PV/T) system in the Tunisian climate to compensate domestic electric and hot water loads. The mathematical model was developed in the MATLAB environment. the combination of the thermo-photovoltaic system with the heat pump makes it possible to reduce the electricity demand by about 30% in a year [16]. Brahim et al. give a review of the historical and recent trend of PVT development technology, in particular the performance and economic feasibility of PVT system for different application area [17] [18].

In order to rationalize and increase the use of renewable sources and simultaneously improve the efficiency of the heat pump when operating in cold climates [15][16], this paper focuses on the possibility of combining a water-water heat pump integrated with other renewable sources. The plant configuration involves a water-water heat pump, thermal solar collector, two thermal storage tanks and a PV generator with batteries. The tank connected with solar collectors is named “solar tank”, the second one in located after the heat pump and connected with the reference building (“secondary tank”). The basic purpose is to use solar thermal collectors and the solar tank to increase COPs by increasing the cold source temperature. When the temperature inside the solar tank is above 50 ºC, the heating demand is met directly from the solar collectors through a motorized three-way valve that directly supplies fan coils of the reference building. The proposed system based on the employment of a water-water heat pump is able to overcome the limitation of air-water devices in cold climates due to the unfavourable outdoor air temperature that could hinder correct functioning. However, to avoid low COPs, the heat pump operation is allowed only when the solar tank temperature is over 5°C, alternatively an auxiliary system (gas boiler) integrated in the secondary tank intervenes. The system performances were investigated in a parametric study by varying solar tank volume and the collecting surface by simulations conducted in the TRNSYS

environment. Proper control strategies were implemented in order to maximize the role of renewable sources to meet heating needs. System efficiency was assessed by considering:

- heating demand covered directly by the system without considering the auxiliary intervention;
- system performance index regarding the non-renewable share;
- system performance index related to the renewable energy share;
- CO_2 emission level.

It is worth noting that the proposed plant, despite requiring a water thermal source, can be planned everywhere, also for the renovation of existing heating systems. Conversely to other investigations already available in the literature this paper, through the parametric analysis, determines analytically the share of renewable energy and the correspondent level of CO_2 emissions that can be achieved and the results compared with two common solutions of heating plant: an air-to-water heat pump with a thermal storage system and connected to a PV generator, with high energy performance and easily installable, and the cheapest solution represented by a gas boiler.

5.2 Methods and materials

In this section, the reference building-plant system and numerical setup are present-ed. The main characteristic of the heat pump, the solar collector and the thermal storage are introduced. The description of the implemented control strategies is also described. Finally, how performance parameters are determined is outlined.

5.2.1 Case study building

The case study building (Figure 5-1) is the typical plan of a multi-storey building with a surface area of approximately 200 m² and an inter-floor height of 2.70 meters. It was decided to analyse a typical plan in order to generalise the application of the proposed system in other contexts. In fact, the surface investigated can be used for one, two or three flats without losing its generality. In the present analysis, the standard plan consists of three flats surface (small, medium and large). The envelope was defined to satisfy current national regulations regarding the energy efficiency of buildings in Italy [21]. The main dispersing surfaces are represented by vertical walls, whose thermal properties of the layers are reported in Table 5-1. The building was simulated as a single thermal zone.

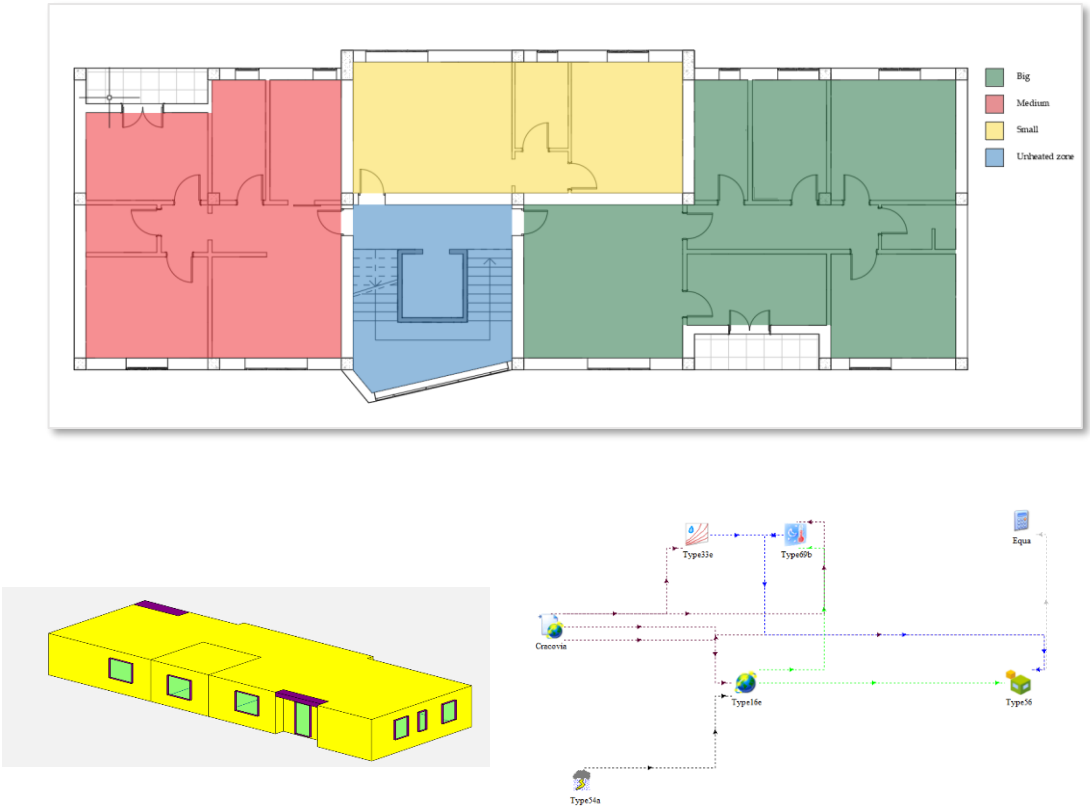

Figure 5-1- Case study building with flats locations and TRNSYS workspace for the design heating load evaluation.

Table 5-1- Thermal properties of the layers composing the external vertical wall.

	External vertical wall (U=0.239 W/m²K)			
Material	Thickness [cm]	Density [kg/m^3]	Specific heat [J/kg K]	Thermal conductivity [W/mK]
Plaster	2	1400	1000	0.700
Bricks	30	850	1000	0.182*
Insulation	8	70	1030	0.035
Skim Coat	2	1400	360	0.470
Plaster	1	1400	1000	0.700

For the aim of the study, the building is supposed located in Milan characterized by a continental climate and classified as subtype “CFb” (Marine West Coast Climate) in the Köppen Climate Classification [22]. This makes the location with a dominant heating climate whereas cooling requirements can be considered negligible. DHW needs, with a low magnitude in terms of energy requirements when compared with the heating ones, were neglected. Internal gains were defined according to the Italian National Standard UNI 11300-1 differentiating them according to a schedule [23]. Similarly, natural ventilation was assumed with a rate of 0.3 air-change per hour (the minimum value

imposed by the current Italian legislation for buildings intended as a Residence of a continuous character). Windows are made by a double-pane glazing 4/15/4 with argon filled, wooden frame and a global thermal transmittance of 2.2 W/m^{2}K (frame to glazed surface ratio of 0.15). The heating loads required to size the heat pump have been quantified by using Type 56 with hourly weather data provided by CTI (Italian Thermo-technical Committee) as Typical Meteorological Year (TMY) [24]. It has to be noticed that transient simulations allow for accounting of the capacity effects of the building fabric that affect the thermal balance of the building-plant system, thus more reliable results were attained [25].

5.2.2 Heating Plant

The proposed system combines the use of solar thermal collectors, the solar tank at the service of the solar collector the secondary tank hosting the auxiliary system, a PV generator connected to batteries and the commercial water-water heat pump [26]. The building is conditioned by fan-coils supplied at 50 °C by the secondary tank.

5.2.2.1 Solar thermal collectors and solar tank

In order to limit winter thermal losses and exploit solar radiation more efficiently, evacuated heat pipe solar collectors have been used. The efficiency of the collector is defined by the following expression [27]:

$$\eta=\eta 0-a1\cdot Tm-a2\cdot G\cdot \mathrm{T\_m\hat{}2} \quad (5.1)$$

with optical efficiency (η0) of 0.75, first order loss coefficient (a1) of 1.18 °C-1 and second order loss coefficient (a2) equal to 0.0095 m²/W°C2 (the values are given in the correspondent datasheet. In the absence of data provided by the manufacturers, it is possible to use the parameters suggested by UNI EN 12975). G is the incident solar radiation (W/m²) and Tm the average water temperature (°C) inside the collectors following the European approach. The solar collectors are tilted at 45° while the surface was varied from 8 to 40 m^2. The thermal energy supplying the heat pump evaporator is provided by a commercial solar tank, with a volume variable between 0.5 m³ and 2 m³, with constant height and changeable diameter, to limit temperature stratification effects

in the vertical direction. The tank is insulated and it was simulated by a proper TRNSYS model without an internal coil on the heat pump side, nevertheless temperature stratification in the vertical direction was anyway considered. Technical features of the tanks are listed in Table 5-2.

5.2.2.2 *Water-water heat pump*

Preliminary simulations in design conditions allowed for choosing the appropriate heat pump rated power, by counting the highest percentage of hours during the heating period in which a precise power interval is required to assure the indoor set-point temperature of 20 °C. The results allowed for identifying a commercial device with a rated heating capacity of 7.93 kW and a rated electric absorption of 2.10 kW (nominal coefficient of performance COP of 3.78). Figure 2 shows the trend of COP as a function of the temperature of the fluid at the evaporator for different values of water temperature at the condenser. The Value of COP decreased with water temperature increasing because to produce hot water at high temperature the condenser has to reject more heat and this requires a greater absorption of electric energy.

Table 5-2 listed main features of the simulated tanks (the values are given in the correspondent datasheet) while in Table 5-3, instead, the main features of the heat pump are re-ported. The device is equipped with an inverter and the accurate sizing allows for avoiding further COP worsening due to the operation in part-load mode. The heat pump con-denser supplies the secondary tank whose features are similar to those of the solar tank (see Table 2) excepting the storage volume that was set constant to 0.5 m³.

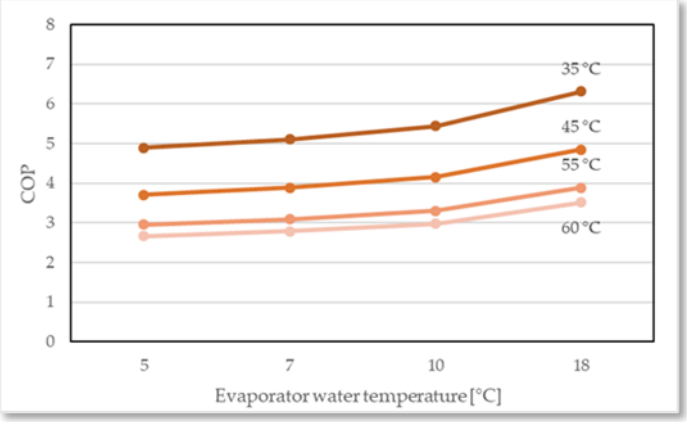

Figure 5-2- Trend of the heat pump COP as a function of the condenser temperature.

Table 5-2- Main features of the simulated tanks.

	Solar tank	**Secondary tank**
Heat transfer fluid	Water	Water
Specific heat capacity	4.182 kJ/kg K	4.182 kJ/kg K
Fluid density	992 Kg/m³	992 Kg/m³
Thermal conductivity of the fluid	0.62 W/m K	0.62 W/m K
Max storage temperature	80 °C	80 °C
Tank volume	parametric	0.5 m³
Tank height	1 m	1 m
Number of tank nodes	5	5
Top loss coefficient	0.923 W/m² K	0.923 W/m² K
Bottom loss coefficient	0.923 W/m² K	0.923 W/m² K
Edge loss coefficient	0.923 W/m² K	0.923 W/m² K

Table 5-3- Main properties of the water-water heat pump.

Heat pump	
Type	Water-to-Water
Rated Heating Capacity	7.93 kW
Rated COP	3.78
Evaporator water flow rate	1722 l/h
Condenser water flow rate	1369 l/h

5.2.2.3 PV generator and electrical storage

To improve the share from renewable sources, 6 kWp (36 m^2) of PV poly-crystalline panels (with properties listed in Table 5-4 [28]) and grid-connected were considered for the provision of a part of the required electric energy [29] [30]. The size of the PV generator was chosen based on the available roof surface and moreover 6 kW represents the threshold values that allow for installing a mono-phase electric plant, as stated by the current Italian regulation. Being the non-synchronism between required electric loads and the availability of solar radiation, the same generator was equipped with an electric storage system to better manage the PV power output surpluses. The simulated batteries were assumed with a capacity of 6000 Wh.

Table 5-4- Electrical Characteristics of PV Panels.

Photovoltaic panels feature	
Panel type	Polycrystalline silicon
Area	1.627 m^2
Nominal Power	280 W
Panels number	22
Voltage at max power	31 V
Current at max power	9.07 A
Short-circuit current	9.76 A
Open circuit voltage	38 V
Temperature coefficient of I_{sc}	-0.31 %/°C

Temperature coefficient of V_{oc}	0.05 %/°C
NOCT	45 °C
Nominal efficiency	0.15

5.2.3 Implemented Control Strategies

A scheme of the proposed plant simulated in the TRNSYS environment is depicted in Figure 5-3. Figure 5-4, instead, shows a flow chart describing the control strategies conceived to increase the renewable share in heating requirements. It can be noticed that the pump of the solar circuit is activated when the outlet temperature from solar collectors is 5°C high-er than the temperature detected at the bottom of the solar tank. Furthermore, the same pump is turned off when the average temperature inside the solar tank exceeds 80°C on the top side. When the temperature level inside the solar tank is above 50°C, the hot water is directly used to supply fan-coils by acting on a three-way valve that bypasses the heat pump, which conversely is activated when the storage temperature range between 5 °C and 50 °C. When the continuous hot water withdrawal from the solar tank causes an abrupt temperature drop, the control system inactivates the heat pump to avoid freezing phenomena, and simultaneously an auxiliary system, represented by a gas boiler connected to the secondary tank, is activated. When the tank connected with the heat pump condenser exceeds 50 °C (the heat pump can operate also at 60°C), another motorized valve regulates water temperature supplying fan-coils to 50°C by recirculating a fraction of the returned flow rate.

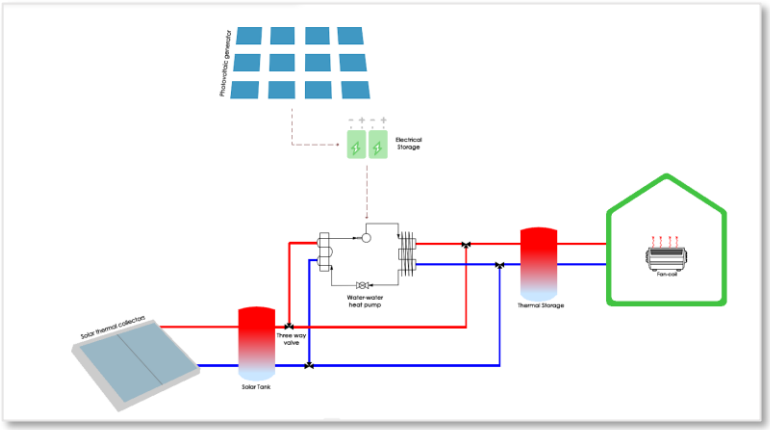

Figure 5-3- Scheme of the simulated SAHP

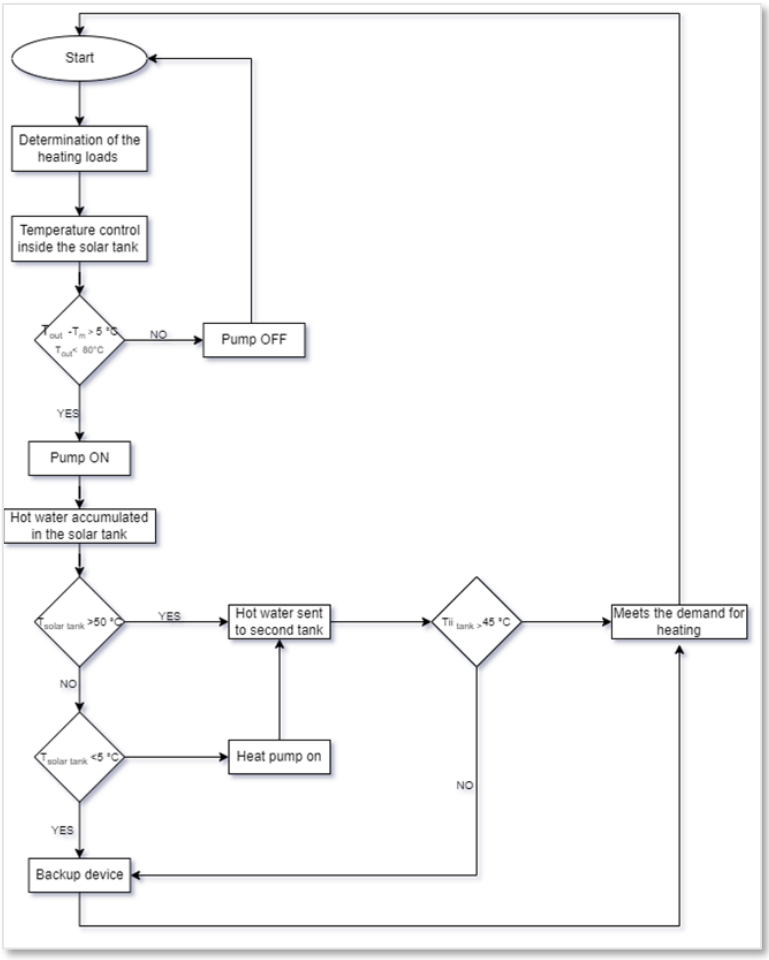

Figure 5-4- Flow chart describing the control strategies adopted for the heating plant

5.2.4 Simulation model

The simulation model was developed in TRNSYS 18 environment [31]. It has to be noticed that the heat pump model was validated by comparison with experimental data of a similar heating plant located at the University of Calabria [19], under typical Mediterranean climatic conditions. To determine the thermal performances in Milan, the building-plant system was simulated by TRNSYS with actual weather data. In light of this, it is worth noting that the obtained performances are relevant to the statistical data reported in the European project TABULA for a similar building typology (multi-storey building) built after 2005 [32]. Simulations were carried out also to determine the perfomances of other plant configurations, employing a PV assisted air-water heat pump without batteries but with a thermal storage system (easy to install and with a high share of renewable primary demand) and with the cheaper solution of a gas boiler supplying radiators.

5.2.5 Primary energy consumption and emission levels

The concept of primary energy factor (PEF) has been chosen by European Community to determine and compare the primary energy demand of different plant configurations in which diverse energy carriers are involved. In particular, PEF allows for the calculation of the total primary energy needed to produce a unit of particular final energy consumed. It includes energy extraction, transmission, storage, distribution and the losses related to the processes. Accordingly, the PEFs reflect the reality of a complete energy system, from energy production to final consumption [33]. In Table 5-5some values related to the energy carriers involved in the proposed system following the current Italian regulation, are reported.

Table 5-5- PEFs and CO_2 emission factors defined according to the Italian national standard.

Energy Carrier	$PEF_{,nren}$	$PEF_{,ren}$	$PEF_{,tot}$	$kgCO_{2eq}$/ kWh
Natural gas	1.05	0	1.05	0.21
Electricity energy from the grid	1.95	0.47	2.42	0.46
Electricity from PV	0.00	1.00	1.00	0.00
Thermal solar collector	0.00	1.00	1.00	0.00

5.3 Result

The system efficiency is assessed through the following parameters:

- the heating demand covered directly by the system without the intervention of the auxiliary generator, as a function of the collecting surface and solar tank volume;
- the seasonal non-renewable performance index, defined as the ratio between the primary energy supplied to the building and the energy absorbed from the external environment;
- the share of the renewable energy employed for covering the heating de-mand;
- the CO_2 emission level.

5.3.1 Calculation of the heating needs of the reference building in the considered climate

Figure 5-5 shows the heating energy requirement (red line) amounts to 12,614 kWh considering the actual weather data associated with the TMY available for Milan. It can be noticed that the maximum hourly energy for heating is slightly over 6 kWh and it differs from the value determined in design conditions because the latter was determined with a constant set-point outdoor air temperature (-5°C). Furthermore, it can be

appreciated that the heating period starts in October to finish in April confirming the dominant heating climate. Despite cooling loads reach also 3 kW, these could be further limited by considering in the simulations the adoption of passive solutions such as shading systems on the transparent surfaces and nightly free-cooling, making them negligible when compared to the heating needs. In order to justify the choice of heat pipe technology, Figure 5-6 reported the total horizontal radiation for Milan between October and April, highlighting the scarce availability of solar radiation that is accompanied by the low values of outdoor air temperature.

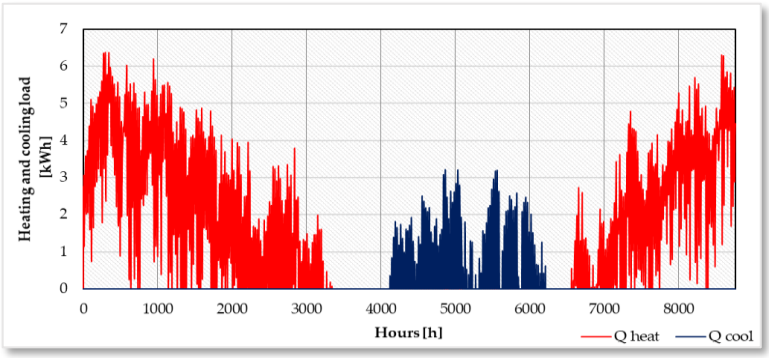

Figure 5-5- Heating and cooling load for the locality of Milan using TMY for weather data.

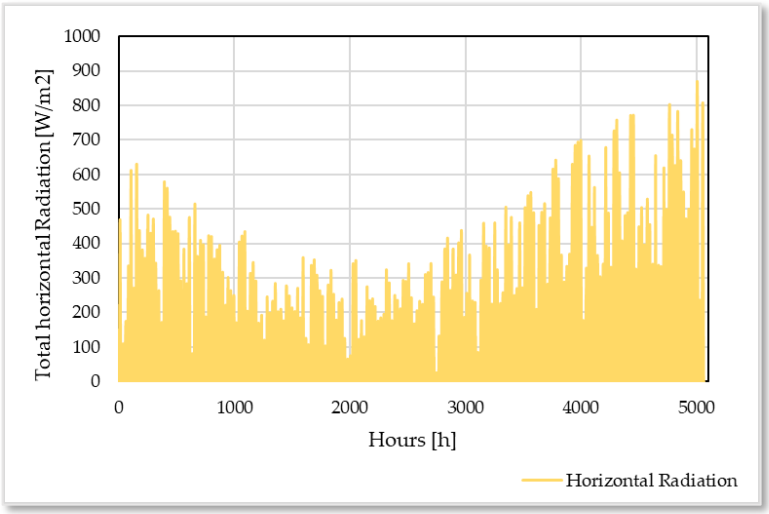

Figure 5-6- Total Horizontal Radiation for Milan between October and April

5.3.2 System operational description

Figure 5-7 shows the percentage of demand covered by each source involved in the proposed heating plant as a function of the collecting surface and the solar tank

volume. In particular, the light green dashed bar represents the share covered directly by solar col-lectors without the heat pump intervention (by the three-way motorized valve), the red bar is the share covered by the auxiliary system (gas boiler) and finally in the dark green dashed line the share provided by the water-water heat pump. It is worth noting that the solar field is mainly involved with large thermal collector surfaces and limited storage tank volumes. Conversely, the heat pump is used more frequently with large collector surface and high solar tank volumes. The functioning of the auxiliary system is reduced under 50% of the heating hours only when the thermal collector surface is greater than 24 m², however the percentage reduces with the collection surface and the solar tank volume growth. This means that the beneficial effect of the solar tank volume growth on the heat pump functioning prevails on the limitation of the share directly provided by the solar field.

Figure 5-7- Percentage of the heating demand covered by the different generators as a function of collecting surface S (m²) and solar tank volume V (m³).

Globally, the percentage of the demand covered by the proposed system increases with the solar tank volume, nevertheless it weighs lesser than the collection surface. The percentage covered by the heat pump and thermal solar collectors is about 20-21% with a collecting surface of 8 m² for every solar tank volume, and this share increases up to 62% for a volume of 2 m^3 and 40 m^2 of collecting surface. The share of energy needs covered directly by the system increases considerably from 8 m^2 to 16 m^2 and from 16 m^2 to 24 m^2 while it is negligible for further increases of the collecting surface.

5.3.3 Electric energy demand and CO_2 emission

Starting from the demand supply by each source, the consumptions of heat pump and auxiliary system are determined. In Table 5-6

, for each combination, is reported the electrical consumption of the heat pump and the gas consumption of the boiler on a seasonal basis as a function of collecting surface S (m^2) and solar tank volume V (m^3).

Table 5-6- Winter electric and gas consumption in the analysed heating plant.

S (m^2)	V=0.5 m^3		V=1 m^3		V=1.5 m^3		V=2 m^3	
	kWh_{ele}	kWh_{gas}	kWh_{ele}	kWh_{gas}	kWh_{ele}	kWh_{gas}	kWh_{ele}	kWh_{gas}
8	695	11765	746	11616	771	11538	785	11483
16	846	9676	969	9333	1033	9156	1069	9048
24	919	8443	1074	7951	1158	7695	1216	7550
32	956	7636	1148	6996	1252	6660	1304	6467
40	983	7084	1172	6331	1294	5938	1369	5705

A considerable portion of the electricity consumption (green bar of Figure 5-8) due to the use of the heat pump is supplied by the PV system combined with the batteries (in red the share covered by the grid, in grey the m^3 of gas consumed by the auxiliary boiler).. With the increase both of solar collector surface and the volume of solar tank increases the percentage of heating demand supply directly by the solar assisted heat pump. For this reason, the electricity consumption increases but simultaneously decreases drastically the consumption of gas. It is worth noting that, from a PV utilization viewpoint, a collecting surface of 16 m^2 is preferable because a sort of ideal combination between PV production and heat pump operation was found. For the other cases, the share covered by the PV generator is almost constant, rather it tends to slightly decrease with the collection surface growth. Similarly, the storage tank volume does not affect the PV share considerably, whereas the augment of the collection surface produces an evident increase in the electricity withdrawal from the grid, due to a wider operation time of the heat pump.

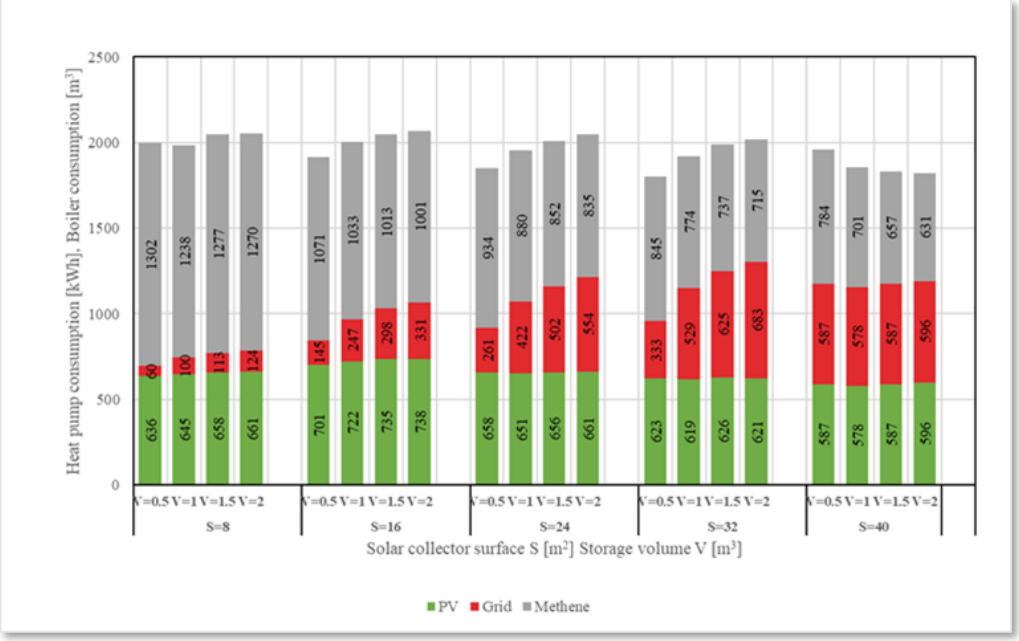

Figure 5-8- Consumptions of gas and electricity in the proposed system as a function of collecting surface S (m²) and solar tank volume V (m³).

Considering the primary energy factors reported in Table 5-5 starting from the calculated consumption reported in Table 6, the renewable and non-renewable primary energy associated with each analysed configuration were listed in Table 5-7.

Table 5-7- Renewable and non-renewable primary energy shares as a function of collecting surface (S) and solar tank volume (V)

	V=0.5 m³		**V=1 m³**		**V=1.5 m³**		**V=2 m³**	
S (m²)	Ep_{ren} [kWh]	Ep_{nren} [kWh]	Ep_{ren} [kWh]	Ep_{nren} [kWh]	Ep_{ren} [kWh]	Ep_{nren} [kWh]	Ep_{ren} [kWh]	Ep_{nren} [kWh]
8	664	12470	692	11941	771	12336	720	12292
16	769	10445	839	10282	875	10192	893	10143
24	780	9371	850	9173	891	9063	921	9003
32	780	8867	867	8377	919	8211	942	8116
40	863	8210	850	7811	863	8116	877	7149

Moving from 8 m^2 to 40 m^2 of collecting surface, independently from the storage volume, a reduction in non-renewable primary energy by about 30% was attained. Furthermore, the renewable share slightly varies with the solar thermal collector area, where-as noticeable deviances have been reordered by increasing the volume of the solar tank.

The system performance index (Figure 5-9) was calculated as the ratio between the thermal energy demand and the non-renewable share of primary energy, so high values denote a plant configuration with an elevated share of renewable energy to satisfy heating needs. This index shows that system performance, in general, improves with the

solar collector area growth, passing from 0.95 with 8 m² and 0.5 m³, up to 1.592 with 40 m² and 2 m³. However, the differences detected by varying the storage volume are negligible. Basically, the percentage of needs covered by the system increases in an evident manner moving from 8 to 40 m² of collecting area rather than the increase in the volume of the solar tank. Figure 5-9 shows the trend of the seasonal COP, which slightly varies around 4.29-4.32 for every heating plant configuration, demonstrating that the solar-assisted heat pump is able to operate with a high-performance index in the considered climatic condition, when compared with the rated values. The COP enhanced by 1.4% only but this in-crease determines a high share of the primary renewable share employed by the proposed system. In particular, these values are greater than those provided by the manufacturer every time the supply hot water is over 45°C and the inlet temperature at the evaporator is lower than 10 °C.

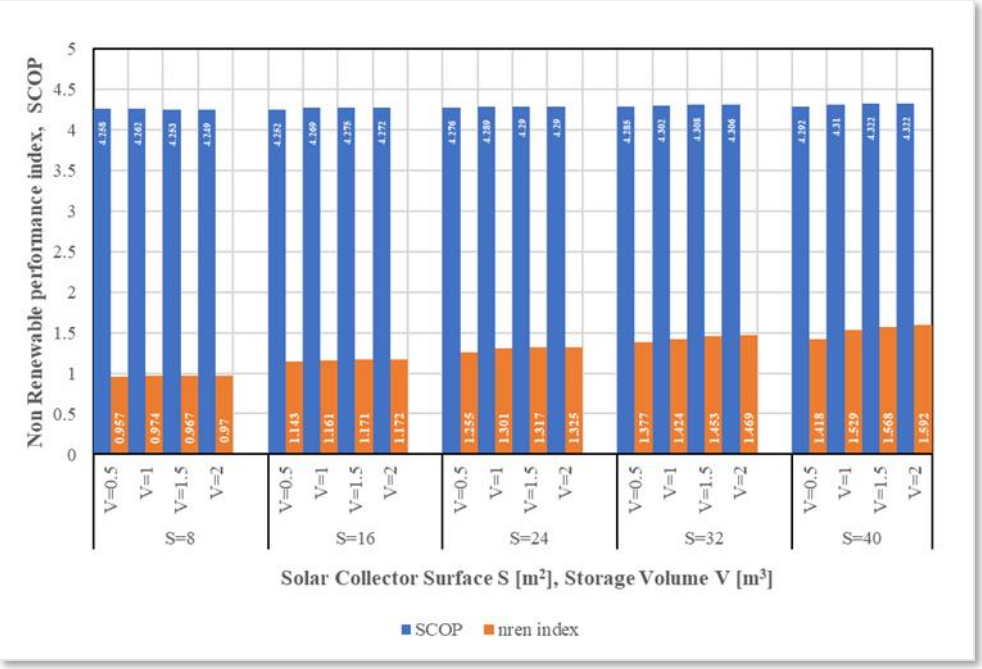

Figure 5-9- Trend of non-renewable performance index as a function of collecting surface S (m²) and solar tank volume V (m³).

When the proposed system is compared with the alternative heating plant using an assisted PV air-to-water heat pump and a storage tank (system 1), primary energy consumption of 5 349 kWh was recorded. Only 990.25 kWh are supplied by the PV system while the remaining is absorbed from the grid. The share of non-renewable primary energy is determined for both systems and these values are reported in Figure 5-10. It is possible to appreciate that for solar collector surfaces larger than 24 m^2 the

proposed system is more performant than the air-water heat pump, in light of the lower shares of non-renewable primary energy. The percentage reduction varies between 4% and 8% with 24 m^2 of solar collectors for the different solar tank volumes. The reduction is bigger in the correspondence of 32 m^2 of the collecting area being 17%. The greatest decrease is recorded for a surface of 40 m^2 and a storage volume of 2 m^3.

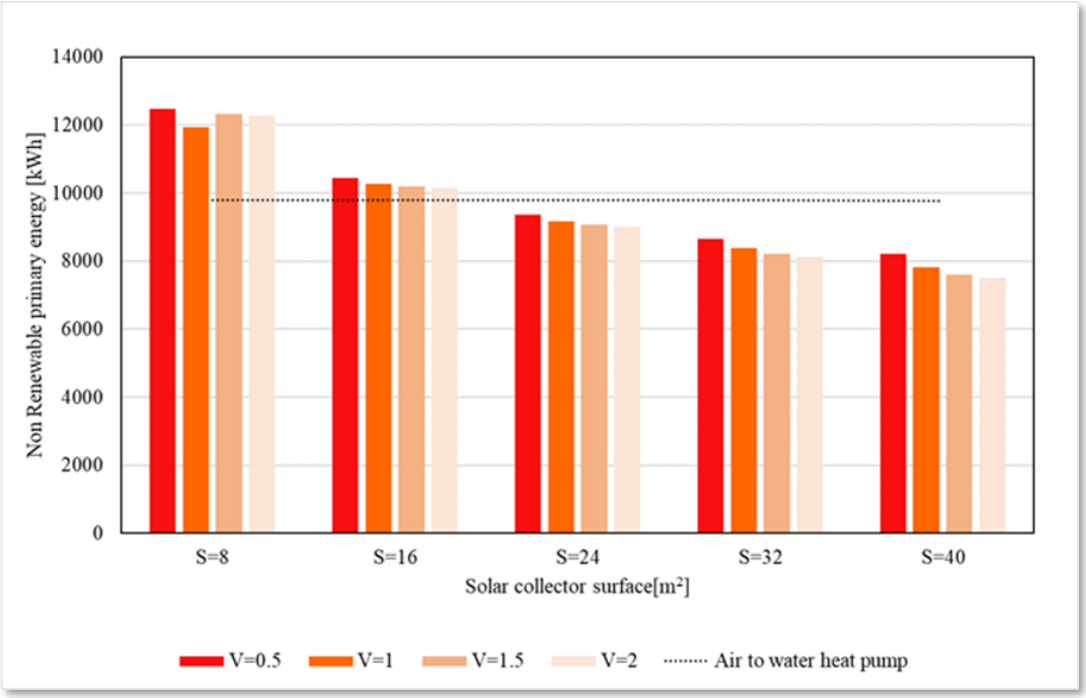

Figure 5-10- share of non-renewable primary energy

When the proposed system, instead, is compared to a traditional gas boiler (system 2, for which an average seasonal efficiency of 0.8 was assumed) a consumption of 14,915 kWh was determined, with a share of non-renewable primary energy of 15,661 kWh. Regarding the previous heating plant configurations, the gas boiler obviously determines the highest consumption and the highest share of non-renewable primary energy. Table 5-8 details the percentage reduction of non-renewable primary energy of each combination compared to system 1 and system 2.

Table 5-8- Non-renewable primary energy (Ep_{nren}) for all heating plants analysed.

S (m^2)	**Ep_{nren}[kWh]**			
	V=0.5 m^3	V=1 m^3	V=1.5 m^3	V=2 m^3
8	12470	11941	12336	12292
16	10445	10282	10192	10143
24	9371	9173	9173	9003
32	8867	8377	8377	8116
40	8210	7811	7811	7496

Air-to-Water Heat Pump	9791,7
Boiler	15661

Table 5-9- Percentage reduction of non-renewable primary energy of each combination compared to system 1 and system 2

	V=0.5 m³		V=1 m³		V=1.5 m³		V=2 m³	
S (m²)	System 1	System 2	System 1	System 2	System 1	System 2	System 1	System 2
8	27.35%	-20.38%	21.95%	-23.75%	25.98%	-21.23%	25.53%	-21.51%
16	6.67%	-33.31%	5.01%	-34.35%	4.09%	-34.92%	3.59%	-35.23%
24	**-4.30%**	**-40.16%**	**-6.32%**	**-41.43%**	**-7.45%**	**-42.14%**	**-8.05%**	**-42.51%**
32	**-9.44%**	**-43.38%**	**-14.45%**	**-46.51%**	**-16.14%**	**-47.57%**	**-17.11%**	**-48.18%**
40	**-12.34%**	**-45.20%**	**-20.57%**	**-50.34%**	**-24.65%**	**-52.89%**	**-26.99%**	**-54.35%**

Figure 5-11 shows the comparison of the share of renewable and non-renewable energy for the three considered configurations of the heating plant.

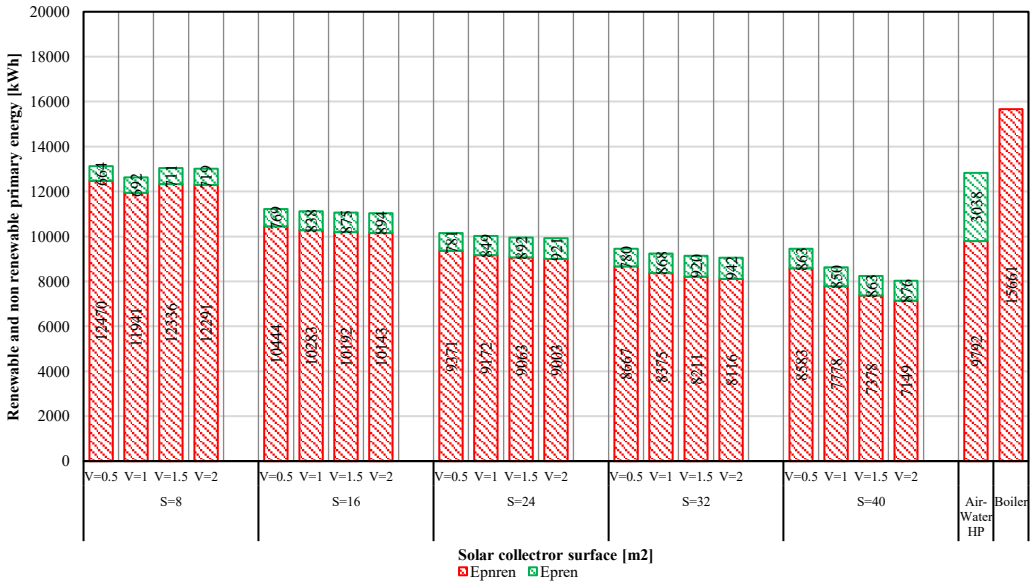

Figure 5-11- The share of total primary energy, including renewable and non-renewable energy for all the systems compared.

As a consequence of the lowest non-renewable primary energy demands, the proposed system allows also a noticeable reduction in CO_2 emissions (Figure 5-12). The equivalent emissions have been calculated through the factors listed in Table 5-5 as a function of the energy carrier. It is possible to appreciate how, compared with a traditional system in which the total thermal load is provided only by a gas boiler, the equivalent CO_2 emissions are lower for each plant configuration. When the system, instead, is compared with the assisted PV air-to-water heat pump, the equivalent CO_2 emissions are

always lower except for a collecting surface of 8 m^2. Globally, the equivalent CO_2 emissions decrease with the solar collector area growth and less with the increase of the accumulation volume. In its best configuration, the proposed system produces a reduction of 33% of emitted CO_2 if compared with the air-water heat pump and 53% if compared with the gas boiler.

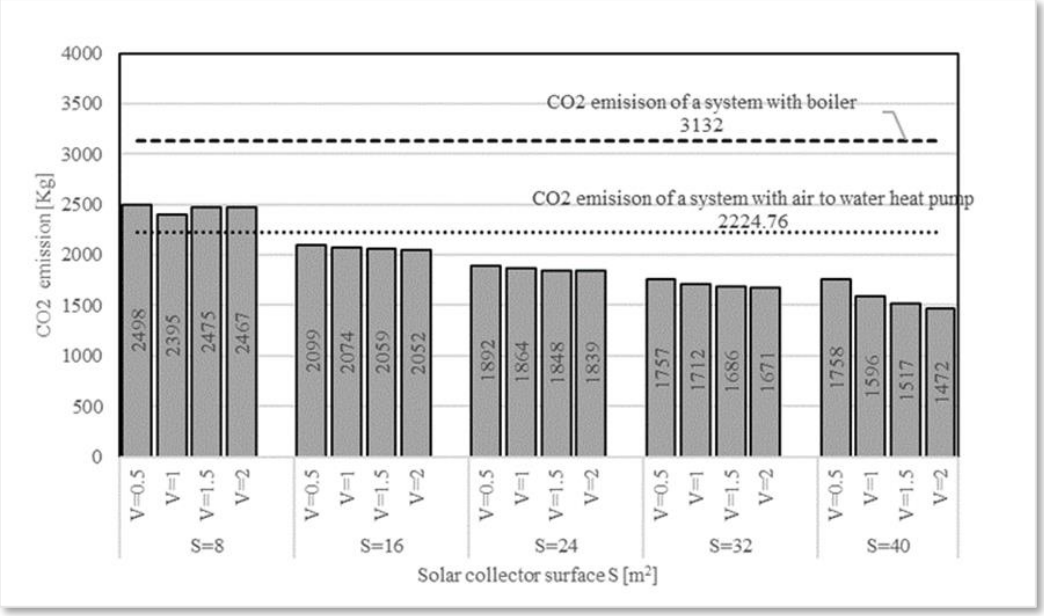

Figure 5-12- Comparison of the CO_2 emissions between the proposed SAHP and the heating plants equipped with assisted PV air-water heat pumps and equipped with a gas boiler.

5.4 Conclusions

This study deals with the energy and environmental evaluations concerning a SAHP system conceived for cold climates that combines the use of solar collector panels, a water-water heat pump, two storage tanks and a photovoltaic system with batteries. Such a combination and the development of proper control strategies allow for better exploitation of the active solar systems, using solar radiation also to operate directly the space heating or, alternatively, to improve the heat pump performance. The electric consumptions are reduced by means of the better COPs, furthermore the batteries allow for overcoming efficiently the mismatching between solar radiation availability and thermal load request. The system performances were investigated by a parametric study by varying solar tank volume and the collecting surface. From the results analysis emerged that the system ensures excellent heat pump performance with an average COP always greater than 4, being the rated value of the simulated commercially available device of 3.78. The heating demand covered by the proposed system increases both with

the collecting surface area and the solar tank volume growth, and a percentage of 22% can be provided directly by 40 m² of solar collectors with a solar tank volume of 0.5 m³.

The percentage covered by the combined use of heat pump and thermal solar collectors moves from 20-21% with a collecting surface of 8 m² up to 62% for a volume of 2 m^3 and 40 m^2. Regarding the primary energy demand, the same configuration permits attaining the lowest non-renewable share. If compared with a heating plant using an assisted PV air-to-water heat pump and a thermal storage system, a decrease of 27% of the required primary energy was detected, because this system in continental climates suffers from unfavourable outdoor air temperatures. The percentage increases up to 75% when the proposed system is compared with the widespread heating plant solution equipped with a gas boiler, corresponding to a CO_2 emissions reduction of 53%.

Currently the cheapest solution for building builders is represented by a heating plant using a gas boiler supplying radiator, nevertheless this solution leads to an energy performance index of about 78 kWh/m² per year. The proposed system allows for a drastic reduction of the energy consumption, producing energy performance indices ranging between 37 kWh/m² and 62 kWh/m², the latter detected with 8 m² of collecting surface and 0.5 m³ of storage volume. These values confirm that the wider investment costs required for the installation of the proposed SAHP are properly counterbalanced by appreciable economic savings achievable by the limitation of operative expense.

5.5 References

[1] I. E. A. IEA, Data and Statistics, https://www.iea.org/data-and-statistics, Accessed on 15th June 2021. 2021.

[2] R. Bruno, N. Arcuri, e C. Carpino, «The passive house in Mediterranean area: Parametric analysis and dynamic simulation of the thermal behavior of an innovative prototype», in Energy Procedia, dic. 2015, vol. 82, pagg. 533–539, doi: 10.1016/j.egypro.2015.11.866.

[3] IEA, «Tracking Buildings 2020», Paris, 2020.

[4] N. Arcuri, R. Bruno, e C. Carpino, «PV Driven Heat Pumps for the Electric Demand-Side Management: Experimental Results of a Demonstrative Plant», in 2018 IEEE International Conference on Environment and Electrical Engineering and 2018 IEEE Industrial and Commercial Power Systems Europe (EEEIC / I&CPS Europe), giu. 2018, pagg. 1–6, doi:10.1109/EEEIC.2018.8493492, doi: 10.1109/EEEIC.2018.8493492.

[5] C. C. Arcuri N., Bruno R., Bevilacqua P., «Strategies for The Reduction of Electricity Consumptions in Heat Pumps : The Role of the Thermal Inertia in Buildings Equipped with Radiant Systems», in BS2019 - Rome, 2019, pagg. 1724–1731, doi:10.26868/25222708.2019.211031, doi: 10.26868/25222708.2019.211031.

[6] Y. Fan et al., «Scientific and technological progress and future perspectives of the solar assisted heat pump (SAHP) system», Energy, vol. 229, n. 2021, pag. 120719, 2023, doi: 10.1016/j.energy.2021.120719.

[7] C. Liang, X. Zhang, X. Li, e X. Zhu, «Study on the performance of a solar assisted air source heat pump system for building heating», Energy & Buildings, vol. 43, n. 9, pagg. 2188–2196, 2011, doi: 10.1016/j.enbuild.2011.04.028.

[8] L. Xu, Y. Zhang, e X. Luo, «Applicability and comparison of solar-air source heat pump systems between cold and warm regions of plateau by transient simulation and experiment», pagg. 1697–1708, 2021.

[9] M. Bakker, H. A. Zondag, M. J. Elswijk, K. J. Strootman, e M. J. M. Jong, «Performance and costs of a roof-sized PV / thermal array combined with a ground coupled heat pump», vol. 78, pagg. 331–339, 2005, doi: 10.1016/j.solener.2004.09.019.

[10] W. W. S. Charters e C. Chaichana, «Solar heat pump systems for domestic hot water», vol. 73, n. 3, pagg. 169–175, 2002.

[11] C. J. Banister e M. R. Collins, «Development and performance of a dual tank solar-assisted heat pump system», Applied Energy, vol. 149, pagg. 125–132, 2015, doi: 10.1016/j.apenergy.2015.03.130.

[12] M. Pinamonti, I. Beausoleil-morrison, A. Prada, e P. Baggio, «Water-to-water heat pump integration in a solar seasonal storage system for space heating and domestic hot water production of a single-family house in a cold climate», Solar Energy, vol. 213, n. August 2020, pagg. 300–311, 2021, doi: 10.1016/j.solener.2020.11.052.

[13] M. S. Buker e S. B. Riffat, «Solar assisted heat pump systems for low temperature water heating applications: A systematic review», Renewable and Sustainable Energy Reviews[1] M. S. Buker e S. B. Riffat, «Solar assisted heat pump systems for low temperature water heating applications: A systematic review», Renewable and Sustainable Energy Reviews. 2016, doi: 10.1016/j.rser.2015.10.157. 2016, doi: 10.1016/j.rser.2015.10.157.

[14] G. Emmi, A. Zarrella, e M. De Carli, «A heat pump coupled with photovoltaic thermal hybrid solar collectors : A case study of a multi-source energy system», Energy Conversion and Management, vol. 151, n. August, pagg. 386–399, 2017, doi: 10.1016/j.enconman.2017.08.077.

[15] Z. Liu et al., «Operating performance of a solar / air-dual source heat pump system under various refrigerant fl ow rates and distributions», vol. 178, n. May, 2020, doi: 10.1016/j.applthermaleng.2020.115631.

[16] B. Taoufik e J. Abdelmajid, «Feasibility Study of Long-Term Dual Tank Photovoltaic / Thermal Indirect Parallel Solar-Assisted Heat Pump Systems», vol. 144, n. August, 2022, doi: 10.1115/1.4053317.

[17] T. Brahim e A. Jemni, «Economical assessment and applications of photovoltaic / thermal hybrid solar technology : A review», Solar Energy, vol. 153, pagg. 540–561, 2017, doi: 10.1016/j.solener.2017.05.081.

[18] T. Brahim e A. Jemni, «Parametric study of photovoltaic / thermal wickless heat pipe solar collector», Energy Conversion and Management, vol. 239, n. March, pag. 114236, 2021, doi: 10.1016/j.enconman.2021.114236.

[19] R. Bruno, F. Nicoletti, G. Cuconati, S. Perrella, e D. Cirone, «Performance indexes of an air-water heat pump versus the capacity ratio: Analysis by means of experimental data», Energies, vol. 13, n. 13, 2020, doi: 10.3390/en13133391.

[20] L. Schibuola, M. Scarpa, e C. Tambani, «Demand response management by means of heat pumps controlled via real time pricing», Energy and Buildings, 2015, doi: 10.1016/j.enbuild.2014.12.047.

[21] Italian interministerial decree 26th June 2015: Application of calculation methods for energy performance and definition of minimum building requirements, «Italian interministerial decree 26th June 2015: Application of calculation methods for energy performance and definition of minimum building requirements», Official Gazzette of Italian Republic n°39 of 15th July 2015, pagg. 1–8, 2015.

[22] M. C. Peel, B. L. Finlayson, e T. A. McMahon, «Updated world map of the Köppen-Geiger climate classification», Hydrology and Earth System Sciences, 2007, doi: 10.5194/hess-11-1633-2007.

[23] «UNI/TS 11300–1. Building energy performance – Part 1: Evaluation of the energy need for space heating and cooling (in Italian). 2014.»

[24] CTI - Italian Thermotechincal Committee, «https://www.cti2000.it/ (accessed on 13 July 2021)», 2021.

[25] R. Bruno, P. Bevilacqua, e N. Arcuri, «Assessing cooling energy demands with the EN ISO 52016-1 quasi-steady approach in the Mediterranean area», Journal of Building Engineering, vol. 24, lug. 2019, doi: 10.1016/j.jobe.2019.100740.

[26] P. Bevilacqua, S. Perrella, R. Bruno, e N. Arcuri, «An accurate thermal model for the PV electric generation prediction: long-term validation in different climatic conditions», Renewable Energy, vol. 163, pagg. 1092–1112, 2021, doi: 10.1016/j.renene.2020.07.115.

[27] G. Oliveti, L. Marletta, N. Arcuri, M. De Simone, R. Bruno, e G. Evola, Solar energy, n. 9783319030739. 2014.

[28] P. Bevilacqua, S. Perrella, D. Cirone, R. Bruno, e N. Arcuri, «Efficiency improvement of photovoltaic modules via back surface cooling», Energies, vol. 14, n. 4, 2021, doi: 10.3390/en14040895.

[29] P. Pinamonti, Maria; Prada, Alessandro;Baggio, «Rule-based control strategy to increase photovoltaic self-consumption of a modulating heat pump using water storages and building mass activation», Energies, vol. 13, 2020.

[30] P. Bevilacqua, R. Bruno, A. Rollo, e V. Ferraro, «A novel thermal model for PV panels with back surface spray cooling», Energy, vol. 255, pag. 124401, 2022, doi: 10.1016/j.energy.2022.124401.

[31] VV.AA., «User Manual: TRNSYS 18 a TRaN sient SYstem Simulation program», TRNSYS Library, Volume 4 Mathematical Reference, Solar Energy Laboratory, University of Wisconsin-Madison, USA. 2016.

[32] N. Diefenbach et al., Application of Building Typologies for Modelling the Energy Balance of the Residential Building Stock, n. June 2009. 2012.

[33] E. Latõšov, A. Volkova, A. Siirde, J. Kurnitski, e M. Thalfeldt, «Primary energy factor for district heating networks in European Union member states», Energy Procedia, vol. 116, pagg. 69–77, 2020, doi: 10.1016/j.egypro.2017.05.056.

6 Optimization of a solar assisted heat pump system to increase thermal efficiency working on the cold sink

Abstract

This study introduces an innovative high-efficiency air conditioning system that utilizes solar-assisted heat pumps to enhance device efficiency by elevating the thermal level of the heat source at lower temperatures. The primary objective is to reduce electrical consumption by achieving a higher coefficient of performance, accomplished through the utilization of solar energy stored in thermal storage to optimize operating conditions with a favourable cold source temperature. The demonstrator for this system will be implemented on the "Chiodo 2" experimental setup at the University of Calabria, where an existing plant equipped with an air- water heat pump is already operational. The simulation model was developed within the TRNSYS environment. The development process of the virtual system model is presented in detail, encompassing solar collectors, thermal storage, heat pump, photovoltaic system, and dry cooler. Through an analysis of the winter operation of the system, the study identifies key requirements, including the optimal thermal storage volume and the optimal size of solar collectors, to maximize energy efficiency. Specific operating conditions are proposed, such as the synergistic use of solar collectors and heat pump in particular thermal scenarios, to enhance performance.

6.1 Introduction

In the road toward the reduction of greenhouse gas emissions and increase sustainability the building sector plays a pivotal role. European Union recent "Fit for 55%" package, set ambitious targets and specifically, the Fit for 55% package underlines the pivotal role of HVAC systems in achieving these goals. For such a reason many countries policies are pushing toward the mandatory adoption of heat pump system for air-conditioning of building, dismissing traditional system based on fossil fuels.

Accurate design of such generator, requires a careful consideration of the real operating condition [1]. Heat pump achieve maximum sustainability when combined with solar energy (solar-assisted heat pumps) [2,3]. In this regard the most used configuration is the use of photovoltaic system to supply electric energy to the heat pump [4]. In recent years however, researchers have focused on integrating heat pumps with solar collectors, photovoltaic panels, and hybrid systems. A study investigated the performance of a

ground source heat pump system with free cooling and photovoltaic/thermal collectors at service of a multi- family building in Stockholm [5]. The optimal design features of photovoltaic-thermal collectors for integration with ground source heat pump systems was investigated considering technical and economic factors [6]. The impact of a control logic aimed at maximizing the utilization of excess renewable in a solar-assisted heat pump system with electrical and thermal storage systems was assesses in [7]. The thermal performance of a direct expansion solar assisted heat pump was analysed for several refrigerants using two collector configurations [8].

The use of appropriate storage system can play an important role in the integration and optimal utilization of renewable energy. In [9], the integration of a modulating water-to-water heat pump in a solar system with a seasonal storage was analysed. In terms of solar fraction, the results showed values reaching 85 %. A solar-assisted raw-water source heat pump [10] was proposed to solve the performance degradation and improve heating performance thanks solar collectors that can increase the entering water temperature. A multi-source energy system including photovoltaic thermal solar collectors, storage tanks for the heat source and domestic hot water and heat pumps was analysed in reference to a single-family dwelling located in North East Italy [11]. Results showed that the multi-energy source systems increased the energy efficiency by 16–25% compared to an ordinary air to water heat pump. A solar hybrid plant consisting of water-based PV-T collectors integrated with an air-to-water heat pump via thermal storage tanks was investigated considering a full-size pilot plant located in Spain and operating under real weather conditions [12] Results showed that thanks to the simultaneous electricity and thermal generation of the PV-T collectors, the plant was overall self-sufficient to satisfy the building energy demand. A solar assisted heat pump solar supplied by thermal-photovoltaic hybrid panels was analysed numerically and experimentally [13]. Results indicated that the system was not properly sized presenting a low solar radiation exploitation. A solar PVT assisted - heat pump system with a cold buffer storage tank on the source side of the heat pump and a hot storage tank for domestic hot water was measured over a nine months period [14]. The uninsulated PVT collector worked as an energy absorber and was able to extract heat form the ambient air and recharge the buffer storage tank to the ambient air temperature when no solar irradiance was available. In the less sunny and colder periods, the PVT added a significant amount of energy to the cold storage tank. In this study solar thermal collectors are employed to increase the

temperature of the cold source of a water-to-water heat pump used for the air-conditioning of a university residential complex in Rende (Italy). Simulations are performed with TRNSYS environment to assess the effect of solar thermal collectors and thermal storage size on the fraction of energy demand covered by solar radiation.

6.2 Methodology

6.2.1 Case study Building

The building considered in the study is part of a student residential complex of University of Calabria named "Chiodo2". The building's energy demand has been calculated within the TRNSYS environment. The building's 3D model was created using Sketchup, incorporating the TRNSYS 3D plug-in to facilitate a comprehensive representation of its geometry. The geometrical representation of the analysed building is reported in Figure 6-1.

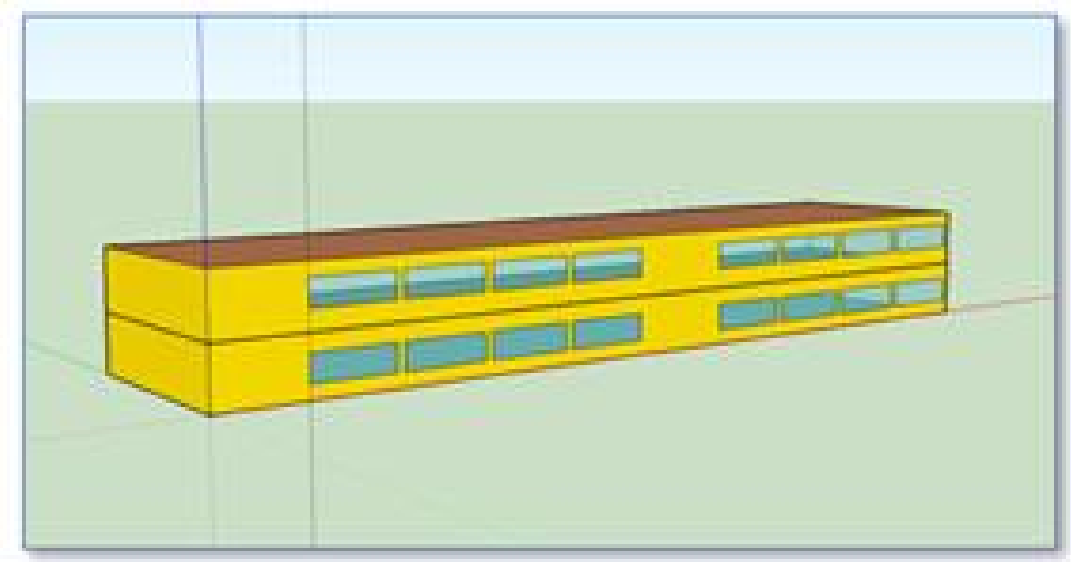

Figure 6-1-3D representation of the building model

The thermal properties and stratigraphy of the main components of the building are reported in Table 6-1and Table 6-2.

Table 6-1- Thermal properties of the external walls

	Thickness [cm]	Conductivity [W/m²K]	Specific heat [J/kgK]	Density [kg/m³]
Plaster	2	0.9	800	1400
Brick masonry	30	0.157	1000	1250
Plaster	2	0.9	800	1400

Table 6-2- Thermal properties of the external roof

	Thickness [cm]	Conductivity [W/m²K]	Specific heat [J/kgK]	Density [kg/m³]
Tiles	2	0.9	800	2000
Screed	14	2	800	900
Insulation	2	0.035	800	55
Plaster	2	0.9	800	1400

Table 6-3 finally reports the U-values of the main building components.

Table 6-3- U-values of the main building components

	U-value
External wall	0.471
External roof/ground floor	0.236
External window	2.89

Internal gains were applied considering and amount of 440 W of radiative and the same amount of convective power. Infiltration were set to 0.5 h-1. The heating plant was considered with a set-point temperature of 20 °C.

6.2.2 The air-conditioning plant

The simulated air-conditioning plant of the building is composed of:

- a field of evacuated tube solar collectors designed to ensure maximum efficiency even under suboptimal solar radiation conditions,
- two thermal storage tanks, one supplied by the solar collector, and supplied by the heat pump,
- a water-to-water heat pump.

The heat pump was sized according to preliminary results of simulation, as reported in section 6.3.1. An available commercial model was chosen for simulation, and

data of COP and thermal power delivered at the different source temperatures were taken from datasheet and provided to Type 927. In particular the selected model is a water-source reversible water condensed heat pump. The heat pump has a nominal power of 12.6 kW and a nominal COP of 3.94.

A commercially available vacuum tube solar collector was chosen for simulation and its parameters were provided to Type 71. The data of the solar thermal collector are reported in Table 6-4.

Table 6-4- Data of the solar thermal collector

Parameter	**Value**
Optical efficiency	0.785
First order coefficient	1.847
Second order coefficient	0.005

The simulation scheme adopted within TRNSYS environment is reported in Figure 6-2.

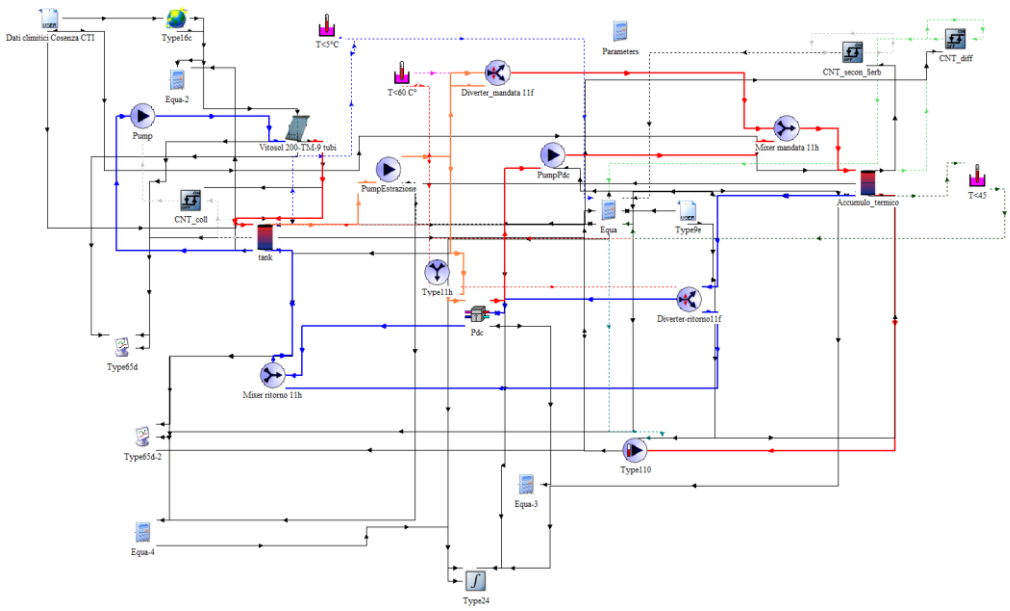

Figure 6-2- Simulation scheme adopted in TRNSYS

The solar collector directly supplies the solar storage tank, according to a control logic that check the temperature difference between the panel outlet temperature and the tank temperature and decide whether activate or not the circulation pump. The solar tank supplies the heat pump acting as a cold source. A proper control strategy, monitoring the

temperature of both tanks, determines if the solar tank supplies directly the user tank or it is used as cold source for the heat pump. More in particular, in winter the system operates according to the following conditions:

If the solar tank temperature is over 60°C or if there is a temperature difference between the two tanks, space heating is directly satisfied by the solar collectors without the assistance of the heat pump. If the solar storage tank is lower than 5 °C the heat pump does not operate and the thermal energy should be provided by an alternative generation system. Since this is a solar-assisted air-conditioning plant, the surface capturing solar radiation and the tank for energy store are of great importance. Therefore, a parametric study of the winter performance of the system was carried out varying the storage volume (V= 800 litres and 1600 litres) and the surface area of the collectors (10, 20, 25, 30, 40 m^2).

6.3 Results and discussion

6.3.1 Building heating load and energy consumption

A preliminary simulation was performed to determine the building heating load and the associated yearly energy consumption. Results of hourly simulation are reported in Figure 6-3.

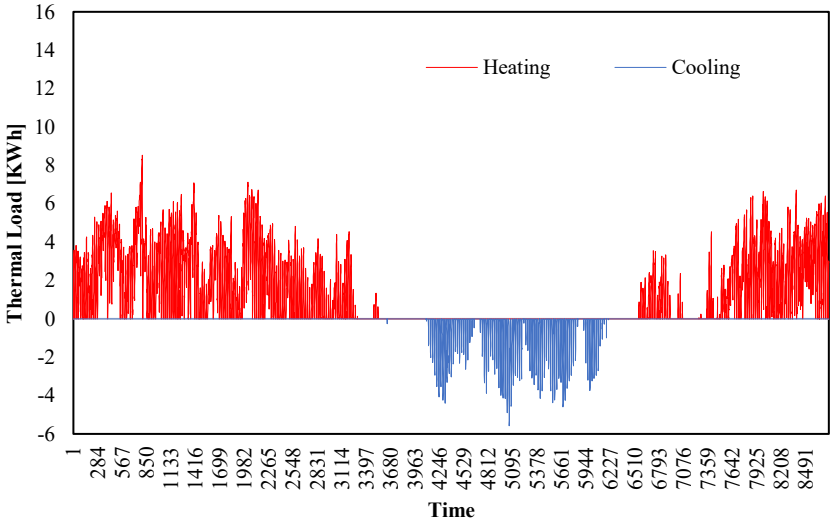

Figure 6-3 Hourly simulation of building thermal need

Accordingly, Figure 6-4 reports the monthly energy demand of the building for winter heating. The months of December showed the highest request with a value of 2182

kWh, followed by January and February with an almost equal amount around 2000 kWh. The total amount of energy needs for winter heating amounts to 10771.7 kWh. Furthermore, a frequency analysis was conducted to quantify the number of hours in which a specific load occurred. Results showed that a load exceeding 12 kW occurred only for a limited number of hours allowing to identify the appropriate capacity for the heat pump, which was selected as 12 kW.

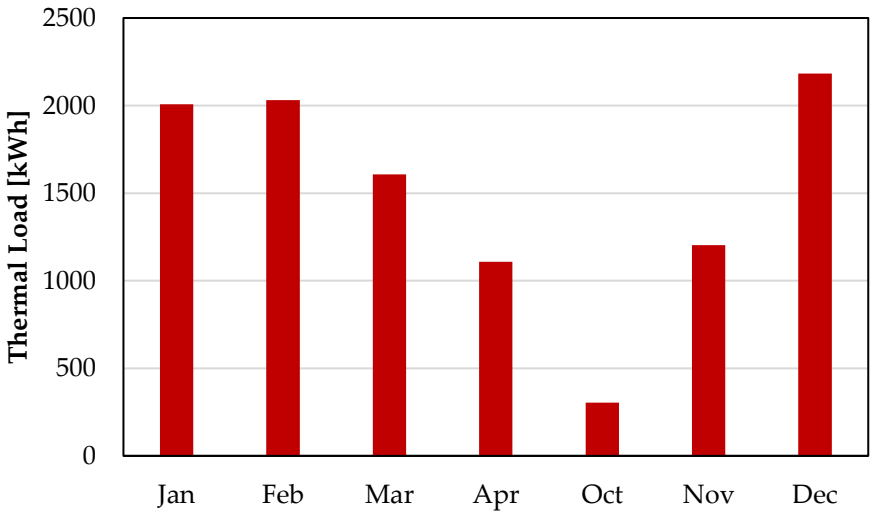

Figure 6-4- Monthly energy demand of the building for winter heating

6.3.2 System thermal performance

For each configuration of the parametric analysis, the percentage of the winter thermal energy demand met by the system has been quantified. Furthermore, concerning the addressed thermal demand, a further distinction has been made between the portion directly handled by the solar collectors and that managed through the heat pump.

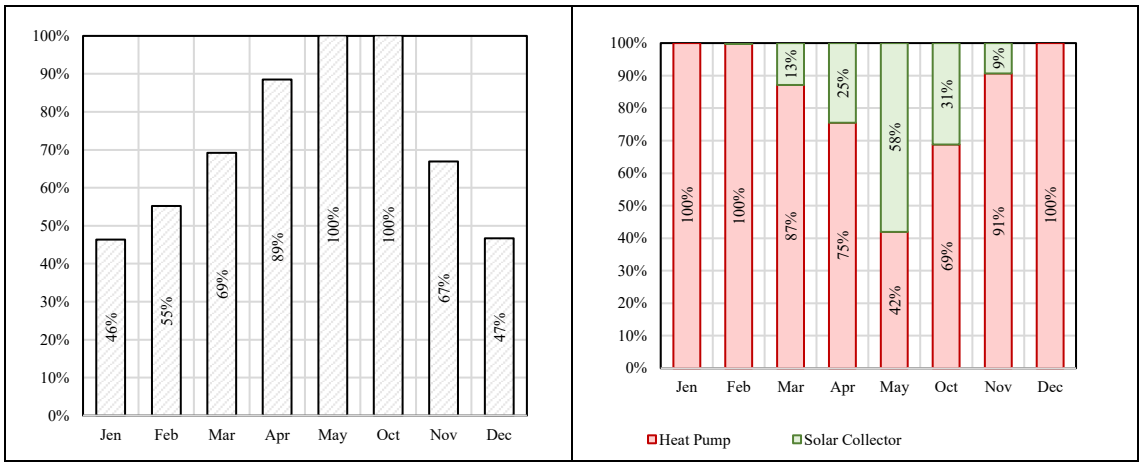

Figure 6-5 Monthly energy demand supplied by the system (left) and percentage of the thermal demand met by heat pump and directly by solar thermal collector (right) A=10 m^2; V=0.8 m^3

In particular, Figure 6-5(left) the monthly percentage of energy satisfied by the SAHP system appears, whereas on the and in Figure 6-5(right) the separated share of energy directly supplied from solar collectors to the user and the share provided by the heat pump is showed. As expected, for low active surfaces of solar panels, the amount of energy provided by the system is not sufficient to completely satisfy the demand in the colder winter months, where the lowest percentage is found in January, being of 46 %. In spring and autumn months the system is able to provide more than 50 % of the energy demand. Interestingly the solar thermal collector is able to directly provide an adequate amount of heating thermal energy in spring and autumn, reaching the maximum value of 58 % in May and the lowest of 9 % in November.

When the solar tank is doubled in its capacity, it is possible to observe better performance in some months. In particular, the system capacity to provide thermal energy increases to 49 % in January and to 57 % in February while in April, May and October the percentages do not vary. Some. As regards the percentage of load directly satisfied by the thermal collector a substantial increase is observed in May, reaching 73 % while in April and October percentages of 27 % and 39 % are observed respectively.

When the solar collector surface is increased to 25 m^2 an overall upward trend shift in all percentages can be observed, as shown in Figure 6-6.

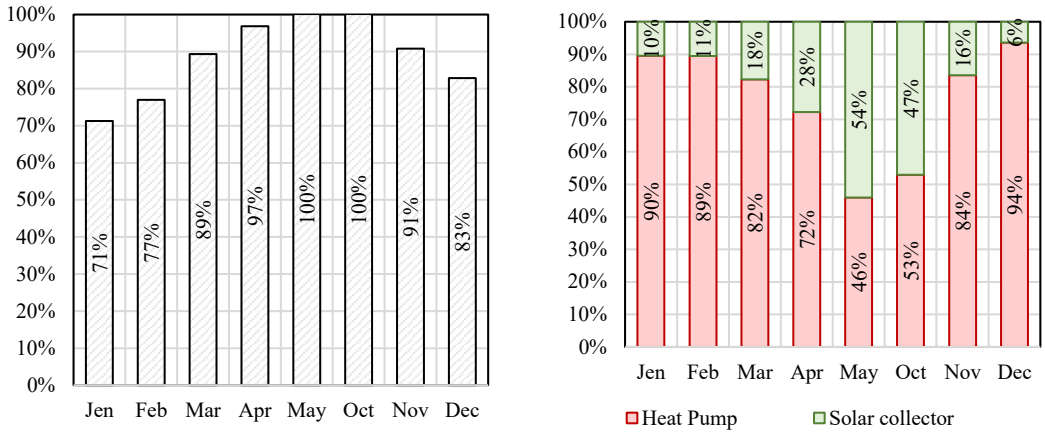

Figure 6-6 Monthly energy demand supplied by the system (left) and percentage of the thermal demand met by heat pump and directly by solar thermal collector (right) A=25 m^2; V=0.8 m^3

From May to November, the ability of the system to provide thermal energy is almost always higher than 90 %, and in the worst condition of January value of 71 % is reached. Solar collector, is in this case, able to directly provide heating to the building in all the months analyzed, with small percentages of 6 % in December and 10 % in January. The best performance is again observed in May where the percentage reaches 54 %. When a solar tank of 1.6 m^3 is used in all the spring and autumn months, the system reaches complete sufficiency (100 %), whereas few increments are observed for the energy directly supplied by the solar collector in winter months, and much more increments are found in May (68%) and October (57%).

In Figure 6-7 the same information is reported for a solar thermal collector surface of 40 m^2 and storage of 800 liters. Clearly the maximum exploitation of solar radiation is achievable in this configuration. In fact, from April to October the system can provide 100 % of energy to the building, and this period extends further to March and November if solar tank volume is augmented to 1.6 m^3. In the latter case, the minimum amount of 87 % is reached in January. When looking at the energy from solar collectors directly used for heating, the amount conspicuously augments in May and October, with percentages of 54 % and 52 % respectively, that further increase to 70 % and 65 % with a 1.6 m^3 solar tank.

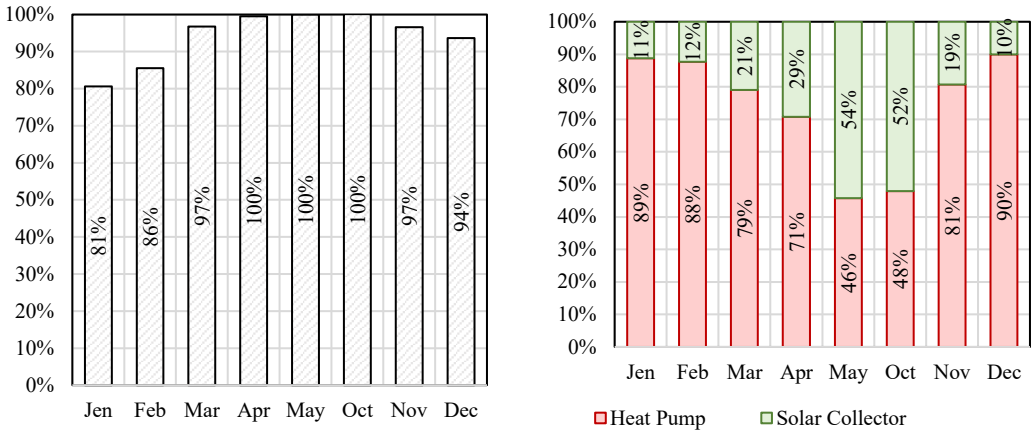

Figure 6-7- Monthly energy demand supplied by the system (left) and percentage of the thermal demand met by heat pump and directly by solar thermal collector (right) A=40 m^2; V=0.8 m^3

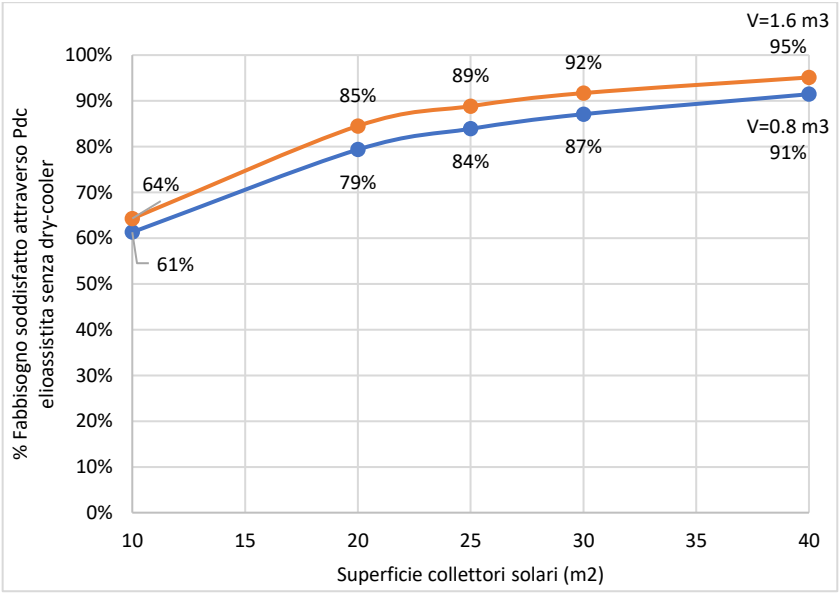

Figure 6-8- Annual energy demand met by heat pump for different solar collector areas and solar tank storages

From Figure 6-8 it is clearly evident that increasing the solar collector surface provides notable increments especially for lower capturing areas. In fact, in the case of the bigger solar tank, moving from 10 m^2 to 20 m^2 produces an increment of 32.8 %; moving from 20 m^2 to 30 m^2 produces instead a much more limited increment of 8.2 %. From the results of simulation, it also emerges that the cost-optimal configuration necessitates a solar panel surface area ranging from 25 to 30 square meters, because gibber areas would not be justified by the relatively small increase in thermal yield.

Furthermore, it was observed that a thermal storage volume of 1.6 cubic meters can ensure the most efficient system performance. This configuration allows for the maximization of energy efficiency while avoiding unnecessary costs. Finally, Table 6-5 reports the average monthly COP of the heat pump along with the yearly average value. The utilization of the solar collector to increase the temperature of the cold source, evidently produces benefits in terms of performance of the heat pump.

Table 6-5- Average monthly COP of the heat pump for the different collector surfaces considered

	S10	**S20**	**S25**	**S30**	**S40**
Jan	3.75	3.86	3.84	3.84	3.87
Feb	3.80	3.91	3.96	3.91	3.95
Mar	3.79	3.91	3.95	3.89	3.96
Apr	3.82	3.97	3.90	3.97	3.87
May	4.08	4.03	4.58	4.02	4.39
Oct	4.10	3.92	3.84	3.89	3.99
Nov	3.70	3.92	3.87	3.91	3.94
Dec	3.72	3.80	3.81	3.88	3.86
Ave	**3.85**	**3.92**	**3.97**	**3.91**	**3.98**

Interestingly the average monthly COP overcome the value of 4 in May for all the collector surfaces. In the other warmer months (October and April), the value is much close to it. In colder months anyway, the COP keep having a relative high value consistent that in January reaches 3.86 for 20 m^3 and in December 3.86 for 40 m^2. For the same months the lowest values of 3.75 and 3.72 are observed for a surface of 10 m^2. The highest value of 4.58 between all the cases is found on May for a surface of 25 m^2. If the yearly average value of COP is considered it can be observed that a maximum value of 3.98 is found for a surface of 40 m^2. However, even in the worst case, the COP assumes a value of 3.85 (for 10 m^2) that can be appreciated to be very much close to the nominal value of the heat pump.

6.4 Conclusions

Heat pumps achieve maximum sustainability when combined with solar energy (solar-assisted heat pumps). In this study solar thermal collectors are employed to

increase the temperature of the cold source of a water-to-water heat pump used for the air-conditioning of a university residential complex in Rende (Italy). The air-conditioning plant of the building is composed of a field of evacuated tube solar collectors and two thermal storage tanks, one at service of the solar collector, that represents the cold source of the water-to-water heat pump.

Simulations are performed with TRNSYS environment to assess the effect of solar thermal collectors and thermal storage size on the fraction of energy demand covered by the system.

When adopting 40 m^2 of solar collector and 1.6 m^3 solar tank the system is able to provide 100 % of energy to the building from March to November. The energy from solar collator directly used for heating amounted to 70 % and 65 % in May and October, respectively. Results of the simulations showed however, that increasing the solar collector surface provided notable increments only for lower capturing areas, whereas moving to higher collector surfaces determined lower marginal increments. It emerged how the cost-optimal configuration requires a solar panel surface ranging from 25 to 30 m^2, and that a thermal storage volume of 1.6 cubic meters can ensure the most efficient system performance. Finally, results showed that utilization of the solar collector to increase the temperature of the cold source of the heat pump produces evident benefits in terms of COP can reach a yearly average value of 3.98 and an average monthly value of 4.58 in May.

6.5 References

[1] Bruno R, Nicoletti F, Cuconati G, Perrella S, Cirone D. Performance indexes of an air-water heat pump versus the capacity ratio: Analysis by means of experimental data. Energies 2020;13. doi: 10.3390/en13133391.

[2] Baggio P, Bee E, Prada A. Demand-Side Management of Air-Source Heat Pump and Photovoltaic Systems for Heating Applications in the Italian Context. Environ 2018, Vol 5, Page 132 2018;5:132. doi:10.3390/ENVIRONMENTS5120132.

[3] Bee E, Prada A, Baggio P, Psimopoulos E. Air-source heat pump and photovoltaic systems for residential heating and cooling: Potential of self-consumption in different European climates. Build Simul 2019;12:453–63. doi:10.1007/S12273-018-0501-5/METRICS.

[4] Nicoletti F, Cucumo MA, Arcuri N. Cost optimal sizing of photovoltaic-battery system and air–water heat pump in the Mediterranean area. Energy Convers Manag 2022;270:116274. doi:10.1016/J.ENCONMAN.2022.116274.

[5] Pourier C, Beltrán F, Sommerfeldt N. Solar photovoltaic/thermal (PVT) technology collectors and free cooling in ground source heat pump systems. Sol Energy Adv 2024;4:100050. doi:10.1016/J.SEJA.2023.100050.

[6] Francisco B, Nelson S, Jaakko E, Hatef M. Empirical investigation of solar photovoltaic-thermal collectors for heat pump integration. Appl Therm Eng 2024;248:123175. doi:10.1016/J.APPLTHERMALENG.2024.123175.

[7] Perrella S, Bisegna F, Bevilacqua P, Cirone D, Bruno R. Solar-Assisted Heat Pump with Electric and Thermal Storage: The Role of Appropriate Control Strategies for the Exploitation of the Solar Source. Build 2024, Vol 14, Page 296 2024;14:296. doi:10.3390/BUILDINGS14010296.

[8] Chata FBG, Chaturvedi SK, Almogbel A. Analysis of a direct expansion solar assisted heat pump using different refrigerants. Energy Convers Manag 2005;46:2614–24. doi:10.1016/J.ENCONMAN.2004.12.001.

[9] Pinamonti M, Beausoleil-morrison I, Prada A, Baggio P. Water-to-water heat pump integration in a solar seasonal storage system for space heating and domestic hot water production of a single-family house in a cold climate. Sol Energy 2021;213:300–11. doi:10.1016/j.solener.2020.11.052.

[10] Han C, Kim J, Cho W, Shin HH, Lee H, Kim Y. Annual performance analysis of solar-assisted raw-water source heat pumps at low water temperatures. Energy 2024;291:130386. doi:10.1016/J.ENERGY.2024.130386.

[11] Emmi G, Zarrella A, De Carli M. A heat pump coupled with photovoltaic thermal hybrid solar collectors: A case study of a multi-source energy system.

Energy Convers Manag 2017;151:386–99. doi:10.1016/J.ENCONMAN.2017.08.077.

[12] Herrando M, Coca-Ortegón A, Guedea I, Fueyo N. Experimental validation of a solar system based on hybrid photovoltaic-thermal collectors and a reversible heat pump for the energy provision in non-residential buildings. Renew Sustain Energy Rev 2023;178:113233. doi:10.1016/J.RSER.2023.113233.

[13] Del Amo A, Martínez-Gracia A, Bayod-Rújula AA, Cañada M. Performance analysis and experimental validation of a solar-assisted heat pump fed by photovoltaic-thermal collectors. Energy 2019;169:1214–23. doi:10.1016/J.ENERGY.2018.12.117.

[14] Dannemand M, Perers B, Furbo S. Performance of a demonstration solar PVT assisted heat pump system with cold buffer storage and domestic hot water storage tanks. Energy Build 2019;188–189:46–57. doi:10.1016/J.ENBUILD.2018.12.042.

7 Solar-Assisted Heat Pump with Electric and Thermal Storage: The Role of Appropriate Control Strategies for the Exploitation of the Solar Source

Abstract

In the EU, the building sector is responsible for 40% of the global energy consumption for final uses and 36% of the carbon dioxide (CO_2) emissions. Heat pumps allow for the replacement of conventional systems based on fossil fuels with the perspective of combining PV and solar thermal collectors. In order to rationalize the use of the solar source, this paper examined the self-consumption electricity share, the CO_2 equivalent emissions, and the domestic hot water demand covered by renewable sources which were determined in two opposite climatic conditions. These involved both electric and thermal storage systems and considered two different control strategies. The first is commonly used for the management of air-conditioning systems, the second was specifically conceived to maximize the exploitation of the solar source. Results showed that the latter significantly reduced grid dependence in both locations, determining the direct satisfaction of 76% of the thermal and electric loads through the PV self-consumption, determined by 18 kWp of installed PV and a battery capacity of 24 kWh. In terms of equivalent CO_2 emissions, when the two control strategies were compared, a remarkable reduction in emissions was registered for the latter, with percentages ranging between 8% and 36% as a function of PV surface and battery capacity. The analysis of domestic hot water supplies revealed disparities between the two localities: the colder first, relied more on heat pumps for water heating, while the warmer second, benefitted from the large availability of solar radiation.

7.1 Introduction

The global environmental landscape has been undergoing profound changes in recent decades [1]. With the growing recognition of the adverse impacts of climate change, the need to transition towards sustainable and environmentally responsible energy sources has become increasingly urgent. As the world grapples with the consequences of greenhouse gas emissions, the pursuit of cleaner and more efficient energy systems has emerged as a central focus of research, policy, and innovation. At the heart of this trans-

formation lies the imperative to harness renewable energy sources. Renewable energy, characterized by its sustainability and low environmental impact, offers a promising avenue for reducing carbon footprint and mitigating the effects of climate change. Solar, wind, hydro, and geothermal energy, among others, have all emerged as key players in the global effort to shift away from fossil fuels. As these sources become more accessible and cost-effective, they present unprecedented opportunities to transform the energy landscape and combat the environmental challenges.

Environmental sustainability has become a central focus, particularly in the building sector and the related energy consumption. This is evidenced by the European Union's re-cent "Fit for 55%" package, which set ambitious targets, including a 55% reduction in greenhouse gas emissions by 2030, compared to 1990 levels. This legislative commitment underscores the growing urgency to address climate-related challenges. Specifically, the Fit for 55% package underlines the pivotal role of HVAC systems in achieving these goals. The legislation encourages the optimization of existing HVAC systems to bolster energy efficiency [2].

Buildings represent one-third of the world's energy consumption and have the potential to significantly reduce carbon emissions [3,4]. In order to achieve this goal, "smart buildings" equipped with innovative air conditioning systems and renewable sources need to be implemented [5].

Heat pumps combined with solar energy (solar-assisted heat pumps) offer high sustainability. Recent research and field applications have made the use of heat pumps necessary as they are efficient, reliable, and environmentally friendly generators for annual air conditioning. Additionally, combining solar power with heat pumps offers a dual ad-vantage. It maximizes the use of solar energy and increases the efficiency of the heat pump, thus optimizing and rationalizing the use of renewable sources [6,7]. The versatility in usage that allows for the provision of both heating and cooling as well as the production of domestic hot water with a single device makes heat pumps particularly suitable for the conditioning of civil buildings. The emission-mitigating potential of heat pumps is contingent upon various factors, including the specific technology employed, geographical location, and the composition of the electricity source [8,9].

In recent years, many researchers have focused on integrating heat pumps with solar collectors, photovoltaic panels, and hybrids for domestic heating. M. S. Bucker et al. and X. Wang conducted reviews on systems that combined heat pumps with solar

collectors, photovoltaic panels, and hybrids. They classified these systems based on their components, the type of use, and the performance achieved in various case studies [10].

Dikici et al. conducted an experimental analysis to evaluate the performance of heat pumps at different sources for domestic heating. They subsequently analysed the performance of multi-heat pump sources to provide a comparison between the various configurations [11]. In another study, F. Huide et al. [12] investigated the performance of an integrated system consisting of a helios-assisted heat pump with photovoltaic/thermal colletors made of heat pipes. The system was used to heat water directly or to act as a heat pump evaporator, depending on different weather conditions [12].

For solar-assisted heat pumps, thermal and electric energy storage systems are pivotal for enhancing self-consumption, narrowing the gap between energy demand peaks and troughs, and increasing the stability of the grid. Over recent years, the widespread adoption of thermal energy storage has been driven by its ability to address the dual requirements of electricity and space heating, while also ameliorating the irregularities in energy demand [13].

Storage systems contribute to enhancing the integration of renewable energy sources into the power grid while boosting system flexibility, all without compromising the security of the transmission and distribution network [14].

Aneli et al. conducted a study to assess how well an energy system, which included an electric heat pump powered by a photovoltaic generator, as well as thermal and electric energy storage, performed. The analysis results showed that systems with around 1000 L of thermal storage and 5.0 kWh of electrical storage can reach self-consumption and self-sufficiency rates of about 80%, which is three times greater than what an energy system lacking storage can achieve. Additionally, this system configuration substantially de-creased grid power exchange [15].

Pinamonti et al. [16] conducted a study on a system that integrated a water-water heat pump with short- and long-term storage, using a dynamic simulation carried out with TRNSYS. The purpose of the long-term storage was to store the surplus solar energy collected by solar collectors during the summer season, which could then be utilized for space heating during the winter months. As a result, the utilization of this system in-creased the solar fraction by five percentage points [16].

Bellos et al., conducted an energy and cost comparison between a solar-assisted heat pump heating system utilizing flat plate collectors, an insulated tank, and a standard

air source heat pump system across twenty European cities through the TRNSYS simulation tool for the entire winter season. The solar-assisted heat pump system demonstrated significant electricity savings, ranging from 30% to 40%, across various insulation scenarios. In these systems, the coefficient of performance (COP) was approximately 4, while for conventional air source systems, it was about 2.5. Notably, the solar-assisted heating system emerged as the financially optimal choice for most of the studied cities, particularly in areas characterized by low insulation levels in buildings [17].

Miglioli et al. [18] provided the state-of-the-art photovoltaic-thermal (PV/T) solar-assisted heat pumps designed for fulfilling thermal energy requirements in buildings. The primary emphasis was given to integration methodologies, potential system configurations, utilization of diverse energy sources, and the design of subsystem components. General guidelines suggested sizing the PV/T area to cover peak thermal demand during the sunniest month and the heat pump according to peak thermal load. Energy storage choices should align with project objectives, favouring water thermal storage (WTS) and advanced control logic for enhanced PV electricity self-consumption and reduced grid de-pendency. Integrating WTS into the solar circuit for direct user or heat pump requirements is advised for optimal solar energy utilization [18].

Furthermore, the integration of heat pumps with thermal storage systems coupled with phase change materials has also been extensively studied. Ning et al. analysed the combination of phase change thermal storage technology with air-source heat pumps, improving the performance coefficient and stability of air-source heat pumps operating in a low-temperature environment. The findings indicated that incorporating phase change materials (PCMs) led to a substantial enhancement in heating time by up to 30.6% and an increase in COP of up to 33.9% at a temperature of 35 °C. However, at 55 °C, this inclusion may trigger an adverse effect [19]. Furthermore, the operation time of the compressor can be reduced by as much as 16.5% at 35 °C, but it increases by up to 15.7% at 55 °C. The study emphasized the importance of balancing sensible and latent heat storage. J. Yao et al. per-formed a numerical simulation to analyse the performance of a system that combined the use of a heat pump associated with solar/photovoltaic panels and thermal storage with PCM [20].

Instead, E. Georges et al. developed an optimization system that allowed load modulation of heat pumps installed in residential buildings to quantify their flexibility of

use by adjusting consumption to electricity prices [21]. Finally, L. Kreuder et al. analysed the combination of heat pump use with demand side management (DSM) strategies [22].

While previous research primarily focused on the effectiveness of the technologies employed, this work aimed to explore the simultaneous impact of combined electrical and thermal storage systems with a control logic aimed at maximizing the utilization of excess renewable energy on the overall performance of solar-assisted heat pump systems. In order to overcome this gap, this paper focused on the possibility of combining an air-to-water heat pump with other renewable sources to increase the use of renewable energy and self-consumption. The proposed system included an air-to-water heat pump, a field of photovoltaic panels with electrical storage, a thermal solar collector, and an insulated tank as thermal storage. The domestic hot water (DHW) is also provided by the tank supplied via thermal solar collectors working in forced convection. The paper's aim was the development of suitable control strategies targeted to optimize the employment of the free solar source. In particular, two different control logics were compared: in the first, the heat pump kept the tank at the set-point temperature, regardless of the presence of renewable energy, whereas the second allowed it to surpass the set point even when the demand for renewable electricity was exceeded in order to store thermal energy in tanks via an appropriate management of renewable surpluses. Simulations were conducted, in the TRNSYS environment for two distinct Italian cities, Milan and Messina, with opposite climatic conditions (heating dominates the first, cooling dominates the second). This analysis also aimed to underscore any potential drawbacks associated with the proposed solution. To quantify the performances of the proposed system, efficiency was chosen as a reference parameter and determined through the analysis of:

- Self-consumption and electricity supplied by the national grid.
- CO2 equivalent emissions.
- Domestic hot water (DHW) supplied by solar collectors.

7.2 Methodology

In this section, the reference building-plant system and numerical setup are present-ed. The main characteristics of the air-to-water heat pump, PV generator, thermal solar collectors, and thermal and electrical storage are introduced. Successively, the implemented control strategies are described. Finally, the method for determining performance parameters is outlined.

7.2.1 Case Study Building

The case study building was a one-story residential structure with a total area of 200 m^2. It was comprised only of thermal zones and had an inter-floor height of 2.7 m (Figure 7-1). The building envelope was designed to meet national energy efficiency regulations for buildings currently mandatory in Italy for new constructions [23]. The U-value of the ex-ternal walls was 0.34 W/m^2K, with the stratigraphy outlined in Table 7-1.

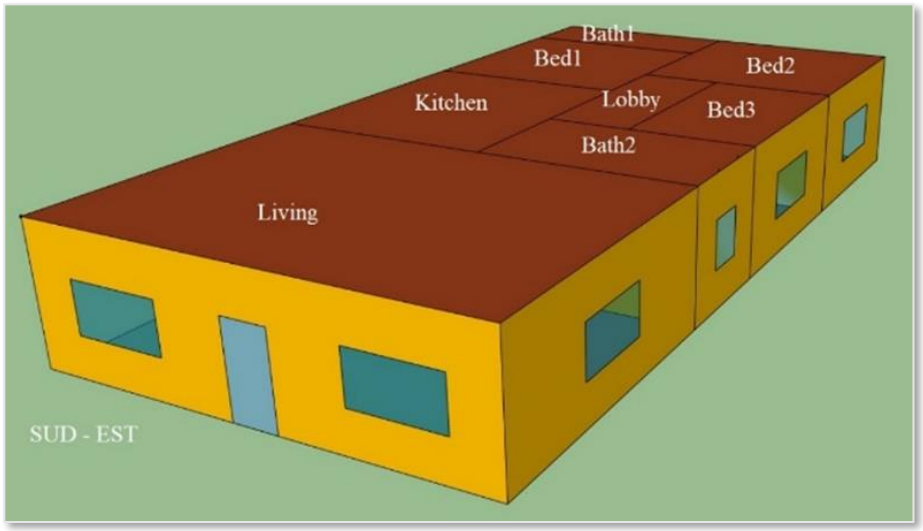

Figure 7-1-3D view of the case study building

Table 7-1- Thermal properties of the external wall layers.

	External Vertical Wall (U = 0.34 W/m²K)			
Material	**Thickness [m]**	**Density [kg/m³]**	**Specific Heat [kJ/kg K]**	**Thermal Conductivity [W/mK]**
Plaster	0.02	900	1.00	0.250
Bricks	0.33	1800	0.84	0.720
Expanded Polystyrene	0.09	20	1.20	0.041
Plaster	0.02	900	1.00	0.250

The ground floor and roof slabs had a thermal transmittance of 0.277 W/m^2K and 0.225 W/m^2K respectively. The layers are listed in Table 7-2 and Table 7-3

Table 7-2- Thermal properties of the ground floor slabs.

	Ground Floor Slabs			
Material	**Thickness [m]**	**Density [kg/m³]**	**Specific Heat [kJ/kg K]**	**Thermal Conductivity [W/mK]**
Tiles	0.010	2.3×10^3	0.84	0.720
Adhesive	0.010	1.53×10^3	1.00	0.720
Sand	0.050	1.73×10^3	0.84	1.400
Expanded polystyrene	0.088	20	1.20	0.041
Bitumen	0.005	1.23×10^3	1.00	0.170
Concrete	0.084	1.93×10^3	0.84	1.060

Bricks	0.330	1.3×10^3	0.84	0.300
Plaster	0.010	2.33×10^3	0.84	0.720

Table 7-3- Thermal properties of the Roof slabs.

Roof Slabs				
Material	**Thickness [m]**	**Density [kg/m³]**	**Specific Heat [kJ/kg K]**	**Thermal Conductivity [W/mK]**
Plaster	0.015	1.83×10^3	1.00	0.700
Concrete and bricks	0.300	1.3×10^3	0.84	0.300
Concrete	0.084	1.93×10^3	0.84	1.060
Bitumen	0.010	1.23×10^3	1.00	0.170
Expanded polystyrene	0.080	203×10^3	1.20	0.041
Sand	0.050	1.73×10^3	0.84	1.400
Adhesive	0.330	13×10^3	0.84	0.300
Plaster	0.010	2.33×10^3	0.84	0.720

The windows consisted of a double-pane 4/15/4 configuration with an argon fill and a thermal transmittance of 2.2 W/m^{2}K. They had a frame-to-glazed surface ratio of 0.15. The building was intended for occupancy by 5 individuals, with a designated sensible heat rate of 75 W per person. An infiltration rate of 0.28 air changes per hour (h−1) was specified. The winter set-point temperature was established at 21 °C, and in summer, it was set to 26 °C. The occupancy profile followed the schedule depicted in Figure 7-2.

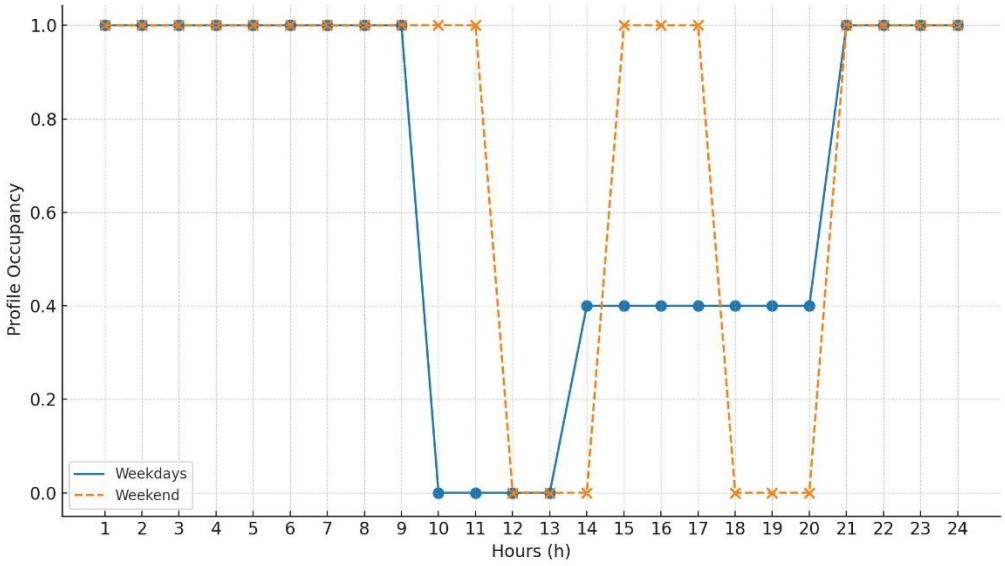

Figure 7-2- Occupancy profiles for weekdays (on the left) and weekends.

Initially, the building was assumed to be located in Milan, characterized by a continental climate classified as subtype 'CFb' (marine west coast climate) according to [19]. Successively, simulations were also conducted in Messina, which features a hot Mediterranean/dry-summer subtropical climate as per the same classification.

7.2.2 Electrical and DHW Loads Profiles

The DHW usage pattern was established based on data collected from residential buildings. Separate profiles were created for weekdays and weekends, and these profiles were used throughout the year. This choice was made as no significant variations were observed in the measured data. The DHW profile, represented in terms of the required thermal energy, is depicted in Figure 7-3.

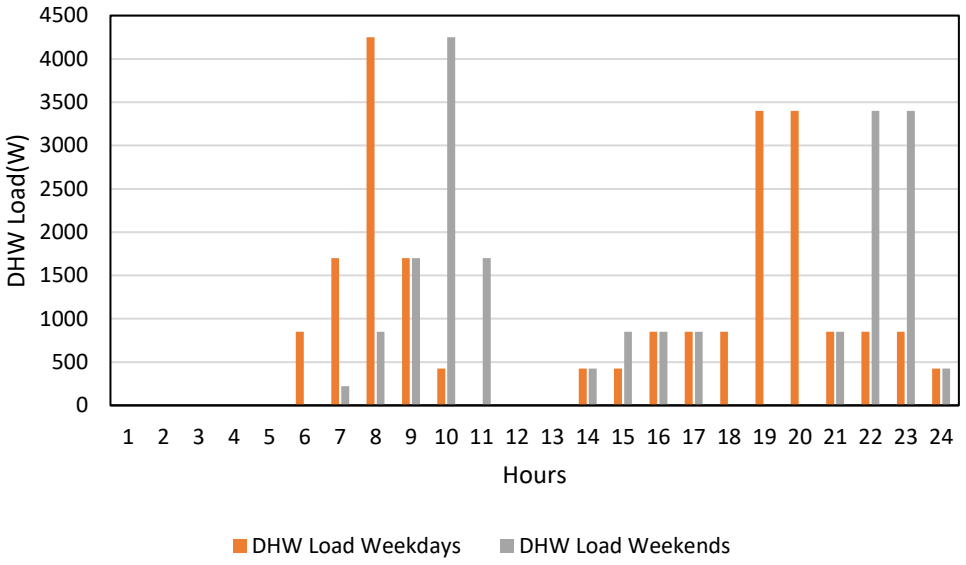

Figure 7-3- Profile of requested thermal power for DHW applications for weekday and weekends.

Similarly, measurements taken on the primary appliances in residential buildings were used to establish an appropriate schedule for the building's electric energy demand. Monitored appliances included the refrigerator, washing machine, dishwasher, phone, iron, personal computers, and television. Data analysis led to the definition of the profiles depicted in Figure 7-4which were categorized for weekdays and weekends.

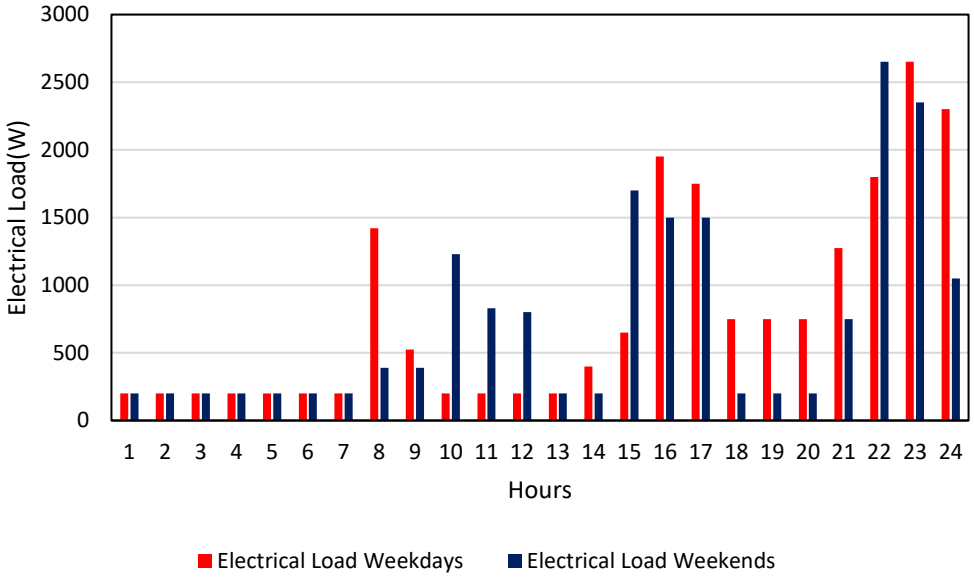

Figure 7-4 Profile of requested electric power on weekdays (left) and weekends (right).

7.2.3 Simulation Model and HVAC Plant

In accordance with recent European directives on energy efficiency, the HVAC system used in the case study relied on an air-to-water heat pump. The plant above was implemented in the TRNSYS 18 environment (

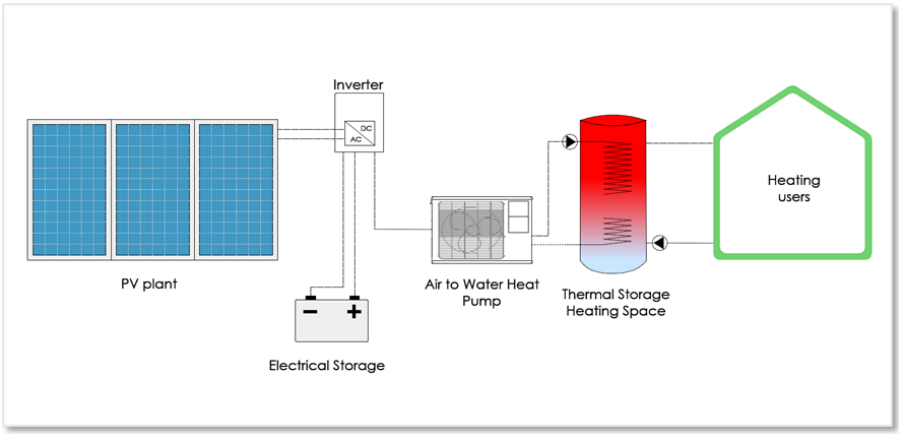

Figure 7-5). TRNSYS 18 is widely recognized as a reliable and versatile tool for energetically simulating complex systems. Its capability to intricately model both the components of the system and their interactions has been crucial in achieving a precise evaluation of the dynamics of the studied system. Additionally, this program incorporates comprehensive libraries of system and technology components, encompassing various types of solar systems, buildings, and heating-cooling loads.

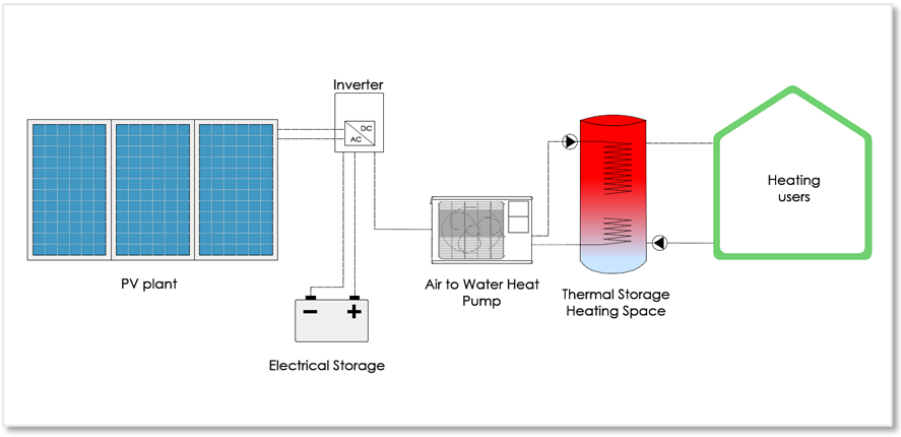

Figure 7-5- Scheme of the simulated plant in TRNSYS 18.

The construction of the model involved the following work-flow (Figure 7-6): construction of the 3D model, a thermophysical definition of the reference building and finally, the mathematical definition. The building's 3D model was created using Sketchup, incorporating the TRNSYS 3D plug-in to facilitate a comprehensive representation of its geometry. TRNBuild establishes the required characteristics of the building envelope and its regime, encompassing radiation mode, infiltration and ventilation, the number of zones/air nodes, as well as the thermal and moisture capacitance of the zone/air node. TRNBuild generates an information file that describes the outputs and inputs required by the Type 56 multi-zone building that in TRNSYS 18, is completely dedicated to modelling the behaviour of even complex buildings. The plant, on the other hand, was primarily modelled using the following types: "type 941" for the air-to-water heat pump, "type 156" for the thermal storage tank, "type 987" to simulate the behaviour of the emission system, "type 103b" for the photovoltaic system, "type 47a" for the electric storage battery, and "type 48b" employed to regulate energy flows.

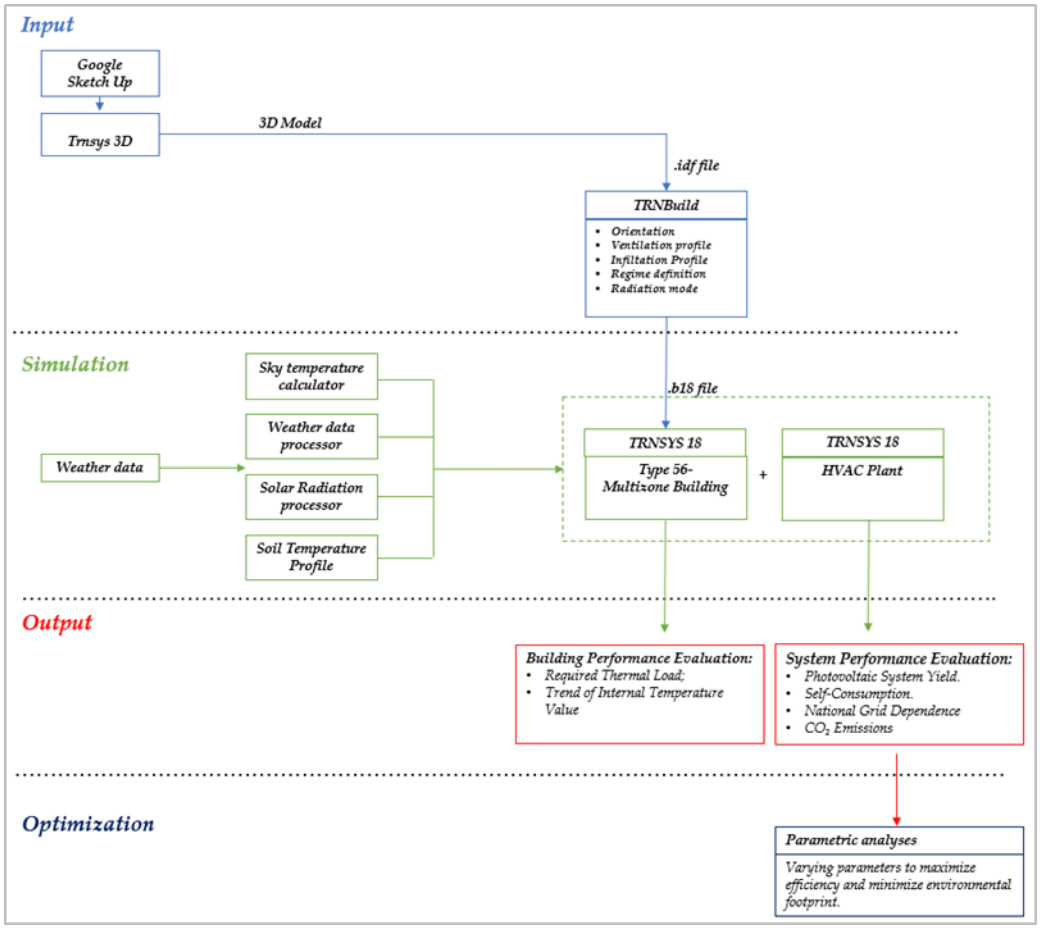

Figure 7-6- Structure of the simulation procedure.

A preliminary building simulation determined the necessary heating capacity of the heat pump, which was then set to 11 kW in set-point conditions for the colder locality.

The heat pump provided direct heating to the thermal storage tank. The key features of the thermal storage are detailed in Table 7-4. The tank was equipped with an immersed heat exchanger in the form of a coiled tube. The fluid in the storage tank interacted with the fluid in the heat exchanger (through heat transfer with the immersed heat exchanger), the environment (through thermal losses from the top, bottom, and edges), and up to two flow streams that passed into and out of the storage tank. The tank was divided into iso-thermal temperature nodes to model water temperature stratification. Each constant-volume node was assumed to be isothermal and interacted thermally with the nodes above and below through fluid conduction and movement.

Table 7-4- Main characteristics of thermal storage.

	Value
Tank height	1 m
Number of nodes	5

Thermal loss coefficient	0.924 W/m²K
Height of inlet 1	0.8 m
Height of outlet 1	0.2 m
Height of inlet 2	0.2 m
Height of outlet 2	0.8 m
Height of HX inlet	0.5 m
Height of HX outlet	0.2 m

An on/off differential controller governed the operation of the heat pump based on the difference between two temperature thresholds (Th and Tl) relative to two hysteresis temperature differences (DTh and DTl). The controller incorporated hysteresis as its control function relied on the previous input function value. For winter operation, the controller permitted the heat pump operation between 50 °C and 55 °C at the outlet (first control log-ic). Additionally, an upper limit condition of 80 °C was in place to prevent the control function from activating if the maximum temperature was exceeded. The building's conditioning was performed by a fan coil heating or cooling the air as it passed over hot or cold liquid flow streams withdrawn from the thermal storage, allowing the outlet flowrate generated via the fan coil to be sent to the building for heating or cooling. Appropriate input variables, such as inlet temperature, humidity, and flowrate, were defined in the building type, where a maximum outlet temperature of 50 °C was allowed to account for real working conditions. It is achieved by mixing the outlet flowrate from the storage with a fraction of the fain coil returning water after passing through a tempering valve. In summer, the thermal storage volume stores chilled water for cooling services, so it cannot be used for DHW. A thermal storage of 300 L was used for DHW with solar collectors working in a forced convection. The solar collectors had an intercept efficiency of 0.8, a first-order loss coefficient of 3.61 W/m^{2}K, and a second-order loss coefficient of 0.139 W/m^{2}K. The circulation pump was activated when the temperature difference between the outlet of the solar collector and the storage was less than 20 °C and stopped when the difference reached 10 °C. The water withdrawn from the solar storage was then mixed with a colder flowrate from the supply network to achieve a set point temperature of 45 °C for domestic applications. The necessary area for the solar collectors was determined through a preliminary simulation to be 8 m^2 to fully meet the defined DHW requirements in Figure 2 for the summer period. In winter, when solar radiation was not sufficient to meet the DHW requirements, the additional energy needed was extracted from the thermal storage connected to the heat pump, giving priority to the solar collectors. To increase efficiency and the share of renewables, a grid-

connected photovoltaic plant was included to provide part of the necessary electricity. The PV modules used were made of mono-crystalline silicon type and the main electric characteristics are reported in Table 7-5.

Table 7-5 Main characteristics of the PV modules.

	Value
Short-circuit current at ref. Isc	8.76 A
Open-circuit voltage at ref. Voc	37.9 V
Voltage at maximum power	31.0 V
Current at maximum power	8.07 A
Temperature coefficient of Isc	0.053 A/K
Temperature coefficient of Voc	−0.485 V/K
Number of cells in series	60
NOCT	47.5 °C
Area	1.64 m^2

The size of the PV plant was left as a parameter for the parametric analysis shown in the following section. Since there is not always synchronization between the required electric loads and the availability of solar radiation, the generator was fitted with an electric storage system—a traditional lead-acid storage battery—in order to better manage the sur-plus of PV power output. The simulated battery worked in conjunction with a solar cell array and power conditioning components, with the capacity of the battery being a variable in the parametric analysis discussed below. In DC source power systems—such as photovoltaic arrays—two power conditioning devices are necessary. The first is a regulator, which distributes DC power from the source to and from a battery (in energy storage systems) and the second component, an inverter. If the battery is fully charged or only re-quires a taper charge, excess power is either discharged or not collected by shutting off parts of the source. The inverter converts the DC power to AC, sending it to the load and/or sending it back to the utility. Type 48 simulates a power regulator and inverter which can be used with a PV array and a battery.

7.2.4 Management Logic

The paper investigated the influence of controllers on the rational use of renewable energy in air-conditioning systems with the aim of improving energy efficiency. Two main control management strategies were proposed. The first strategy activated the heat pump based on the temperature levels monitored on its outlet and the thermal storage, in order to maintain the tank at the desired set-point temperature, irrespective of the

availability of renewable energy. This approach is currently the most commonly used logic in air-conditioning systems, although it gives little attention to the optimization of renewable sources. The second strategy, referred to as smart control, allowed for the tank temperature to exceed the set point, as the heat pump was activated even when the renewable electricity exceeded the demand. This meant that the tank could function as an electric storage unit for any PV surpluses in terms of hot/cold water produced through the heat pump. In other terms, PV surpluses were transformed into heating/cooling loads by the heat pump and stored in the tank for deferred uses. In this case, the combination of a heat pump and tank is considered an electrical storage system for managing excess photovoltaic electricity, therefore it can be exploited also when heating or cooling loads are not required. If the storage tank is saturated, thermal energy can be stored in the building structure by modifying the internal set-point values with strategies such as overheating in winter or under-cooling in summer. To avoid eventual discomfort, indoor temperatures cannot exceed 22 °C in winter and 25 °C in summer. Thus, the implemented smart control strategy has the potential to optimize the use of renewable energy and improve energy efficiency in air-conditioning systems. In this paper, only the system's performance during the winter season was analysed.

Energy Carrier	$kgCO_{2eq}/kWh$
Natural gas	0.21
Electricity energy from the grid	0.46
Electricity from PV	0.00

7.2.5 CO_2 Equivalent Emission

The equivalent emissions were calculated through the factors listed in Table 7-6as a function of the energy carrier [24]. The calculation process involved multiplying the respective emission factor for each energy carrier by its corresponding energy consumption in kilowatt-hours.

Table 7-6- Emission factors for each energy carrier.

7.3 Results

A study was conducted to identify the optimal configuration for each management strategy using parametric analysis. Various parameters were tested, including thermal

storage volume, number of photovoltaic panels, and battery capacity. Photovoltaic system simulations were conducted using 18, 36, and 72 panels for peak powers of 6, 12, and 24 kW, respectively. Electrical storage was tested with two different capacities, 1.2 × 104 Wh and 2.4 × 104 Wh. Tank volume was tested with 0.5 m^3 and 1 m^3 capacities. The results showed that energy efficiency was not significantly affected by tank volume variation and hence not reported in the text. Therefore, only the results of the other two analysed parameters were reported and referred to a tank storage volume of 1 m^3. The efficiency of the system was measured by determining the self-consumption of photovoltaic electricity, the percentage of electricity supplied by the grid and CO_2 emissions. The study also examined the percentage of DHW supplied by solar collectors.

7.3.1 . Calculation of the Heating Loads of the Reference Building in the Considered Climate

In Figure 7-7, the thermal loads for the building are illustrated, with Milan depicted in red and Messina in orange.

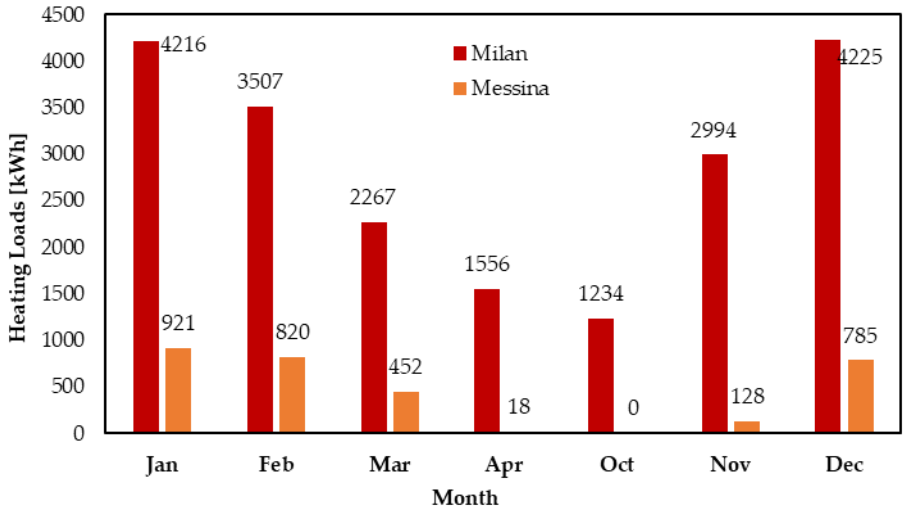

Figure 7-7- Heating Loads for Milan and Messina.

The monthly load data presented represents the dynamic simulation results obtained through TRNSYS for a building based on actual weather data provided by a typical meteorological year (TMY) that is a collation of selected weather data for a specific location, providing hourly records of solar radiation and meteorological elements over a one-year period. These values were derived from a database with a duration significantly longer than a year, typically spanning at least 12 years. The selection was

specifically tailored to encompass the full range of weather phenomena for the given location, while still providing annual averages that aligned with the long-term averages for that particular geo-graphic area.

The load data for the building in Milan reveals significant variations throughout the year. Notably, the highest heating demands were observed during the winter months (January, February, and December), with substantial values reaching up to 920.70 kWh. These load patterns aligned with Milan's continental climate, characterized by cold winters and warm summers. In contrast, the load data for the building in Messina reflected a substantially different climatic profile. The heating demands in Messina were considerably lower than in Milan, with minimal winter loads that almost reached zero. This discrepancy was due to Messina's Mediterranean climate, featuring mild winters and hot summers.

The graphs in Figure 7-8 depict meteorological variations between Milan and Messina, presenting a comparison of air temperature (°C) and solar radiation on the horizontal plane (kJ/h·m^2). These data provide insights into the availability of solar energy in their respective regions.

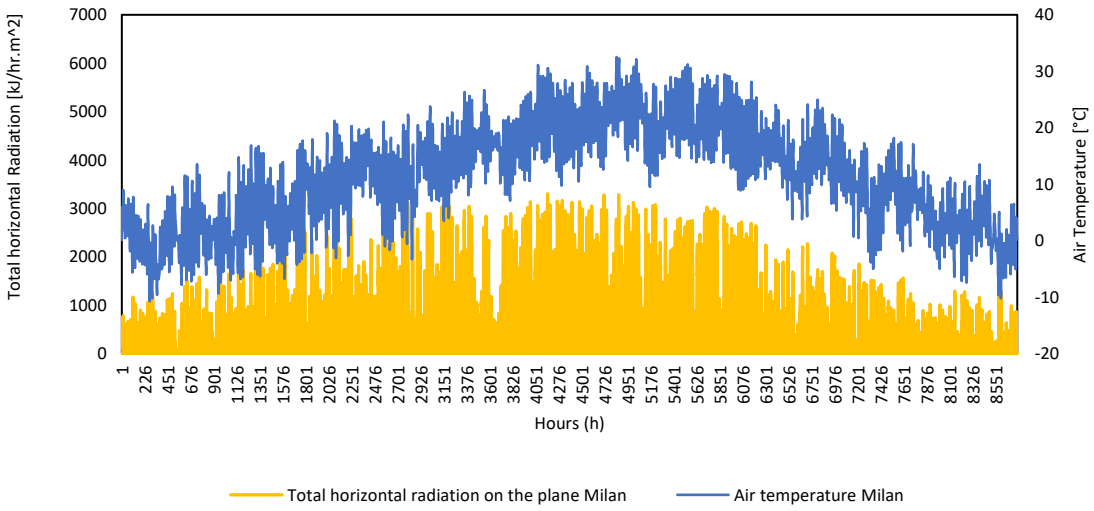

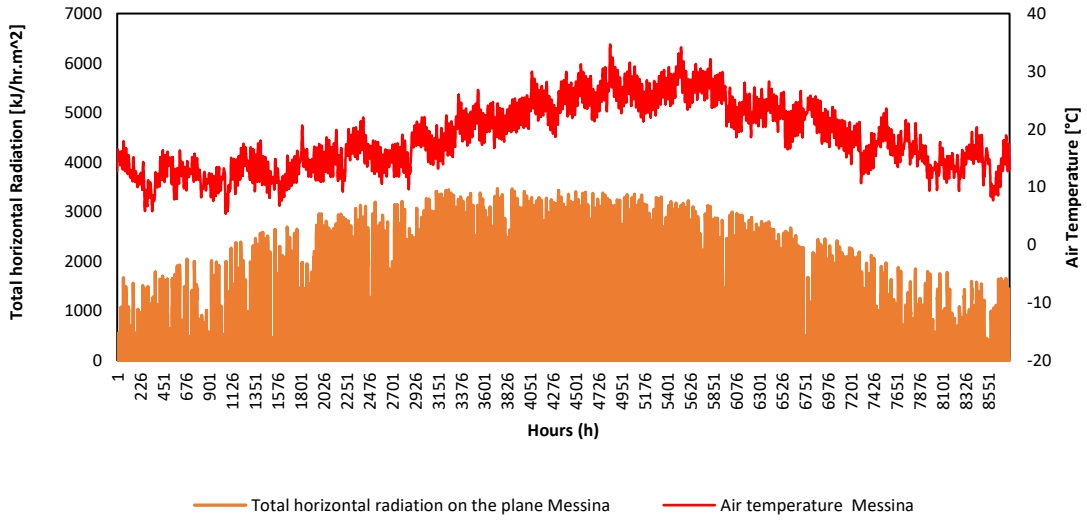

Figure 7-8- Weather conditions in selected localities: comparison of air temperature and total horizontal radiation on the plane in Milan and Messina.

This analysis underscores the importance of tailoring HVAC systems to the specific climatic conditions of each location. In Milan, the focus should be on effective heating solutions for winter, while in Messina, a strong emphasis on cooling systems is essential to address the summer heat. These insights were crucial for optimizing energy efficiency and ensuring occupant comfort in both regions.

7.3.2 Self-Consumption and Electricity Supplied by the National Grid

This analysis investigated the impact of varying peak installed power (PV panels) and battery capacity on the system's performance, with a focus on the heating season (from October to April). The key parameters evaluated include PV generation, electrical storage, electricity from the grid, PV self-consumption, and building power consumption. Six scenarios were considered: Scenario 1: 18 PV panels and 1.2 × 104 Wh battery capacity. Scenario 2: 36 PV panels and 1.2 × 104 Wh battery capacity. Scenario 3: 72 PV panels and 1.2 × 104 Wh battery capacity. Scenario 4: 18 PV panels and 2.4 × 104 Wh battery capacity. Scenario 5: 36 PV panels and 2.4 × 104 Wh battery capacity. Scenario 6: 72 PV panels and 2.4 × 104 Wh battery capacity.

Simulations were conducted for all the scenarios listed above, carefully examining both the application of the first and the second control logic. In these simulations, the behaviour of the systems under different conditions was analysed, considering both traditional management, based on the first logic, and the more advanced approach of the

second control logic. This allowed us to evaluate how each system performed in terms of energy demand coverage, self-consumption, and the use of renewable sources in various scenarios and environmental conditions.

The following charts depict the percentage distribution of the electrical load provided by each component: the contribution from the direct photovoltaic system is shown in green, that of the electrical storage in light green, and finally, the national electrical grid in red.

7.3.2.1 Milan

From the graphs depicted in Figure 7-9 (from Scenario 1 to Scenario 3), it can be seen that as the peak photovoltaic power installed increased, the percentage of energy demand coverage directly from the photovoltaic system and battery increased, consequently the dependence on the national grid decreased. In particular, the maximum percentage of dependence on the grid, recorded in December with 18 panels, decreased to 76% in December with 72 panels installed. By doubling the battery storage capacity (from Scenario 4 to Scenario 6), the use of photovoltaics and batteries increased proportionally to the number of photovoltaic panels. It is particularly noticeable that the benefits were lower in colder months and higher in April, October, and November. In October, with 72 panels and a battery capacity of 2.4 × 104 Wh, almost complete energy self-sufficiency was achieved compared to the national grid.

First control logic

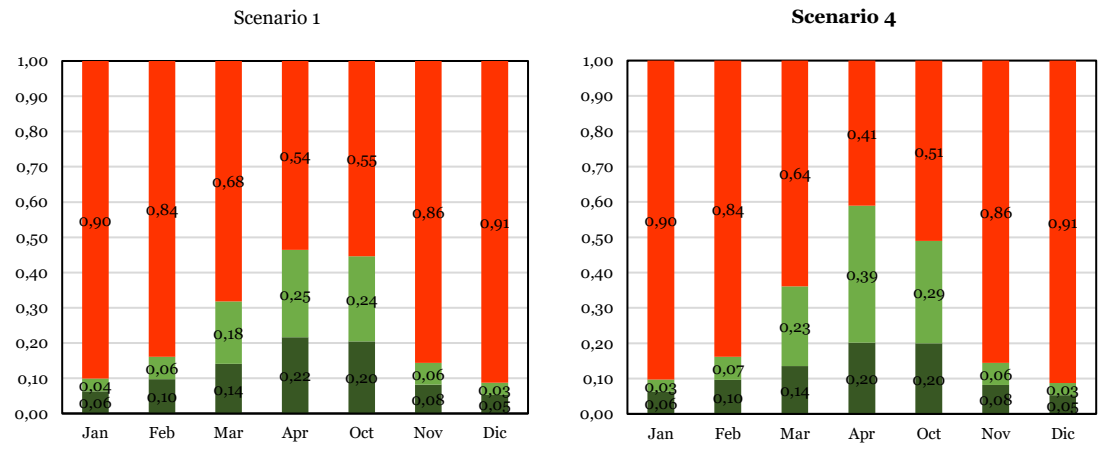

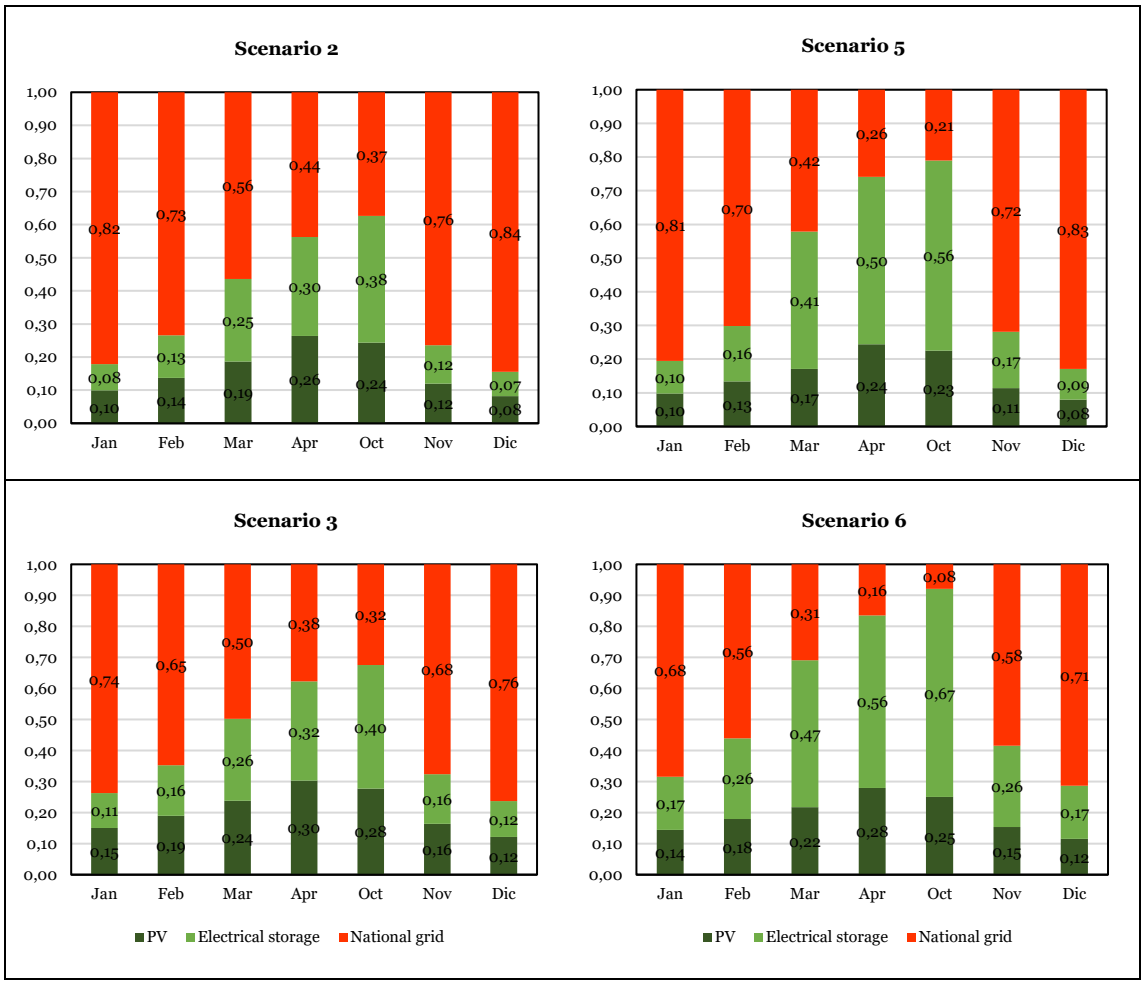

Figure 7-9- Percentage of load managed by each component varying the scenarios for the first control logic in Milan.

The diagrams in Figure 7-10 (from Scenario 1 to Scenario 3) show the percentage of load managed by each component through the implementation of the second control logic, while the number of photovoltaic panels increased and a 1.2 × 104 Wh storage battery was used. Comparing it with the graph in Figure 7-9, it can be noticed that for 18 panels, the situation remained essentially unchanged. However, the situation was different for the con-figuration with 36 and 72 panels. In the latter case, it was evident that the storage of excess photovoltaic energy as thermal energy can halve the usage of the national grid, especially in March, April, and October.

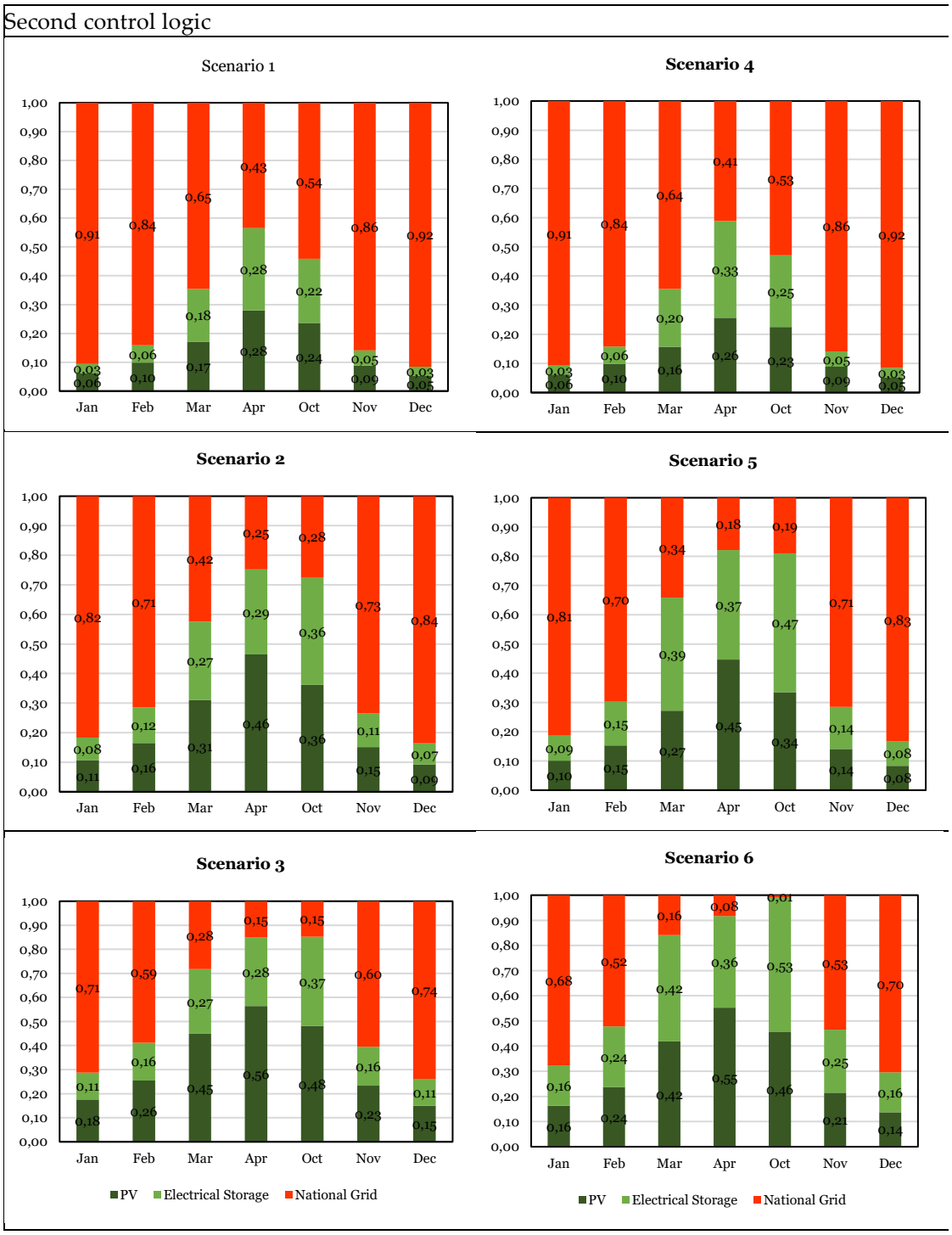

Figure 7-10- Percentage of load managed by each component varying the scenarios for the second control logic in Milan.

The charts in Figure 7-10 (from Scenario 4 to Scenario 6) depict the percentage of load regulated by each component via the second control logic, as the quantity of photovoltaic panels increased and a 2.4 × 104 Wh storage battery was employed. By comparing the per-centages in the graph shown in Figure 7-10 with those in Figure 7-9

(the same combination but with a different control logic), it can be deduced that in this case as well, a control logic that was more focused on managing the surplus energy produced did not lead to improvements to the configuration with 18 panels. In fact, in this configuration, excess pro-duction compared to demand rarely occurred. On the other hand, the situation was different compared to the other two combinations. A smart control strategy allowed for almost always satisfying 50% of the thermal load using renewable energy sources.

In Figure 7-11, the annual percentages of self-consumed energy during the heating period are shown relative to the energy produced. It can be observed that this percentage de-creased as the peak power installed increased. It was also evident that greater electrical storage capacity allowed for better utilization of solar radiation, resolving the problem of the mismatch between demand and solar radiation presence. Through the use of building envelope overheating strategies (second control logic), it was possible to increase the per-centage of self-consumed energy by approximately 10%, maximizing the use of a clean energy source, except for a number of panels equal to 18.

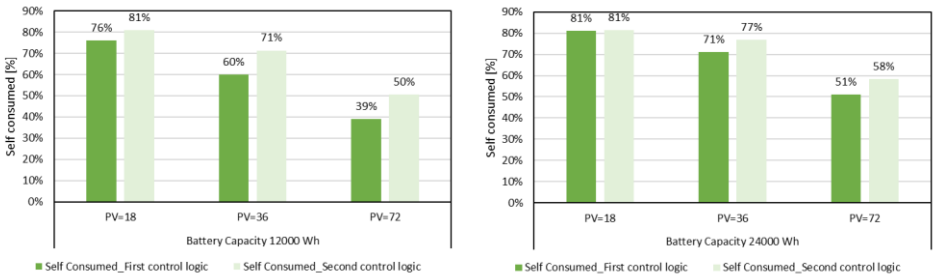

Figure 7-11- Annual percentages of total self-consumed electric energy in Milan.

Table 7-7 provides an annual breakdown of the percentage distribution of electrical load managed by various components within different scenarios. These scenarios were assessed under two distinct management logics: first control logic and second control logic. The results revealed notable variations in energy utilization patterns between the two logics. Under the first control logic, the systems exhibited a significant reliance on the national grid, ranging from 65% to 75% of energy sourced externally, highlighting substantial grid dependency. However, self-consumption rates were remarkable, surpassing 70% in certain scenarios, particularly during colder months. Conversely, the second control logic' showcased a substantial reduction in grid dependence across all scenarios. The percentage of grid-sourced energy significantly diminished, occasionally dropping as low as 38%, emphasizing the efficiency of this logic

in optimizing local energy utilization. Moreover, self-consumption levels remained notably high, exceeding 70% in several scenarios. These findings underscored the reliability of the second control logic' in maximizing self-generated energy consumption while mitigating dependence on the national grid.

Table 7-7 Annual percentage distribution of electrical load managed by each component in different scenarios, comparing the two management logics in Milan.

Management Logic	Scenario	PV	Electrical Storage	National-Grid	Self-Consumed
First control logic	Scenario 1	12%	12%	75%	76%
	Scenario 2	16%	19%	65%	60%
	Scenario 3	21%	22%	57%	39%
	Scenario 4	12%	16%	72%	81%
	Scenario 5	15%	28%	56%	71%
	Scenario 6	12%	11%	76%	55%
Second control logic	Scenario 1	14%	12%	73%	81%
	Scenario 2	24%	19%	58%	71%
	Scenario 3	33%	21%	46%	50%
	Scenario 4	13%	14%	73%	81%
	Scenario 5	22%	24%	54%	77%
	Scenario 6	31%	30%	38%	58%

7.3.2.2 Messina

In the graphs of Figure 7-12, the percentages provided by each component of the first control logic are shown concerning the simulations conducted in the city of Messina.

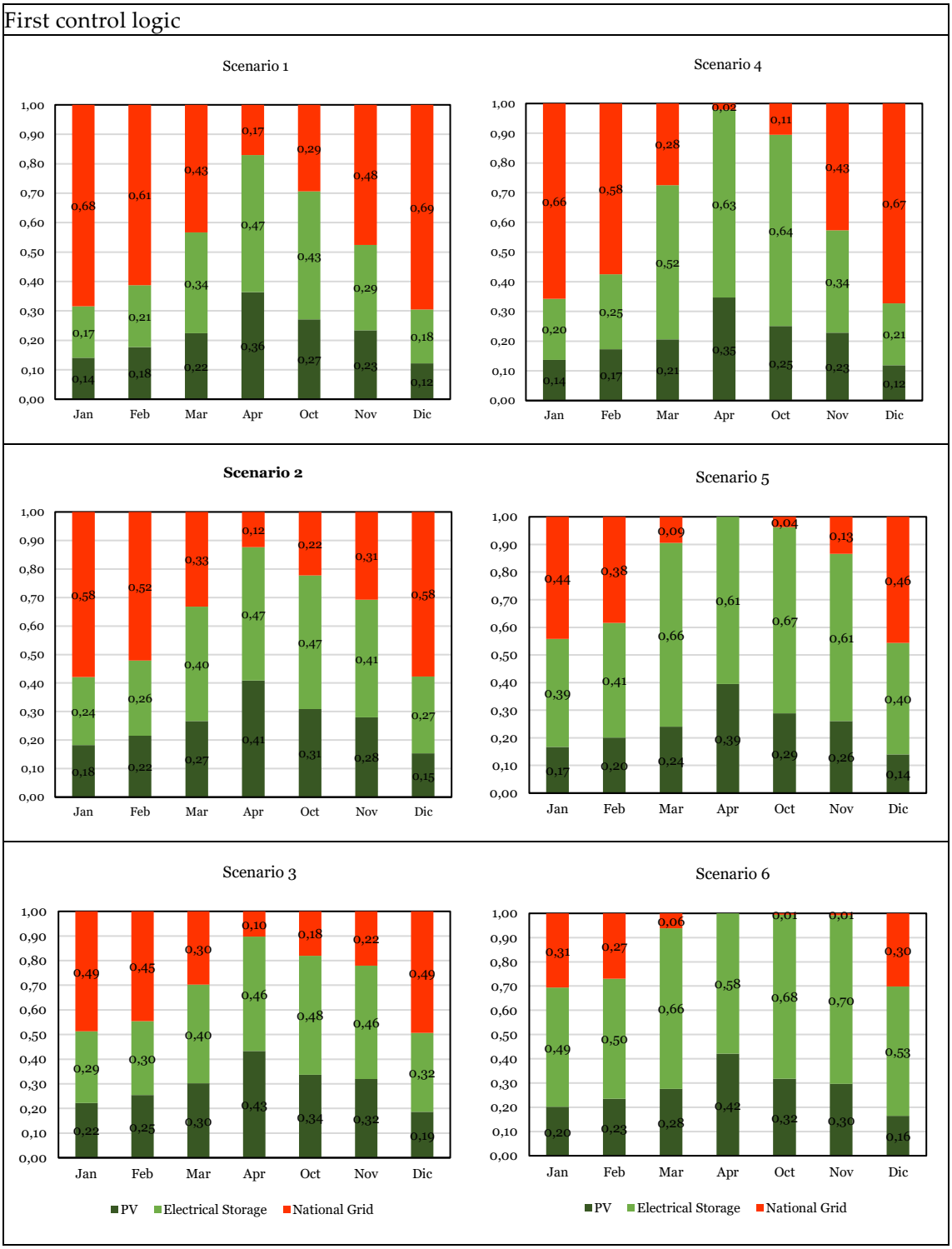

Figure 7-12- Percentage of load managed by each component varying the scenarios for the first control logic in Messina.

Similar to the simulations conducted in Milan, the data from the Messina simulations also revealed the impact of varying the number of photovoltaic panels while maintaining a constant 1.2 × 104 Wh battery capacity (Scenario 1 to 3) and the influence of doubling the battery capacity (Scenario 4 to 6) with an increasing number of panels.

In the Milan simulations, the results showed that as the peak photovoltaic power in-stalled increased, the percentage of energy demand covered directly by the photovoltaic system and battery increased. Conversely, the reliance on the national grid decreased. For instance, the highest grid dependence in Milan was observed in December with 18 panels, covering 75% of the energy demand. However, with 72 panels installed, this dependence dropped to 49% in January, underscoring the potential for greater energy self-sufficiency as photovoltaic capacity increased.

Similarly, to Milan, in the Messina simulations, the trend of increasing photovoltaic power leading to greater self-sufficiency was observed. The percentage of load directly supplied via the photovoltaic system (represented by the green bars) and the contribution of the electrical storage system (light green bars) both grew, while the percentage of grid-supplied energy (red bars) decreased. Notably, in Messina, with 72 panels and a 2.4 × 104 Wh storage battery, nearly complete energy self-sufficiency was achieved in October compared to the national grid, similar to the results obtained in Milan.

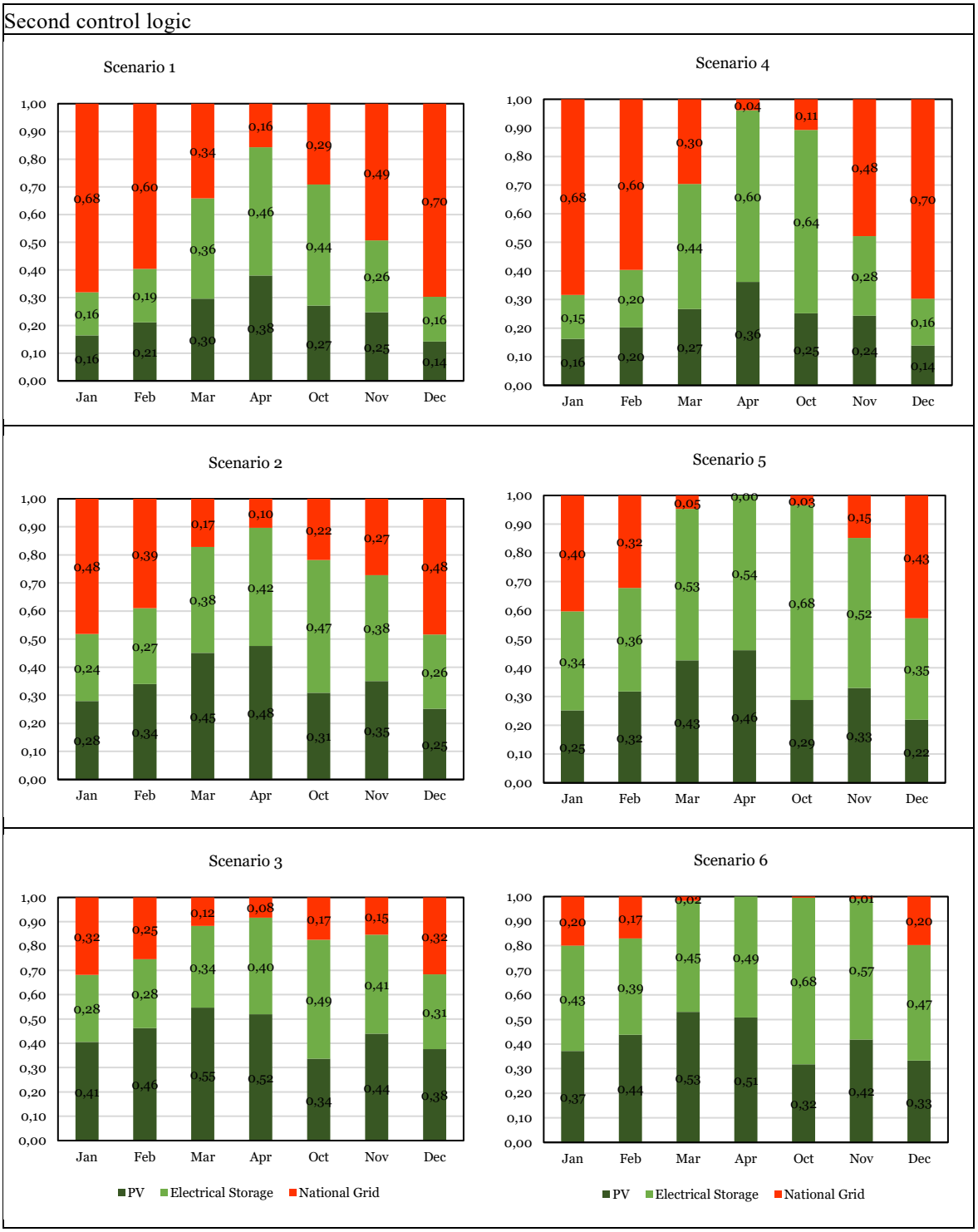

Figure 7-13- Percentage of load managed by each component varying the scenarios for the second control logic in Messina.

Regarding the simulations conducted in Messina during the heating period with the second control logic, the data (Figure 7-13) exhibited a similar trend to what was observed in the Milan simulations. Increasing the number of solar panels from Scenario 1 to Scenario 3 while maintaining a constant battery capacity of 1.2 × 104 Wh, the

percentage of energy supplied directly via the solar panels rose from 16% to 22%, while the battery contribution varied from 16% to 28%. Concurrently, energy drawn from the national grid decreased from 68% to 49%. These results underscore the second control logic's capacity to promote greater grid independence, in parallel with the increase in solar panels.

Comparing these simulations with those of the first control logic in Messina revealed some significant differences. While the second control logic demonstrated reduced grid dependency, especially with a growing number of solar panels, the first logic maintained a higher percentage of energy supplied by the grid. Furthermore, the effect of doubling the number of panels and battery capacity, from Scenario 4 to Scenario 6, was less pronounced in the first logic, with a more modest variation in the energy drawn from the grid, ranging from 68% to 38%.

Table 7-8 provides a summarized presentation of the detailed outcomes derived from an analysis of the percentage distribution of electrical load across various scenarios, considering the implementation of two management logics. These data distinctly showcased the disparities between the two logics and their impact on the integration of renewable energy sources in the construction sector. Specifically, the second control logic emerged as the more efficient approach, demanding less energy from the national grid. For instance, in Scenario 1, it allowed for the direct satisfaction of 76% of the load through self-consumption, thereby reducing reliance on the national grid to 47%. This outcome holds profound significance in fostering enhanced integration of renewable energy sources within the building context, thereby aiding in diminishing the reliance on the national grid and optimizing the energy system's efficiency.

Table 7-8- Annual percentage distribution of electrical load managed by each component in different scenarios, comparing the two management logics in Messina.

Management Logic	Scenario	PV	Electrical Storage	National Grid	Self-Consumed
First control logic	Scenario 1	22%	30%	48%	68%
	Scenario 2	26%	36%	38%	42%
	Scenario 3	29%	39%	32%	24%
	Scenario 4	21%	40%	39%	78%
	Scenario 5	24%	54%	22%	54%
	Scenario 6	27%	59%	14%	31%
Second control logic	Scenario 1	24%	29%	47%	76%
	Scenario 2	35%	35%	30%	54%
	Scenario 3	44%	36%	20%	34%
	Scenario 4	23%	35%	41%	80%
	Scenario 5	33%	47%	20%	63%
	Scenario 6	42%	50%	9%	39%

However, it is noteworthy that the results obtained in Messina with the second control logic differed from those in Milan during the heating period. Despite an identical number of solar panels, regional and climatic variables led to considerable variations in the outcomes. This variation underscored the importance of adapting energy management strategies to local specifics to maximize self-consumption and reduce grid dependence.

Within the context of the two control logics under examination, these climatic differences dictated how energy was generated, managed, and utilized within the system. The first control logic was more effective in the mild climate of Messina, where heating demands necessitated lower thermal capacity and thermal storage could be employed more efficiently. Conversely, the second control logic was advantageous in Milan, where lower temperatures required greater thermal capacity, and thermal storage became vital for heating.

These differences hold considerable significance in the design and optimization of the energy system, as they impact efficiency, self-consumption, and grid dependence in a climate-specific manner.

7.3.3 Calculation of CO_2 Equivalent Emissions

In conclusion, the annual equivalent CO_2 emission percentages were calculated using the emission factors reported in Table 6 for all analysed configurations. The results are presented in Figure 7-14 for Milan.

It was found that the highest CO_2 production was achieved with 18 photovoltaic panels, regardless of battery capacity and control logic, with an amount of approximately 3.0 × 103 kg of CO_2. However, increasing the battery capacity and peak power installed led to a reduction in this production. On the other hand, the lowest CO_2 production was observed with 72 photovoltaic panels and a 2.4 × 104 Wh battery, using the second control logic. In this case, the CO_2 production was around 1.86 × 103 kg. This represents a significant re-duction compared to a traditional heating system with a gas boiler, which produces ap-proximately 5. ×103 kg of CO_2.

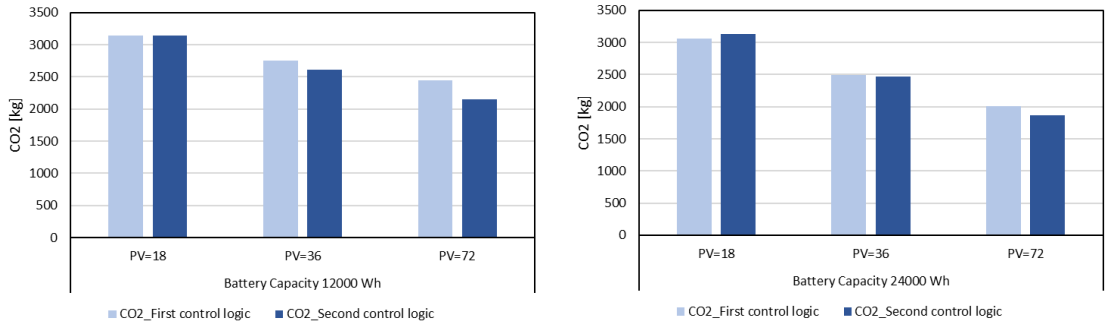

Figure 7-14- Annual amount of equivalent CO2 emissions for Millan.

The graphs in Figure 7-15 display CO_2 emissions observed during simulations con-ducted in Messina across various scenarios managed using two distinct control logics: the first traditional logic and the second "smart" logic. A comparative analysis of these two strategies revealed that the second "smart" logic led to a substantial reduction in CO2 emissions compared to the traditional logic across all considered scenarios. In the initial three scenarios (Scenario 1, 2, and 3), the adoption of the second "smart" logic resulted in reductions of CO2 emissions by 8%, 23%, and 36%, respectively, in comparison to the traditional logic. This trend continued in subsequent scenarios (Scenario 4, 5, and 6), with reductions in CO_2 emissions amounting to 0.1%, 13%, and 37%, respectively.

The data highlighted that the second "smart" logic had a significant impact on reducing CO_2 emissions, particularly in the first three scenarios. These findings underscored the importance of implementing advanced control strategies to enhance energy efficiency and mitigate environmental impact, especially in climatic contexts akin to Messina.

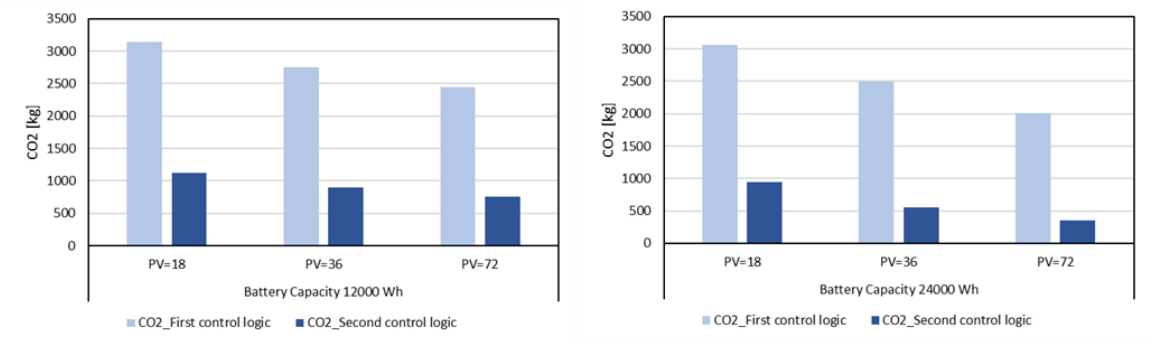

Figure 7-15- Annual amount of equivalent CO_2 emissions for Messina.

7.3.4 Domestic Hot Water Supplied by the Solar Collectors

During the summer season, the thermal storage system was used to store chilled water for cooling purposes and cannot be utilized for DHW. For this reason, a supplementary 300 L thermal storage unit was employed with solar collectors to provide DHW. The solar storage output was combined with a cooler flow rate from the supply network to attain a temperature of 45 °C for household usage. In the winter season, when solar radiation was insufficient to meet DHW demands, the heat pump took energy from the thermal storage system, with the solar collectors being given priority.

In Figure 7-16, the graph presents the coverage percentages for each component throughout every month of the year in the city of Milan. Furthermore, in Figure 7-17, an analogous graph is provided, which pertains specifically to the city of Messina.

In Milan, the data in the table showed that the use of solar collectors covered approximately 38% to 57% of the demand for DHW. However, the city relied more on heat pumps, which satisfied between 43% to 62% of the demand. This suggested that in Milan, the efficiency of solar collectors in providing hot water was relatively lower compared to Messina. The colder climate in Milan led to a higher dependence on heat pumps to heat water, resulting in less reliance on solar collectors.

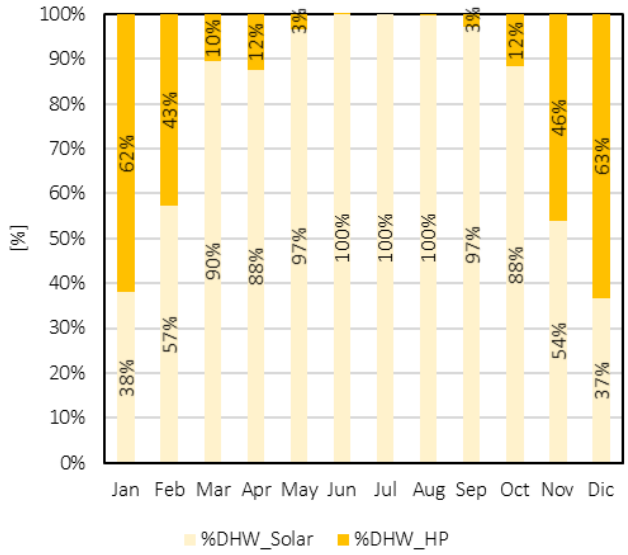

Figure 7-16- Coverage percentages for each component throughout every month of the year in the city of Milan.

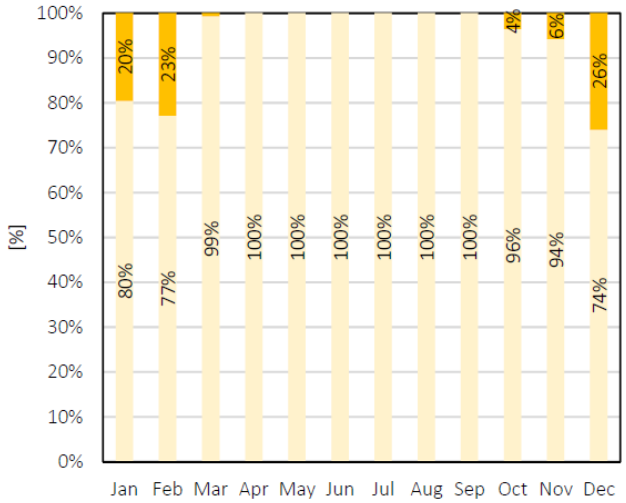

Figure 7-17 Coverage percentages for each component throughout every month of the year in the city of Messina.

Turning our attention to Messina, the data indicated that solar collectors were significantly more effective in covering the demand for hot water. In Messina, the use of solar collectors ranged from 74% to 100% in meeting the demand, highlighting the city's ability to harness solar energy efficiently. The use of heat pumps in Messina remained notably low, ranging from 0% to 26%. This outcome underscored the favourable climate conditions in Messina, which allowed for extensive utilization of solar energy and a reduced reliance on heat pumps for water heating.

7.4 Conclusions

In this study, the energy and environmental implications of a system that combines the use of an air-water heat pump with photovoltaic panels and electric and thermal storage systems were analysed. Performances were compared between two different control strategies, the first commonly used for the management of air-conditioning systems, and the second one specifically conceived to maximize the employment of renewable solar sources.

A comprehensive parametric analysis was conducted to determine the optimal con-figuration for energy management strategies, considering various parameters such as thermal storage volume, the number of photovoltaic panels, and battery capacity. Increasing peak photovoltaic power enhanced direct coverage of energy demand by the photo-voltaic system and battery, reducing reliance on the national grid. Comparative analysis of traditional and advanced "smart" control logics underscored the latter's efficiency in optimizing local energy utilization, significantly reducing grid dependence. The "smart" logic maximized self-generated energy consumption, mitigating national grid dependence. CO_2 equivalent emissions analysis revealed substantial reductions, especially in initial scenarios, emphasizing the advanced control's role in enhancing energy efficiency and environmental sustainability in climates akin to Messina.

Evaluation of domestic hot water supply highlighted differences between Milan and Messina. In Milan, solar collectors covered 38–57% of demand, while heat pumps satisfied 43–62%. Conversely, Messina exhibited higher solar efficiency, covering 74–100% of demand with less reliance on heat pumps. Results underscored local climatic influence on solar energy effectiveness for water heating.

In conclusion, the study emphasized tailoring energy management to regional climates. Advanced control logic benefits energy efficiency, reduces carbon emissions, and promotes sustainable energy use in Milan and Messina. These insights can guide optimal energy systems and enhance environmental sustainability in diverse climatic contexts.

7.5 References

1. IEA. Data. Statistics. Available online: https://www.iea.org/data-and-statistics (accessed on 1 January 2021)

2. Available online: https://www.europarl.europa.eu (accessed on 13 December 2023)

3. Korol, E.; Shushunova, N. Analysis and Valuation of the Energy-Efficient Residential Building with Innovative Modular Green Wall Systems. Sustainability 2022, 14, 6891. https://doi.org/10.3390/su14116891.

4. IEA. Tracking Buildings 2020; IEA: Paris, France, 2020.

5. Shushunova, N.; Korol, E.; Luzay, E.; Shafieva, D. Impact of the Innovative Green Wall Modular Systems on the Urban Air. Sustainability 2023, 15, 9732. https://doi.org/10.3390/su15129732.

6. Bee, E.; Prada, A.; Baggio, P.; Psimopoulos, E. Air-source heat pump and photovoltaic systems for residential heating and cooling: Potential of self-consumption in different European climates. Build. Simul. 2019, 12, 453–463. https://doi.org/10.1007/s12273-018-0501-5.

7. Baggio, P.; Bee, E.; Prada, A. Demand-side management of air-source heat pump and photovoltaic systems for heating applications in the Italian context. Environments 2018, 5, 132. https://doi.org/10.3390/environments5120132.

8. Popescu, L.L.; Popescu, R.; Catalina, T. Improving the energy efficiency of an existing building by dynamic numerical simulation. Appl. Sci. 2021, 11, 12150. https://doi.org/10.3390/app112412150.

9. Gaur, A.S.; Fitiwi, D.Z.; Curtis, J. Energy Research & Social Science Heat pumps and our low-carbon future : A comprehensive review. Energy Res. Soc. Sci. 2021, 71, 101764. https://doi.org/10.1016/j.erss.2020.101764.

10. Wang, Z.; Guo, P.; Zhang, H.; Yang, W.; Mei, S. Comprehensive review on the development of SAHP for domestic hot water. Renew. Sustain. Energy Rev. 2017, 72, 871–881. https://doi.org/10.1016/J.RSER.2017.01.127.

11. Dikici, A.; Akbulut, A. Exergetic performance evaluation of heat pump systems having various heat sources. Int. J. Energy Res. 2008, 32, 1279–1296. https://doi.org/10.1002/er.1414.

12. Huide, F.; Tao, Z. Performance Analysis of an Integrated Solar-assisted Heat Pump System with Heat Pipe PV/T Collectors Operating under Different Weather Conditions. Energy Procedia 2017, 105, 1143–1148. https://doi.org/10.1016/j.egypro.2017.03.485.

13. Zhao, H.; Wu, Q.; Hu, S.; Xu, H.; Nygaard, C. Review of energy storage system for wind power integration support. Appl. Energy 2015, 137, 545–553. https://doi.org/10.1016/j.apenergy.2014.04.103.

14. Carvalho, A.T.G.M.L. Life Cycle Assessment of Stationary Storage Systems within the Italian Electric Network. Energies 2021, 14, 2047.

15. Aneli, S.; Arena, R.; Tina, G.M.; Gagliano, A. Improvement of energy self-sufficiency in residential buildings by using so-lar-assisted heat pumps and thermal and electrical storage. Sustain. Energy Technol. Assess. 2023, 60, 103446. https://doi.org/10.1016/j.seta.2023.103446.

16. Pinamonti, M.; Beausoleil-morrison, I.; Prada, A.; Baggio, P. Water-to-water heat pump integration in a solar seasonal storage system for space heating and domestic hot water production of a single-family house in a cold climate. Solar Energy 2021, 213, 300–311. https://doi.org/10.1016/j.solener.2020.11.052 .

17. Bellos, E.; Tzivanidis, C. Energetic and fi nancial sustainability of solar assisted heat pump heating systems in Europe. Sustain. Cities Soc. 2017, 33, 70–84. https://doi.org/10.1016/j.scs.2017.05.020.

18. Miglioli, A.; Aste, N.; Del Pero, C.; Leonforte, F. Photovoltaic-thermal solar-assisted heat pump systems for building applications: Integration and design methods. Energy Built Environ. 2023, 4, 39–56. https://doi.org/10.1016/j.enbenv.2021.07.002.

19. Ning, Z.; Zhang, X.; Ji, J.; Shi, Y.; Du, F. Research progress of phase change thermal storage technology in air-source heat pump. J. Energy Storage 2023, 64, 107114, . https://doi.org/10.1016/j.est.2023.107114.

20. Long, J.Y.; Zhu, D.S. Numerical and experimental study on heat pump water heater with PCM for thermal storage. Energy Build. 2008, 40, 666–672. https://doi.org/10.1016/j.enbuild.2007.05.001.

21. Georges, E.; Cornélusse, B.; Ernst, D.; Lemort, V.; Mathieu, S. Residential heat pump as flexible load for direct control service with parametrized duration and rebound effect. Appl. Energy 2017, 187, 140–153. https://doi.org/10.1016/j.apenergy.2016.11.012.

22. Kreuder, L.; Spataru, C. Assessing demand response with heat pumps for efficient grid operation in smart grids. Sustain. Cit-ies Soc. 2015, 19, 136–143. https://doi.org/10.1016/j.scs.2015.07.011.

23. UNI/TS 11300–1. Building energy performance—Part 1: Evaluation of the energy need for space heating and cooling (in Ital-ian). 2014 ,https://www.uni.com (access on 1 October 2014).

24. Italian Higher Instutute for Environmental Protection and Research (ISPRA), https://www.isprambiente.gov.it/en/istitute, (ac-cess on 1 January 2022).

8 The choice of appropriate generator systems to enhance the renewable energy share in buildings. A comparison between PV-assisted heat pumps and biomass boilers

Abstract

Low-energy buildings are generally equipped with generation systems driven by renewable sources. Regarding heating and DHW production, two choices appear appropriate: PV assisted heat pumps and biomass boilers. In this paper, by means of TRNSYS dynamic simulations, the non-renewable primary energy was determined for two buildings located in different climatic contexts by varying the PV size to consider the actual self-consumed electricity of commercial devices. Results showed that in cold climates biomass boilers are more suggested, especially in unfavourable climatic zones, whereas the COP of air-water heat pumps is strongly penalized by the outdoor temperatures and in many cases the self-consumed PV electricity does not limit the grid intervention adequately. However, in building with limited thermal energy demands and in favourable climates, suitable PV sizes make heat pumps more performant than biomass boilers. The same calculations were conducted with the quasi-steady approach, in accordance with the Italian building energy certification procedure, observing a favorable scenario in a heating plant equipped with a PV assisted heat pump because it assumes the renewable electricity entirely absorbed, while the accounting of the actual self-consumed share produces a greater demand of non-renewable energy.

8.1 Introduction

Because in recent years the issue related to the global warming caused by the use of fossil fuels have increased, it has become mandatory to expand the use of renewable energy source in the building sector. Indeed, currently the world housing account for 2,109,205 thousand tons of oil equivalent of consumed energy (21.2% of total energy consumption), with a correspondent amount of CO_2 emission of 2033 Mton per year [1]. For this purpose, in Europe the promulgation of the Directive 28/2009/CE has promoted the use of renewable energy in the building sector to reduce the percentage of 40% on the final energy consumption that contributes for the 36% of GHG emissions [2]. Recently, in October 2020 the regulation amending the Energy Performance of Buildings Directive (2018/844/EU) has introduced new targets as part of the so-called “European Green

Deal", by presenting an action plan with concrete regulatory, financing and promoting measures to boost the penetration of renewable technologies in the building sector [3]. Among the several generation systems employed in residential buildings for heating and DHW production purposes, electric heat pumps assisted by PV generators and biomass boilers are able to allow a rational exploitation of the renewable sources [4]. Indeed, the firsts use the renewable energy contained in the air, water or ground to supply appropriate emitters for the air-conditioning and to produce Domestic Hot Water (DHW) by absorbing electricity from the grid, that could be properly limited by the self-consumed PV electricity [5,6]. Biomass boilers, instead, benefit of the neutral CO_2 emission that allows for considering the majority of the embodied primary energy as fully renewable [7]. Consequently, it is interesting to compare these generations systems in terms of exploited renewable energy, in order to determine how they act on the limitation of the fossil primary energy and on the external environment.

The comparison is justified by the fact that modern biomass boilers have performance indexes considerably lower than those detectable in heat pumps, therefore they could seem naturally penalized. On the other hand, in heat pumps the advantage could be largely counterbalanced by the electricity absorbed from the grid, whose conversion factor required to quantify the fossil primary energy share is almost 10 times greater than that employed in biomass boilers [8]. Moreover, when heat pumps use the outdoor air as thermal source, the absorbed electricity strongly depends on the external temperature levels [9], therefore the actual performances have to be evaluated in different climatic contexts.

A preliminary comparison between biomass boilers and heat pumps was conducted in [10] in which authors compared the generation systems exclusively in economic and environmental terms for small-detached houses located in Poland. They determined that the operating cost savings of the heat pump did not compensate the large installation costs in an acceptable period, moreover the CO_2 emission level were larger than biomass boilers. In [11], heat pumps and biomass boilers were analysed in terms of LCA, in order to compare these generation systems with the other available for tertiary buildings. Biomass boilers and other devices supplied by fossil fuels were compared in [12], whereas the limitations of air-water heat pumps in cold climate was deeply investigated in [13]. Some studies suggest to use rationally the rejected heat from biomass boilers as thermal source for heat pumps in hybrid systems [14], whereas no studies were

found to compare the renewable primary energy share attainable in different plant configurations equipped with these devices. Therefore, regarding heating and DHW production, in this paper the generation systems were compared in terms of non-renewable primary energy by referring to two different buildings located in different climatic zones of the Italian territory. In particular, the buildings have different thermal energy requirements, whereas the PV size was varied in presence of heat pumps to quantify the benefits that could be achieved in terms of reduction of the electricity absorbed from the grid. Dynamic simulations of the building-plant systems were conducted in TRNSYS to determine in detail the electricity absorbed by a commercial air-water heat pump as function of the sources temperature and of the operation in part-load mode [15]. Furthermore, for the renewable electricity, it was assumed to give the priority to drive the generation systems, whereas the remaining part to supply internal appliances and the surpluses used to charge a thermal storage system or transferred to the grid. Regarding the biomass boilers, the primary energy was determined by varying the device efficiency as a linear function of the capacity ratio, in accordance with values listed in commercial datasheets. In the considered climatic zones, the simulated buildings are the same from the geometrical point of view whereas the thermal characteristics of the dispersing elements were changed in function of heating degree-day (HDD). Specifically, the insulation thickness in opaque walls was increased whereas the thermal transmittance of the windowed surfaces was reduced with the HDD growth, in order to meet the national regulations in terms of minimum energy performance requirements for new buildings [8]. The same calculations were repeated by adopting the quasi-steady approach [16–18], because currently in Italy it is used for the building energy certification and often used as a reference to establish building energy performances, allowing also to quantify the deviances between the results provided by dynamic and simplified procedures.

8.2 Material and Method

8.2.1 Buildings description

Energy evaluations were conducted by dynamic simulations carried out in TRNSYS on the detached houses of Figure 8-1, with gross surface on the ground of 100 m² and net heated surfaces equal to 57.7 m² and 115.4 m² respectively for the single-storey and the double-storey building. The first structure represents a modular unit and

the second building was designed by superimposing two modular units, so that the aspect ratio (ratio between the gross dispersing surface S and gross heated volume V) is equal to respectively 0.75 m-1 and 0.625 m-1. The first was simulated in TRNSYS with a single air node (ground floor), whereas for the second one two air nodes (ground and first floor) have been used and connected to the same generation system [19]. Both the buildings have the same Window to Wall Ratio (WWR) on each exposure, equal to 13%, 10% and 4% for North/South, East and West [20]. Internal gains (332 W per floor, whose 50% is radiative) [21,22] and natural ventilation (0.5 air-change per hour) were set in accordance to Italian standards. These structures, in fact, have been thermally designed in order to meet the minimal energy requirements regulated by the national legislation [8]. In particular, the following aspects were imposed:

a) mean global thermal exchange coefficient of the envelope lower than a specific threshold, the latter defined as function of the building aspect ratio and the HDD;
b) heating and cooling thermal requirements lower than the correspondent values determined for a reference building with the same geometry but with different envelope thermal parameters;
c) mean seasonal global efficiency for the heating and the DHW systems greater than a limit value, the latter determined as function of heating and DHW plants and of the heat generators features;
d) global primary energy requirements, determined as sum of the correspondent terms for heating and DHW, lower than the correspondent value for the reference building including the share provided by renewable systems;
e) 50% of the domestic hot water produced by a renewable system;
f) 2 kWp of installed PV per 100 m² of gross surface area on the ground.

Because in the parametric study the number of HDD changes, the respect of the points a), b) and d) has imposed the variation of the insulation thickness (EPS, λ= 0.041 W/mK [23]) inside the dispersing opaque surfaces (vertical walls, ground floor and flat roof) and the change of the windows thermal transmittances (Uw) and of the normal solar factor ($g_{\perp}$), in accordance with the values listed in Table 8-1. It can be noted that the buildings were located in five different climatic zone, uniformly distanced by about 500-550 HDD.

Figure 8-1- Perspective views of the single-storey and double-storey building involved in TRNSYS simulations

Table 8-1- Insulation thickness in dispersing opaque walls and windows thermal transmittance set in the simulated buildings, as function of the climatic zone

	EPS Insulation thickness [mm]			U_w [W/m²K] and $g_\perp$ [-]
HDD	Ground floor	Flat roof	Vertical walls	Windows
772	60	80	50	1.69 – 0.66 (low-ε double pane)
1317	60	90	100	1.69 – 0.66 (low-ε double pane)
1861	100	110	100	1.69 – 0.66 (low-ε double pane)
2394	110	140	130	1.40 – 0.70 (clear triple pane)
2897	110	140	130	1.40 – 0.70 (clear triple pane)
3445	120	160	160	1.1 – 0.62 (low-ε triple pane)

The localities with the HDD listed in Table 8-1 have the position depicted in Figure 8-2; it can be appreciated that these have more or less similar latitudes in order to attain similar PV producibility, between 1300-1400 kWh/kWp assuming a polycrystalline technology [24,25]. The PV generator is facing South and tilted of 30°C, made of modules with main electric data listed in Table 8-2. The size of the PV was varied between 2 kWp (required minimum installed peak power) to 6 kWp (to avoid three-phase installations). The remaining components of the PV plant have been considered in simplified way by setting a BOS (Balance of System) efficiency of 0.85 throughout the year.

Regarding the DHW production, the required water flow rate was determined as function of the net plan surface, in accordance to Italian standard [17], obtaining 100 and 172 liters per day respectively for the single and the double-storey building, and scheduled at daily level as indicated in Table 8-3. For the weather data, TMYs were used and simulations were conducted for the whole year with a timestep of 0.125 h, setting a continuous functioning situation of the heating plant in order to compare the TRNSYS results with those provided by the quasi-steady procedure.

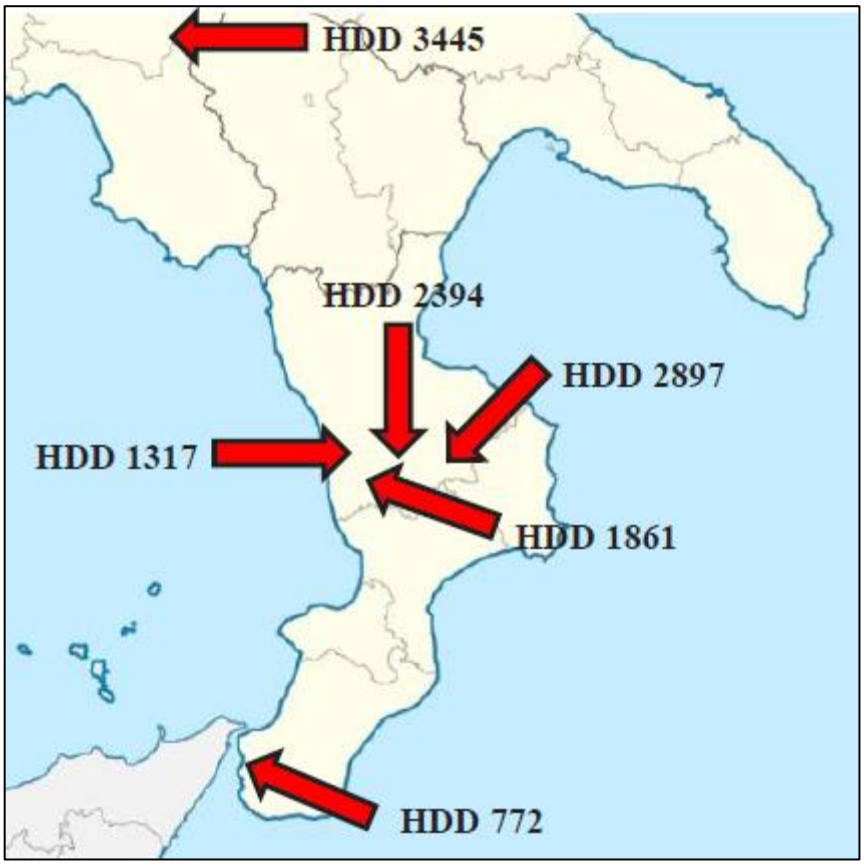

Figure 8-2- Position of the considered localities considered for the buildings energy performance analysis

Table 8-2- Main electric features of the polycrystalline PV panels considered in simulations

Short-circuit current at STC	9.17 A
Current at max power point in STC	8.80 A
Open-circuit voltage in STC	35.17 V
Voltage at max power point in STC	28.49 V
Temperature coefficient of short-circuit current	0.0052 A/K
Temperature coefficient of open-circuit voltage	-0.0081 V/K

Table 8-3- Scheduled water flow rate (in liters per hour) requirements for the calculation of the annual DHW energy needs in the considered buildings

	DHW flow rate (l/h)						
	00:00-07:00	07:00-10:00	10:00-12:00	12:00-14:00	14:00-18:00	18:00-21:00	21:00-00:00
Single-storey	0	12.5	0	12.5	0	12.5	0
Double-storey	0	21.5	0	21.5	0	21.5	0

8.2.2 Heating plant with the air-water heat pump

The heating plant is equipped with a commercial and modulating air-water heat pump (AWHP), and the produced hot water supplies a radiant floor inside every thermal zone whose indoor temperature is regulated by a thermostat with a dead band of 1°C and

a set-point of 20°C. The cut-off temperature of the heat pump is -20°C, with thermal power and the coefficient of performance trends showed in Figure 8-4 as function of the outdoor air temperature, by setting the set-point water temperature to 45°C. Preliminary simulations have allowed for determining the size of the air-water heat pump, by choosing as nominal power the value with the highest frequency detected during the heating period. Thermal powers of about 4 kW and 8 kW respectively for the single and the double-storey building were determined, so two commercial air-water heat pumps, with a minimum modulation factor of 30%, were identified and simulated. Among the different climatic zones, it is worth noting that the nominal power values remain almost the same because the increase of the envelope insulation allowed for compensating the thermal losses detectable with the HDD growth, maintaining similar design loads. Radiant floors were implemented in TRNSYS with a pipe spacing of 25 cm, an internal diameter of 10 mm, embedded in a lightweight concrete layer thick 9 cm. The AWHP thermal plant was simulated by considering a vertical tank of 3 m^3 as thermal storage system equipped with an electric resistance as backup, maintained at a set-point temperature of 40°C for a rational exploitation of the AWHP and to manage PV surpluses rationally (see Figure 8-3). Indeed, the control system activates the heat pump also when heating loads are not required if the tank temperature is lower than the set-point and the PV electricity is available. The inlet temperature in the radiant floors was set constant to 35°C, by implementing a motorized 3-way valve that recirculate a fraction of the returning water flow rate from the same emitters. The latter was always retained supplied by the grid, in accordance with national regulation that hinders the electricity used by Joule effect to be covered by the PV production [8].

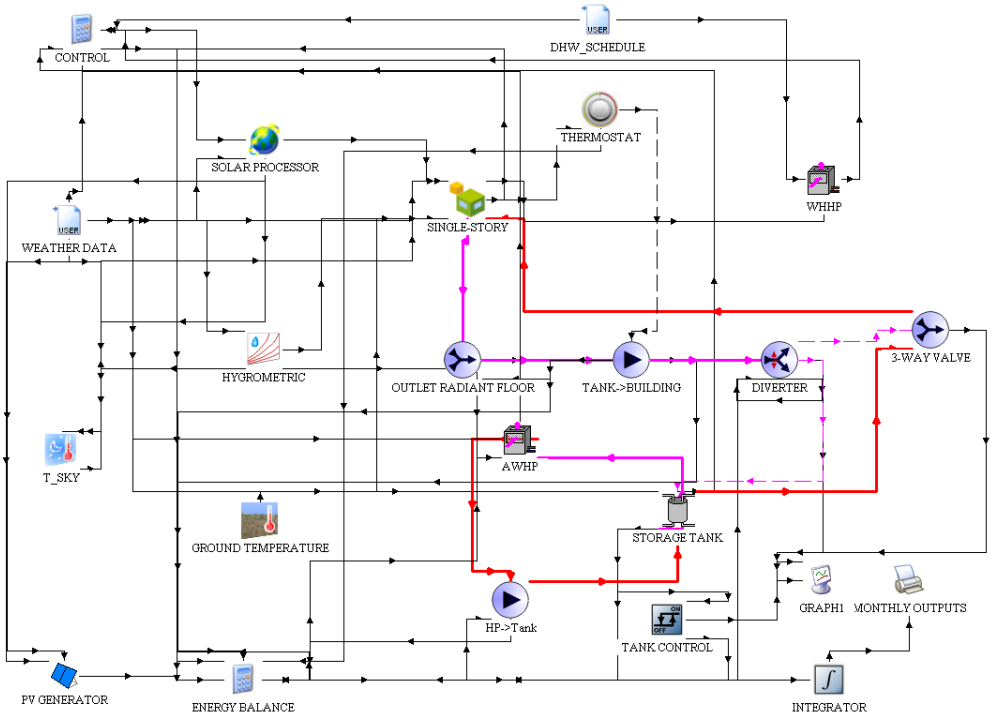

Figure 8-3- Project implemented in the TRNSYS interface for the building-plant system with the AWHP

It is worth noting that the TRNSYS model employed to simulate the AWHP determines the electric consumptions by considering the COP variation with the temperature sources, assuming a full load operation. Actually, the presence of the storage tank determines noticeable functioning times in part load mode, therefore the performance index is further modified when the heat pump capacity ratio (CR) is lower than minimum modulation factor (30% in accordance with datasheet). In order to consider this aspect, a further correction factor fc was introduced to determine an actual COP in part-load mode by means of the relation:

$$COP_{real} = f_c \cdot COP_{NOM}\,(t_{oa}, 45°C) \qquad if\ \ CR < 30\% \tag{8.1}$$

in which the nominal COP was determined by TRNSYS as function of the outdoor air temperature (T_{oa}) and by the setting the supplied water flow rate at a temperature of 45 °C. The correction factor, instead, was calculated by a TRNSYS equation for every timestep t in accordance with the procedure described in the EN 14825 [25]:

$$f_c(t) = \frac{CR(t)}{1 - C_c + C_c \cdot CR(t)} \quad 8.2$$

in which Cc is the device degradation factor set to 0.9, as suggested by the standard when manufacturer does not provide pertinent information. Regarding the capacity ratio, it was calculated as:

$$CR(t) = \frac{P_{h,real}}{P_{h,NOM}(t_{oa}, 45°C)} \quad 8.3$$

namely the real thermal power provided by the AHWP to the storage tank and the thermal power that the heat pump could produce in nominal condition when the outdoor air temperature value is t_{oa} and the water flow rate temperature is 45°C. Therefore, Eq. (2) was implemented inside TRNSYS to determine the real COP in accordance to Eq. (8.1), and successively used to quantify the actual electric consumptions starting from the real provided thermal power. Regarding the DHW production, an independent water heater heat pump (WHHP) equipped with an electric booster and with performance depicted in Figure 8-4, assuming DHW at 55 °C, was simulated. Again, for the same reason discussed for the AWHP, the electric energy of the WHHP booster was considered completely absorbed from the grid. The correction of the COP described by Eq. (8.1) was not implemented, assuming a functioning always in full load mode. The produced renewable electricity was considered to operate the AWHP and WHHP electric demands, excluding backup and booster systems, and to drive the hydronic pumps. So, the global electric energy absorbed from the grid determined the non-renewable primary energy, by applying a conversion factor of 1.95 as indicated by Italian rules [8].

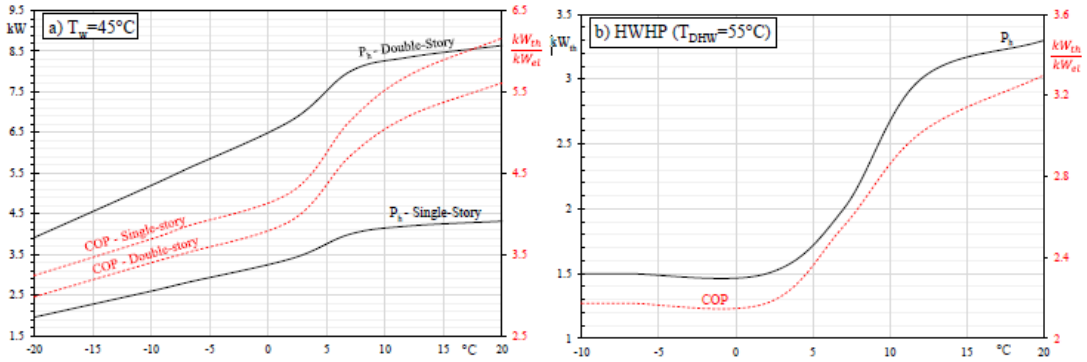

Figure 8-4- Trends of the thermal power and COP as function of the outdoor air temperature in nominal conditions for: a) AWHP (Tcut,off=-20°C) b) WHHP (Tcut,off=-10°C)

8.2.3 Heating plant with the biomass boiler

Regarding the heating plant equipped with a boiler supplied by solid biomass, a commercial device with a burner working with a forced air system, supplies directly radiators by a water flow rate at a constant temperature of 80°C, in accordance with the plant scheme depicted in Figure 8-5. Again, a zone thermostat controls the indoor air temperature with a dead band of 1 °C and a set-point of 20°C. The biomass boiler has a combined functioning; therefore, the same device is used to provide heating and DHW, but exclusively in winter. In order to cover the DHW demand in summer and to respect the constrain to produce at least the 50% by means of a renewable system [8], the buildings were equipped with 4 m² of plane solar thermal collectors with selective surfaces, including a storage tank of 0.5 m³ operating by natural circulation. The building-plant system involves a 2 kWp of PV panels (minimum required peak power), whose electricity was used to meet auxiliary consumptions, mainly represented by the hydraulic pumps and the fan of the biomass boiler. In simulations, the energy input in the generation system was computed by considering a boiler efficiency depending on the capacity ratio, by means of the linear relation (determined by interpolating the datasheet values):

$$\eta_{th} = 0.0769 \cdot CR + 0.8431 \qquad 8.4$$

that provides a value of 0.92 in nominal conditions (CR=1) and of 0.86 at the minimum modulation factor (CR=0.22).

Regarding the fan consumptions, the absorbed electric power was determined by the formula:

$$\dot{Q}_{el,boiler} = -325.8 \cdot CR^2 + 730.8 \cdot CR + 15 \qquad 8.5$$

that produces a consumption of 420 W in nominal conditions, of 160 W at the minimum modulation factor and 15 W with a switched-off burner. The boiler capacity ratio was calculated as:

$$CR(t) = \frac{P_{b,real}}{P_{b,NOM}} \qquad 8.3$$

namely the ratio between the actual produced thermal power and that achievable in nominal condition operation. For the latter, design evaluations on the two simulated edifices have allowed to identify a nominal thermal power of 14 kW (assuming a suitable contemporary factor for heating and DHW) for the single-storey building and of 20 kW for the double-storey building. Finally, the non-renewable primary energy was computed by associating a conversion factor of 0.2 for the energy input of the biomass boiler and again of 1.95 for the electricity absorbed from the grid.

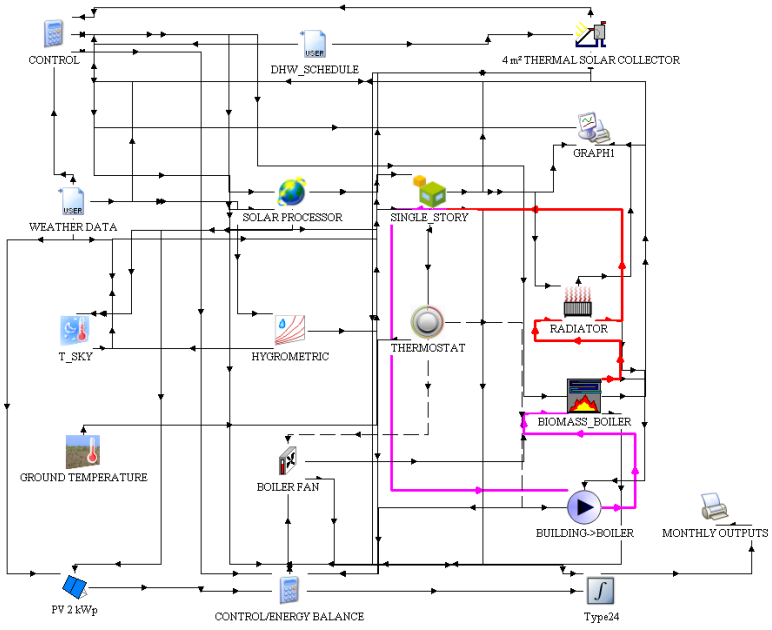

Figure 8-5- Project implemented in the TRNSYS interface for the building-plant system with the biomass boiler

8.3 Results

In Figure 8-6, with reference to the single-storey building (S/V=0.75), the yearly non-renewable primary energy per square meter of heated net surface (non-renewable Energy Performance index, EP [kWh/m²]) is depicted as a function of the considered HDD and, only for the heating plant equipped with the AWHP, of the PV size. It is clear that, despite the augment of the envelope insulation level with the HDD growth, the fossil share increases with the number of HDD due to the prolonged employment of the generation system and the unfavourable outdoor air temperatures. However, for the single-storey building, the performances of the AHWP assisted by the PV generator are always better than the biomass boiler, indicating that the magnitude of the electricity absorbed from the grid is not in such amount to be affected excessively by the penalizing conversion factor in fossil primary energy. Furthermore, it is worth noting that the increase of the PV size does not produce an evident limitation of the primary fossil demand. Indeed, the precise and instantaneous electric energy balance carried out by TRNSYS has highlighted that, in every climatic zone and in continuous functioning conditions, the thermal storage system and its control strategy are not sufficient to relieve the mismatching between PV production and thermal load request. In particular, greater heating loads are required prevalently at night, with a quick discharge of the storage system, and consequent activation of the AWHP that uses electricity from the grid. The slight reduction of the fossil primary energy share with the PV size growth is essentially due to the wider availability of renewable electricity during the AHWP and the WHHP operation that in some circumstances allows for limiting the electricity absorbed from the grid.

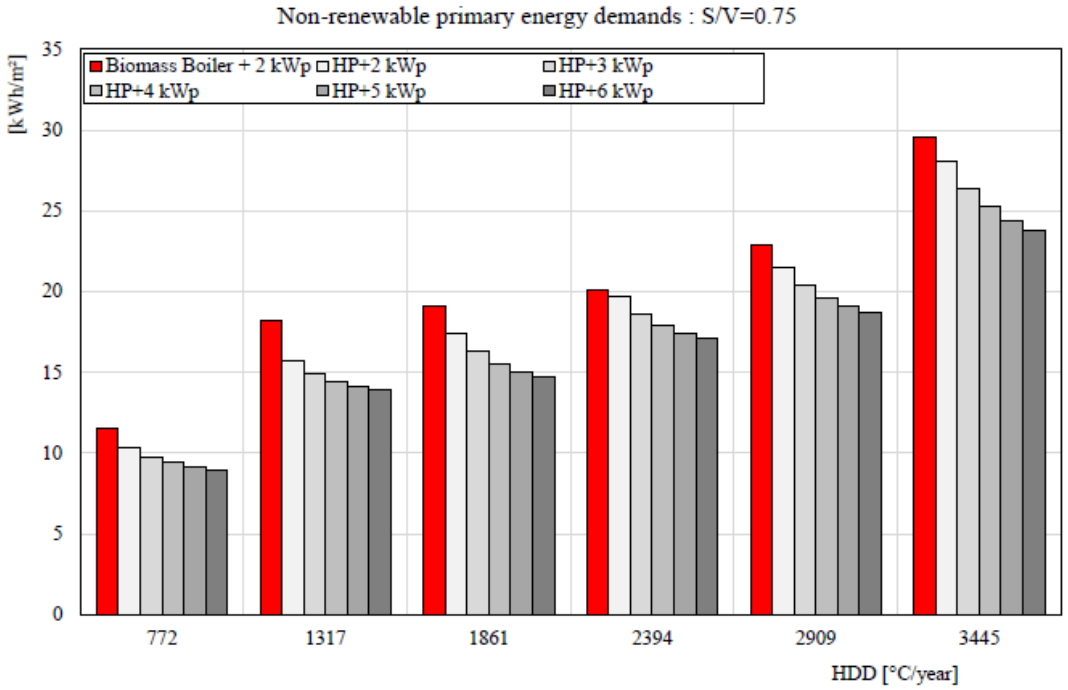

Figure 8-6- Single-storey building: fossil primary energy per square meter of net heated surface as function of the HDD number and for the different heating plant configurations

A different situation was detected instead for the double-storey building (S/V=0.625), which requires more thermal energy to maintain the indoor set-point temperature and for the DHW production. In this case, the employment of the biomass boiler can be suggested rather than other heating plant configurations equipped with the AHWP, as depicted in Figure 8-7. In particular, it appears that the biomass boiler becomes more performant when the HDD number increases; this is due to the higher electric consumption of the heat pumps for the greater thermal requirements in colder zones [29]. Therefore, in such severe climates, it is difficult for the assisted AWHP to compete with the biomass boiler. On the contrary, from the same graph, it is possible to appreciate that larger PV peak powers allow for counterbalancing the gap with the biomass boiler when the climatic zone is favourable. Nevertheless, this aspect is not always true because the non-renewable primary energy depends strongly on the combination of weather data and building-plant features, as demonstrated by the location with 1317 HDD in which the heating plant equipped with the AWHP can be used rationally with every PV size. Nevertheless, the detected trends suggest to prefer biomass boilers especially in the locations with high HDD, whereas in more favourable climatic contexts the gap can be recovered with AWHP by properly increasing the PV size. It is worth noting that, in comparison with the single-storey building, the smaller EPs are due to the smaller

building aspect ratio: in fact, the doubling of the heated volume does not correspond with the doubling of the dispersing surface.

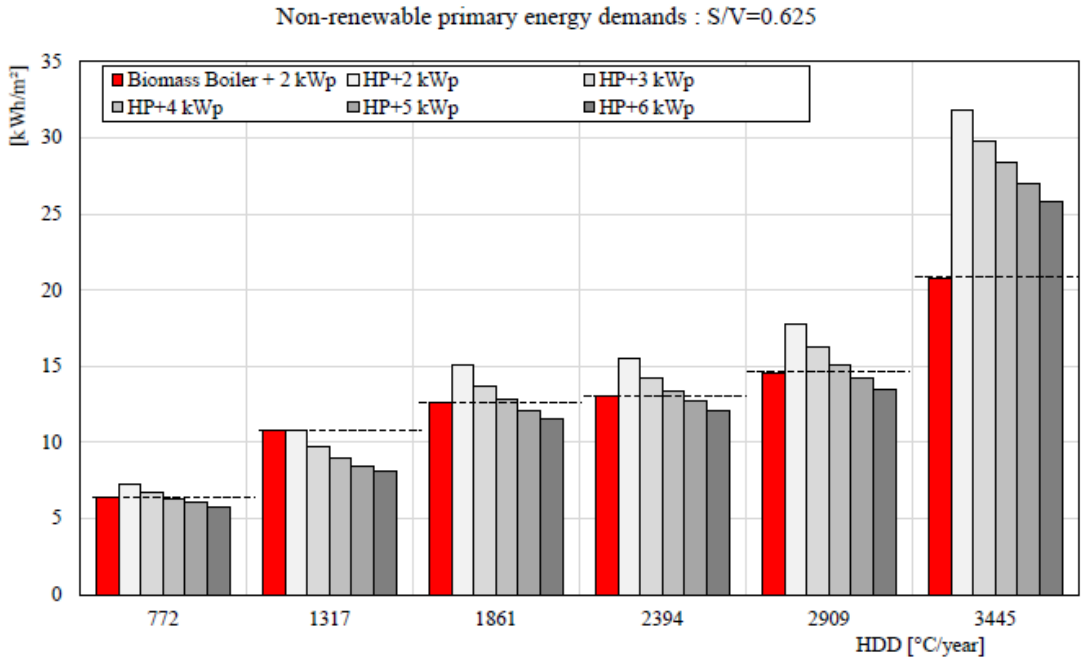

Figure 8-7- Double-storey building: fossil primary energy per square meter of net heated surface as a function of the HDD number and for the different heating plant configurations

The same evaluations conducted on the double-storey building were repeated by adopting the quasi-steady calculation, in accordance to the standard currently employed in Italy for the building energy certification (Figure 8-8). The differences in results are obviously due to the different approaches used to determine the thermal and primary energy requirements, however, it is clear the evident simplification to consider the whole PV producibility completely used to satisfy heating and DHW requirements in the quasi-steady approach. Indeed, this hypothesis produces fossil primary energies that reduce linearly with the PV size and, for the location with 3445 HDD, the AWHP assisted by a 6 kW_P PV generator offers an EP lower than the one detected for the biomass boiler, in contradictory with the results highlighted in Figure 8-7. Therefore, considering the whole PV production instead of the actual self-consumed PV electricity produces a very different scenarios in presence of large PV surfaces that do not reflect the actual energy balance of the building-plant system. The results reported in Figure 8-6 and Figure 8-7 give information concerning the energy performance worsening of the heat generator systems prevalently due to the outdoor temperature reduction observable with the HDD

growth, whereas the same results are independent of the PV performances due to similar producibility among the considered locations. For this reason, in order to define the role of the PV producibility on the AWHP performances, further dynamic simulations have been carried out by considering two localities with different latitudes but similar HDD. In particular, the EPs were determined as a function of the PV size for the location with 3445 HDD considered in the previous evaluations (Lat. 41 °N) and another location with 3452 HDD but with a higher latitude (about 45°N). The results showed in Figure 8-9 for the double-storey building demonstrate the important role of the PV production, with an EP worsening detected when moving toward higher latitudes. In particular, these results are due to the limited availability of solar radiation that determines deviances of non-renewable energy ranging between 5.7 and 8.2 kWh/m²; whereas at a seasonal level the available aerothermal energy can be considered similar due to the equivalent HDD of the two localities. For the same reason, the PV cell thermal drift effects are comparable and do not contribute to the PV producibility, affected exclusively by the limited availability of solar radiation. It is worth noting that the gap tends to reduce with the PV size growth, by confirming that the differences in terms of solar radiation can be recovered by increasing the caption surface because the probability to meet PV production and thermal load request increases.

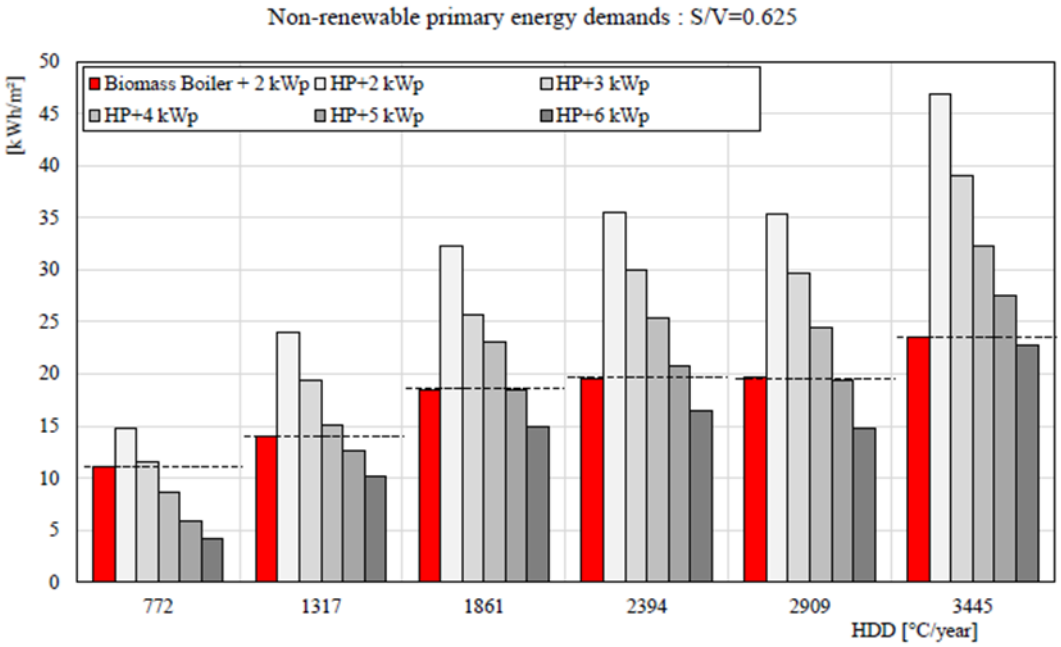

Figure 8-8- Double-storey building: fossil primary energy per square meter of net heated surface as a function of the HDD number and for the different heating plant configurations determined with the quasi-steady model

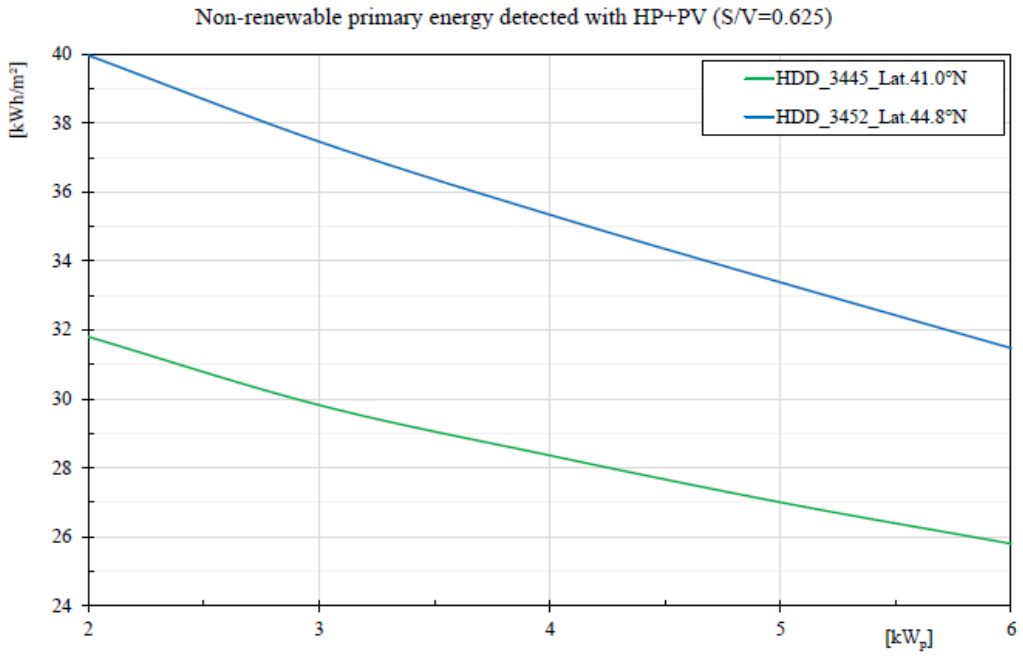

Figure 8-9- Double-storey building: fossil primary energy per square meter of net heated surface as a function of the PV size for two localities with similar HDD

The analysis conducted has demonstrated that the role of the self-consumed PV electricity is decisive to attain the share of primary renewable energy employed to satisfy heating and DHW production requirements. Nevertheless, the increase of the self-consumed PV electricity share does not mean necessarily a preference for the heat pump systems. Figure 8-10 shows the monthly values of self-consumed PV electricity (in kWh_{el} per square meter of heated surface), with the correspondent percentage referred to the PV production for the single and double-storey buildings for the locality with 3445 HDD assuming a PV peak power of $6kW_p$. It can be noticed a greater self-consumed share for the double-storey building, especially in the coldest months, concluding that the greater operation of the heat pumps systems led to better exploitation of the PV generator. Nevertheless, in light of the results in Figure 8-7, still, the renewable primary energy shares are worse than those detected for the biomass boiler, meaning that the remaining part absorbed from the grid assumes a prevalent role in the fossil primary consumptions forming. Therefore, it is confirmed that heat pump systems are preferable in presence of contained energy consumptions, even with the thermal storage system, and consequently in severe climatic zones is mandatory to limit as possible the thermal energy requirements in buildings. Moreover, it can be appreciated how the self-consumed PV electricity ranges between a maximum value of 48.6% in December and minimum values around 0.5-1%

in summer, assuming a mean seasonal percentage of 9.4% and 26% for the single and the double-storey respectively. In order to investigate how to increase the self-consumed PV electricity, in Figure 8-11 for the single-storey building equipped with the heat pumps and for the locality with 1861 HDD, the non-renewable energy shares were determined by assuming a heating plant functioning closer to the actual conditions. In particular, in such locality, the indoor set-point temperature can be 20 °C for a maximum of 12 hours per day, as listed in the schedule of Table 8-4, whereas in the remaining part of the day an attenuation operation mode was simulated by supplying the radiant floors at a temperature of 25 °C. Furthermore, a PV peak-power of 6 kW_p was set.

Table 8-4- Time slots of the indoor set-point temperatures for the calculation of the primary energy requirements in the considered buildings assuming a non-continuous operating regime of the heating plant

Indoor set-point temperature [°C]						
00:00-06:00	06:00-10:00	10:00-12:00	12:00-15:00	15:00-17:00	17:00-22:00	22:00-00:00
Attenuated	20°C	Attenuated	20°C	Attenuated	20°C	Attenuated

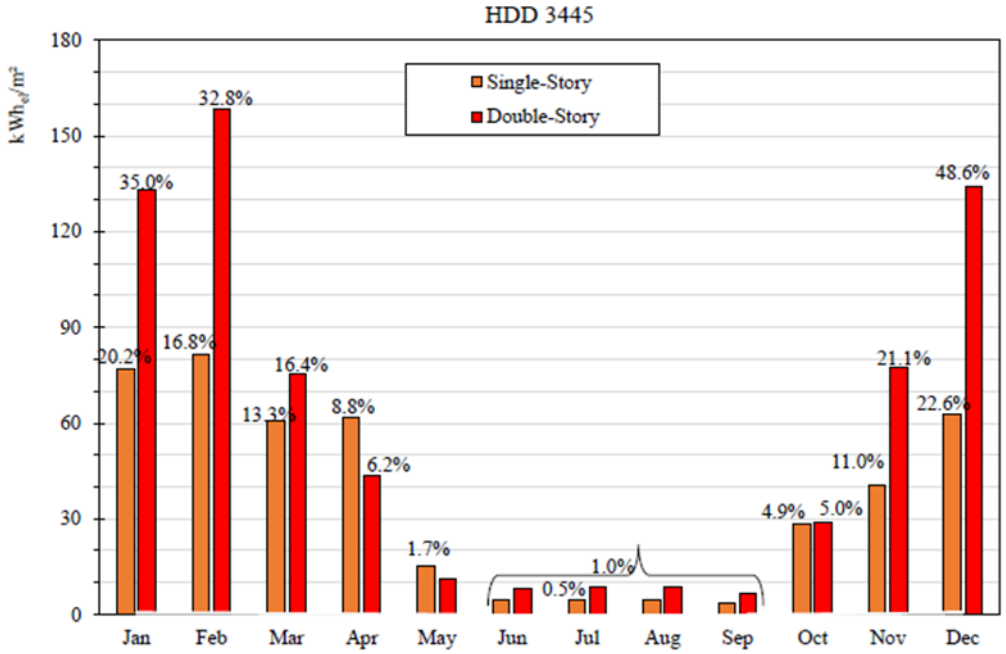

Figure 8-10- Self-consumed PV electricity and percentage value referred to the monthly producibility for the two buildings located in the locality with 3445 HDD equipped with a PV generator of 6 kWp

It is worth noting that the new management of the heating plant, and especially of the storage system, leads to better use of the PV generator because the mean seasonal percentage of the self-consumed electric energy increases from 9.7% of the base case up to 19.9% of the actual scenario. This allows for achieving a better Energy Performance

index that reduces from 14.71 kWh/m² of the base case down to 12.33 kWh/m². Nevertheless, despite the self-consumed PV electricity doubled, the non-renewable primary energy improvement is limited because it reduces of about 137 kWh. This means that the building energy performances continue to be strongly penalized by the high conversion factor in fossil primary energy despite the electricity absorbed from the grid was reduced.

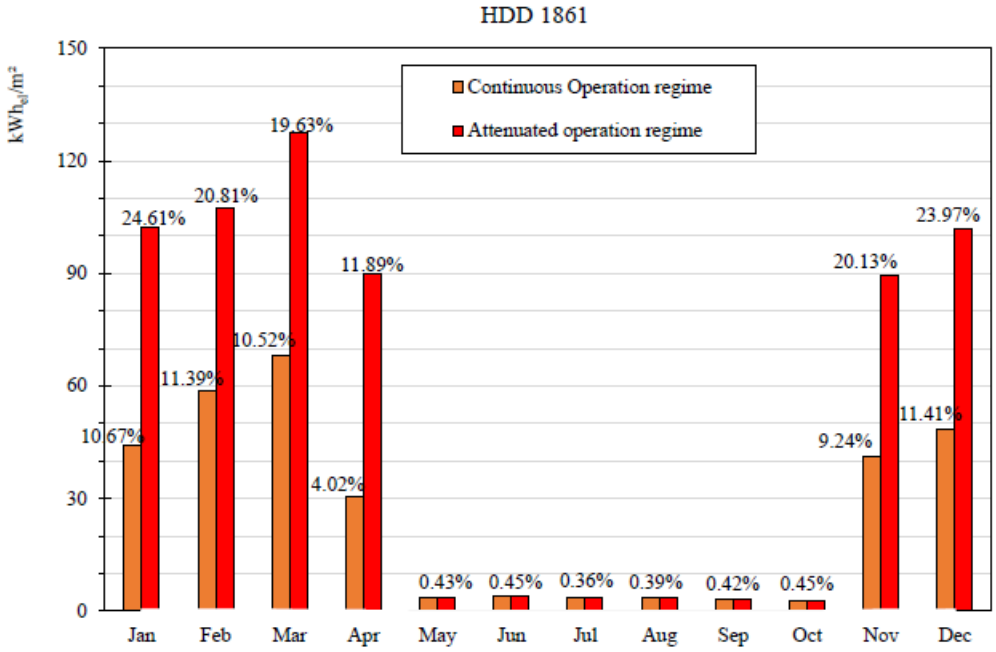

Figure 8-11- Self-consumed PV electricity and percentage value referred to the monthly producibility for the single-storey buildings located in the locality with 1861 HDD equipped with a PV generator of 6 kWp and assuming a continuous and an attenuation operation regime of the heating plant

8.4 Conclusion

In this paper, the non-renewable shares of two different heat generator systems, represented by a boiler supplied by solid biomass and connected to high-temperature emitters and a PV assisted air-water heat pump supplying radiant floors, were calculated in a transient regime by considering different HDD and by varying the size of the PV generator. The non-renewable share includes also the primary energy required for the DHW production, obtained in a combined manner with the biomass boiler and with an independent water heater heat pump in presence of PV assisted heat pumps. Finally, two typologies of buildings were simulated and designed in order to meet the minimum energy requirements required by Italian legislation. The same calculation has been

repeated adopting the quasi-steady model in order to highlight the deviances when the energy certification procedure is carried out. The results can be summarized as follow:

- assisted air-water heat pumps offer better performance in buildings with reduced thermal energy needs because the electricity from grid is limited. Consequently, the share of fossil primary energy is reduced despite the employment of the highest conversion factor among the energy carriers;
- with the increase of the building thermal energy demands and with the HDD growth, biomass boilers produce better results because the electric energy from the grid becomes significant, furthermore, the non-renewable share is penalized further by low outdoor air temperatures that penalize the COP increasing the electric consumptions;
- whit limited HDD, the gap between biomass boilers and heat pumps can be recovered easily by increasing the PV generator size;
- the results obtained with the quasi-steady approach show a different scenario because the PV electricity is considered completely absorbed from heating and DHW devices. Dynamic simulations, instead, showed an evident winter mismatching between solar radiation availability and thermal load request, still difficult to solve by adopting thermal energy storage systems, even if managed by suitable control strategies;
- under similar climatic conditions, the renewable shares determined with heat pumps are strongly affected by the locality latitude due to the different PV producibility. By augmenting the caption surface, a self-consumed PV electricity growth was observed because the probability to meet PV production and thermal load request increases.
- by assuming continuous functioning conditions and despite the priority of the PV production was given to the generation systems, it was difficult to assess PV self-consumed electricity greater than 50%. Nevertheless, these percentages improve as thermal energy requirements increase and with the PV size growth.
- in attenuated functioning conditions, the PV self-consumed electricity increases due to a better exploitation of the thermal storage tank.

Globally, in cold climates biomass are recommended to increase the share of the renewable primary energy. PV assisted heat pumps are negatively affected by lower COP detectable in localities with high HDD, which requires a larger use of the electricity from

the grid, especially at night. Since localities with high HDD numbers usually do not require cooling, the advantage to use the same heat pumps in summer fails. Conversely, climatic zones with high HDD are generally located in mountainous regions where there is a wider availability of solid biomass, making these devices able to exploit “local” fuel. The thermal storage systems managed by appropriate control strategies can improve the heat pump performance in favourable climates, however, a suitable PV size has to be installed. Nevertheless, to contrast the issues related to the aleatory nature of the renewable source and the misalignment with the building thermal loads, a great role could be assumed by the energy communities assuming the building-plant system able to rationalize the energy produced in-situ by exchanging thermal and/or electric energies with other structures, making heat pumps more competitive.

8.5 References

[1] I. E. A. IEA, Data and Statistics, Https://Www.Iea.Org/Data-and-Statistics, Accessed on 15th June 2021 (2021)

[2] European Commission, Directive 28/2009 of the European Parliament and of the Council of 23 April 2009on the Promotion of the Use of Energy from Renewable Sources and Amending and Subsequently Repealing Directives 2001/77/EC and 2003/30/EC (2009), p. L 140/16-62

[3] European Commission, Directive (EU) 2018/844 of the European Parliament and of the Council of 30 May 2018 Amending Directive 2010/31/EU on the Energy Performance of Buildings and Directive 2012/27/EU on Energy Efficiency (2018), pp. 1–17

[4] N. Aste, P. Caputo, C. Del Pero, G. Ferla, H. E. Huerto-Cardenas, F. Leonforte, and A. Miglioli, Energy 206, (2020)

[5] Eng. 2018 IEEE Ind. Commer. Power Syst. Eur. (EEEIC / I&CPS Eur. (IEEE, 2018), pp. 1–6, doi:10.1109/EEEIC.2018.8493492

[6] Arcuri N., Bruno R., Bevilacqua P., Carpino C., in BS2019 - Build. Simul. Assoc. Rome Conf. (2017

[7] M. Carpio, M. Zamorano, and M. Costa, Energy Build. 66, 732 (2013)

[8] Italian iterministerial decree 26th June 2015: Application of calculation methods for energy performance and definition of minimum building requirements, Off. Gazzette Ital. Repub. N°39 15th July 2015 1 (2015)

[9] R. Bruno, F. Nicoletti, G. Cuconati, S. Perrella, and D. Cirone, Energies 13, (2020)

[10] T. Olkowski, S. Lipiński, and A. Olędzka, E3S Web Conf. 19, (2017)

[11] J. A. Lozano Miralles, R. López García, J. M. Palomar Carnicero, and F. J. R. Martínez, Renew. Energy 152, 1439 (2020)

[12] M. J. Stolarski, M. Krzyzaniak, K. Warmiński, and D. Niksa, Energy Convers. Manag. 121, 71 (2016)

[13] A. Saari, T. Kalamees, J. Jokisalo, R. Michelsson, K. Alanne, and J. Kurnitski, Appl. Energy 92, 76 (2012)

[14] B. Hebenstreit, R. Schnetzinger, R. Ohnmacht, E. Höftberger, J. Lundgren, W. Haslinger, and A. Toffolo, Biomass and Bioenergy 71, 12 (2014)

[15] VV.AA., TRNSYS Libr. Vol. 4 Math. Ref. Sol. Energy Lab. Univ. Wisconsin-Madison, USA (2016)

[16] Italian Unification Institution, UNI TS 11300-1: Energy Performance of Buildings - Part 1: Evaluation of Energy Need Far Space Heating and Cooling (2014)

[17] Italian Unification Institution, UNI 11300-2: Energy Performances of Buildings-Part 2- Evaluation of Primary Energy Need and of System Efficiency for Space Heating, Domestic Hot Water Production, Ventilation and Lighting for Non-Residential Buildings (2014), pp. 37–40

[18] Italian Unification Institution, UNI TS 11300-4. Energy Performances of Building: Renewable Energy and Other Generation Systems for Space Heating and Domestic Hot Water Production (2016)

[19] . TRANSSOLAR & Energietechnik GmbH, TRNSYS Doc. (2016)

[20] J. Szyszka, Energies 13(3), (2020)

[21] B. Gil, S. Rosiek, J. Kaspersky, M. Nems, A. Nems, ECOS 2019 - Proceedings of the 32nd International Conference on Efficiency, Cost, Optimization, Simulation and Environmental Impact of Energy Systems, pp. 2559-2570,

[22] G. Evola and L. Marletta, Energy and Buildings 65, pp. 448-457 (2013)

[23] M. Cucumo, V. Ferraro, D. Kaliakatsos, M. Mele, Energy and Buildings 158, pp. 677-683, (2018)

[24] R. Bruno, P. Bevilacqua, L. Longo, and N. Arcuri, in Energy Procedia (2015)

[25] P. Bevilacqua, R. Bruno, and N. Arcuri, Energy 195, 116950 (2020)

[26] EN 14825:2018, Air conditioners, liquid chilling packages and heat pumps, with electrically driven compressors, for space heating and cooling - Testing and rating at part load conditions and calculation of seasonal performance

[27] M. Dongellini, C. Naldi, G.L. Morini, Applied Thermal engineering 90, (2015)

[28] . European Commission, Directive 92/42/EEC of the European Parliament and of the Council of 21 May 1992 on efficiencyrequirementsfornewhot-waterboilersfiredwithliquidorgaseousfuel, p. L 167/17

[29] S. Korol, N. Shushunova, T. Shushunova, MATEC Web of Conferences, Volume 193, Article Number 0507

9 Synoptic analysis of research results

9.1 Introduction

In an era where the energy and environmental crisis constitutes one of the most urgent global challenges, it is essential to steer energy consumption towards a sustainable development model that reduces dependence on fossil fuels and CO_2 emissions. The increase in energy demand necessitates the adoption of effective and sustainable solutions, supported by regulations that promote the expansion of renewable sources and energy efficiency. In this context, the construction sector has a significant impact on the environment, requiring innovative solutions to minimize energy consumption and pollutant emissions. The European Union has recognized this urgency, adopting ambitious policies to reduce greenhouse gas emissions, enhance energy efficiency, and promote the use of renewable energy through a series of targeted measures aimed at facilitating the energy transition, with particular focus on the building sector. One of the main pillars of these initiatives is the "2030 Climate and Energy Framework," which aims to reduce greenhouse gas emissions by 40%, increase the share of renewable energy to 32%, and improve energy efficiency by 32.5% by 2030. A key initiative is the Energy Performance of Buildings Directive, which imposes stringent standards for the energy efficiency of new and renovated buildings, entailing the adoption of advanced technologies such as heat pumps and solar thermal systems. Moreover, the European Green Deal represents a broader strategic framework to make Europe the first climate-neutral continent by 2050. The Green Deal envisions significant investments in renewable energy, modernization of energy infrastructure, and technological innovation. The European Commission estimates that Europe will need to invest approximately 1.7 trillion euros by 2030 to achieve these objectives.

9.2 Methodology

In the context of energy transition strategies, the implementation of advanced energy management solutions represents a crucial element for maximising the efficiency and sustainability of buildings. In this framework, heat pumps emerge as a strategic technology for building climate control. These devices, capable of transferring heat from a low-temperature source to a higher-temperature one, provide heating services, cooling, and domestic hot water production with high efficiency. Their versatility and ability to integrate with other renewable energy sources make them particularly suitable for reducing dependence on fossil fuels and minimising the environmental impact of buildings.

A crucial aspect of heat pumps lies in their potential to harness solar radiation. In fact, these devices become significantly more efficient when integrated with systems that utilise solar energy, such as solar thermal collectors and photovoltaic panels coupled with both thermal and electrical storage systems. Solar radiation, abundant and free, thus becomes a key element in enhancing the performance of heat pumps, especially during periods of high solar irradiance. This approach not only optimises the energy efficiency of buildings but also contributes to reducing CO_2 emissions, promoting a more sustainable use of natural resources.

One of the most widely adopted approaches to improving the energy efficiency of buildings involves integrating photovoltaic (PV) panels with heat pumps (HP). This configuration harnesses solar energy to power heating and cooling systems, significantly contributing to the reduction of greenhouse gas emissions and energy costs. It is essential to consider that the electrical energy generated by photovoltaic panels is a valuable resource, also utilized for domestic loads such as appliances and lighting systems. In addition to this approach, further system configurations have been examined to optimize energy management. Specifically, the integration of solar thermal collectors has been evaluated for the production of domestic hot water and for supporting heating systems, thereby maximizing the use of solar thermal energy. Moreover, the implementation of advanced control logics has proven crucial for the rationalization of renewable resource utilization. These control logics enable dynamic and optimized energy management based on predictive and regulatory algorithms that modulate energy delivery according to real-time demand and the availability of renewable sources. This integrated approach allows for maximizing self-consumption, reducing energy losses, and improving the overall

system efficiency, ensuring high standards of residential comfort and environmental sustainability.

This research has explored various methodologies and proposals for integrating heat pumps with renewable technologies that harness solar radiation, highlighting how each study, despite addressing different contexts and approaches, converges on the objective of identifying best practices for the implementation of sustainable energy systems, each with particular attention to climatic specificities and building characteristics. Specifically, the guiding principle behind the configuration of various integrated systems has been the necessity to move towards an intelligent building model, capable of rationally managing energy flows from renewable sources, implementing strategies to retain the surplus produced within the building-plant system. Consequently, the surplus produced will no longer constitute a waste factor but will transform into a virtuous component of the system, further enhancing energy efficiency.

Multiple configurations of integrated systems have been analysed, exploring various levels of complexity and technological integration.

9.3 Results

9.4 Synergies and challenges in the efficiency of heat pumps in centralized configurations: the strategic role of thermal storage

In the context of building energy efficiency, one of the central challenges is the high energy consumption associated with heating and cooling. This study examined a complex of four terraced houses located in Crotone, characterized by a "Csa" climate according to the Köppen classification. This case study was selected due to its representative status as buildings with very limited energy performance, making them prime candidates for energy retrofit interventions. The buildings, arranged over two floors, have a gross floor area of approximately 60 m² per floor and a ceiling height of 3 meters. The energy consumption for heating and cooling in the four analyzed buildings (B1, B2, B3, B4) indicates a higher energy demand for cooling, particularly during the summer months.

A key question emerging from this analysis is: *How can the integration of a centralized system with heat pumps and photovoltaic technology address the issue of high energy consumption in a climate like that of Crotone?* To answer this question, the study

compared three scenarios: the base case with a gas boiler, an autonomous heat pump system, and a centralized system with a heat pump supported by a photovoltaic system.

The results show significant differences in terms of energy consumption, CO_2 emissions, and operating costs. As reported in Table 9.1, the base case with a gas boiler results in annual energy consumption of 17,700 kWh, CO_2 emissions of 12,400 kg/year, and a total annual cost of €4,960. The adoption of an autonomous heat pump system reduces energy consumption to 16,203.5 kWh and emissions to 9,800 kg/year, with annual costs of €4,050. Finally, the integration of a centralized system with heat pumps and a 16-kW photovoltaic system leads to further reductions, with energy consumption of 15,489.1 kWh, CO_2 emissions of 7,559 kg/year, and an annual cost of €3,500.

Table 9-1Comparison of different scenarios in terms of energy consumption, CO_2 emissions, and annual operating costs

Scenarios	**Energy Consumption** [kWh/year]	**CO_2 Emissions** [kg/year]	**Total Cost** [€/year]
Base Case	17,700	12,400	4,960
Autonomous Heat Pump	16,203.5	9,800	4,050
Centralized PV System	15,489.1	7,559	3,500

Figure 9.1 clearly illustrates the variations in energy consumption, CO_2 emissions, and total costs across the different scenarios. The centralized system with photovoltaic panels shows a 12.45% reduction in energy consumption compared to the base case, and a drastic decrease in CO2 emissions of 39.10%, underscoring the effectiveness of this integrated solution.

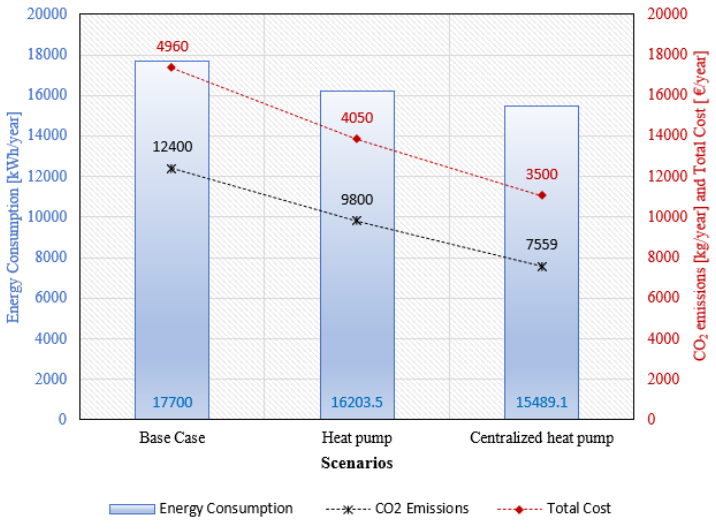

Figure 9-1 Variations in energy consumption, CO_2 emissions, and total costs among the three main scenarios

A strategic aspect deserving attention is the use of a thermal storage tank. *To what extent can this storage system further enhance the efficiency of the overall system by increasing solar energy self-consumption and reducing reliance on the electrical* **grid?** The data indicate that integrating a thermal storage tank optimizes solar energy use, maximizing self-consumption and minimizing the energy demand from the grid, which is particularly relevant in a climate like that of Crotone.

From an economic perspective, the results show that adopting the centralized system with photovoltaics allows for a reduction in annual operating costs of approximately 29.44% compared to the base case. This is evident in Figure 9.1, which highlights the significant savings associated with the implementation of sustainable technologies.

Finally, the reduction of CO_2 emissions is a crucial objective. The centralized system with a photovoltaic system demonstrated a significant reduction in emissions, confirming the importance of technological choices for building sustainability. In summary, this study demonstrates that the integration of sustainable technologies, such as heat pumps and photovoltaic systems, can serve as a key solution for buildings located in areas with high cooling demand, while simultaneously improving environmental sustainability and reducing operating costs.

9.5 The function of solar energy in optimizing the efficiency of heat pumps in cold climate conditions: an innovative analysis

One of the primary issues encountered in cold climates is the reduction in efficiency of traditional heat pumps, particularly air-to-water systems, due to low external temperatures. To address this challenge, a cutting-edge solution involves the integration of solar thermal collectors, which enhance the thermal potential of the cold source utilized by the heat pump, thereby contributing to an overall improvement in system performance. Through this integration, solar collectors are tasked with heating the heat transfer fluid, optimizing the coefficient of performance (COP) of the heat pump, and significantly reducing electricity consumption. During periods of adequate solar irradiation, it is even possible to achieve complete coverage of the heating demand, resulting in the elimination of the economic impact associated with electricity consumption.

The investigation focuses on a key question: *how can the integration of solar collectors enhance the efficiency of heat pumps* even under challenging climatic

conditions? Additionally, *what configuration in terms of collector area and storage volume ensures optimal energy performance?* To address these questions, the study examines two specific cases in Italy: a residential building in Milan and the 'Chiodo 2' student housing complex at the University of Calabria in Rende.

The analysis focuses on identifying key variables, such as the surface area of the solar collectors and the thermal storage volume, to determine the optimal configuration capable of maximizing energy efficiency under adverse climatic conditions.

9.5.1.1 Milan

The objective of this study was to evaluate the energy efficiency and environmental impact of a solar-assisted heat pump (SAHP) system operating in cold climates. The research analysed the system's performance through a parametric analysis that varied the solar tank volume and collector area. The reference building used in the study, assumed to be located in the Italian city of Milan, is a typical multi-storey building with an area of approximately 200 m² and a floor height of 2.70 m. The analysis was conducted considering three apartments of different sizes (small, medium, and large), with the building envelope complying with current Italian energy efficiency regulations. The building was simulated as a single thermal zone.

The system's efficiency was evaluated based on several key parameters. These include the percentage of energy demand covered without the aid of a secondary generation system, the average seasonal COP (SCOP) to measure system efficiency during the heating season, the share of renewable and non-renewable energy supplied, and CO_2 emissions. The examined configurations varied by solar collector area and solar storage tank volume. The main configurations are:

- Configuration A: storage volume 0.5 m³, solar collector area ranging from 8 to 40 m² with a step of 8 m².
- Configuration B: storage volume 1 m³, solar collector area ranging from 8 to 40 m² with a step of 8 m².
- Configuration C: storage volume 1.5 m³, solar collector area ranging from 8 to 40 m² with a step of 8 m².
- Configuration D: storage volume 2 m³, solar collector area ranging from 8 to 40 m² with a step of 8 m².

The main results are summarized in Table 9-2, which shows the key energy and environmental parameters for each configuration in relation to the minimum (8 m²) and maximum (40 m²) solar collector area:

Table 9-2 Key energy and environmental parameters for each configuration in relation to the minimum and maximum solar collector area

	Configuration A 8-40 m²	Configuration B 8-40 m²	Configuration C 8-40 m²	Configuration D 8-40 m²
Solar collectors [%]	1÷22	2÷20	1÷18	1÷17
Heat Pump [%]	20÷31	21÷28	21÷42	22÷44
Auxilary[%]	79÷47	78÷42	77÷40	77÷39
Ep_{ren} [kWh]	664÷863	692÷850	771÷863	720÷877
Ep_{nren} [kWh]	12.470÷8210	11941÷7811	12336÷8166	12292÷7149
CO_2[kg]	2498÷1758	2395÷1596	2475÷1517	2467÷1472
SCOP	4.258÷4.298	4.262÷4.31	4.253÷4.322	4.249÷4.322
Ep_{ren} reduction VS air-water heat pump	27.35÷12.34%	21.92 ÷20.57%	25.98%÷24.65%	21.51% ÷54.35%
Ep_{ren} reduction VS Boiler [%]	20.38÷45.20	23.75÷50.34	21.23÷52.89	21.58÷54.35
CO_2 reduction VS air-water heat pump [%]	20÷44%	24÷49	21÷52	21÷53
CO_2 reduction VS Boiler [%]	0÷21%	0÷28%	0÷32%	0÷34%

The analysis shows that the heating demand coverage by the different generators varies based on the collector area and the solar tank volume. The percentage of demand covered by the proposed system increases with the increase in the solar tank volume, but the main influence is exerted by the solar collector area. The analysis showed that the proposed SAHP system guarantees excellent heat pump performance, with an average COP always above 4, compared to the nominal value of 3.78 of the simulated commercial devices. The heating demand covered by the system increased with the increase in

collector area and solar tank volume, reaching a coverage of 61% with 40 m² of solar collectors and a tank volume of 2 m³. The optimal configuration achieved the lowest share of non-renewable energy, with a reduction of 27% compared to a heating system with air-water heat pump assisted by photovoltaic and thermal storage systems, and 54% compared to a traditional gas boiler system. This highlights the innovation and effectiveness of this solution compared to traditional heating systems and air-water heat pumps assisted by photovoltaics.

The charts in Figure 9-2 illustrate interactively how the seasonal COP (SCOP), equivalent carbon dioxide emissions, and their percentage reduction compared to a traditional boiler system vary for each configuration as a function of collector area. On the x-axis, the SCOP value is reported, while on the y-axis, the equivalent carbon dioxide emissions are indicated. A colour scale represents the percentage reduction in emissions compared to the traditional system

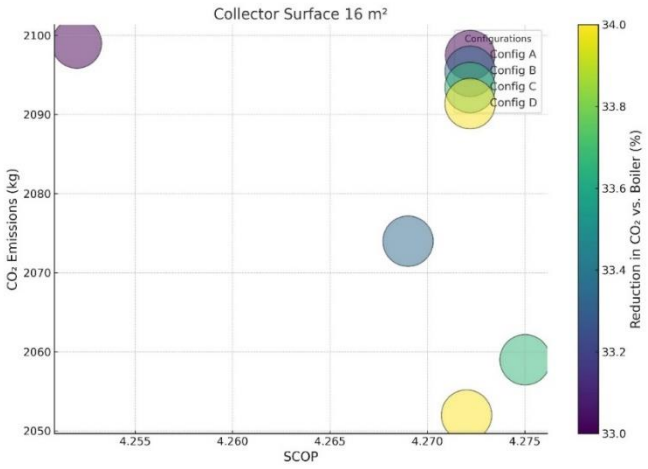
Collector Surface 16 m²
Configurations
Config A
Config B
Config C
Config D
CO₂ Emissions (kg)
SCOP
Reduction in CO₂ vs. Boiler (%)

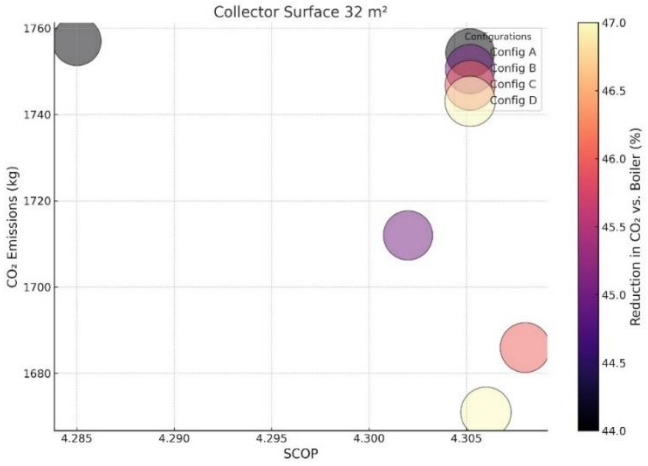
Collector Surface 32 m²
Configurations
Config A
Config B
Config C
Config D
CO₂ Emissions (kg)
SCOP
Reduction in CO₂ vs. Boiler (%)

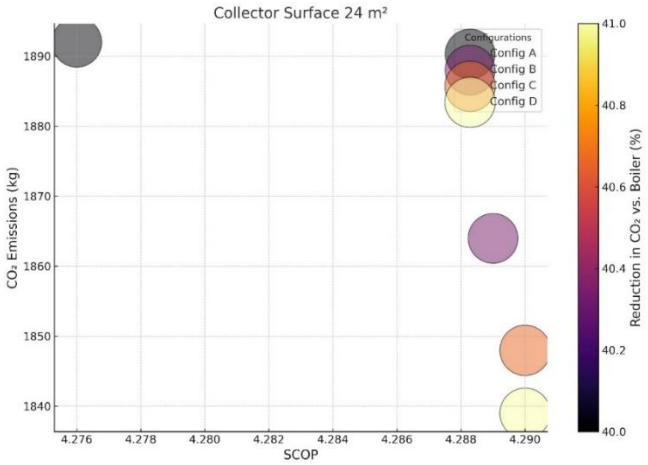
Collector Surface 24 m²
Configurations
Config A
Config B
Config C
Config D
CO₂ Emissions (kg)
SCOP
Reduction in CO₂ vs. Boiler (%)

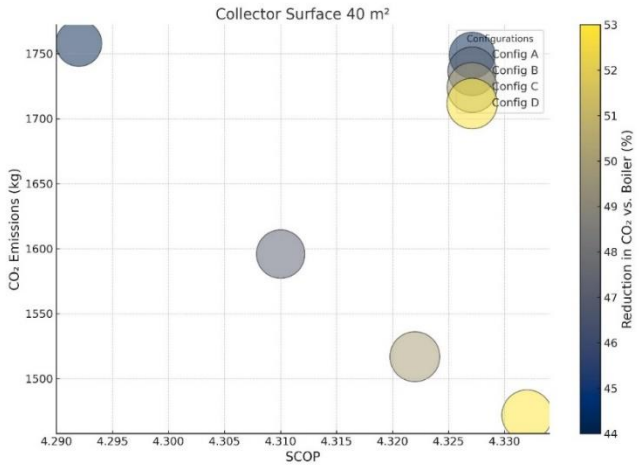

Figure 9-2- Variation of the Seasonal Coefficient of Performance (SCOP), equivalent carbon dioxide emissions, and the percentage reduction of the latter compared to a traditional boiler system for each configuration as a function of collector area.

9.5.1.2 Rende

This study describes the implementation of the aforementioned system at the experimental site "Chiodo 2" of the University of Calabria, where an air-water heat pump is already operational. The main objective is to reduce electrical consumption by achieving a higher coefficient of performance (COP) through the use of solar energy stored in a thermal storage tank, thereby optimizing operational conditions with a favourable cold source temperature.

The simulated air conditioning system includes:

- A field of evacuated tube solar collectors.
- Two thermal storage tanks, one powered by the solar collectors and the other by the heat pump.
- A water-water heat pump, sized according to the preliminary simulation results.

The system's control strategy includes specific conditions for winter operation, such as the direct use of solar energy when the solar tank temperature exceeds 60°C. The surface area of the solar collectors and the thermal storage volume were varied to study their effect on the fraction of energy demand met by the system. Simulations showed that the adoption of 40 m² of solar collectors and a solar tank of 1.6 m³ allows the system to meet 100% of the building's energy demand from March to November. Solar energy directly used for heating reached 70% in May and 65% in October. However, increases

in the surface area of the solar collectors produced marginal benefits beyond a certain threshold, identifying the optimal configuration as a surface area of 25-30 m² and a storage volume of 1.6 m³. The use of solar collectors to increase the temperature of the cold source significantly improved the heat pump's COP, achieving an annual average value of 3.98 and a maximum monthly value of 4.58 in May. The main results are reported in Table 9-3

Table 9-3 Main results of the study

Parameter	Value
Solar collector Surface area	25÷ 30 m^2
Thermal storage volume	1.6 m^3
Annual average COP	3.98
Maximum monthly COP	4.58
Direct solar energy	70% (May), 65%(October)
Percentage of energy provided	100% (from March to November with 40 m^2

Below are the graphs with colour maps related to the percentage of demand directly covered by the analysed system without the use of an auxiliary device (Figure 9-3) and the monthly COP (Figure 9-4), both related to the increase in the surface area of the solar collectors.

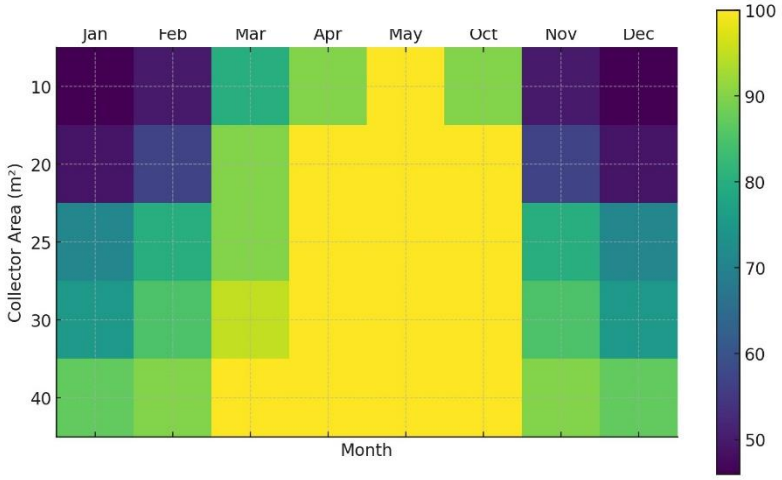

Figure 9-3-Percentage of energy demand met by the system

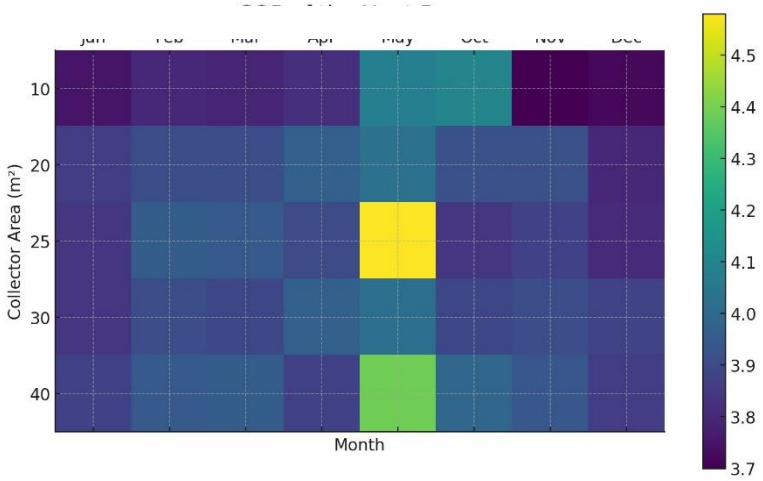

Figure 9-4-COP of the water-water heat pump

Figure 9-4 presents the COP performance of the heat pump across different solar collector surface configurations (25 m², 30 m², and 40 m²). We observe that the COP does not increase linearly with larger collector surfaces. This seemingly counterintuitive behaviour occurs primarily during months with higher solar radiation. During these periods, larger collector surfaces (such as 30 and 40 m²) allow the solar storage tank to reach temperatures high enough to meet the heating demand directly, without activating the heat pump. As a result, the COP reported in the figure reflects only those periods when the heat pump is in operation and does not account for direct heating, leading to a lower COP for configurations with larger surfaces during high-radiation months.

9.6 From passive storage to active management: analysis of the impact of advanced control strategies on heat pump efficiency through the utilization of photovoltaic surplus as thermal storage.

The efficiency of heat pumps can be significantly enhanced through the implementation of advanced control strategies aimed at rationalizing the flow of renewable energies and maximizing their utilization, even during periods of surplus production. In this context, heat pumps are positioned as strategic elements in demand management, contributing to the realization of smart grids. The integration of heat pumps with thermal storage systems and photovoltaic generators provides an alternative means of storing surplus electricity generated in the form of thermal energy, effectively decoupling electricity consumption from heat demand and offering the operational flexibility required for a more efficient energy system.

This raises pertinent questions: *how can advanced control strategies optimize the accumulation of photovoltaic surplus as thermal energy*, thereby improving the overall energy efficiency of the system? *What is the optimal configuration*, in terms of the number of photovoltaic panels and storage volume, *to ensure effective integration between renewable energy production and heat demand?*

This study analysed an air-water heat pump system assisted by solar energy, equipped with both electrical and thermal storage, implemented in two residential buildings located in Italy: Milan, characterized by a continental climate and high heating demands during the winter months, and Messina, which features a Mediterranean climate with significantly lower thermal loads. Two different control strategies were examined:

- **Conventional Control Strategy**: This strategy manages the air conditioning system based on the immediate demand of the building, without considering the optimization of the available solar energy use. The main objective is to maintain the thermal comfort of the occupants, activating the heat pump and storage units based on the instant heating, cooling, and domestic hot water production needs.
- **Solar Energy Optimized Control Strategy**: This strategy is designed to maximize the self-consumption of the solar energy generated by photovoltaic panels. It includes proactive management of the charging and discharging of electric batteries and thermal storage, synchronizing the use of the heat pump with the periods of highest solar production through thermal storage in the tank or directly in the structure by increasing the internal set-point. This reduces the dependence on the electrical grid and increases the use of renewable energies to meet the building's thermal and electrical needs.

A parametric analysis was conducted by varying the peak photovoltaic power, battery capacity, and storage volume. The influence of the storage volume was negligible. Despite the substantial climatic differences between the two analysed locations, a similar trend was observed in the system's behaviour. The increase in peak photovoltaic power led to an increase in the energy coverage provided by the system, reducing dependence on the national electrical grid. This effect is due to the greater energy generation capacity of the photovoltaic panels during optimal solar irradiation hours, which allows for greater energy storage in the batteries. CO_2 emissions were significantly reduced compared to traditional boiler-based systems. The integration with solar collectors allowed almost complete fulfilment of the hot water demand using renewable energy. Moreover, the

second control logic led to a significant increase in photovoltaic energy self-consumption and a reduction in CO_2 emissions. In Milan, the reduction in emissions ranges from 8% to 36% depending on the surface area of the photovoltaic panels and the battery capacity. Messina showed similar results with better exploitation of the available solar energy.

The graphs in Figure 9-5 and Figure 9-6 show data on grid dependence, self-consumption, and the contribution of electrical storage as a function of installed peak power and battery capacity, comparing conventional and intelligent control logics for Milan and Messina, respectively.

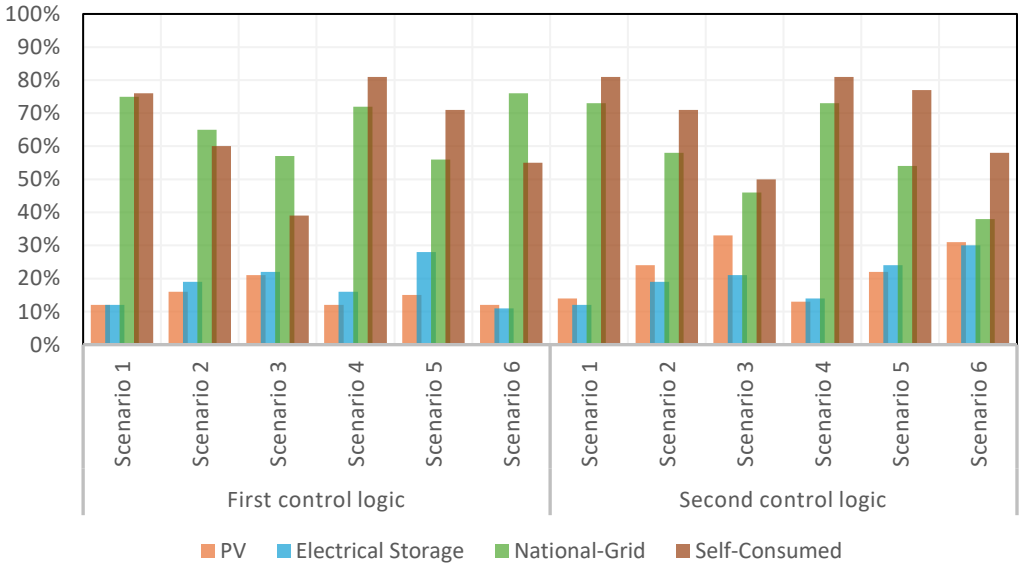

Figure 9-5 Grid Dependence, Self-Consumption, and Electrical Storage Contribution for Milan

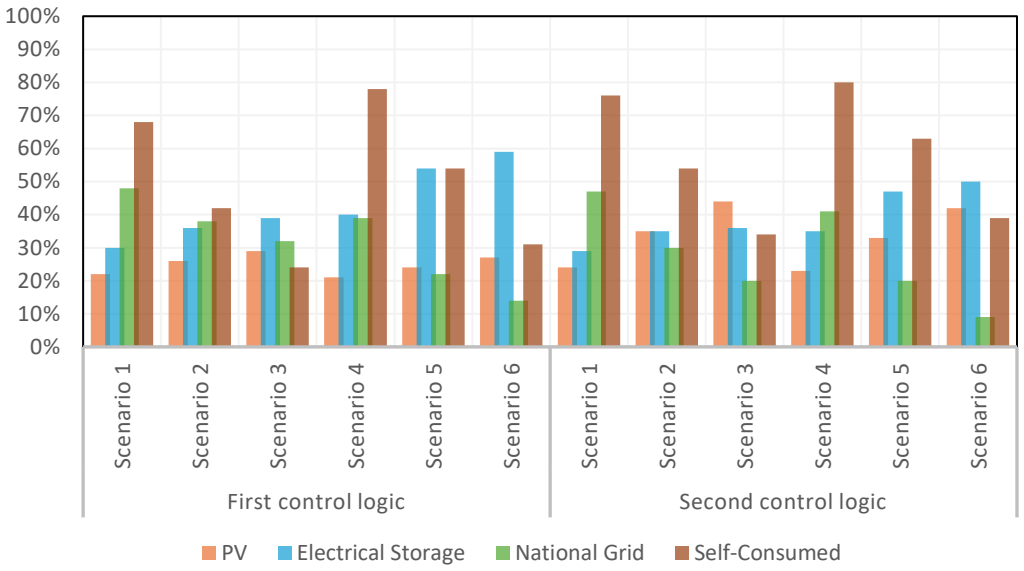

Figure 9-6-Grid Dependence, Self-Consumption, and Electrical Storage Contribution for Messina

9.7 Heat pumps versus biomass boilers: primary energy consumption analysis across different climatic contexts

Previous studies have highlighted the effectiveness of heat pumps assisted by renewable sources, such as photovoltaic and solar thermal systems, in improving energy efficiency and reducing CO_2 emissions in residential buildings. However, with the aim of defining highly integrated solutions tailored to the climatic specificities and energy needs of buildings, the fourth case study proposes to compare, in terms of non-renewable primary energy, the performance of air-to-water heat pumps assisted by photovoltaic systems with that of biomass boilers.

The objective is to determine the climatic contexts and energy demand profiles under which each technology demonstrates optimal efficiency. In this regard, two principal research questions arise*: what are the comparative advantages of heat pumps versus biomass boilers* in terms of primary energy consumption and CO_2 emissions across distinct climatic zones? Furthermore, to what extent does the energy demand of buildings with varying consumption levels influence the effectiveness of each solution?

Biomass represents an important alternative energy source due to its renewability and more favorable carbon balance. Composed of rapidly renewable organic materials such as agricultural and forestry residues, biomass can significantly contribute to sustainable waste management, reducing methane emissions and supporting the production of clean energy. The use of biomass also stimulates local economic

development by creating jobs and enhancing the energy security of communities. Additionally, the versatility of biomass allows it to be used for the production of heat, electricity, and biofuels, facilitating an energy transition towards more sustainable and less polluting sources.

Simulations have shown that air-to-water heat pumps assisted by photovoltaics offer excellent performance in buildings with low energy demands and in mild climates, where the availability of solar energy is higher. These systems significantly reduce dependence on grid electricity, optimizing the use of renewable resources and improving the overall energy efficiency of buildings. However, in cold climates and buildings with high energy demands, biomass boilers are more efficient due to their ability to use local fuels and the lesser impact of low external temperatures on system efficiency. The main results are shown in Table 9-4.

Table 9-4 Comparison of heat pumps and biomass boilers in different climates and building types

		Heat Pump			Boilers		
Climate	**Building Type**	**Energy consumption (kWh/m²)**	**CO_2 (kg/m²)**	**Costs (€)**	**Energy consumption (kWh/m²)**	**CO_2 (kg/m²)**	**Costs (€)**
Temperate	Low Demand	15	7.5	1000	18	5	1200
Temperate	High Demand	20	10	1200	25	7	1400
Cold	Low Demand	25	12	1500	22	6	1600
Cold	High Demand	30	15	1800	28	9	2000

The graph in Figure 9-7 provides a comparative analysis of the efficiency of heat pumps assisted by photovoltaics and biomass boilers in temperate and cold climates. It illustrates the energy consumption (kWh/m²), CO_2 emissions (kg/m²), and annual costs (€) for buildings with low energy demand (LF) and high energy demand (HF).

In particular, regarding a temperate climate, heat pumps assisted by photovoltaics demonstrate remarkable efficiency. For buildings with low energy demand, the energy consumption is 15 kWh/m², while for buildings with high energy demand, the consumption rises to 20 kWh/m². In comparison, biomass boilers consume 18 kWh/m² and 25 kWh/m² respectively. Therefore, heat pumps are more efficient, with a reduction in energy consumption of up to 20% for low-demand buildings and 25% for high-demand buildings. CO_2 emissions from heat pumps are 7.5 kg/m² for low-demand buildings and 10 kg/m² for high-demand buildings, while biomass boilers emit 5 kg/m² and 7 kg/m²

respectively. Annual costs for heat pumps are €1000 for low-demand buildings and €1200 for high-demand buildings, while for biomass boilers the costs are €1200 and €1400 respectively, with a cost reduction of 17% and 14%.

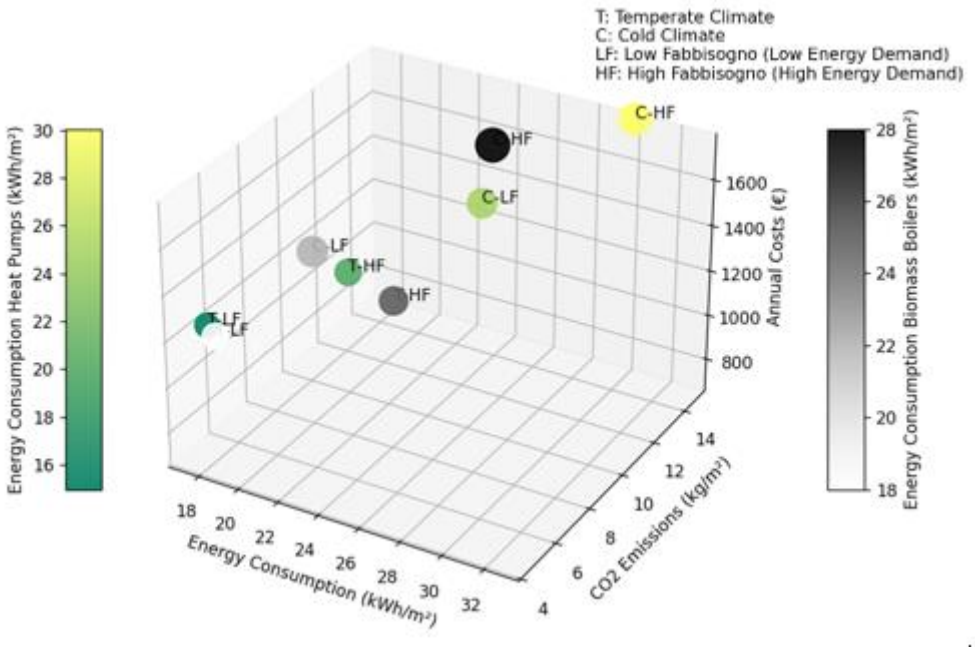

Figure 9-7 Comparative efficiency of photovoltaic-assisted heat pumps and biomass boilers in temperate and cold climates. The graph shows energy consumption (kWh/m²), CO_2 emissions (kg/m²), and annual costs (€) for buildings with low (LF) and high (HF) energy demand.

10 Conclusions

The analysis of the research results highlights the usefulness, effectiveness, and advantages of adopting sustainable development model in the building sector to reduce dependence on fossil fuels and CO_2 emissions through the implementation of advanced technologies. The widespread adoption of integrated technologies such as heat pumps and solar systems is crucial for achieving energy sustainability goals. These technologies not only provide practical solutions for reducing CO_2 emissions but also represent a fundamental step towards energy security and building resilience, effectively addressing the challenges posed by global climate change.

The specific climatic conditions and structural characteristics of buildings significantly influence the performance and efficiency of the analysed energy systems. Research on integrated systems of heat pumps, solar thermal collectors, and photovoltaic plants has demonstrated their effectiveness in meeting the energy demands of buildings while simultaneously reducing dependence on fossil fuels. Simulations conducted using TRNSYS software have produced multiple results, highlighting how intelligent energy management strategies, storage systems, and the utilization of solar energy are essential for optimizing the efficiency and resilience of systems under various operating conditions.

The studies reviewed cover a broad range of contexts and approaches, all aimed at identifying best practices for the implementation of sustainable energy systems, with particular attention to climatic specifics and building characteristics. The five studies included in this analysis offer a comprehensive and detailed overview of technological solutions for optimizing heat pumps integrated with renewable energy sources, also identifying usage limitations. Each study contributes to outlining a coherent and innovative framework for the decarbonization of the building sector, highlighting the potential and challenges of different plant configurations.

The integration of heat pumps with solar thermal collectors and storage tanks can mitigate performance penalties due to low external temperatures in cold climates. Advanced configurations, such as water-to-water heat pumps combined with solar systems, significantly improve the Coefficient of Performance (COP) and reduce electricity consumption, increasing the share of renewable energy used for heating buildings. This approach allows for higher energy efficiency while reducing environmental impact.

Configurations that combine heat pumps with thermal storage and photovoltaic systems significantly increase the energy self-sufficiency of buildings, reducing dependence on the electrical grid and enhancing renewable energy self-consumption. Studies emphasize the importance of advanced control logics to rationalize the flow of renewable energies and maximize their utilization, even during surplus production periods.

The comparison between different heat generation technologies, such as photovoltaic-assisted heat pumps and biomass boilers, is particularly relevant in cold climates. Biomass boilers can offer advantages in terms of efficiency and CO2 emissions reduction compared to heat pumps, which may be penalized by low external temperatures. However, in milder climates and for buildings with low thermal requirements, photovoltaic-assisted heat pumps demonstrate superior energy performance and sustainability.

In conclusion, the joint research of these solutions represents a significant step towards the realization of energy-efficient and sustainable buildings, aligned with global objectives for reducing CO_2 emissions and transitioning towards a cleaner and more resilient energy future.